INHIBITORY SYNAPTIC PLASTICITY IN THE CEREBELLUM

A thesis submitted for the Degree of Doctor of Philosophy
in the University of London, Faculty of Science

By

Ian Charles Duguid, B.Sc.(Hons.)

Department of Pharmacology,
School of Pharmacy,
29/39 Brunswick Square,
London WC1N 1AX.

June 2001

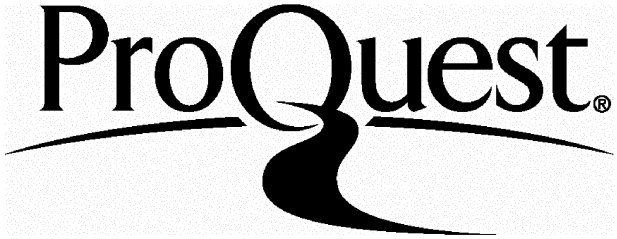

To my parents

Janet and Kenneth

ABSTRACT

Learning and memory within the brain are thought to be based on long lasting changes in synaptic efficacy. Purkinje neurones, which focus their output on descending projection pathways and constitute the sole inhibitory output from the cerebellum, display two forms of synaptic plasticity termed 'depolarisation-induced suppression of inhibition' (DSI) and 'rebound potentiation' (RP). Purkinje neurone depolarisation induces a rapid rise in $[Ca^{2+}]_i$ triggering both the release of a retrograde transmitter and activation of a variety of protein kinases. The phenomena of DSI underlies a transient (lasting <60s) decrease in the mean frequency of mIPSCs, occurring immediately after stimulus cessation, while RP manifests itself as a robust increase in the mean amplitude of spontaneous and miniature inhibitory postsynaptic currents (IPSCs).

The present study examined the relationship between pre- and postsynaptic plasticity during the induction phase of DSI and rebound potentiation in cultured cerebellar Purkinje neurones. Depolarisation caused an immediate decrease in the frequency of mIPSCs (lasting ~40s), followed by a transient increase in mIPSC frequency lasting approximately 5 minutes before recovering. A robust potentiation of the mean mIPSC amplitude was observed throughout all experiments and persisted for the duration of recording. The initial frequency decrease (DSI), was abolished by a specific group II mGluR antagonist, LY 341495, while the subsequent transient frequency potentiation was abolished by the specific N-methyl-D-aspartate receptor (NMDAR) antagonist, D-APV. Removal of extracellular sodium, the main current carrying ion through NMDARs, mimicked the application of D-APV by abolishing the frequency potentiation while having no effect on the induction of DSI. Immunocytochemical staining of mixed cerebellar preparations identified cerebellar basket/stellate cells as displaying immunoreactivity for NMDAR NR1 subunits but not $mGluR_{2/3}$ at putative presynaptic release sites.

These results provide the first evidence for, 1) the involvement of presynaptic NMDARs in the transient enhancement of GABA release during rebound potentiation and 2) the possibility that a novel group II mGluR splice variant/subtype underlies the induction of cerebellar DSI. A model is proposed to explain the relationship between DSI and rebound potentiation.

`INHIBITORY SYNAPTIC PLASTICITY IN THE CEREBELLUM`

LIST OF TABLES

Chapter 1

Chapter 2

Chapter 3

Chapter 4

Chapter 5

Chapter 6

Chapter 7

LIST OF FIGURES

Chapter 1

Chapter 2

Chapter 3

Chapter 4

Chapter 5

Chapter 6

Chapter 7

Chapter 8

Chapter 1
INTRODUCTION

The Cerebellum

The cerebellum (*Latin, little or lesser brain*) is a highly ordered region of the brain, involved in the regulation of movement and posture. Inputs to the cerebellum derive from many areas of the neuraxis and result in indirect regulation of movement and posture by adjusting the output of the major descending motor pathways. The cerebellum receives inputs concerning the initiation of movement and information about motor performance during muscle activity. These two types of feedback information processing termed internal and external feedback, respectively, allow the cerebellum to assess central information and compare between intended goal and actual motor response. Output from the cerebellum, as a result of information processing, will manifest itself as 'sculpted' coordinated movements of limbs and correct posture. Damage, resulting in lesions within one or more of these pathways, causes disruption of limb and eye movements, impaired balance, decrease muscle tone and jerky under-overshoot movements (dysmetria) (Kandel *et al.* 1991). However, complete removal of the cerebellum does not impair either sensory perception or muscle strength indicating that the cerebellum plays a central role in modulating the output of downstream motor centres without itself being directly involved in muscle stimulation.

The cerebellum receives input from the periphery and all levels of the central nervous system via three symmetrical pairs of peduncles termed inferior cerebellar peduncle, middle cerebellar peduncle (*branchium pontis*) and superior cerebellar peduncle (*brachium conjunctivum*). The surface of the cerebellum contains many parallel transverse convolutions subdivided by deep transverse fissures to create both a posterior and an anterior lobe. Shallower fissures subdivide the aforementioned lobes to create lobules containing a multitude of small offshoots termed folia (*Latin, leaves*). A simplified schematic diagram of the circuitry and morphology of the cerebellum can be seen in Fig. 1.1. and Fig. 1.2.

Fig. 1.1. Schematic diagram of excitatory and inhibitory inputs in the cerebellum.

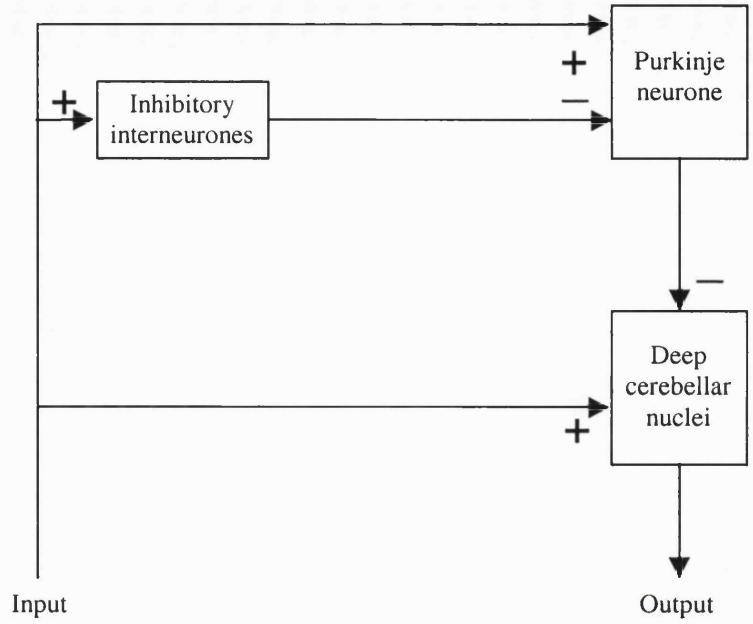

Fig. 1.2. Section through the cerebellum identifying (1) arbor vitae, (2) cerebellar cortex, (3) folia and (4) medullary centre. The cerebellar cortex consists of the three cellular layers; granular, Purkinje and molecular (England & Wakely, 1991).

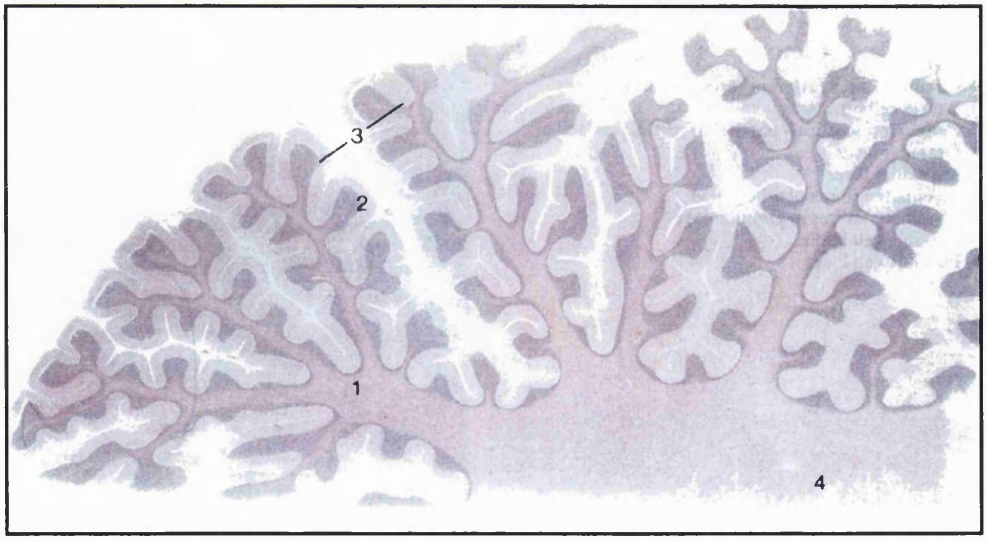

The cerebellar cortex

Each folium consists of a cell rich layer, the *cerebellar cortex*, and a core of myelinated fibres projecting to (afferent) and from (efferent) the overlying cortex. The cerebellar cortex is a simplistic structure consisting of 3 highly organised layers possessing only five different types of neurones: stellate; basket; Purkinje; Golgi and granule cells (Fig. 1.3.).

Purkinje cell layer

The Purkinje cell layer possesses the large (20-60μm) cell bodies of the Purkinje neurones arranged in a single, juxtaposed, uniform layer. Each Purkinje neurone projects an extensive, wide branching dendritic tree deep into the relatively cell-sparse molecular layer, located superior to the Purkinje cell layer. The 'trunk' of the dendrite is a large, flat structure bifurcating to produce secondary and tertiary branchlets. Branchlets developmentally form spines as both excitatory (parallel and climbing fibres) and inhibitory (stellate and basket cell) inputs form synapses with the Purkinje neurone dendrites during synaptogenesis. Purkinje neurones form the sole (inhibitory) output of the cerebellum, their axons arise from the basal aspect of the soma and project through the granular (granule cell) layer, subcortical white matter and finally terminate in either the cerebellar or vestibular nuclei. Purkinje neurone axons release the inhibitory neurotransmitter γ-aminobutyric acid (GABA) resulting in the overall 'dampening' of the excitability of the downstream cerebellar or vestibular nuclei.

Granular layer

This densely packed region of the cerebellum contains an abundance of small (5-8μm) granule cells, their axons ascend deep into the molecular layer where upon they bifurcate producing parallel fibres (PFs). PFs run parallel to the long axis of the folium and pass through the dense dendritic arbour of the Purkinje neurone, forming synapses with spiny branchlets on secondary and tertiary dendrites. An example of PF-Purkinje neurone synapse is displayed in Fig. 1.4. Granule cells release excitatory neurotransmitter (glutamate/aspartate) from axon terminals resulting in the overall excitation of the Purkinje neurone. A secondary cell type present in the granular layer is

Fig. 1.3. Cross-section through the cerebellar cortex (modified from Kandel *et al.*, 1991).

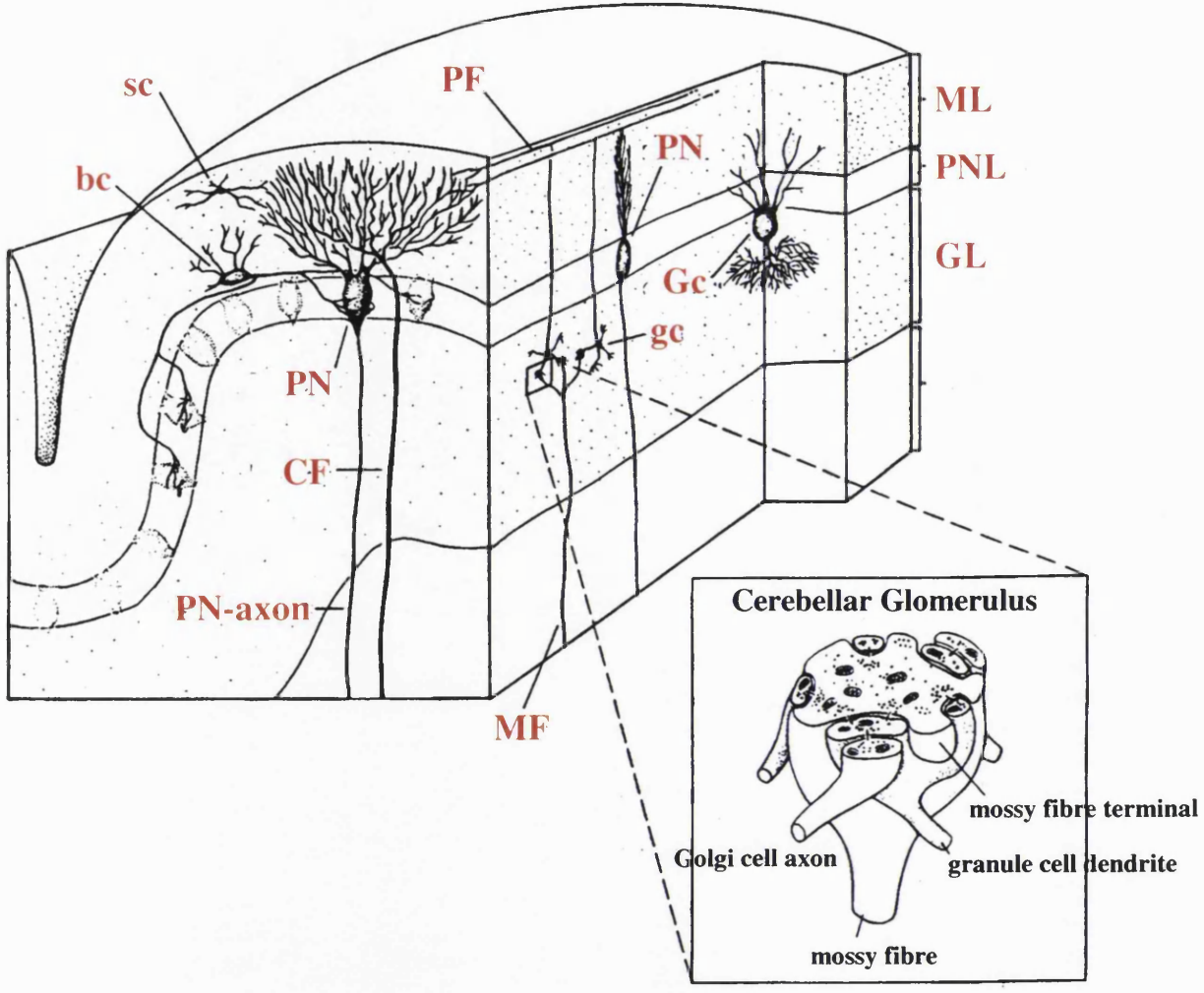

ML – molecular layer
PNL – Purkinje neurones layer
GL – granular layer

PN – Purkinje neurone
sc – stellate cell
bc – basket cell
CF – climbing fibre
PF – parallel fibre
MF – mossy fibre
Gc – Golgi cell
gc – granule cell

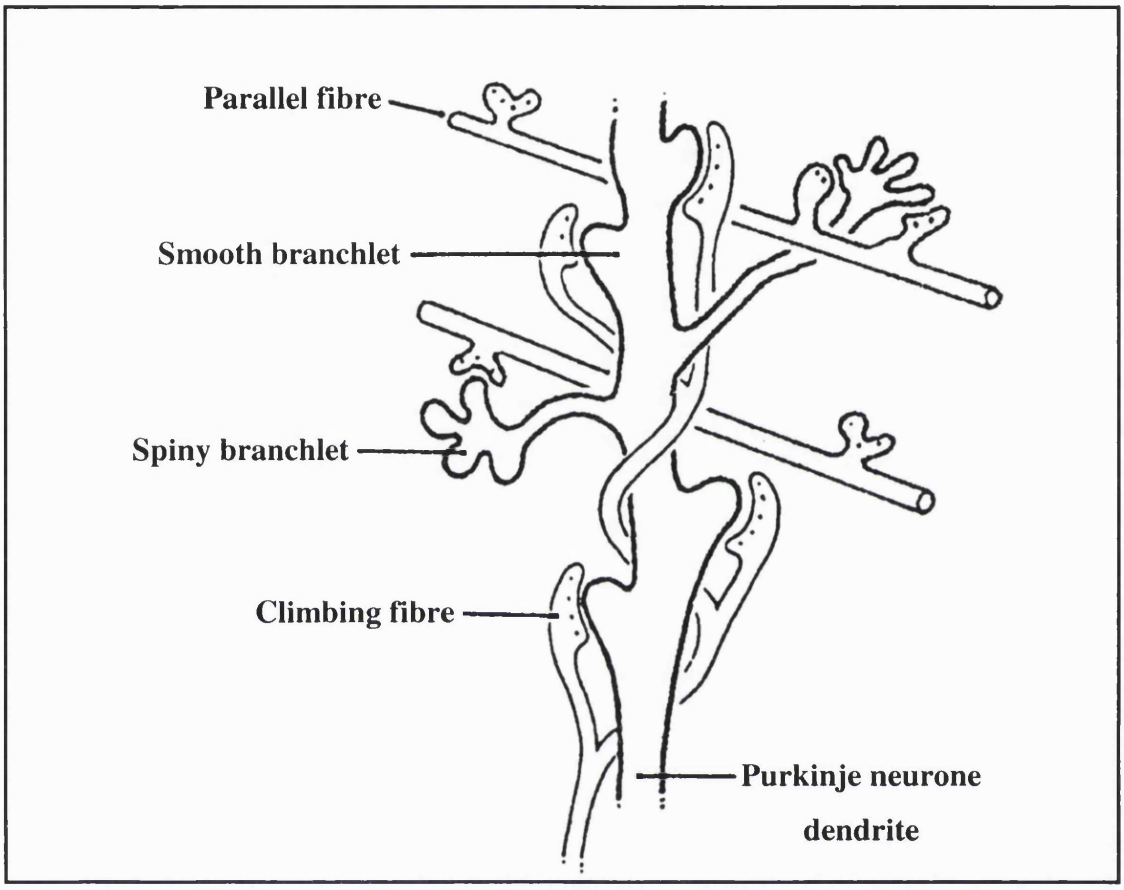

Fig. 1.4. Diagram of climbing and parallel fibre synaptic connections with spiny branchlets of mature Purkinje neurone dendrites. Climbing fibres induce fast depolarisation of the Purkinje neurone by releasing aspartate/glutamate while parallel fibres release glutamate to activate downstream signalling cascades after the initial depolarisation (Haines *et al.*, 1997).

a somewhat larger cell (18-25μm) than the granule cells, termed Golgi cells. They are positioned juxtaposed to the Purkinje cells bodies with dendrites extending primarily into the molecular layer without regard to plane of orientation. Axons of Golgi cells extend back into the granular layer in order to synapse with granule cell dendrites, releasing the neurotransmitter GABA and thus constituting the second GABAergic inhibitory interneurone of the cerebellum.

Molecular layer

The molecular layer contains relatively fewer cell bodies compared to the granular layer but does possess considerably more cell processes. These include parallel fibres (bifurcating from granule cells). Purkinje cell dendrites, Golgi cell dendrites, climbing fibres and processes of cells intrinsic to the molecular layer. The intrinsic cell types of the molecular layer are the remaining interneurones of the cerebellum, stellate and basket cells. Stellate cells are located in outer regions of the molecular layer and are frequently referred to as superficial or outer stellate cells. The extent of dendritic and axonal fields of the stellate cells is limited compared to basket cells, therefore influencing a more compact section of Purkinje neurones in the sagittal plane. As inhibitory interneurones, stellate cells release GABA onto proximal and distal dendrites of the Purkinje neurone directly modulating the excitability of the cell. Basket cells, their name being derived from the 'basket-like' formation of their branched axons round the Purkinje neurone soma, lie directly above the Purkinje cell layer. The axon, from a single basket cell, extends to a multitude of Purkinje neurones causing a far greater area of effect in comparison to the more focal actions of stellate cell stimulation. Therefore, release of GABA from conjunctive activation of both basket and stellate cells induces tight control of the excitability and eventual release of neurotransmitter from the Purkinje neurone, the sole (inhibitory) output of the cerebellum.

Cerebellar afferent fibres

The three types of afferent input to the cerebellum arises from mossy fibres, climbing fibres and multilayered (monoaminergic) fibres.

Mossy fibres originate from cell bodies in the cerebellar nuclei (nucleocortical fibres) and a variety of other nuclei in the spinal cord, medulla and pons. Mossy fibres

branch extensively, and their terminals synapse with other cells at irregular intervals (termed the mossy fibre rosette). The rosette, constituting the central component of the cerebellar glomerulus, gives the fibre a mossy appearance. Each individual mossy fibre may form up to 50 rosettes, where each rosette may synapse with 10 to 15 granule cells in a cerebellar glomerulus. An example of the cerebellar glomerulus is displayed in Fig. 1.3, inset.

Inferior olivary nuclei extend their axons deep into the cerebellar cortex as climbing fibres (CFs) terminating in the molecular layer by entwining with the soma and dendritic branches of Purkinje neurones. Each Purkinje cell receives input from a single climbing fibre, but olivocerebellar axons branch to enlist a multitude of Purkinje neurones. The neurotransmitter glutamate/aspartate is released from climbing fibre axon terminals causing an overall excitation of the downstream Purkinje neurones.

Multilayered fibres (monoaminergic or peptidergic) stem from the hypothalamus (some are histaminergic), the raphe nuclei (serotonergic) and the locus ceruleus (noradrenergic). These afferent inputs enter the cerebellum via the cerebellar peduncles, branching extensively throughout the molecular layer influencing the excitability of intrinsic neurones. Modulation of the cerebellar output, via activation of multilayered fibres, is achieved in two ways. Firstly, they modulate the spontaneous discharge rates of the Purkinje neurone. Secondly, they modulate the responsiveness of the Purkinje neurone to the excitatory afferent inputs from both climbing and mossy fibres. Therefore, during the initial stages of postnatal development (P1-7), at a stage where postsynaptic PN $GABA_ARs$ are present but minimal GABAergic innervation exists (Woodward *et al.*, 1971; Smart, 1992), multilayered fibres may exert indirect inhibitory control of PN excitability thus controlling cerebellar output.

Therefore, the output from the cerebellar cortex is a complex integration of both excitatory and inhibitory afferent input. Feedforward and feedback mechanisms of synaptic circuitry aid in the control of Purkinje neurone output, culminating to produce controlled, 'sculpted' movements of limbs and the maintenance of correct posture.

Mammalian $GABA_A$ receptors

γ-Aminobutyric acid (GABA) is a major inhibitory neurotransmitter found throughout the mammalian central nervous system (CNS). GABA induced activation of the $GABA_A$ receptor plays a pivotal role in the regulation of excitability in a wealth of cell types. Cloning studies have identified $GABA_A$ receptors as members of a channel superfamily that includes nicotinic acetylcholine receptors (AChRs), serotonin-type 3 ($5\text{-}HT_3$) receptors and glycine receptors (GlyRs) (Barnard *et al.*, 1987; Schofield *et al.*, 1987; Unwin, 1993). Mammalian $GABA_A$ receptors are formed from different hetero-oligomeric (pentameric) arrangements of the 16 $GABA_A$ receptor subunits, each approximately 50,000 Daltons in size ($\alpha_{1\text{-}6}$, $\beta_{1\text{-}3}$, $\gamma_{1\text{-}3}$, ε, δ, π, θ) (Burt and Kamatchi, 1991; Davies *et al.*, 1997; Whiting *et al.*, 1997; Hedblom and Kirkness, 1997; Bonnert *et al.*, 1999). The variation in $GABA_A$ receptor subunit composition produces a vast array of functional diversity throughout the mammalian CNS, that is contributed to by alternative exon splicing of the pre-mRNA for the α_6, β_2, β_4, and γ_2 subunits (Whiting *et al.*, 1995). The $GABA_A$ receptor topology consists of a large glycosylated N-terminal extracellular domain, four transmembrane domains (TM1-TM4), a large intracellular region spanning TM3-TM4 (site of protein kinase consensus sequences) and a short extracellular carboxy-terminal region (Fig. 1.5.). The $GABA_A$ receptor is postulated to be a pentameric structure where each TM2 region of the five independent subunits forms part of the ion channel pore through which anions can selectively pass. The existence of channel vestibules in the pore region, with a high positive charge density, is consistent with the theory of an anion-selective channel. In contrast, cation-selective channels have a high negative charge density at the same point on TM2 (Bormann *et al.*, 1987).

To date, controversy still surrounds the actual subunits involved in the preferred pentameric receptor combination. Initial studies identified 2α, 2γ and 1β (Backus *et al.*, 1993) or 2α, 2β and 1γ (Chang *et al.*, 1996) subunits as the preferred pentameric combination. Recent data has suggested that a total of four alternating α and β subunits are linked by a single γ subunit in a pentameric $GABA_A$ receptor assembly (Tretter *et al.*, 1997). The preferred subunit composition of native $GABA_A$ receptors may vary

between different regions of the mammalian brain but generally the $\alpha_1\beta_2\gamma_2$ combination is thought to be representative of the major $GABA_A$ receptor isoform in the CNS (Whiting *et al.*, 1995).

The binding site for GABA is postulated to be on the N-termini of all receptor isoforms determined from site-directed mutagenesis studies (Amin & Weiss, 1993). Of all the $\alpha\beta\gamma$ subunit combinations forming functional receptors, only $\alpha\beta$, $\alpha\beta\gamma$, $\beta_{1/3}\gamma$ and $\beta_{1/3}$ allow transmembrane ion flux (Sigel *et al.*, 1990). The α subunit, in conjunction with mediating GABA affinity, also mediates benzodiazepine (BZ) type pharmacology. The α_1 subunit has a residue on the N-terminus, glycine at position 201, which confers BZ type I pharmacology while the α_3 subunit has a glutamate at the same position, conferring BZ type II pharmacology (Luddens *et al.*, 1995). Differentiation between subunit composition of native $GABA_A$ receptors can be achieved by using subunit-specific benzodiazepines displaying either of the two pharmacologies. The β subunit is involved in a variety of effects ranging from efficient assembly of $GABA_A$ receptor complexes to coupling ligand binding to channel activation acting as a target for numerous drugs (Verdoorn *et al.*, 1990; Sigel *et al.*, 1992). Studies, using recombinant receptors, identified the pivotal role played by the β subunit in cell surface insertion and channel activation of the $GABA_A$ receptor complex (Connolly *et al.*, 1996; Connolly *et al.*, 1999). While it has been well established that the α subunit confers the BZ pharmacology of the $GABA_A$ receptor, incorporation of the γ subunit has an interactive influence on BZ pharmacology and more importantly is required for allosteric modulation of receptor function. $GABA_A$ receptors, containing γ_1 subunits display atypical BZ responses, while receptors containing γ_{2s} subunits display typical native neuronal BZ sensitivity and relative insensitivity to Zn^{2+} (Draguhn *et al.*, 1990; Smart *et al.*, 1991). Co-expression of a γ subunit with α and β subunits has the effect of increasing the unitary conductance of the $GABA_A$ receptor channel (Verdoorn *et al.*, 1991). The existence of multiple subunit isoforms, coupled with the heterogeneous subunit composition of $GABA_A$ receptors, provides the mammalian CNS with a vast array of functionally diverse effects upon $GABA_A$ receptor activation, creating a complex but highly co-ordinated inhibitory neural network.

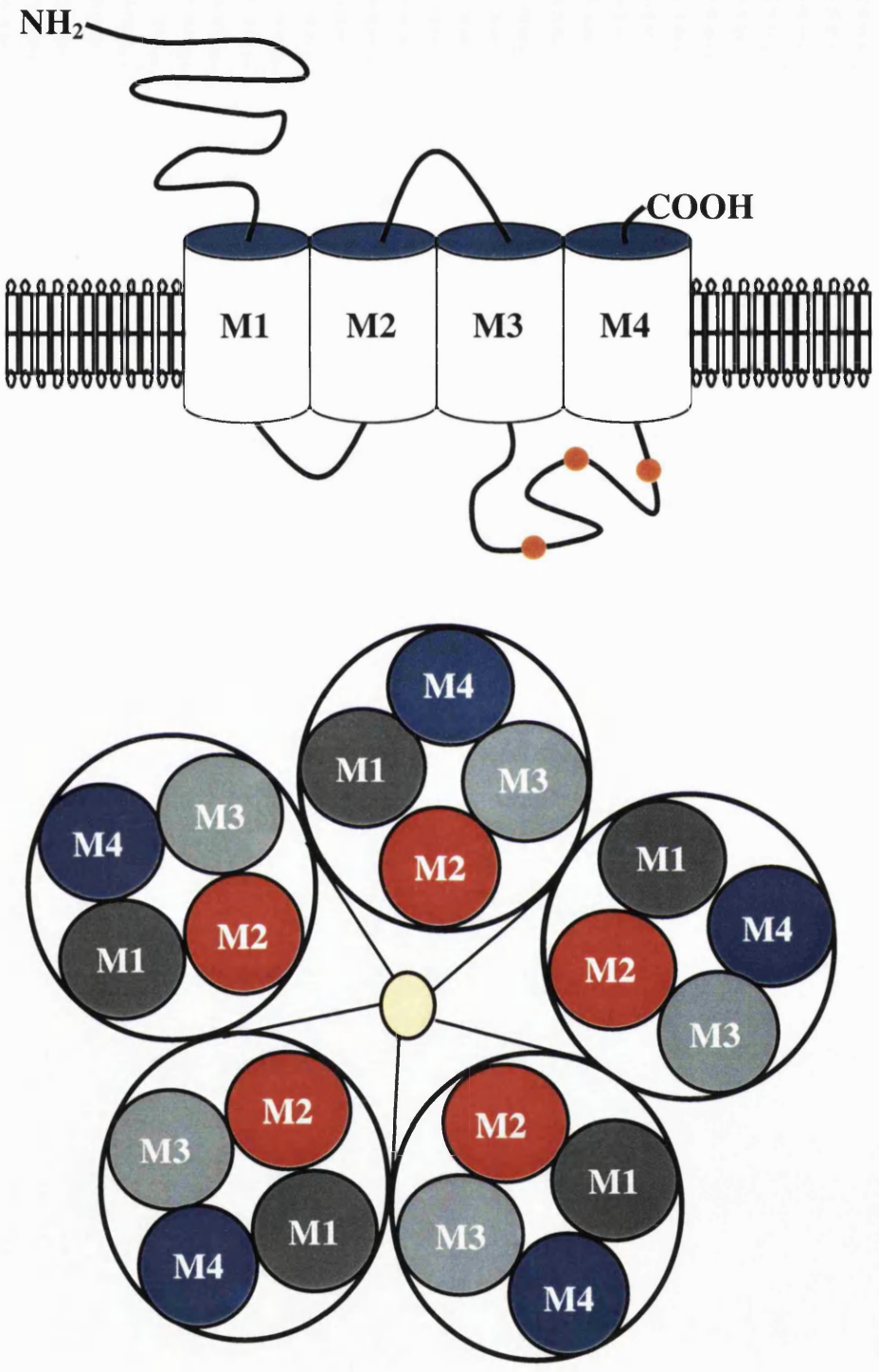

Fig. 1.5. (above) Transmembrane topology of the mammalian $GABA_A$ receptor and (below) putative pentameric subunit arrangement. (●) Putative consensus sites for phosphorylation by protein kinases.

$GABA_A$ receptors in the cerebellum

Work, spanning over quarter of a century, has led to the detailed identification of the $GABA_A$ receptors and GABAergic networks involved in the control and maintenance of neural networks within the cerebellum (Ito , 1984; Somogyi *et al.*, 1989; Llinas and Walton, 1990). Therefore, this brain structure provides a good model for examining and comparing recombinant receptor combinations with known pharmacological profiles of native $GABA_A$ receptors. Elucidation of the reasons for differential expression of $GABA_A$ receptors between different neurones can be attempted due to the relatively simple neuronal network of the cerebellum.

$GABA_A$ receptor expression in Purkinje neurones has been most extensively studied in the rat. *In situ* hybridisation studies identified strong expression of α_1, β_2, β_3 and γ_2 mRNA, where β_2 mRNA levels were in excess of β_3 (Laurie *et al.*, 1992a; Persohn *et al.*, 1992). In addition, spliced subunit-specific oligonucleotides used during *in situ* hybridisation identified γ_{2L} as the abundant γ_2 gene splice variant (Miralles *et al.*, 1994). Immunocytochemical evidence identified the co-localisation of α_1, $\beta_{2/3}$ subunits on both the dendritic shafts and spines of Purkinje neurones (Somogyi *et al.*, 1989) and it is suspected that the γ_{2L} subunit co-localises with the α, β complex (Benke *et al.*, 1991a; Gutierrez *et al.*, 1994). Fritschy and colleagues (1992) used double and triple immunofluorescence to identify the presence of a second α subunit (α_3). According to this group the pattern of α subunit expression revealed α_1 solely in the soma and α_3 present on both the soma and dendrites of mature Purkinje neurones. Therefore, the question still remains whether Purkinje neurones express a single type of receptor in the soma (α_1, β_2/β_3, γ_{2L}) and dendrites (α_3, β_2/β_3, γ_{2L}) or whether the 2α and 2β subunits form heterogeneous $GABA_A$ receptor complexes. The most compelling evidence still suggests that the abundant $GABA_A$ receptor subunit composition is α_1, β_2/β_3, γ_{2L}. Interestingly, light microscopy studies have displayed little β subunit expression (using BD-17 antibody) on the soma of mature Purkinje neurones (Richards *et al.*, 1987; Somogyi *et al.*, 1989; Benke *et al.*, 1991; Gutierrez *et al.*, 1994). Purkinje cell innervation arises from stellate cell activation of dendritic $GABA_A$ receptors in conjunction with innervation of somatic $GABA_A$ receptors by basket cells. Electrophysiological data has identified the occurrence of spontaneously occurring

inhibitory synaptic currents measured after whole-cell patch clamping of the Purkinje neurone soma from slices of juvenile (P11-P17) rat cerebellum (Konnerth *et al.*, 1990). The variability in size and frequency of $GABA_A$ receptor-mediated currents suggests the involvement of an array of basket cells which form a variety of synapses with differing synaptic strengths (Konnerth *et al.*, 1990). Llano and colleagues (1988) and Smart (1992) identified multiple conductance states of $GABA_A$ receptors (28-30pS) by recording from outside-out patches of Purkinje cell soma and these conductance states are comparable to that of recombinant α_1, β_2, γ_2 channels (Verdoon *et al.*, 1990). The discrepancy between low level β subunit immunofluorescence and the definitive electrophysiological data identifying the existence of β subunit containing synapses was only resolved at the electron microscopic level. Analysis, at this resolution, identified the existence of α, $\beta_{2/3}$ subunits co-localising at the basket cell-Purkinje soma synapse (Somogyi *et al.*, 1989).

The molecular layer contains a significant number of $GABA_A$ receptors and these are located on both basket and stellate cells. *In situ* hybridisation has identified that these neurones express α_1, β_2, γ_2 subunits with equal amounts of γ_{2L} and γ_{2S} (Laurie *et al.*, 1992a; Persohn *et al.*, 1992; Miralles *et al.*, 1994). Low level amounts of α_3 mRNA has been detected in the molecular layer, although the signal is too weak to identify the loci of expression (Laurie *et al.*, 1992a). The possibility remains that stellate and basket cells express α_3 containing receptors but this signal could be derived from Golgi cells or the dendritic arbour of Purkinje neurones. Llano and Gerschenfeld (1993) determined the single channel conductances of rat stellate cells as 28pS, which is comparable to both Purkinje neurone and recombinant $GABA_A$ receptors which contain α_1, β_2, γ_2 subunits.

The pharmacological profile of $GABA_A$ receptors in Purkinje neurones and molecular layer interneurones further compounds the evidence for $GABA_A$ receptors containing α_1, β_2/β_3, γ_{2L} subunits. In the rodent, the majority of BZ binding sites in the molecular layer selectively bind β-carbolines, CL 218 872 and zolpidem and are therefore designated BZ type I (Faull *et al.*, 1987; Niddam *et al.*, 1987; Olsen *et al.*, 1990; Bureau and Olsen, 1993). Electrophysiological data displaying dissociated rat Purkinje neurones as having BZ I type pharmacology concurs with the previous binding

data and reveals an abundance of α_1, β_2/β_3, γ_{2L} subunit containing $GABA_A$ receptors (Yakushiji *et al.*, 1993). As previously mentioned the inclusion of γ_2 subunit confers Zn^{2+} relative insensitivity on α_1, β, γ_2 receptors (Draguhn *et al.*, 1990; Smart *et al.*, 1991). Co-application of 10μM Zn^{2+} and 1μM GABA had no effect on the GABA mediated currents recorded from cultured Purkinje neurones (Zempel and Steinbach, 1995). The wealth of evidence surrounding the expression of only α, β, γ_2 containing $GABA_A$ receptors provides a simplistic inhibitory network in which to evaluate the role of these subunits in neuronal activity.

Interestingly, Purkinje neurones at the point of birth (P0) possess functional $GABA_A$ receptors even though GABAergic innervation does not occur until P7 (Woodward *et al.*, 1971; Smart, 1992). Evidence displaying the presence of α_1, β_2, γ_2 mRNA in Purkinje neurones at birth concurs with the observations of functional $GABA_A$ receptors being present at this early stage. Subunit mRNA levels accumulate postnatally through the first few weeks reaching an equilibrium at P21 (Zdilat *et al.*, 1991, 1992; Laurie *et al.*, 1992b; Luntz-Leydman *et al.*, 1993). Innervation to the Purkinje neurone, if compromised, does not seem to affect the expression or function of native $GABA_A$ receptors. In the *reeler* mutant cerebellum, resulting in a defect of cell migration, granule cell and basket cell innervation is lost while Golgi cells and mossy fibres induce heterologous synaptic activation. In this situation the Purkinje neurone $GABA_A$ receptor subunit composition is unperturbed (Frostholm *et al.*, 1991). A mutation causing the failure of granule cells to migrate from the external to internal layers during the early stages of development termed *weaver* cerebellum, results in a removal of this type of excitatory input. Although this may in fact compromise the development of the mature Purkinje neurone they still express α_1, β_2, γ_2 subunits (β_3 subunit levels were not analysed) (Beattie *et al.*, 1995). Therefore, the $GABA_A$ receptor subunit expression seems to be largely "hard wired" into the Purkinje neurone differentiation program irrespective of excitatory or inhibitory synaptic activation (Wisden *et al.*, 1996)

Cerebellar granule cells possess a somewhat more extensive range of $GABA_AR$ subunits throughout development when compared to PNs. Initially, granule cells contain an abundance of Bz sensitive $GABA_ARs$ most likely containing α_1, α_2, α_3, $\beta_{2/3}$ and γ_2

subunits. During development there is a substantial increase in the expression levels of the α_1, α_6, β_2, β_3, γ_2 and δ subunits, while the expression levels of α_2 and α_3 are down-regulated. At this stage $GABA_A$Rs become increasing less sensitive to Bz agonists most likely as a result of the incorporation of α_6 into the receptor complexes. As with the subunit gene expression in PNs, granule cells seem to possess an intrinsic "hard wired" subunit gene expression programme, which in the case of cultured granule cells, can be altered to various degrees by environmental influences (Wisden *et al.*, 1996).

$GABA_A$ receptor subunit phosphorylation

$GABA_A$ receptor phosphorylation occurs on the large intracellular domains between TM3 and TM4 of both β and γ subunits as they contain consensus sites for serine (S) / threonine (T) and tyrosine (Y) protein kinases. A summary of subunit consensus sites within the major intracellular domains is displayed in Table 1.1.

Table 1.1. $GABA_A$R subunit protein kinase consensus sites.

Subunit	Consensus site	Kinase
β1	S409	PKA, CaMKII, PKG, PKC
β2	S410	PKA, CaMKII, PKG, PKC
β3	S408/S409	PKA, CaMKII, PKG, PKC
γ1	Y372/Y374	PDGF receptor, src
γ2L/γ2S	S327	PKA, PKC, CaMKII
γ2L/γ2S	S343/S349	PKA, PKC, CaMKII, PKG
γ2L/γ2S	Y365/Y367	PDGF receptor, src
γ2L	S353	PKA, PKC, CaMKII
γ3	T333	PKA, PKC, PKG, CaMKII

(modified from Moss & Smart, 1996)

Functional significance of $GABA_A$ receptor phosphorylation

As with many of the protein kinases, protein kinase A (PKA) phosphorylation of $GABA_A$ receptors has been extensively studied with contrasting results. Application of vasoactive intestinal peptide (VIP) and noradrenaline (NA) to retinal and cerebellar Purkinje cells respectively, causes an enhancement in $GABA_A$ receptor mediated responses (Veruki and Yeh, 1992, 1994; Parfitt *et al.*, 1990). Therefore, enhancement of

PKA activity leads to the phosphorylation of $GABA_A$ receptors and an upregulation in GABAergic responses. In contrast, PKA induces $GABA_A$ receptor desensitisation and decreases receptor activation in cortical and spinal neurones and synaptoneurosomes (Harrsion and Lambert, 1989; Heuschneider and Schwartz 1989; Tehrani *et al.*, 1989; Porter *et al.*, 1990; Schwartz *et al.*, 1991; White *et al.*, 1992). The contrasting results probably reflect the subunit heterogeneity of $GABA_A$ receptors differentially regulated by PKA phosphorylation. One major drawback of utilising drugs that stimulate PKA mediated phosphorylation (e.g. forskolin) are that these hydrophobic drugs themselves have direct effects on the $GABA_A$ receptor which are independent of phosphorylation (Leidenheimer *et al.*, 1991). Phosphorylation induced by intracellular dialysis of the catalytic subunit of PKA or with cAMP provides the only strategy to circumvent the inherent problems associated with the use of membrane permeable second messengers. Recombinant receptor studies on receptors composed of α_1, β_1 or α_1, β_1, γ_{2s}, expressed in HEK cells, identified the serine residue at position 409 on the β_1 subunits as the phosphorylation site inducing the time-dependent decrease of $GABA_A$ receptor-mediated currents (Moss *et al.*, 1992). Similar studies, using the catalytic subunit of PKA, have demonstrated comparable modulation of the $GABA_A$ receptor in cultured superior cervical ganglia (SCG), spinal cord neurones and cerebellar granule cells (Porter *et al.*, 1990; Moss *et al.*, 1992; Robello *et al.*, 1993). Interestingly, the effects of PKA phosphorylation can have the opposite effects in neuronal preparations. Application of cAMP analogues can mimic the enhancement of GABA-mediated currents seen with the application of NA and can be completely abolished by the application of the specific PKA inhibitor (PKIP) (Kano and Konnerth, 1992). Depolarisation of the Purkinje neurone after climbing fibre activation, results in a rise in the intracellular calcium concentration inducing a similar enhancement of $GABA_A$ receptor function (Kano *et al.*, 1992). The reasons for differential regulation of $GABA_A$ receptor function within these different preparations by PKA might be accounted for by the type of β subunit present in the majority of expressed $GABA_A$ receptors. Recent work by McDonald and colleagues (1998) demonstrated that the function of β_1 subunit containing $GABA_A$ receptors were inhibited; β_2 subunit containing receptors were

unaffected and β_3 subunit containing receptors were enhanced by PKA-induced phosphorylation.

Activation of protein kinase C (PKC) using phorbol esters results in a significant inhibition of GABA-mediated whole-cell currents. Recombinant $GABA_A$ receptors composed of α_{1-5}, β_{1-2}, γ_2 subunits all display a marked inhibition after phosphorylation by PKC (Sigel *et al.*, 1991; Leidenheimer *et al.*, 1992, 1993) and this inhibition persists irrespective of the presence of γ_{2L} or γ_{2S} subunits. The residues identified as putative PKC phosphorylation sites are S409 within the β_1 subunit, S327 in both γ_{2L}/γ_{2S} subunits and S343 within the γ_{2L} subunit (Kellenberger *et al.*, 1992; Krishek *et al.*, 1994). Recent evidence has identified the role of PKC phosphorylation in the inhibition of synaptic $GABA_A$ responses in hippocampal CA1 neurones. Inclusion of PKCI (specific peptide PKC inhibitor) causes a marked enhancement of $GABA_A$-mediated inhibitory postsynaptic potentials (Weiner *et al.* 1994). Therefore, PKC phosphorylation, unlike the differential effects of PKA, seems to play a predominantly inhibitory role in the mammalian CNS. However there are some reports of PKC induced enhancement in $GABA_A$ receptor function (Lin *et al.*, 1994) although this is difficult to reconcile with the more recent studies demonstrating that PKC can cause $GABA_A$ receptor internalisation (Bueno *et al.*, 1998; Connolly *et al.*, 1999).

Interestingly, the functional effects of the two remaining serine/threonine kinases (cGMP-dependent protein kinase (PKG) and Ca^{2+}/calmodulin-dependent protein kinase II (CaMKII)) are poorly understood. $GABA_A$ receptor-mediated currents are inhibited by cGMP in neurones from the nucleus of the tractus solitarius (Glaum and Miller, 1993). Ca^{2+} induced activation of CaMKII has differential effects depending upon the neuronal population being studied (Stelzer, 1992). The induction of rebound potentiation of $GABA_A$-mediated currents in rat cerebellar Purkinje neurones requires the activation of CaMKII during the induction stimulus (Kano *et al.*, 1996). Phosphorylation of $GABA_A$ receptor subunits by CaMKII causes the potentiation of inhibitory synaptic currents but the specific sites of phosphorylation still remain unresolved (Wang *et al.*, 1995).

The role of tyrosine phosphorylation of $GABA_A$ receptors has received an increasing amount of attention in the past decade. Two tyrosine residues on the γ_{2L}

subunit, Y365 and Y367, have been identified as the major substrates for the tyrosine kinase, src, in $GABA_A$ receptors composed of α_1, β_1, γ_{2L} subunits. Phosphorylation induces a significant enhancement of GABA-induced currents in HEK cells (Moss *et al.*, 1995; Valenzuela *et al.*, 1995; Wan *et al.*, 1997). Neuronal $GABA_A$ receptors are also modulated by tyrosine phosphorylation. A significant reduction in $GABA_A$ receptor mediated whole-cell currents is observed with the addition of tyrosine kinase inhibitors while enhancements are seen with the addition of tyrosine phosphatase inhibitors (Moss *et al.*, 1995). Increases in mean open time and probability of channel opening are the mechanisms underlying tyrosine kinase induced enhancement of $GABA_A$ receptor function. Recent evidence has suggested a link between the activation of Src via TrkB and mGluR1-mediated pathways in cerebellar Purkinje neurones. Phosphorylation mediated by the non-receptor tyrosine kinase, Src, led to a 39% increase in the mean mIPSC amplitude suggesting a role for tyrosine kinase phosphorylation in the modulation of GABAergic synapses in Purkinje neurones (Boxall, 2000).

The functional significance of $GABA_A$ receptor phosphorylation at the synaptic level still remains to be fully understood. Evaluation of the specific roles played by individual and coincident subunit phosphorylation may aid in the identification of specific protein kinases underlying differential cellular functions such as rebound potentiation.

Metabotropic glutamate receptors

Classification: Structure and function

Metabotropic glutamate receptors (mGluRs) are G-protein coupled receptors (GPCRs), classified into three different groups depending upon their receptor pharmacology (Schoepp *et al.*, 1990; Nakanishi, 1992; Schoepp & Conn, 1993; Conn & Pin, 1997; Schoepp *et al.*, 1999; Cartmell & Schoepp, 2000). The various mGluR groupings are shown in Fig. 1.6. There is around 70% homology within a group and approximately 30% homology between different groupings. Surprisingly, GluRs show no sequence homology with other GPCRs. All mGluRs posses a large extracellular amino-terminal domain, 7 transmembrane domains which are separated by short intra- and extracellular loops and a variable length intracellular carboxyl-terminal domain. Nineteen separate cysteine residues, on predicted extracellular domains and loops, are conserved throughout all classifications of mGluRs suggesting a putative role in receptor structure or intramolecular transduction.

Fig. 1.6. Diagram of mGluRs: Classification, homology and major transduction pathways

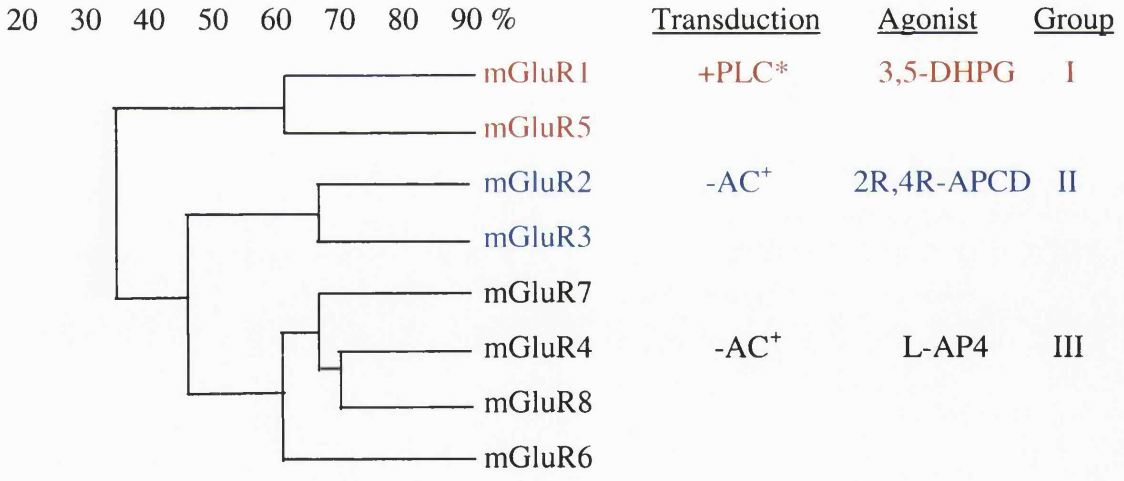

PLC* - phospholipase C & AC^+ /AC^+ - adenylate cyclase

Identification, by O'Hara and co-workers (1993) identified a weak sequence similarity of the extracellular domain of mGluRs with bacterial periplasmic binding proteins (PBP), especially with the leucine, isoleucine, valine binding protein (LIVBP). A model based on previously reported three-dimensional structures of several PBPs was constructed for the agonist-binding region of mGluRs consisting of two globular domains incorporating a hinge region. This model allowed the identification of two residues, S165 and T188, thought to underlie the glutamate binding site. Mutations of these specific residues in mGluR1 resulted in changes in glutamate affinity (O'Hara *et al.*, 1993).

G-protein coupling has been extensively studied for many GPCRs and the N-terminal end of the second intracellular loop (I2) has been identified as playing a pivotal role in G-protein coupling and activation (Savarese and Fraser, 1992; Ostrowski *et al.*, 1992). Specificity of GPCRs for specific G-proteins is conferred by the third intracellular loop, particularly the interaction with the α subunit of the G-protein complex (Liu *et al.*, 1995). Interestingly, the DRY signature is omitted from any of the mGluR intracellular loops whilst the third intracellular loop (I3) is conserved throughout all members of the mGluR family making this site unlikely to play a major role in G-protein selectivity. Studies using chimeras of different mGluRs has identified the second intracellular loop as mediating G-protein selectivity (Pin *et al.*, 1994; Gomeza *et al.*, 1996). Therefore, it seems evident that I2 of mGluRs plays a role comparative to that of I3 in most other GPCRs. The large (300 amino acid) carboxy-terminal domain, proposed to facilitate the coupling of G-proteins to the receptor complex (Pin *et al.*, 1992; Pickering *et al.*, 1993; Gabellini *et al.*, 1993; Prezeau *et al.*, 1996), may have a conjunctive role of targeting the receptor to specific compartments in neurones (Pin and Bockaert, 1995). This domain also contains a multitude of serine and threonine residues that could potentially be sites for interaction with GPCR kinases (GRK) (Alaluf *et al.*, 1995). Phosphorylation at these sites and the various SH3 binding sites could potentially regulate the overall activity of the mGluRs and subsequent activation of downstream signalling cascades.

Purkinje neurone mGluR receptors

Cerebellar Purkinje neurones have been shown to express high levels of mRNA (Fotuhi *et al.*, 1993; Masu *et al.*, 1991) and protein (Baude *et al.*, 1993; Fotuhi *et al.*, 1993; Hampson *et al.*, 1994; Martin *et al.*, 1992; Nusser *et al.*, 1994; Shigemoto *et al.*1994) for $mGluR_{1/1a}$ and $mGluR_{1b}$ (Mateos *et al.*, 2000). Subcellular distributions of both $mGluR_{1a}$ and $mGluR_{1b}$ were reported to be similar each having a predominantly perisynaptic localisation (Mateos *et al.*, 2000). To date, mRNA for other mGluR subtypes ($mGluR_2$, $mGluR_3$, $mGluR_4$, $mGluR_5$ $mGluR_6$ and $mGluR_8$) has not been detected in Purkinje neurones (Abe *et al.*, 1992; Duvoisin *et al.*, 1995; Nakajima *et al.*, 1993; Nakanishi 1992; Ohishi *et al.*, 1993; Tanabe *et al.*, 1993). This group 1 mGluR is coupled to the phospholipase C_β pathway via the G-protein, $G_{q/11}$ and stimulates the hydrolysis of membrane phospholipids into inositol trisphosphate (InsP3) and diacylglycerol (DAG) (Bockaert *et al.* 1993). InsP3 binds to $InsP_3$ receptors on the endoplasmic reticulum (ER) of Purkinje neurones, causing the 'all-or-none' wave release of calcium into the cytoplasm. The consequent rise in intracellular Ca^{2+} ($[Ca^{2+}]_i$) has been proposed to be a crucial step in the induction of cerebellar synaptic plasticity such as long-term depression and rebound potentiation (Linden *et al.*, 1991; Shigemoto *et al.*, 1994; Llano *et al.*, 1991; Kano *et al.*, 1992), and may underlie the process of motor learning within the cerebellum. The localisation of postsynaptic $mGluR_1$ and $mGluR_5$ receptors seems to be under the regulation of a family of "Homer" proteins which contain "postsynaptic density zone-like" protein-interaction domains (Brakeman *et al.*, 1997). The Homer family selectively binds $mGluR_1$ and $mGluR_5$ regulating the position of these receptor subtypes with respect to their second messenger pathways ($InsP_3$ and DAG) in the postsynaptic neurone (Ciruela *et al.*, 1999; Worley, 1999).

Presynaptic mGluRs: Regulation of neurotransmitter release

Immunoperoxidase localisation studies have aided in the identification of sites of mGluR expression within the mammalian brain. The majority of studies investigating group 1 mGluR expression have identified a postsynaptic locus of expression (Fig. 1.8), where most staining occurs at sites distant from active release zones (Martin *et al.*, 1992; Baude *et al.*, 1993; Nusser *et al.*, 1994; Lujan *et al.*, 1996, 1997). Using similar techniques group II mGluRs have been identified in both presynaptic (Shigemoto *et al.*,

1997) and postsynaptic densities (concentrated at the periphery) in the hippocampus (Petralia *et al.*, 1996). One interesting finding is that, unlike group II mGluRs, group III mGluRs are located solely at presynaptic sites and are abundant in or close to active zones (Shigemoto *et al.*, 1997) (Fig. 1.8). Differential expression of group III mGluRs is displayed within the hippocampus where immunoreactivity for $mGluR_7$ is localised exclusively at glutamatergic terminals while the splice-variant $mGluR_{4a}$ is located at both glutamatergic and non-glutamatergic synapses (Bradley *et al.*, 1996). The differential loci of mGluR subtype expression may underlie the physiological roles played by each subtype. The comparatively high potency of glutamate (3-40μM) at $mGluR_4$ receptors identifies a role for this subtype in activation by glutamate spilling over following release from adjacent glutamatergic synapses. Their perisynaptic location, coupled with their presence on non-glutamatergic synapses, leads to the hypothesis that $mGluR_4$ subtypes may form presynaptic heteroreceptors, leading to the modulation of neurotransmitter release. This hypothesis also applies to presynaptic group II mGluRs displaying perisynaptic localisation. Glutamate is a highly potent agonist at group II receptors (displaying EC_{50} values of 0.3-20μM) but preterminal localisation of $mGluR_2$ receptors at the hippocampal mossy fibre synapse would predict that the receptor would only be activated under conditions of high neurotransmitter release (Yokoi *et al.*, 1996). The distinct lack of $mGluR_7$ receptors on non-glutamatergic terminals is expected, as it is unlikely that the "spillover" glutamate concentration would rise to such an extent so as to activate this receptor subtype (EC_{50} for glutamate >500μM). Therefore, it is possible that perisynaptic mGluR receptors are inactive under normal physiological conditions only being activated after intense neurotransmitter release (Scanziani *et al.*, 1997).

A high level of expression of mGluRs has been identified at glutamatergic synapses throughout the CNS, implying an important role in the modulation of glutamate release. All three mGluR groups have displayed a negative modulation of transmitter release at specific synapses. The negative modulatory effect of selective group II agonist DCG-IV in the medial (Kilbride *et al.*, 1998) and lateral (Bushell *et al.*, 1996) perforant path of the dentate gyrus, striatum (Lovinger and McCool., 1995), olfactory bulb (Hayashi *et al.*, 1993), cerebellum (Glitsch *et al.*, 1996) and spinal cord

Fig. 1.7. Agonist and antagonist structures for mGluR group I, II & III.

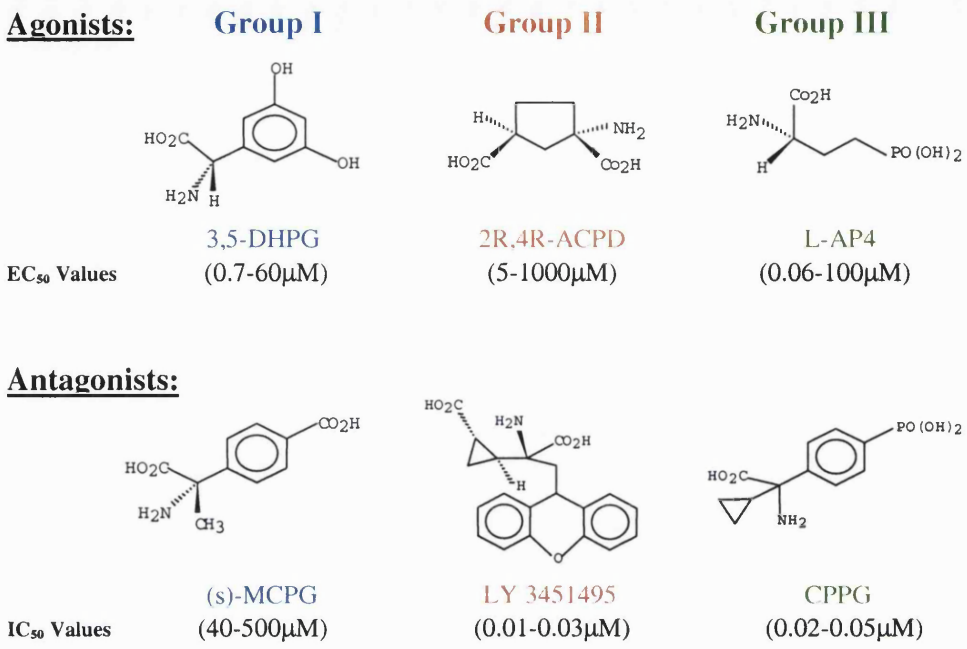

Fig. 1.8. Putative localisation of metabotropic glutamate receptors at a theoretical CNS synapse

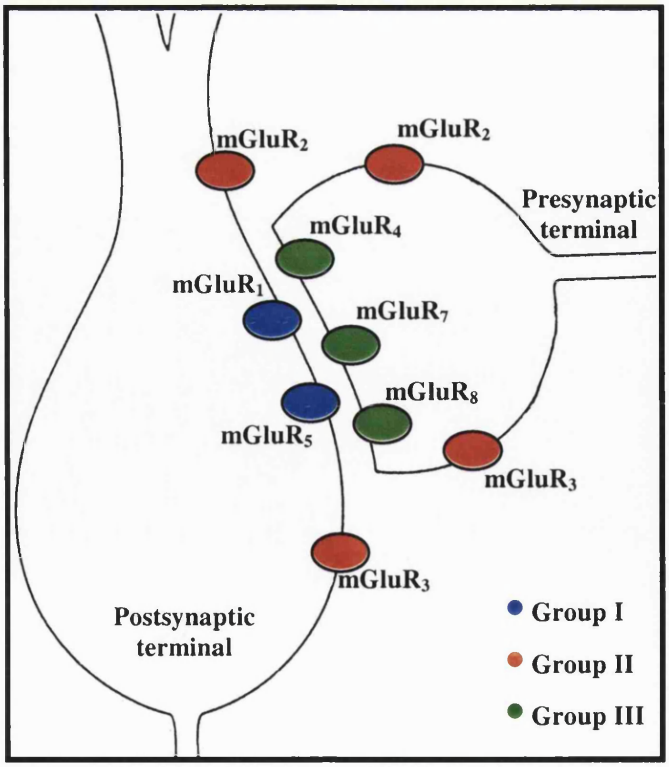

motorneurones (Ishida *et al.*, 1993) has been well established. Application of the group III selective agonist, L-AP4, produced similar effects on glutamatergic release in the hippocampal CA1 region (Baskys and Malenka, 1991; Gereau and conn, 1995), the medial and lateral perforant path of the dentate gyrus (Koerner and Cotman, 1981), striatum (Pisani *et al.*, 1997) and olfactory bulb (Trombley and Westbrook, 1992). Interestingly, electrophysiological studies have identified a negative modulatory role for group I mGluRs in the CA1 region of the hippocampus (Baskys and Malenka, 1991; Gereau and Conn, 1995; Manzoni and Bockaert, 1995). These findings are contrary to the belief that group I mGluRs are located exclusively at postsynaptic sites and may possibly have a role in both positive and negative modulation of glutamate release in the mammalian CNS.

Presynaptic modulation of neurotransmitter release, via mGluRs, is by no means restricted to glutamatergic synapses. Increasing evidence suggests that presynaptic mGluRs have a role in modulating the release of a wealth of different neurotransmitters throughout the brain. Electrophysiological reports suggest that mGluRs regulate the release of GABA from interneurones of the hippocampus, cerebellum, thalamus and olfactory bulb. Initial studies involved the use of the non-specific agonist 1S,3R-ACPD and its ability to reduce the amplitude of GABA-mediated inhibitory postsynaptic currents in the CA1 region of the hippocampus (Liu *et al.*, 1993; Jouvenceau *et al.*, 1995) and in the cerebellum (Llano and Marty, 1995). In the latter case, the application of t-ACPD induced effects was deemed to be due to two independent modes of action. First, t-ACPD altered the intrinsic firing rate of interneurones, presumed to be due to an action on somatic conductance mechanisms. Second, was a decrease in the efficacy of both interneurone-interneurone and interneurone-Purkinje neurone synapses, deemed to be an action on the vesicle release machinery of the GABAergic terminal.

Therefore, further identification of presynaptic mGluR subtypes and their resultant effects on endogenous neurotransmitter release, will aid in the understanding of the role played by mGluRs in maintaining/modulating neurotransmission in the mammalian CNS.

N-methyl-D-aspartate receptors

Ionotropic glutamate receptors are ligand-gated ion channels that mediate the vast majority of excitatory neurotransmission in the brain. N-methyl-D-aspartate (NMDA) receptors allow the influx of calcium into neurones, facilitating in the induction of higher order processes such as learning and memory (Asztely and Gustafsson, 1996) and in a variety of neurological disorders including epilepsy and ischaemic brain damage. In recent years, a tentative link between excessive NMDA receptor activation and neurodegenerative disorders such as Parkinson's and Alzheimer's diseases, Huntington's chorea and amyotrophic lateral sclerosis, has been forged (Kornhuber & Weller, 1997; Sonsalla *et al.*, 1998; Loopuijt & Schmidt, 1998).

Sequence similarities within the NMDA receptor family have led to the identification of 3 gene families encoding separate receptor subunits, termed NR1, NR2 and NR3 respectively. The subunit families of NR1, NR2 and NR3 all possess splice variants (Sun *et al.*, 1998; Winkler *et al.*, 1999) The NR1 subunits can form homomeric receptors whereas NR2 subunits cannot, requiring the co-expression with NR1 subunits for the formation of functional receptors (Dingledine *et al.*, 1999).

Receptor structure, subunit stoichiometry and ligand binding site

Resolution of the NMDA receptor subunit structure identified a topology somewhat different to $GABA_A$ and nAChR subunits. Individual subunits possessed only three transmembrane domains (M1, M3 and M4, Fig. 1.9), contrary to the expected topology of four transmembrane domains of nAChR (M1-M4). A re-entrant membrane loop facing the cytoplasm substitutes for the missing M2 transmembrane domain producing the atypical subunit structure. The identification of the re-entrant loop arises from the pattern of accessibility, from both sides of the membrane, of charged sulfhydryl reagents to cysteines substituted by mutagenisis for M2 residues (Kuner *et al.*, 1996). Each subunit possesses a large, extracellular N-terminal domain with various glycosylation sites and a shorter intracellular C-terminal tail. The NMDA receptor agonist binding site, typical of glutamate receptors, is composed of a conserved amino acid-binding pocket. This pocket formation consists of two globular domains (S1 and S2, Fig. 1.9) encompassing sequences adjacent to the M1 and the M3-M4 loop,

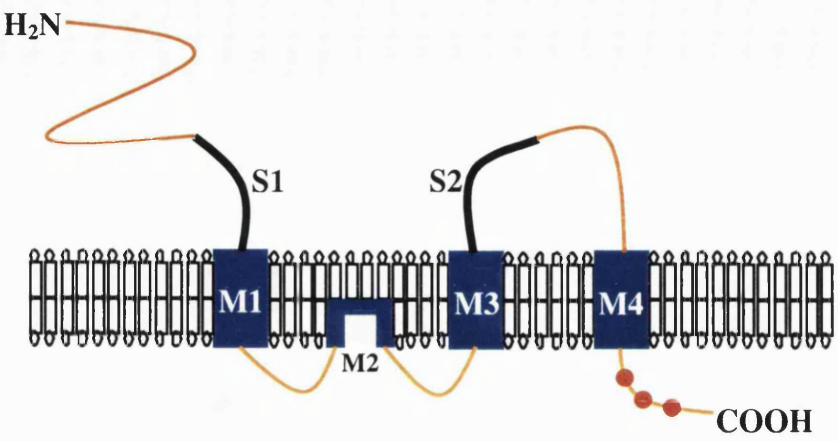

Fig. 1.9. Putative structure of NMDA receptor subunits. Subunit consists of 3 transmembrane spanning domains (M1, M3 & M4); 1 re-entrant loop (M2) and 2 ligand binding domains (S1 & S2). (●) Putative consensus sites for phosphorylation by protein kinases.

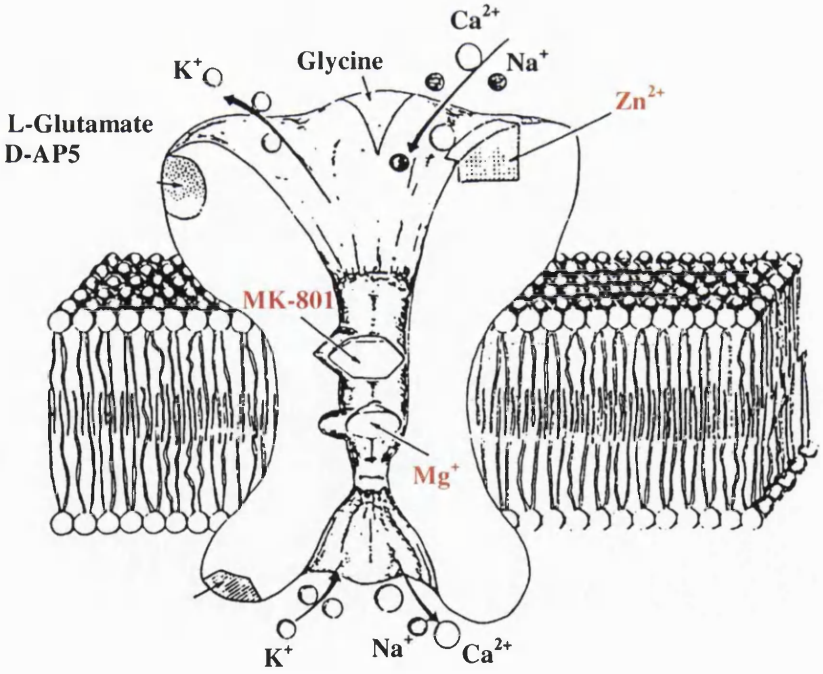

Fig. 1.10. Schematic representation of the NMDA receptor ion channel and ligand binding sites (modified from Wong and Kemp, 1991).

respectively (Stern-Bach *et al.*, 1994; Kuusinen *et al.*, 1995; Arvola and Keinanen, 1996). These and similar findings support the idea that NMDA receptor subunits are modular, consisting of a pore-forming domain and two separate domains that form a single agonist binding site. The N-terminal 400 amino acids seem devoid of function with respect to ligand binding, but may however, play a functional role in NMDA receptor modulation. Speculation as to the induction of channel opening, after agonist binding, has led to the hypothesis that closure of the S1 and S2 lobes may place a torque on the receptor. This conformational change may be transmitted to the channel region, facilitating in the uncovering of the channel pore region itself and propelling the receptor from a 'closed' state to that of an 'open' state (Dingledine *et al.*, 1999).

In order to attain the full 'open' state of the NMDA receptor, binding of glutamate and the co-agonist glycine is required (Johnson & Ascher, 1987). Analysis of NR1 and NR2 mutants has led to the assumption that glutamate binds exclusively to the NR2 subunit while glycine (co-agonist) binds exclusively to NR1 subunits (Kuryatov *et al.*, 1994; Hirai *et al.*, 1996; Laube *et al.*, 1997; Anson *et al.*, 1998). Early work on NMDA receptor stoichiometry favoured a pentameric structure for all glutamate receptors, based on evaluation of the size of cross-linked NMDA receptor protein (Brose *et al.*, 1993) or functional analysis of combinations of native and mutant subunits possessing differential sensitivity to channel blockers (e.g. Ferrer-Monteil and Montal, 1996). Premkumar and Auerbach (1997) used single channel analysis of native and recombinant subunits to infer a pentameric stoichiometry for NMDA receptors, consisting of three NR1 and two NR2 subunits. Previous to these findings Behe and colleagues (1995) concluded that the receptor structure consisted of a more basic tetrameric structure consisting of two NR1 and two NR2. Rosemund and colleagues (1998) and concurrent studies, identifying the similarity of potassium channels (Doyle *et al.*, 1998) or cyclic nucleotide-gated channels (Liu *et al.*, 1996) to the proposed subunit stoichiometry of the NMDA receptor, corroborated these early findings. Therefore, it remains relatively unclear as to the exact subunit composition of native NMDA receptors with a spilt between tetra- and pentameric structure. The advent of physical methods, with which to unequivocally determine the number of subunits in a functional NMDA receptor, will aid in the understanding of NMDA receptor structure and function. Immunoprecipitation studies have aided in the identification of subunits

coexisting in native NMDA receptor complexes. Immunoprecipitation strategies have identified NR1 and NR2B subunits coexisting in mammalian brain extracts (Sheng *et al.*, 1994; Blahos and Wenthold, 1996; Luo *et al.*, 1997; Chazot and Stephenson, 1997) and NR1 with either NR2A or NR2B (Dunah *et al.*, 1998).

NMDA receptor phosphorylation

Phosphorylation plays an important regulatory role in ion channel function and has been implicated in the induction of synaptic plasticity. Phosphorylation serves to enhance or potentiate the response to agonist binding in order to facilitate in the activation of downstream signal transduction pathways. NMDA receptors can be phosphorylated on serine/threonine residues by PKA, PKC and CaMKII, causing an enhancement of receptor function. Dephosphorylation by Calcium/calmodulin-dependent phosphatase, calcineurin, results in an inhibition of NMDA receptor function (Lieberman and Mody, 1994). In the mammalian brain, between 10 and 70% of NR1 and NR2 subunits seem to be phosphorylated at one or more sites by PKA and PKC. The variation in receptor phosphorylation provides a substantial level of molecular and functional heterogeneity within the NMDA receptor population (Leonard and Hell, 1997). PKC activation serves to enhance NMDA receptor function and has been observed in several different neuronal preparations (Moss & Smart, 1996). Parameters affected by PKC phosphorylation include an increase in open probability in conjunction with a decrease in the affinity for extracellular magnesium (Chen and Huang, 1992). Although the effects of PKC phosphorylation are profound, the underlying mechanisms of action are unknown. Zheng and Sigworth (1997) identified an amplification of PKC phosphorylation of NMDA receptors due to calcium influx through the receptor itself. This finding identifies a role by which NMDA receptor activation itself provides a positive feedback mechanism to facilitate the activation of alternative downstream signalling mechanisms. Modulation of NMDA receptor function by PKA and CaMKII still remains unclear. Evidence supporting specific residues phosphorylated by PKA (NR1, S879; Tingley *et al.*, 1997) and CaMKII (NR2B S1303; Omkumar *et al.*, 1996) remains inconclusive and sparse, while the physiological effects of this phosphorylation seem indirect. In the hippocampus, PKA activation by β adrenergic receptors enhances

the NMDA receptor mediated currents via an indirect block of calcineurin (Raman *et al.*, 1996).

In contrast to NMDA receptor potentiation, serine and threonine phosphatases 1, 2A, or 2B (calcineurin) facilitate the inhibition of NMDA receptor function. Calcineurin can be activated by the flux of calcium entering the cell during receptor activation and serves to reduce the open time of the NMDA receptor (Liberman and Mody, 1994). Activation of phosphatase 1 and 2A resulted in a reduction in the open probability of NMDA receptors in hippocampal neurones (Wang *et al.*, 1994).

Tyrosine kinase induced enhancement of NMDA receptor-mediated responses has been illustrated in neurones (Lu *et al.*, 1998; Zheng *et al.*, 1998). The endogenous, non-receptor tyrosine kinase, Src, seems to play a regulatory role in the function of neuronal NMDA receptors. Application of a high-affinity peptide (which activates Src) resulted in an increase in the open probability of the receptor and anti-Src antibodies co-immunoprecipitated NR1 from synaptic membranes (Yu *et al.*, 1997). The data suggests that Src plays a role in NMDA receptor phosphorylation and may be a component of the subsynaptic protein complex that contains NMDA receptors. Activation of tyrosine kinases has been implicated in the induction of long term potentiation (LTP) in the hippocampus. Application of tyrosine kinase inhibitors and inhibition of Src using a Src-blocking peptide both resulted in an inhibition of LTP induction while Src induced enhancement of NMDA receptor function can be inhibited by NMDA receptor antagonists (O'Dell *et al.*, 1991; *Lu et al.*, 1998). As with the serine and threonine kinases, endogenous tyrosine phosphatases may also regulate channel opening probability and therefore the activation properties of the NMDA receptor. Therefore, the activation of protein kinases and phosphatases plays pivotal role in adjusting the functional properties of the NMDA receptor, allowing a co-ordinated activation of downstream signalling cascades.

NMDA receptor pharmacology

Fast excitatory neurotransmission in the mammalian brain requires the activation of AMPA, Kainate and NMDA receptor subtypes. The putative endogenous neurotransmitter candidate for receptor activation is L-glutamate, whereas L-aspartate seems to exclusively activate NMDA receptors (Patneau and Mayer, 1990). Glycine,

initially thought to potentiate NMDA receptor-mediated responses has now been identified as an essential co-agonist at NMDA receptors (Johnson & Ascher, 1987; Klecker and Dingledine, 1988). The advent of new NMDA receptor antagonists has provided a better understanding of the physiological functions of NMDA receptors and native receptor subunit combinations. The first type of organic compounds to be synthesised as NMDA receptor antagonists were those which impeded the binding of glutamate/aspartate to the agonist binding site. The first compounds were D-isomers of simple longer chain glutamate analogues, D-α-aminoadipate (D-α-AA). These relatively low potency compounds were superseded by structures which had the ω-carboxylic acid of D-α-AA replaced with a phosphonic acid group to give D-2-amino-5-phosphovalerate (D-APV). This competitive antagonist displayed good selectivity and low micromolar affinity for the agonist binding site. D-AP5 has played a pivotal role in the identification of NMDA receptor function in the CNS (Watkins, 1984). An alternative site for NMDA receptor block is the ion-channel site or pore region of the receptor. The receptor requires to be in an activated state allowing the uncovering of the antagonist-binding site within the pore lining. One such compound is MK-801, a noncompetitive, use-dependent NMDA receptor antagonist (Huettner and Bean, 1988; MacDonald *et al.*, 1991; Jahr, 1992; Dzubay and Jahr, 1996). Activation of the NMDA receptor requires the binding of the co-agonist glycine to the strychnine-insensitive glycine binding site found on the NR1 subunit and thus was a potential target for antagonism. Kynurenic acid, a "broad spectrum" glutamate receptor antagonist, produced a noncompetitive block of NMDA receptor mediated responses via antagonism at the glycine binding site. Development of a structural analogue of Kynurenic acid, 7-chloro Kynurenic acid (7-Cl KYNA) displayed a 70-fold increase in affinity for the glycine modulatory site and completely depressed all NMDA responses in rat cortical tissue (Kemp *et al.*, 1988) (Fig. 1.10).

Voltage-dependent magnesium (Mg^{2+}) block of NMDA receptors

The NMDA receptor is unique in comparison to other ligand-gated ion channels due to the dual dependence of function on agonist binding and membrane potential. The voltage dependence of channel activation stems from the submillimolar concentration block by Mg^{2+} as opposed to the voltage dependence of conformational changes

(Nowak *et al.*, 1984; Westbrook & Mayer, 1987; Jahr and Stevens, 1990a,b). The function of the NMDA receptor is governed by the strong voltage dependence of Mg^{2+} block, where, at normal resting membrane potentials (-70mV) most NMDA receptors will undergo Mg^{2+} block, resulting in a considerable reduction in the NMDA receptor component of synaptic currents. Alleviation of the block occurs when the neurone becomes depolarised, via action potential generation (AP) or intense activation of colocalised AMPA receptors. Depolarisation, above –30mV, will partially relieve the Mg^{2+} block allowing ion flux through the activated NMDA receptor. The resulting influx in Na^{+}, Ca^{2+} and efflux of K^{+} triggers a multitude of downstream signalling cascades culminating in the maintenance of neuronal function mediated via various protein kinases and phosphatases (Dingledine *et al.*, 1999).

Presynaptic NMDA receptors

Excitatory neurotransmission in the brain follows the dogma that postsynaptic NMDA receptors are activated upon release of glutamate from a presynaptic release site. In recent years there has been an increasing volume of evidence supporting a putative role for presynaptic NMDA receptors in the mammalian CNS. The majority of the evidence results from immunohistological evidence at the light and electron microscopic level. Paquet and Smith (2000) provided convincing immunocytochemical evidence for the existence of presynaptic NMDA receptor subunit immunoreactivity in termini of GABAergic interneurones. Ultrastructural data identified strong NMDAR1 immunoreactivity in subpopulations of GABA-immunoreactive boutons in the bed nucleus of the stria terminalis, the paraventricular hypothalamic nucleus and the arcuate nucleus in rat brain. At the light microscopic level, immunoreactive terminal-like varicosities were identified in other nuclei in the basal forebrain, midline thalamus and periventricular hypothalamus. This compelling data suggests that the existence of presynaptic NMDA receptors is a more generalised phenomenon than previously thought. Specificity of presynaptic NMDA receptor expression and function is maintained due to there being an absence of presynaptic immunoreactivity in the midbrain, brainstem and cortical levels (Paquet & Smith, 2000). Previous to these findings, the only direct immunocytochemical evidence of NMDAR1 immunoreactivity

in GABAergic terminals came from DeBiasi *et al.* (1996), who found NMDAR1 and NMDAR2A/B-positive terminals forming symmetric synapses in the rat cerebral cortex.

Therefore, it is possible that GABAergic terminals of cerebellar interneurones may possess functional NMDA receptors. Purkinje neurones display dense staining for NMDAR1 compared to relatively little if any staining for NMDAR2A/B (Petralia *et al.*, 1994) which is consistent with the lack of functional NMDA receptors in the adult Purkinje neurones (Moriyoshi *et al.*, 1991). The NMDAR1 staining is concentrated in the cell bodies and dendritic arbours of Purkinje neurones in slice preparations from early developmental stages through to adulthood (Hafidi and Hillman, 1997; Thompson *et al.*, 2000). Developmental expression of NMDAR1 in basket, stellate and Golgi cells occurs after P15 continuing to increase up to P20 where expression levels are maintained (Hafidi and Hillman, 1997). Interneurones of the adult cerebellum displayed differential staining for secondary NMDA receptor subunits with Golgi cells displaying prominent staining for NMDAR2B and basket and stellate cells for NMDAR2A (Thompson *et al.*, 2000). The existence of data supporting NMDA receptor subunit expression at terminals of GABAergic interneurones of the cerebellum still remains elusive. The lack of immunocytochemical data may arise from the lack of functional data suggesting a role for presynaptic NMDA receptors in the interneurone-Purkinje neurone synapse. Glistch and Marty (1999) identified the NMDA receptor induced increase in GABA release on application of NMDA. The receptors were postulated to be present on axonal domains of GABAergic interneurones due to NMDA effects persisting in the presence of 0.2μM TTX. Further electrophysiological and immunocytochemical data is required to identify the existence of functional presynaptic NMDA receptors in the cerebellum. Presynaptic NMDA receptors would facilitate the release of GABA by two possible mechanisms. First, the microdomain increase in intracellular calcium, mediated via the NMDA receptor, is likely to facilitate the exocytotic release of vesicular GABA. Second, the increased level of sodium may cause a depolarisation of the terminal, which could result in reversal of the GABA transporter, inducing a release of GABA from the cytoplasmic pool (Attwell *et al.*, 1993; Levi and Raiteri, 1993).

AMPA, Kainate & NMDA receptors: Presynaptic regulation of transmitter release

The presence of postsynaptic, fast ionotropic glutamate receptors has long been established in the mammalian brain. More recently, data suggests that a presynaptic localisation of ionotropic receptors could play an influential role in modulating the effects of either excitatory or inhibitory inputs to target neurones. Interestingly, the activation of the same ionotropic receptor on different neuronal preparations induces complicated and often contradictory effects on the neurotransmitter release process. The activation of these presynaptic receptors is as a result of glutamate 'spillover' from neighbouring excitatory neurones. A wealth of information exists as to the physiological reasons for 'spillover' and its modulatory effects on distant neurones, but to date, there are only a handful of investigations into the possible roles of retrograde messenger activation of presynaptic ionotropic receptors.

Satake and colleagues (2000) examined the effects of repetitive CF stimulation on the release of GABA from adjacent basket cells in the rat cerebellum. CF stimulation produced the documented AMPA-mediated postsynaptic EPSC in the recorded Purkinje neurone (Konnerth *et al.*, 1990) but also induced a transient depression of the GABAergic inhibitory transmission between cerebellar interneurones and PNs, termed 'disinhibition'. Examination of paired pulse (PP) ratio changes after CF stimulation in conjunction with the evaluation of coefficient of variation of IPSC amplitudes identified a presynaptic locus for the reduced inhibitory transmission. Further examination, using a multitude of pharmacological tools, identified AMPA receptors as the presynaptic ionotropic receptor subtype initiating the interneurone-PN 'disinhibition'. The CF-mediated reduction in IPSC amplitude, somewhat similar to DSI, was deemed to be due to glutamate spillover from the CF as opposed to release of a retrograde transmitter from the PN. Therefore, the effect of glutamate release from CFs is twofold. Firstly, glutamate binds to postsynaptic AMPA receptors causing an overall depolarisation of the PN. Secondly, glutamate diffuses from the synaptic cleft to adjacent sites of inhibitory transmission causing an AMPA mediated depression of GABA release, thereby accentuating PN depolarisation.

These findings are in direct contrast to that of an earlier study by Bureau and Mulle (1998) examining the effects of the AMPA/KA receptor agonist, domoate, on the amplitude and frequency of sIPSCs in cerebellar stellate cells. During the application of domoate a large increase in the frequency of sIPSCs was observed with no discernible change in the mean amplitude while a large decrease in sIPSC frequency and amplitude was observed immediately after cessation of agonist application. Therefore, the exact effects of AMPA/KA receptor activation on the release of GABA from cerebellar interneurones still remains controversial.

In parallel with the identification of presynaptic AMPA receptors on basket cells, Carter and Regehr (2000) identified the existence of both AMPA and NMDA receptors at putative release sites on cerebellar stellate cells. The main finding of this work was that repetitive stimulation of PFs caused a prolonged EPSC in the adjacent stellate cells. This EPSC consisted of both a fast and slow component corresponding to presynaptic AMPAR and NMDAR activation, respectively. Glutamate, released during PF stimulation, accumulated in the cleft before diffusing to adjacent interneurone synaptic sites causing a prolonged EPSC. The EPSC was composed of a fast AMPA and somewhat slower NMDA-mediated component. Interestingly, block of glutamate transporters, required for the termination of glutamate effects after release, caused an increase in the PF-mediated EPSC in stellate cells. Therefore, glutamate transporters play a fundamental role in the regulation of 'spillover' of glutamate after intense synaptic stimulation.

Presynaptic ionotropic receptors can also act as autoreceptors being activated subsequent to the release of their own endogenous transmitter (MacDermott *et al.*, 1999; Parnas *et al.*, 2000). Application of NMDA at the PF-PN synapse in the cerebellum resulted in a transient depression of PF-mediated EPSCs recorded in PNs (Casado *et al.*, 2000). This depression was initially thought to involve a reduction in transmitter release mediated via presynaptic NMDA receptor activation. However, on further examination it was revealed that calcium entry, via presynaptic NMDARs, caused a depression of postsynaptic EPSCs via the release of a trans-synaptic messenger. The presynaptic microdomain increase in calcium resulted in the production and release of the soluble messenger nitric oxide (NO). Synaptic depression is thought to occur due to the diffusion of NO from a pre- to postsynaptic site whereupon it could conceivably

augment the phosphorylation of AMPARs, possibly via PKG, and this might result in an overall reduction in EPSC amplitude.

Finally, kainate receptors are also implicated in the regulation of neurotransmitter release in the mammalian brain (Khakh & Henderson, 2000). Controversy surrounds this ionotropic receptor subtype as it plays differential roles depending on the neuronal preparation. Activation of presynaptic kainate receptors, deemed to have an axon terminal locus of expression, causes an increase in the release of GABA from hypothalamic neurones (Liu *et al.*, 1999). Conversely, presynaptic kainate receptor activation in hippocampal interneurones causes a marked depression of GABA release (Rodriguez-moreno *et al.*, 1997; Min *et al.*, 1999). Interestingly, one hypothesis for this depression in transmission involved direct activation of a $G_{i/o}$ subtype G-protein-coupled pathway upon presynaptic kainate receptor activation (Rodriguez-moreno & Lerma, 1998). Subsequent work by Frerking and colleagues (1999) proposed that presynaptic kainate receptor activation resulted in a kainate-induced increase in the spontaneous release of GABA. However, this initial increase in presynaptic transmitter release resulted in an overall decrease in sIPSCs due to $GABA_B$ autoreceptor inhibition of further release. The possibility still remains that kainate receptors may have a direct coupling to G-protein-mediated signalling pathways whereby influencing the release of neurotransmitter, however this remains to be evaluated.

Clearly, further work is required to elucidate the specific signal transduction cascades involved in ionotropic receptor-mediated modulation of neurotransmitter release processes. There remains a complex signalling network in the cerebellum involving both excitatory and inhibitory inputs, differentially regulating both their own target receptors and the excitability of adjacent neuronal inputs.

Excitatory amino acid transporters (EAATs)

Glutamate, the most widespread excitatory neurotransmitter in the brain, can allow neurones to relay and process information while also being the precursor to global neuronal destruction. In situations such as brain hypoxia (perinatal asphyxia) and cerebrovascular ischaemia (stroke), glutamate concentrations rise to levels sufficient to induce excitotoxicity and resulting neuronal death (Szatkowski and Attwell, 1994). Glutamate release during normal exocytosis will spread throughout the synaptic cleft in order to activate all excitatory amino acid receptors surrounding the cleft (postsynaptic and presynaptic autoreceptors). Termination of glutamate activity requires the re-uptake of glutamate into presynaptic boutons or uptake into postsynaptic neurones or glia. This action of EAATs, present on the plasma membranes of neurones and glial cells, results in the complete removal of glutamate from the extracellular space and thus eliminates the possibility of glutamate-induced excitotoxicity.

Protein structure

The family of mammalian excitatory 'amino acid transporters consists of five isoforms termed EAAT(1-5). Each displays approximately 36-65% sequence homology and all are dependent upon the concentration gradient of sodium ions for transport. Structural features which are common throughout the mammalian EAAT family are the absence of a cleavable signal sequence, suggesting a cytosolic localisation of the NH_2 terminus; the presence of a sequence motif AA(I,V,L)FIAQ, probably located in a membrane-spanning domain, which is conserved throughout all amino acid transporters; an increased level of sequence conservation in the COOH-terminal compared to the NH_2 terminal; the presence of six highly conserved putative membrane-spanning domains in the NH_2-terminal half of the proteins; and the presence of two cannonical sites for N-linked glycosylation on the extracellular hydrophilic loop EL2 between TM3 and TM4 (Danbolt *et al.*, 1992; Lehre *et al.*, 1995; Levy *et al.*, 1993; Rothstein *et al.*, 1994; Schulte & Stoffel, 1995). EAAT3 has been identified as possessing 6 α-helical transmembrane domains in the NH_2 terminal domain of these proteins (Kanai and

Heidiger, 1992). Controversy still surrounds the structure and function of the COOH terminal domain of the protein, and this is where the largest level of sequence homology is found. There exists a long hydrophobic stretch of amino acid residues displaying no tendency to form α-helical structures in this region. Unfortunately, three independent groups have identified two, four and six extra classical transmembrane domains within this COOH terminal domain of the protein, resulting in inconsistencies in the identification of the overall sequence of EAATs (Pines *et al.*, 1992; Kanai and Heidiger, 1992; Hofmann *et al.*, 1994; Storck *et al.*, 1992). One finding, common to all the aforementioned studies, was the cytosolic localisation of the COOH terminus.

Stoichiometry

The exact stoichiometry of individual EAATs varies among the five members of the transporter superfamily. Glutamate uptake, for many cell types, is electrogenic and driven by the cotransport of Na^+ and the countertransport of K^+ with a first-order dependence on external glutamate and $[K^+]_i$ and a sigmoidal dependence on external Na^+, which suggests a stoichiometry of 3 Na^+ : 1 glutamate : 1K^+ (Barbour *et al.*, 1988; Kanner and Sharon, 1978). In conjunction with the movement of Na^+, K^+ and glutamate there is a flux of pH-changing ions, cotransport of 1H^+ or counter-transport of 1 OH^- (Bouvier *et al.*, 1992; Erecinska *et al.*, 1983; Nelson *et al.*, 1983). This would confer a stoichiometry of 1 glutamate: 2 Na^+: 1 K^+: 1 OH^- which would still be electrogenic. Controversy still surrounds the exact stoichiometry of the different EAATs, for example EAAT3 has been shown to have a stoichiometry of 1 Na^+ : 1 glutamate : 1H^+ : 1K^+ (Zerangue and Kavanaugh, 1996), 2 Na^+ : 1 glutamate : 1K^+ : 1H^+ / OH^- (Kanai *et al.*, 1995) and 3 Na^+ transported per glutamate (Zerangue and Kavanaugh, 1996). Discrepancies in evaluation of the true stoichiometry of EAAT3 are derived from the different experimental conditions in which the results were obtained. To date the most compelling evidence suggests that glutamate uptake is driven by the cotransport of 2 Na^+ into the cell (Stallcup *et al.*, 1979; Baetge *et al.*, 1979; Erecinska *et al.*, 1983), the counter-transport of 1K^+ (Kanner and Sharon, 1978; Burckhardt *et al.*, 1980; Amato *et al.*, 1994), and either the cotransport of 1H^+ or the counter-transport of 1OH^- (Bouvier *et al.*, 1992). This is diagrammatically represented in fig. 1.11.

Fig. 1.11. Stoichiometry of glutamate uptake for EAAT3

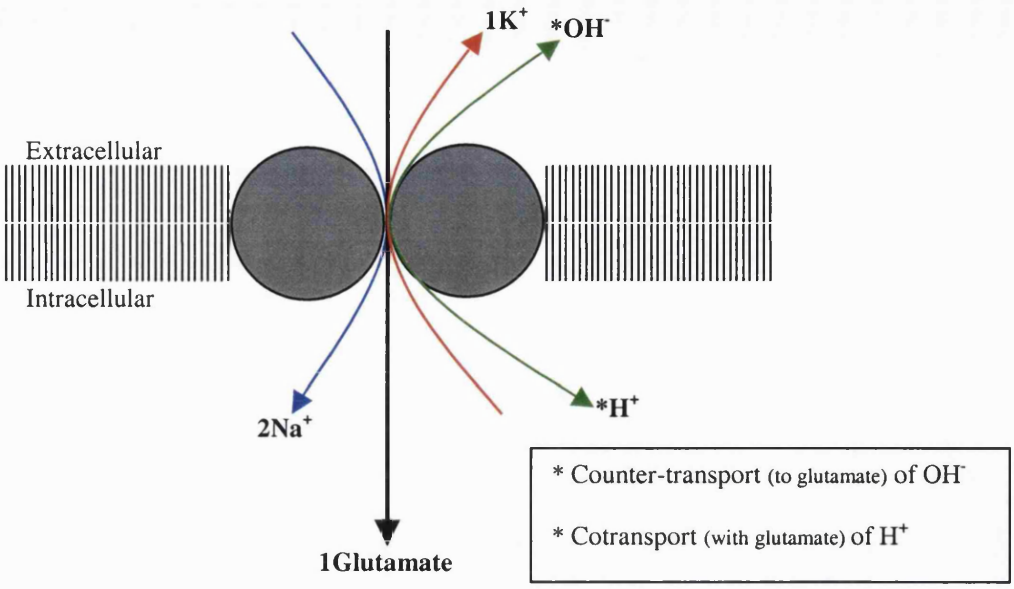

Mechanism of transport

The translocation of glutamate requires the ordered binding of two or three Na^+ in order to facilitate the binding of a single glutamate molecule. Cooperativity of Na^+ and glutamate binding for EAAT3 suggests that one Na^+ ion binds with low affinity then glutamate binds inducing the binding of the second Na^+. This Na^+/glutamate complex is then translocated whereupon both ions become independent. Subsequent to the complex translocation, K^+ bind and translocate to the extracellular face allowing a new glutamate uptake cycle to begin. If pH changes occur then simultaneous translocation of glutamate and H^+ or K^+ and OH^- will occur (Kanner, 1993). Sodium ion and glutamate concentrations provide the major driving force for glutamate translocation, where at low extracellular Na^+ concentrations the binding of Na^+ to the extracellular face becomes the rate-limiting step. Conversely, when the extracellular sodium concentration is high the rate-limiting translocation step becomes the extracellular concentration of L-glutamate.

Physiological role of neuronal EAATs

The strict control of extracellular glutamate concentration is paramount in order to eliminate the possibility of glutamate-induced neurotoxicity. Neurones

contain glutamate concentrations four orders of magnitude higher than that in the extracellular fluid of the synaptic cleft (10mM in neurones and low millimolar in glial cells) (Benveniste *et al.*, 1984; Burger *et al.*, 1989; Kanner and Schuldiner, 1987; Rothstein *et al.*, 1996). The block of glutamate transport by non-selective glutamate blockers (threo-β-hydroxyaspartate, (THA) and dihydrokainate, (DHK) raise the extracellular glutamate concentration, alter postsynaptic potentials and result in neurotoxicity *in vitro* (Barks and Silverstein, 1994; Isaacson and Nicol, 1993; Mennerick and Zorumski, 1994; Robinson *et al.*, 1993; Rothstein *et al.*, 1993; Sarantis *et al.*, 1993) and *in vivo* (Lucas and Newhouse, 1957; Olney and Sharpe, 1969; Olney *et al.*, 1971). Evidence suggests that glial transporters (EAAT1 and EAAT2) regulate the extracellular glutamate concentration rather than transporters which are located on neurones (EAAT3 and EAAT4) (Peghini *et al.*, 1997; Tanaka *et al.*, 1997). Therefore, specific partial knockouts of EAAT1-2 cause progressive paralysis and neurodegeneration in rats (Rothstein *et al.*, 1996). These findings do not exclude EAAT3-4 in the induction of neurodegeneration, as the possible reversal of these uptake transporters may increase extracellular glutamate levels to such an extent so as to initiate excitotoxicity, this will be discussed later. The cerebellum contains four of the five subtypes of EAATs (1-4) located differentially throughout the different cell types. Glial cells contain an abundance of EAAT1 while Bergmann glia contain EAAT2 (Chaudhry *et al.*, 1995; Lehre *et al.*, 1995; Rothstein *et al.*, 1994).

Purkinje neurones express an abundance of EAAT4 with predominant immunoreactivity in the dendrites and spines. However, immunogold-labelling studies have identified EAAT4 as having extrajunctional loci of expression. This infers that EAAT4 functions to uptake glutamate from the synaptic cleft so as to minimise glutamate spillover, as opposed to quenching the glutamate released from PF or CFs (Tanaka *et al.*, 1997). Studies by Coco and colleagues (1997) identified a non-synaptic localisation of the EAAT3 glutamate transporter in cultured hippocampal neurones. Immunoreactivity was present in the somatodendritic compartments with specific localisation on dendritic shafts and spine necks, juxtaposed to the active zone. The loci of expression for EAAT3 and EAAT4 would argue against a role in synaptic glutamate clearance and would predict an unconventional non-synaptic function for both transporters. Purkinje neurones display a similar somatodendritic localisation of EAAT3

(Furuta *et al.*, 1997). Therefore, the presence of EAAT3 and EAAT4 in GABAergic Purkinje neurones may aid in the block of glutamate spillover, modulation of GABA synthesis or play an as yet unidentified role in the regulation of intra/extracellular glutamate concentrations.

Glutamate release during EAAT reversal

Under normal transmembrane gradients of Na^+, K^+, pH and voltage, glutamate will be removed in order to minimise the extracellular glutamate concentration ($[glutamate]_o$ ~0.2μM) (Attwell *et al.*, 1993). During situations such as brain hypoxia or ischaemia the normal transmembrane gradients become disrupted. Anaerobic conditions, which exist during ischaemia and hypoxia results in a change in the H^+ ion concentration on both sides of the plasma membrane, eventually causing a change in the pH level to approximately 6.1. Persistent lack of oxygen to the brain will cause a reduction in ATP levels resulting in a slowing of the Na^+/K^+ ATPase pump and eventual rundown of the transmembrane gradients for $[K^+]$, $[Na^+]$ and the resting membrane potential. Interestingly, the extracellular K^+ concentration rises relatively slowly until around two minutes after cessation of oxygen whereupon $[K^+]_o$ rises rapidly to around 60mM, $[Na^+]_o$ falls and the cells depolarise to –20mV. The disruption to the transmembrane gradients leads to the reversal of the glutamate transporter and a rapid rise in the extracellular glutamate concentration (Szatkowski *et al.*, 1990; Billups and Attwell, 1996). During ischaemia and hypoxia, it is predicted, assuming an average value of 3mM $[glutamate]_i$, that when $[K^+]_o$ rises the reversal of neuronal EAATs will result in $[glutamate]_o$ rising to 260μM (Attwell *et al.*, 1993). This concentration of glutamate is sufficient to induce neuronal death if it persists for more than a few minutes (Choi *et al.*, 1987). This phenomenon is not unique to the cerebellum and is postulated to underlie neuronal death in a variety of brain tissues. In the hippocampus, non-specific blockers of EAATs have prevented damage to neurones subjected to hypoxia and ischaemic conditions, thus identifying the major role played by EAATs during the induction of excitotoxicity and eventual neuronal death (Roettger and Lipton, 1996; Katsumori *et al.*, 1999).

Ca^{2+} in Purkinje neurones: Sources and homeostasis

AMPA receptors and voltage-activated calcium channels (VACCs)

Fast excitatory neurotransmission in the cerebellum releases glutamate from both parallel fibres (PFs) and climbing fibres (CFs) thus activating postsynaptic glutamate receptors present on Purkinje neurones (Llano *et al.*, 1991; Konnerth *et al.*, 1990). Only during very early postnatal stages (P0-5) do Purkinje neurones express calcium-permeable NMDA receptors. Mature Purkinje neurones (P21) do not possess functional NMDARs (Farrant and Cull-Candy, 1991; Llano *et al.*, 1991; Rosemund *et al.*, 1992). Therefore, CF and PF activation results in the activation of AMPA receptors and mGluRs mediating a postsynaptic rise in cytosolic calcium levels. Studies using *in-situ* hybridisation and RT-PCR (Lambolez *et al.*, 1992; Tempia *et al.*, 1996) identified the presence of all AMPA receptor subunits (GluR1-4) in mature Purkinje neurones. Large amounts of the GluR2 subunit is expressed, which confers a low calcium permeability on heteromeric recombinant AMPA receptors and inwardly-rectifying current-voltage relationship (Verdoorn *et al.*, 1991; Burnashev *et al*, 1992; Ozawa, 1998), indicating that Purkinje neurone AMPA receptors have a low calcium permeability. Further investigation calculated that calcium carries 0.6% of the total ion flux through the AMPA receptor during activation (Burnashev *et al.*, 1995). The role of the AMPA receptor is predominantly in neuronal depolarisation and does not contribute significantly to calcium rises, underlying many forms of synaptic plasticity within the cerebellum.

Depolarisation, induced by PF and CF activation of AMPA receptors, causes activation of voltage-activated calcium channels (VACCs) present on the Purkinje neurone plasma membrane. Neurones express a range of VACCs classified in two groups depending upon their pharmacological and physiological properties, either low voltage-activated (LVA, T-type channels) or high voltage-activated (HVA, L, N, P, Q and R types) (Miller, 1987; Tsien *et al.*, 1988; Bean, 1989; Swandulla *et al.*, 1991; Llinas *et al.*, 1992; Wheeler *et al.*, 1995). At a membrane potential of –10mV, all types of VACCs will open resulting in an influx of calcium and rapid rise in cytosolic calcium levels. The majority of calcium currents are mediated via HVA P-type calcium

channels, first found in Purkinje neurones and subsequently identified in a variety of other tissue types (Llinas *et al.*, 1992). Pharmacological properties of this type of calcium channel include insensitivity to dihydropyridines and ω-conotoxin GVIA, modulators of L-type and N-type channels, respectively. One compound that displays a specific, potent block of P-type calcium channels is ω-Aga IVA (a component of funnel web spider venom, *Agelenopsis aperta*; Mintz *et al.*, 1992 a & b). Depolarisation of the Purkinje neurone membrane results in the opening of P-type calcium channels located throughout the neurone, causing a large scale increase in cytosolic calcium, the precursor step thought to underlie persistent synaptic changes in the cerebellum (Sakurai, 1990; Konnerth *et al.*, 1992; Kano *et al.*, 1992).

Calcium release from intracellular stores

Calcium elevation in Purkinje neurones can be further aided by the 'wave-like' release of calcium from two independent intracellular stores located on the endoplasmic reticulum (ER) (Berridge, 1996; Mikoshiba, 1996). The stores are ligand-gated, calcium permeable channels termed ryanodine receptors (RyRs) and inositol 1,4,5-trisphosphate receptors (IP_3Rs). Ryanodine receptors are composed of three subtypes, two from muscle; the skeletal muscle type (RyR1) and cardiac muscle (RyR2) and one from the brain (RyR3) (McPherson & Campbell, 1993; Sorrentino & Volpe, 1993; Hamilton *et al.*, 2000). All isoforms are present in Purkinje neurones with RyR2 being the most prominent (Kuwajima *et al.*, 1992). Interestingly, Purkinje neurones possess RyR1 which has been postulated, with the dihydropyridine receptor acting as a voltage sensor, to be involved in depolarisation-induced release of calcium in skeletal muscle (Hamilton *et al.*, 2000). RyR2 and RyR3 are activated when cytosolic calcium levels reach micromolar concentrations, where calcium facilitates the release of calcium from ER stores in a process termed calcium-induced-calcium release (CICR) (Mikoshiba, 1996). Therefore, the calcium signal mediated by activation of VACCs is subsequently prolonged by the release of intracellular calcium. However, to date there is no evidence for the release of calcium from ryanodine sensitive stores after intense CF and PF stimulation of Purkinje neurones. In accordance with this, measured calcium transients, as a result of depolarisation, show only a monotonic rise in calcium with no secondary component (Eilers *et al.*, 1995; Llano *et al.*, 1994; Kano *et al.*, 1995). Application of the

RyR agonist, caffeine, resulted in a transient increase in cytosolic calcium levels in both the soma and dendrites of mature Purkinje neurones. This rise can be blocked by the application of Ruthenium Red but not mimicked by membrane depolarisation inducing long-term changes in synaptic transmission (Kano *et al.*, 1995). This provides compelling evidence that RyRs do not play a pivotal role in the induction phase of long term synaptic plasticity within the cerebellum.

PF activation of Purkinje neurone mGluR type 1 receptors resulted in the $InsP_3$ via the phospholipase C pathway. Intense CF and PF stimulation caused an increase in the cytosolic concentration of $InsP_3$ (10-20μM), accumulating in the spines and dendrites of the Purkinje neurone where $InsP_3Rs$ are located (Satoh *et al.*, 1990; Takei *et al.*, 1992). Binding of $InsP_3$ to the type 1 $InsP_3R$, the predominant receptor subtype in Purkinje neurones, caused a 'wave-like' release of calcium into the cytosol. Initially, a fast calcium transient is observed due to VACC opening, followed by a secondary peak due to calcium liberation from the $InsP_3$ stores (Takechi *et al.*, 1998; Finch & Augustine, 1998). Therefore, it seems likely that PF activation induces the release of calcium from $InsP_3$ stores and not ryanodine-sensitive stores during the induction phases of long-term plasticity.

Purkinje neurones contain large concentrations of the calcium binding proteins calbindin-D_{28K} and parvalbumin. Calbindin-D_{28K} is located throughout the Purkinje neurone and shows a high level of immunoreactivity in the nucleus, constituting 15% of the soluble protein of this cell type (German *et al.*, 1997; Baimbridge *et al.*, 1982). Rapid calcium sequestration by calbindin-D_{28K} occurs due to it possessing three to four high-affinity, cooperative binding sites (Cheung *et al.*, 1993) that exhibit rapid binding kinetics and that the protein itself is mobile (Roberts, 1993). In conjunction with rapid calcium sequestration by calcium binding proteins, sarco-endoplasmic reticulum calcium pumps (SERCA), plasma membrane calcium pumps (PMCA) and Na^+-Ca^{2+} exchangers, all provide conjunctive and alternative mechanisms for calcium sequestration (Fierro *et al.*, 1998). Efficient spatio-temporal modulation of neurone calcium underlies the maintenance of the majority of cellular functions and could potentially play a pivotal role in cerebellar Purkinje neurone synaptic plasticity.

Long-term depression (LTD) in the cerebellum

Long lasting, activity-dependent depression of synaptic transmission, termed long-term depression (LTD), has been established at synapses between parallel fibres (PF) and Purkinje neurones. LTD is manifest as a significant reduction in the PN response to the release of glutamate from PFs, induced as a result of repetitive PN stimulation. The induction of LTD of PF-mediated responses requires, *in vivo*, the coincident activation of postsynaptic ionotropic AMPA receptors and metabotropic glutamate receptors. Climbing fibre (CF) stimulation induces AMPA receptor activation resulting in a fast depolarisation of PNs leading to the opening of voltage-activated calcium channels and subsequent increase in $[Ca^{2+}]_i$. LTD induction can be blocked by simultaneous stimulation of CF and cerebellar interneurones, probably due to hyperpolarisation of the PN and thus blocking the Ca^{2+}-dependent plateau potentials (Ekerot and Kano, 1985; Ekerot and Oscarsson, 1981). Reduction of free cytosolic calcium using EGTA blocks LTD, therefore, identifying the rise in cytosolic calcium as being the crucial step in the induction phase (Sakurai, 1987). Coincident stimulation of PFs causes activation of mGluR type 1 receptors known to be coupled to the phospholipase C pathway (Baude *et al.*, 1993). Stimulation of this enzyme pathway leads to the production of $InsP_3$ and DAG (Pin and Duvoisin, 1995). The result of stimulation of this pathway is twofold. Firstly, $InsP_3$ binds to $InsP_3R$ located on the ER of neurones to induce the release of calcium from intracellular calcium stores. This release of calcium into the cytosol induces the secondary wave-like release from ryanodine-sensitive stores due to 'calcium induced calcium release' (Ellisman *et al.*, 1990; Walton *et al.*, 1991; Kuwajima *et al.*, 1992; Nakanishi *et al.*, 1992; Ross *et al.*, 1992). Secondly, DAG directly activates the protein kinase, PKC. Induction of LTD, in acute slices and cultures, requires the activation of PKC following PF-$mGluR_1$ activation (Crepel and Krupa, 1988). Therefore the underlying mechanism of LTD induction requires the wave-like increase in cytosolic calcium and subsequent protein kinase C activation.

The downstream mechanisms causing depression of the PF-PN synapse are still largely unresolved. Recent studies have identified a predominant role for nitric oxide in the induction phase of LTD. One major drawback with this hypothesis is that RT-PCR

studies on PNs have failed to detect any presence of the enzyme, nitric oxide synthase (NOS) (Crepel *et al.*, 1994). However, both CF and cerebellar basket cells possess an abundance of NOS and could therefore be the source of NO production (Bredt *et al.*, 1990; Southam *et al.*, 1992). It was hypothesised that, following a rise in cytosolic calcium in PNs after CF/PF stimulation, a K^+ efflux (via Ca^{2+}-activated K^+ channels) would induce a local depolarisation of presynaptic PFs to such an extent so as to stimulate the NOS pathway. Diffusion of NO, back across the synaptic cleft, would result in the activation of guanylate cyclases and subsequent activation of protein kinase G in nearby PNs. This hypothesis is supported by experiments displaying a robust LTD in patch-clamped PNs after raising the extracellular K^+ concentration and that this LTD can be completely abolished by NOS inhibitors (Crepel *et al.*, 1994). Therefore, PKC and PKG activation seems to underlie the induction of a robust LTD of the PF-PN synapse. Early experiments identified a reduction in the responsiveness to iontophoretic application of glutamate after depolarisation of the PN (Ito *et al.*, 1982). This led to the hypothesis that the induction of LTD may lead to a long-term desensitisation of the postsynaptic AMPA receptors of PNs. Analysis of the coefficient of variation for EPSCs during LTD illustrated an entirely postsynaptic loci of depression (Blond *et al.*, 1997). The use of compounds which, either reduced AMPA receptor desensitisation or induced persistent phosphorylation of the AMPA receptor, caused a marked reduction or enhancement, respectively, of LTD. Recent studies have identified the possibility that a large proportion of LTD induction may underlie the clathrin-mediated endocytosis of AMPA receptors. This receptor internalisation coupled with changes in AMPA receptor unitary conductance, kinetics or glutamate affinity may account for LTD of the PF-PN synapse (Wang & Linden, 2000; Hirai, 2001; Xia *et al.*, 2000).

There still remains a multitude of unanswered questions concerning the area of long-term synaptic depression. Subsequent work, identifying the intermediary steps in the signalling cascades, may help to uncover the true nature of LTD and its role in the process of motor learning.

Depolarisation induced suppression of inhibition (DSI)

Regulation of inhibitory synaptic inputs in both the hippocampus and cerebellum plays a pivotal role in the control of neuronal excitability (Alger, 1991; Stelzer, 1992). In cerebellar Purkinje neurones (Llano *et al.*, 1991; Vincent *et al.*, 1992; Vincent and Marty, 1993) and in hippocampal CA1 pyramidal cells (Alger *et al.*, 1996; Pitler and Alger, 1992, 1994), depolarisation, causing a wave-like rise in cytosolic calcium concentration, induces a transient depression of GABAergic IPSCs. This depression, lasting for many seconds, was termed depolarisation-induced suppression of inhibition (DSI). Evaluation of $GABA_A$ receptor properties identified no apparent changes in receptor response as assessed by analysis of spontaneous (Llano *et al.*, 1991; Pitler and Alger, 1994), evoked (Alger *et al.*, 1996) or miniature (Morishita and Alger, 1997) IPSCs. Therefore, the transient decrease in IPSCs was though to be mediated by a retrograde messenger released after depolarisation of either the Purkinje neurone or CA1 pyramidal cell. More recent work by Alger *et al.* (1996), examining the coefficient of variation of IPSC amplitudes, has identified a purely presynaptic loci of DSI where the phenomenon results in an increase in the magnitude of presynaptic failures (Alger *et al.* 1996; Vincent *et al.*, 1992). Thus, calcium entry into both the pyramidal cell and Purkinje neurone induces the release of retrograde messenger suppressing the release of GABA from presynaptic terminals.

Only recently has the true nature of the calcium dependence of DSI, in both the hippocampus and cerebellum, been fully resolved. Application of a single 100ms depolarisation to 0mV in both CA1 pyramidal cells and PNs induces a half-maximal DSI (Lenz and Alger, 1999; Glitsch *et al.*, 2000). Interestingly, basal calcium levels in both neuronal types lies between 20 and 100nM and half saturation DSI in PNs occurs when calcium levels reach 200 and 40nM in dendrites and soma, respectively. Therefore, it remains a possibility that DSI could be tonically active at resting states in both hippocampal CA1 pyramidal cells and cerebellar Purkinje neurones (Pitler and Alger, 1992; Morishita *et al.*, 1997).

Although hippocampal and cerebellar DSI require comparable induction protocols and share a similar calcium dependence, there still remains a subtle difference in the presynaptic receptors activated upon retrograde transmitter release. In the

cerebellum, DSI is mimicked by the application of DCG-IV, a specific agonist of group II metabotropic glutamate receptors and enhanced by the application of forskolin (Glitsch *et al.*, 1996). These results suggest that group II mGluRs play a pivotal role in cerebellar DSI and transiently reduce GABA release via blockade of the adenylate cyclase pathway. This hypothesis is supported by *in situ* hybridisation experiments identifying the existence of group II mGluRs on cerebellar interneurones (Ohishi *et al.*, 1993). In contrast, hippocampal CA1 DSI can be mimicked by the application of the mGluR group I agonist, quisqualate (at low concentration), and completely inhibited by the addition of (s)-MCPG, a group I and II antagonist (Morishita *et al.*, 1998). It remains likely that hippocampal DSI is mediated via mGluR type 5 ($mGluR_5$) receptors, as this receptor type is densely distributed throughout the CA1 region whereas $mGluR_1$ is confined to a subgroup of neurones in the stratum oriens (Shigemoto *et al.*, 1997).

Retrograde messenger: Putative release mechanisms

Early studies identified the possibility that retrograde signalling could underlie part of the induction phase of long-term potentiation in the hippocampus. Controversy surrounded this novel signalling pathway and subsequently two candidate substances were postulated to play the role. The first was arachidonic acid (AA) (Dumuis *et al.*, 1988) and the second, nitric oxide (Bohme *et al.*, 1991). This early pioneering work, although controversial, paved the way for the identification of other retrograde messengers throughout the mammalian CNS.

Recent work by Reyes *et al.* (1998) reported an inhibition of glutamate release in the excitatory synapse between pyramidal cells and bitufted interneurones of the hippocampus. The retrograde transmitter in this case was identified as GABA, which on release from the bitufted interneurone, activated presynaptic $GABA_B$ receptors causing an overall decrease in transmitter release. In contrast, the retrograde transmitter postulated to be involved in hippocampal CA1 DSI, cerebellar DSI and suppression of synaptic inhibition at the hippocampal pyramidal-FSN (fast-spiking non-accommodating) neurone synapse is glutamate or a glutamate-like substance (Glitsch *et al.*, 1996; Morishita *et al.*, 1998). Therefore, it remains plausible that individual neuronal networks or even individual neurones possess specific retrograde transmitters

recruited to perform a particular function during the induction of short- or long-term synaptic changes.

The exact nature of the retrograde transmitter release mechanism still remains largely unclear. Reversal of an excitatory amino acid transporter, resulting in an efflux of glutamate from the cytosol into the synaptic cleft, would be inconsistent with the stoichiometry of known glutamate transporters, such that under normal transmembrane ion gradients EAATs will only run in the forward direction (removing glutamate from the synaptic cleft) and will not reverse (Attwell *et al.*, 1993). In agreement with this is the finding that application of EAAT blockers enhance the level of DSI seen in the hippocampus (Morishita and Alger, 1999). Therefore, it seems likely that the calcium-dependent release of a retrograde transmitter results from a novel form of postsynaptic vesicular release. Glial cells and cholinergic neurones have been shown to release glutamate through calcium-dependent vesicular release (Parpura *et al.*, 1994; Dan & Poo, 1994). Zilberter (2000) completely abolished the release of glutamate from FSN neurones in the hippocampus by disrupting two components of the vesicle release machinery. Firstly, botulinum toxin type D was added to the intracellular solution to induce enzymatic cleavage of vesicle recycling proteins. Secondly, GDP-β-S was introduced, via the patch pipette, as GTP-binding proteins are necessary for several steps in vesicle docking and trafficking during exocytosis (Watson, 1999). This work produced compelling evidence that the release of glutamate was indeed a novel postsynaptic vesicle release process, although to date there is no EM evidence to support this theory. Further work is required to elucidate the signal cascade(s) involved in connecting the crucial cytosolic rise in intracellular calcium to the possible vesicular release of a retrograde transmitter.

Rebound potentiation

Early studies examining the effects of PN depolarisation identified a late phase potentiation of $GABA_A$ receptor-mediated responses to the exogenous application of GABA (Llano *et al.*, 1991). Induction of the potentiation required the same depolarising protocol as DSI and could be entirely blocked by the inclusion, in the patch pipette

solution, of 30mM BAPTA. Interestingly, this $GABA_A$ receptor potentiation persisted in the presence of TTX arguing against a polysynaptic mechanism. Subsequent work by Kano and colleagues (1992) identified a robust increase in the mean amplitude of PN IPSCs (analysed 20 minutes after stimulus induction) following repetitive CF stimulation, this was termed rebound potentiation. The frequency of IPSCs was unaffected by the repetitive depolarisation. Inclusion of 30mM BAPTA in the patch pipette solution completely abolished rebound potentiation indicating that the rise in cytosolic calcium is the crucial step in the induction of this phenomenon (Kano *et al.*, 1992; Hashimoto *et al.*, 1996; Khodakhah and Armstrong, 1997) (Fig. 1.12). Induction of LTD has been proposed to involve the calcium activation of signal cascades resulting in protein kinase activation. As previously described, $GABA_A$ receptor-mediated currents display both up and down regulation after phosphorylation, this being dependent upon the kinase involved and receptor subunit composition. Previous studies have implicated PKA in the upregulation of $GABA_A$ receptor-mediated mIPSCs in PNs. Application of membrane permeable 8-bromo-cAMP caused a significant increase in the mean amplitude of GABA-induced whole-cell currents and mIPSCs (Kano and Konnerth, 1992). However, it is still relatively unclear whether PKA directly phosphorylates $GABA_A$ receptor subunits or is an intermediary step in the induction phase of rebound potentiation. An alternative kinase involved in the induction and possible maintenance of rebound potentiation is CaMKII. Specific inhibitors of this calcium-activated kinase completely blocked rebound potentiation if applied prior to or during the induction stimulus. Application of CaMKII inhibitors after the stimulus failed to affect the induction of a robust rebound potentiation (Kano *et al*, 1996). Therefore, CaMKII is involved in the initial phosphorylation process during depolarisation leading to a robust potentiation of $GABA_A$ receptor-mediated synaptic currents. Biochemical data indicate that CaMKII undergoes an autophosphorylation process whereby it no longer requires calmodulin to maintain its activity (Saitoh and Schwartz, 1985; Kindler and Kennedy, 1996), and so could play a pivotal role in the maintenance of rebound potentiation. As previously described both β and γ subunits of the $GABA_A$ receptor have consensus sequences for the phosphorylation by CaMKII. Interestingly, CaMKII activation may induce direct phosphorylation of $GABA_A$

receptor subunits or itself may activate an intracellular signalling cascade leading to the persistent functional/structural modification of the $GABA_A$ receptor.

A recent study by Kawaguchi and Hirano (2000) identified a role for postsynaptic $GABA_B$ receptors in the suppression of rebound potentiation. Concurrent stimulation of presynaptic GABAergic interneurones and postsynaptic PNs caused the abolition of rebound potentiation of evoked and mIPSCs. Cerebellar PNs abundantly express $GABA_BR1$ and $GABA_BR2$ subunits and thus may play a role in the suppression of synaptic plasticity. Activation of PKA and specific block of G_i/G_o proteins inhibited the suppression of rebound potentiation. These findings suggest that $GABA_B$R-dependent suppression of rebound potentiation occurs via activation of G_i/G_o, resulting in a decrease in intracellular cAMP concentration and a downregulation of PKA activity. Interestingly, suppression of rebound potentiation only occurred at inhibitory synapses active during PN depolarisation. This synapse-specific suppression by presynaptic activity may play a pivotal role in information processing and storage within the cerebellum.

Hippocampal CA1 neurones have provided a very good model for studying suppression of GABAergic inhibition (DSI) and the transduction cascades. However, recent work published by Caillard and colleagues (1999) displayed a form of long-term potentiation of GABAergic synapses impinging on CA3 pyramidal neurones, termed $GABA_{LTP}$. Repetitive stimulation of the CA3 neurones, using induction protocols similar to that of DSI and rebound potentiation, caused a persistent (>1h) increase in the frequency of spontaneous and mIPSCs with no discernible change in amplitude. Block of the initial postsynaptic rise in calcium, using specific VACC blockers or BAPTA, resulted in the complete abolition of $GABA_{LTP}$. The locus of plasticity was deemed to be purely presynaptic resulting in an increase in the probability of release, rather than an upregulation of postsynaptic $GABA_A$ receptor surface numbers or conductance. Therefore, there remains the possibility that presynaptic control of transmitter release is as much a source of synaptic plasticity as direct enhancement of postsynaptic receptor function. Elucidation of all the receptor subtypes present on putative presynaptic release sites throughout the mammalian CNS will aid in the eventual true understanding of synaptic plasticity.

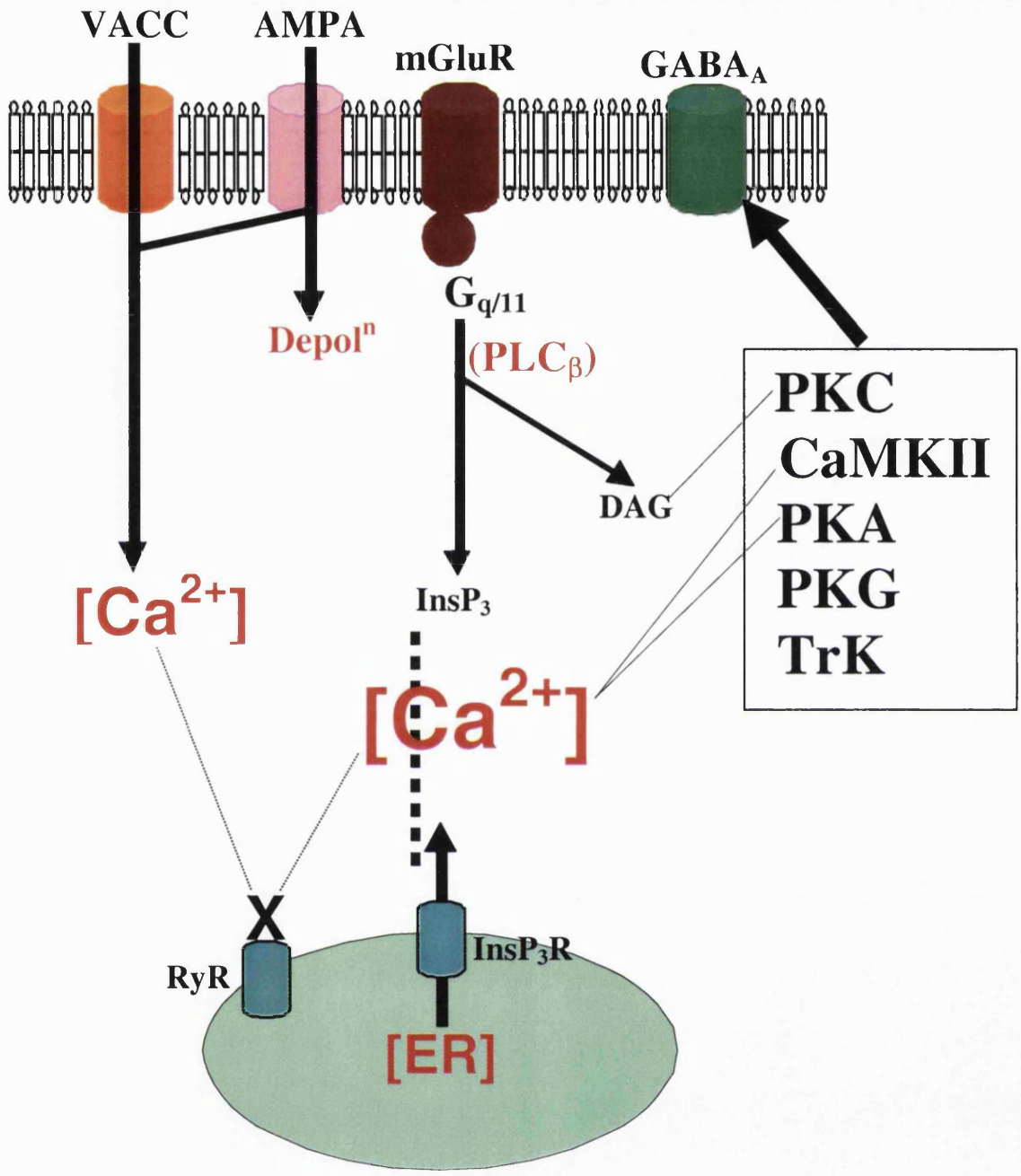

Fig. 1.12. Schematic diagram representing the signal transduction pathways involved in the induction of rebound potentiation of Purkinje neurone $GABA_A$ receptors. Depolarisation and mGluR-mediated increases in cytosolic calcium are the crucial steps involved in the alternative forms of cerebellar synaptic plasticity, DSI and LTD.

Chapter 2
MATERIALS AND METHODS

2.1. Mixed cerebellar cultures

Sterile glass coverslips (22mm diameter) were dipped in ethanol, flamed and placed individually in 33mm plastic dishes. Poly-D-lysine (500μg/ml) was coated on each coverslip and left overnight at 4°C before being washed 3 times with distilled H_2O (dH_2O) and air-dried in a laminar flow hood.

Cerebella from postnatal Sprague Dawley rats (Postnatal day 1 (P1)) were removed after cervical dislocation then decapitation and placed in ice-cold Ca^{2+}/Mg^{2+} free phosphate buffered solution (PBS). Meninges were subsequently removed and whole cerebella were placed in a 0.1% w/v trypsin solution at (20-25°C) for 3 mins. The trypsin solution was then removed and replaced with 1ml DNase (type I) solution (0.05% w/v). Whole cerebella were triturated sequentially with a series of 3 fire-polished Pasteur pipettes (20, 60 and 95% reduction in bore size) until a single cell suspension was obtained. The suspension was centrifuged at 210 X g for 3 minutes, resuspended in 1-2ml of Ca^{2+}/Mg^{2+} free PBS and passed through a 30μm mesh to eliminate large debris and cell clumps. The suspension was then further centrifuged (210 X g for 3 minutes) before being resuspended in 50μl DNase and 800μl horse serum-containing medium. Cells were counted and plated at a density of $5X10^6$ cells/ml. After 24 hours the serum and DNase-containing medium was changed to a serum-free medium (1.5-2ml per dish). Cultures were maintained for >18 days when the morphology, at this stage, is consistent with mature Purkinje neurones (Baptista *et al.*, 1994). Medium was changed every four days, replacing 1 ml of medium per dish (Morrison & Mason, 1998).

2.2. Culture solutions

Ca^{2+}/Mg^{2+} free PBS (per litre) was composed of: NaCl, 140mM; KCl, 4mM; glucose, 11mM; $NaH_2PO_4.H_2O$, 3.6mM; KH_2PO_4, 2.98mM; $NaHCO_3$, 2ml of 2% w/v

stock; phenol red, 0.5ml of 0.5% w/v solution; pH 7.4. Eagle's basal medium (BME) stock solution contained: powdered complete BME mix for 1litre; 980ml dH_2O; 20ml 1M $NaHCO_3$; pH 7.4. Serum containing medium, per 100ml, consisted of: 84ml BME stock solution; 4.8ml of 10% w/v glucose solution; penicillin-streptomycin, 10units/ml; L-glutamine, 0.32mM; 10ml heat-inactivated horse serum; 71µl of 10% w/v NaCl solution; 769µl dH_2O; pH 7.4. Serum-free medium (per 100ml) contained: 1g bovine serum albumin; 93ml BME stock solution; 4.8ml of 10% w/v glucose solution; 1ml serum-free supplement (Final concentrations: 5µg/ml insulin; 5µg/ml apo-transferrin; 5ng/ml sodium selenite); penicillin-streptomycin, 10units/ml; L-glutamine, 0.32mM; 79µl of 10% w/v NaCl solution; 851µl dH_2O; pH 7.4. All serum containing and serum-free medium was prepared fresh on the day of the dissection.

2.3. Composition of superfusing media

The extracellular medium was based on a Krebs solution containing (mM): NaCl, 140; KCl, 4.7; $MgCl_2$, 1.2; $CaCl_2$, 2.52; glucose, 11; HEPES, 5; pH 7.4 (1M NaOH). All experimental protocols required the addition of 10µM 6-cyano-7-nitroquinoxaline-2, 3-dione (CNQX) and 500nM tetrodotoxin (TTX) in order to block non-N-methyl-D-aspartate (NMDA) receptor activation and action potential generation, respectively.

Experiments examining the effects of Na^+ removal were based on using a Krebs solution containing (mM): N-methyl-D-glucamine, 120; KCl, 3; $MgCl_2$, 1.5; $CaCl_2$, 2.5; glucose, 11; HEPES, 10; Mannitol, 27.5; pH 7.4 (6M HCl). To enhance NMDA receptor activation, a nominally zero Mg^{2+} Krebs (Mg-free) containing 10µM glycine and 1µM strychnine was used (Johnson & Ascher, 1987; Mayer & Westbrook 1987; Dingledine *et al.*, 1999)

2.4. Composition of patch clamp internal solution

The patch clamp electrolyte solutions were Cs^+ based containing (mM): CsCl, 150; $MgCl_2$, 1.5; HEPES, 10; Cs-BAPTA, 0.1; Na_2ATP, 2; pH 7.2 (1M CsOH).

Equimolar extracellular and intracellular Cl^- concentrations produced an equilibrium potential for Cl^- +0.69mV. In order to minimse the generation of action potentials within the postsynaptic cell 5mM (N - (2,6 – dimethylphenyl carbamoylmethyl) triethylammonium bromide (QX-314), an internal blocker of voltage-activated sodium channels (Strichartz, 1973) was included.

2.5. Electrophysiological techniques

2.5.1. Whole-cell recording

Individual glass coverslips, coated with mature mixed cerebellar neurones (18-28 days *in vitro* (DIV)), were transferred into a recording chamber (1.5ml) (Fig. 2.1.) and fully superfused with Krebs solution (10.5 ± 0.3ml/min) maintained at 30-32°C. Purkinje neurones (PN) were identified using a Nikon inverted Eclipse TE300 microscope with differential interference contrast microscopy (DIC).

Fig. 2.1. Photograph of the experimental set-up used for whole-cell patch clamp recording.

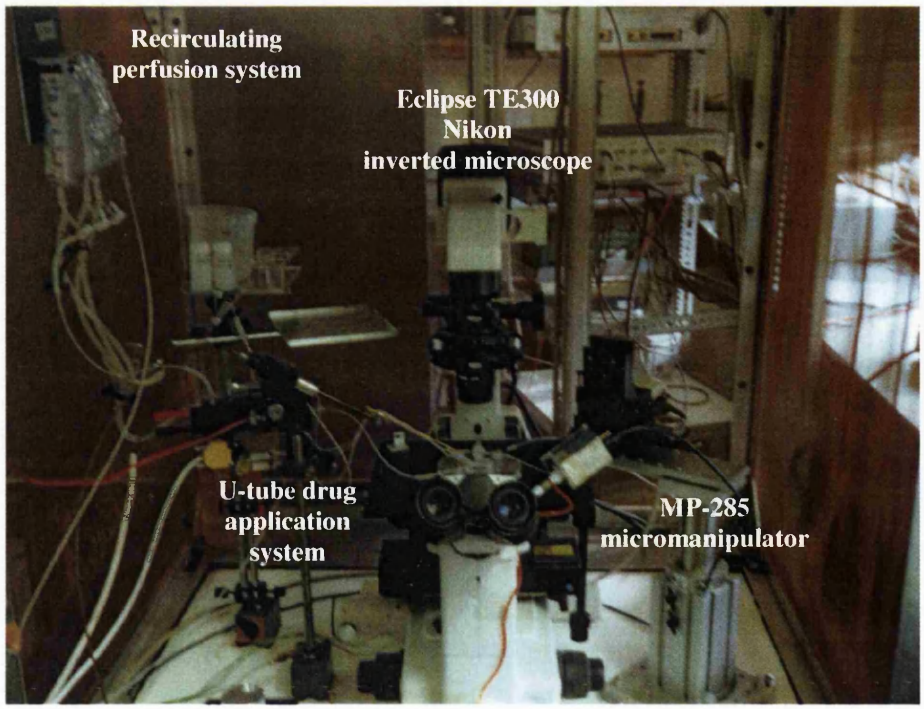

A 20X objective was used for locating Purkinje neurones within the mixed monolayer culture while a 40X objective was used for patch electrode placement and during the attainment of the whole-cell configuration. Purkinje neurones were identified as large, round neurones (soma>20μm) possessing one or two large, flat dendrites.

Microelectrodes were pulled from borosilicate non-filamented, thin-walled glass capillaries (Clark electromedical instruments, GC150T-10) using a Narashige PC-10 vertical, automated micropipette puller. The two stage heat settings allowed the production of stable electrode resistances of 3.5 ± 0.6 MΩ for whole-cell recording of Purkinje neurones and 5.1 ± 0.5 MΩ for recording from interneurones. Microelectrodes were housed in a DB2 holder (constructed to ensure maximal stability due to supporting the electrode at 2 independent points) (G23 Instruments, UCL) and inserted into an axon instruments headstage (1/100 gain). Manipulation of the electrode was achieved using an MP-285, 3-dimensional micromanipulator (Sutter Instruments). Electrodes were brought to 200μm above the cell by executing a pre-programmed robotic series, before manually manoevouring towards the cell surface. Bath electrode/whole-cell capacitance and series resistance compensation was achieved using a patch clamp amplifier (AxoPatch 1C, Axon Instruments). Slight positive pressure was maintained on the patch electrolyte until contact with the cell, then alleviated to induce the cell-attached configuration (R_{patch}>5GΩ). Sharp negative pressure achieved the whole-cell configuration allowing the equilibrium of patch pipette solution with the intracellular milieu. Cells were hyperpolarised and maintained at a holding potential of –70mV.

Table. 2.1. Cell membrane properties of PNs in whole-cell configuration (n=12).

Cell membrane properties	Mean ± s.e
Access resistance	9.3 ± 0.5 MΩ
Resting potential	-56.1 ± 1.97 mV
Series resistance	6.66 ± 0.4MΩ
Membrane capacity	40.5 ± 3.7ρF

2.6. Data recording and electrical stimulation

2.6.1. Seal-test configuration

Electrode resistance measurements, cell-attached configuration and whole cell configuration were achieved in 'Seal-Test' mode in Axon Instruments data acquisition program, Clampex 8. Hyperpolarising pulses (-5mV step, 10ms duration at 50Hz) were applied to the electrode to monitor seal resistance, capacitance and input resistance. Once a stable whole-cell configuration had been achieved 'Test-Seal' mode was terminated and the main 'Scope' window (Clampex 8) activated. All gap-free recording and stimulation protocols were observed in the main 'scope' window as shown in Fig. 2.2.

Fig. 2.2. Clampex 8 'scope' window during gap-free recording of miniature inhibitory postsynaptic currents (mIPSCs), using a holding current of –100pA (ordinate) against real time (ms, abscissa).

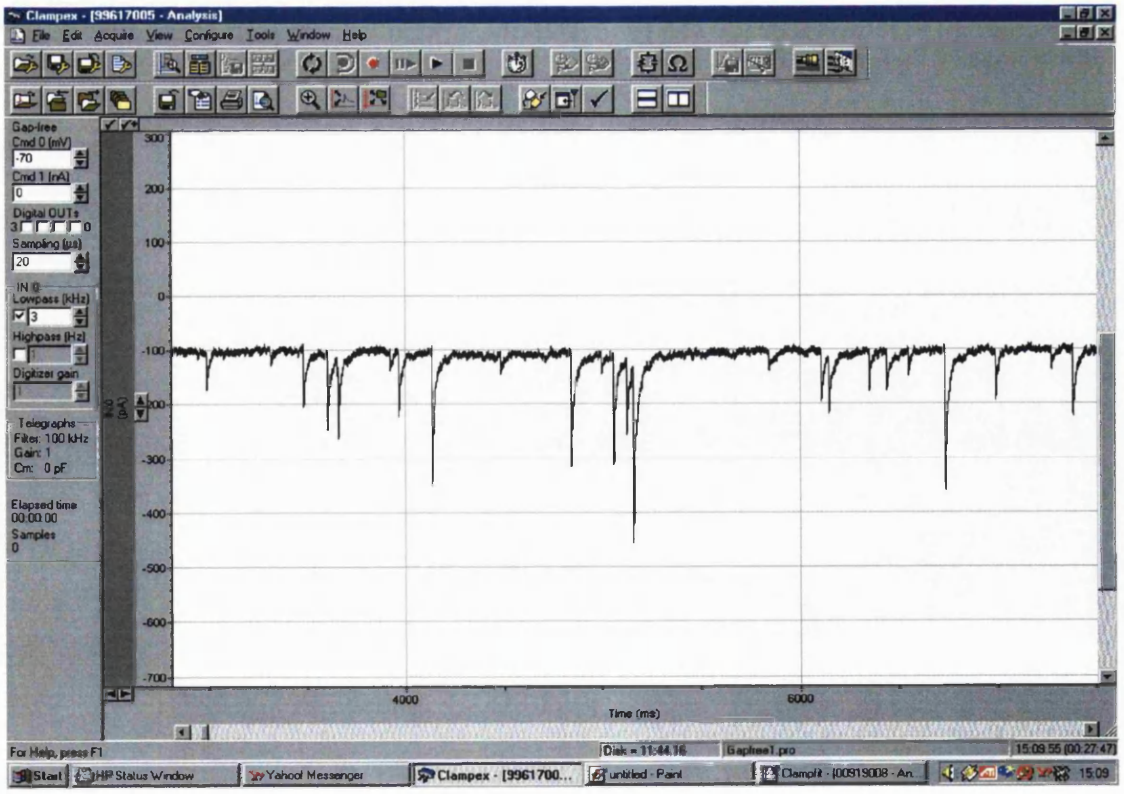

2.6.2. Gap-free recording

Individual cells were left for 3 minutes after going whole-cell in order to attain an equilibrium concentration of Cl^- throughout the cell soma and dense dendritic arbor. Spontaneous mIPSCs were recorded in Gap-free mode, downstreaming directly to a pentium II P400MHz computer (digitising at 20μs per sampled point). All recordings were filtered with an 8-pole Bessel filter at 3kHz (-3dB cut off) using a gain of unity during seal-test configuration and X5 gain during all recording periods. Gap-free recording ceased briefly after the control period to allow stimulation of the cell before returning to Gap-free mode to record for the remainder of the experiment.

2.6.3. Electrical stimulation

Synaptic plasticity was induced by electrical stimulation of the recorded neurone. Depolarisation of the Purkinje neurone was achieved using an episodic stimulation protocol. The membrane potential was depolarised from –70mV to 0mV for the duration of 100ms. This depolarisation was repeated 8 times with an interval between each step of 2s. During each experiment R_{access} (R_a) and R_{series} (R_s) were monitored where possible to identify significant changes. If R_a or R_s increased above 12MΩ the experiment was terminated. A change in holding current to >500pA would also induce the termination of the experiment.

2.6.4. Fast drug application

Focal drug application was achieved using a gravity-fed U-tube controlled by 2 independent solenoids, releasing either drug solution or Krebs (wash-off). The U-tube was positioned approximately 100-200μm leftward of the recording electrode inducing a mean drug onset time of 371±19.7ms. Solutions used in fast drug application were maintained at ambient room temperature (20-25°C) and were applied for 4 seconds before wash-off. The dose-cycle used was 2 minutes to ensure no receptor desensitisation would occur during the duration of the experiment. A diagrammatic representation of the fast drug application is shown in Fig. 2.3.

Fig. 2.3. Fast drug application set-up

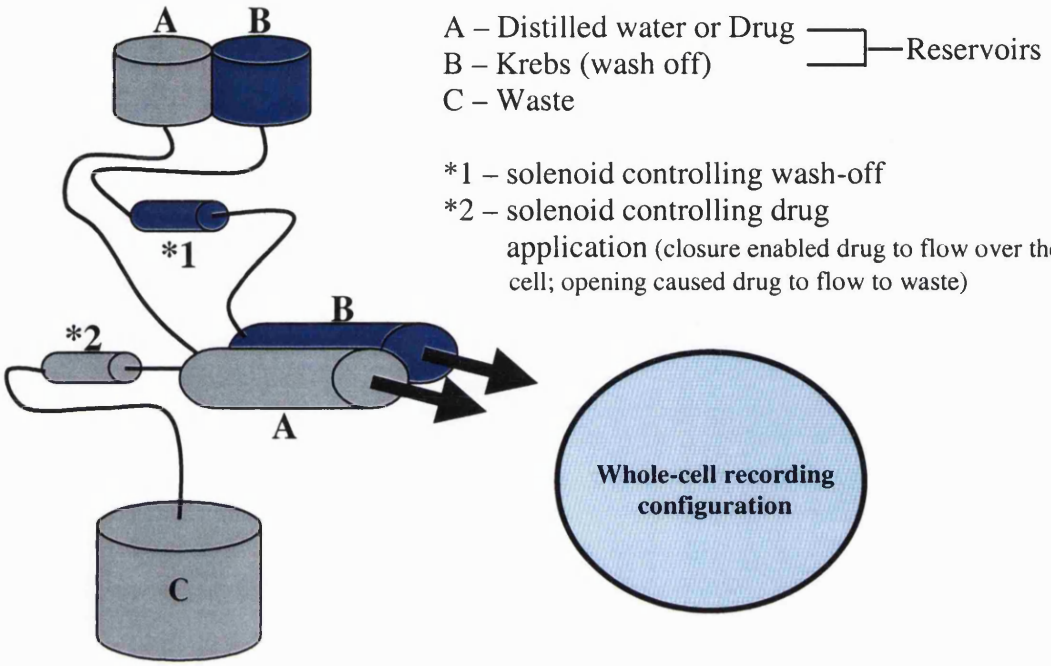

2.7. Immunocytochemical staining

Mixed cerebellar cultures were washed twice with phosphate buffered (PBS) solution before being fixed in 4% paraformaldehyde (in PBS – Sigma electron microscopy grade) for 15 minutes. The paraformaldehyde was quenched with 50mM NH_4Cl (in PBS) before being rinsed thoroughly with PBS. Cells were then permeabilised using 10% v/v foetal calf serum (FCS), 0.5% w/v bovine serum albumin (BSA), 0.1% v/v Triton X in PBS for 20 minutes. To remove Triton X (permeabilising agent) the cells were washed twice in PBS and once in 0.5% BSA, 10% FCS in PBS solution. Permeabilisation was required as all antibodies used during immunocytochemistry recognised either epitopes on intracellular sites of receptor complexes or intracellular proteins. Primary antibody solutions (50µl per coverslip)

were pipetted onto parafilm before placing the coverslip cells-side-down onto the droplet. Antibodies were left to incubate for 30 mins before being washed three times with 0.5% BSA and 10% FCS in PBS solution. Coverslips were then placed on to secondary antibody conjugate solutions (50μl per coverslip) and left to incubate for a further 30 minutes. Aluminium foil was used to cover the coverslips in order to minimise 'photolytic bleaching' of the fluorophores. The final washing process involved two rinses with 0.5% BSA and 10% FCS in PBS and five washes in PBS before coverslips were mounted on glass slides using glycerol gelatin.

2.7.1 Single, double and triple immunocytochemical staining

Identification of Purkinje neurones and their developing morphology was achieved using an antibody recognising an epitope on the calcium binding protein, Calbindin D_{28K}. Purkinje neurones possess an abundance of the calcium binding protein Calbindin D_{28K} in both the soma and nucleus and are the only cell type in the cerebellum to express this protein (German *et al.*, 1997). Therefore, immunocytochemical staining using an anti-calbindin D_{28K} antibody will identify only Purkinje neurones in a mixed cerebellar culture preparation.

Double and triple immunocytochemical staining required careful selection of antibodies in order to minimise the chance of cross-reactivity between the differing antibodies. Primary antibodies were required to have been raised in different host species (e.g. rabbit, mouse, goat). Secondary conjugated antibodies were required to have been raised in the same host species but be directed against the different primary antibody species (e.g. Donkey anti-rabbit, Donkey anti-mouse, Donkey anti-goat). All antibody concentrations were titrated to find the minimal concentration providing adequate staining while minimising the risk of non-specific staining of alternative cellular structures. All antibodies and antibody concentrations are displayed in Table. 2.2.

Table. 2.2. Primary and secondary antibodies* combined with working dilutions.

PRIMARY ANTIBODY	DILUTION	SECONDARY CONJUGATE	DILUTION
1)Anti-Calbindin D_{28K} (mouse)	**1:1,600**	Goat anti-mouse TRITC & FITC	**1:50**
2)Anti-Parvalbumin (mouse)	**1:1,000**	Goat anti-mouse TRITC	**1:50**
3)Anti-$mGluR_{2/3}$ (rabbit)	**1:100**	Donkey anti-rabbit FITC	**1:30**
Anti-Synaptophysin (mouse)	**1:50**	Donkey anti-mouse Cy5	**1:50**
Anti-GAD (goat)	**1:10**	Donkey anti-goat TRITC	**1:30**
4)Anti-Parvalbumin (mouse)	**1:1,000**	Donkey anti-mouse TRITC	**1:50**
Anti-$mGluR_{2/3}$ (rabbit)	**1:100**	Donkey anti-rabbit FITC	**1:30**
5)Anti-Calbindin D_{28K} (mouse)	**1:1,600**	Donkey anti-mouse TRITC	**1:50**
Anti-NR1 (rabbit)	**1:25**	Donkey anti-rabbit FITC	**1:30**
6)Anti-NR1 (rabbit)	**1:25**	Donkey anti-rabbit FITC	**1:30**
Anti-Synaptophysin (mouse)	**1:50**	Donkey anti-mouse Cy5	**1:50**
Anti-GAD (goat)	**1:10**	Donkey anti-goat TRITC	**1:30**

* Refer to 'drugs and their application' for abbreviations and sources of antibodies.

2.8. Confocal Microscopy

Mounted slides were then viewed using a Leica DMRE fluorescence microscope using both X40 (PL APO) and X63 (HCX PL APO) oil immersion objectives. Confocal microscopy was achieved using a Leica TCS SP multi-band confocal imaging spectrophotometer with argon, krypton and helium-neon laser lines (maintained <18°C). The excitation and emission spectra of the fluorophores used during the immunocytochemical staining process are shown in Fig. 2.4.

Fig. 2.4. Excitation and emission spectra for FITC, TRITC and Cy5 fluorophores

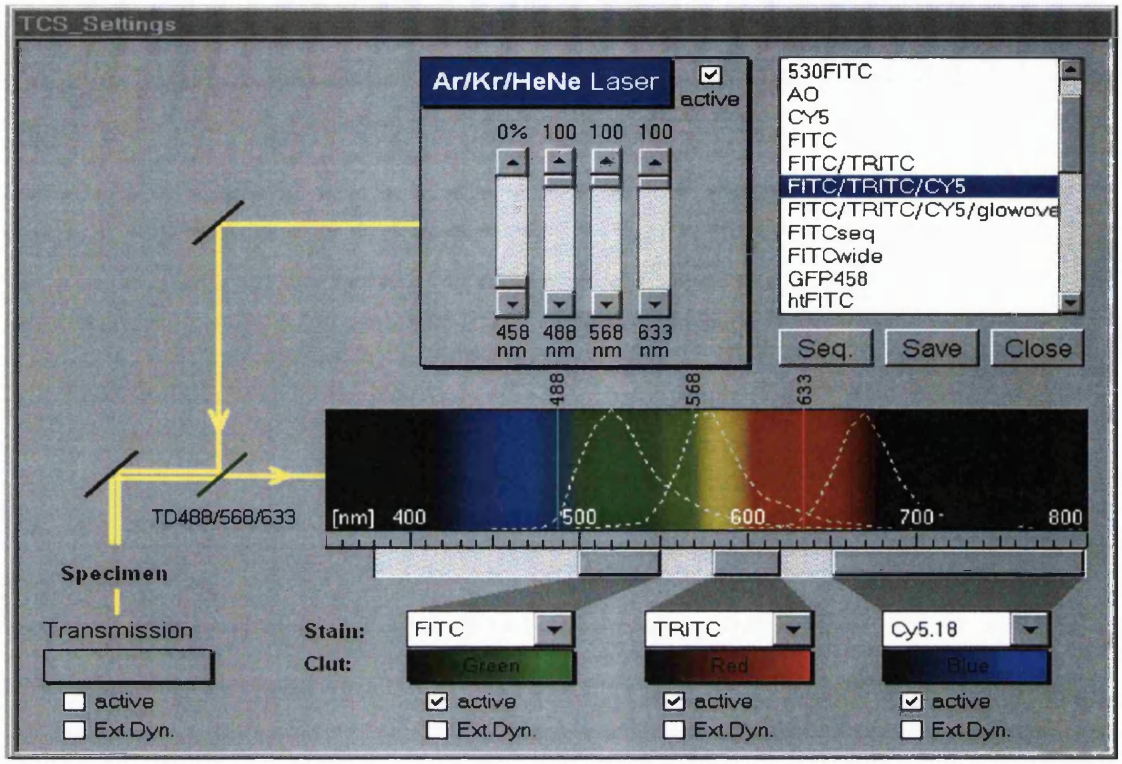

*Laser excitation wavelengths are indicated as solid lines and emission spectra as white dashed lines.

Leica TCS NT acquisition software, running on a Windows NT based operating system, acquired digital fluorescent images. During the acquisition stage only one laser line was switched on (e.g. brightfield + 488nm argon or 568nm krypton or 633nm helium/neon) in order to maximise the acquisition parameters (e.g. photomultiplier tube settings and laser intensity (0-100%)) for each fluorophore independently, ensuring minimal 'bleedthrough'. This technique guaranteed there was no emission at any other wavelengths other than the predicted emission wavelength for that particular fluorophore. Excitation producing emission at more than one wavelength for a single fluorophore is termed 'bleedthrough'. This 'bleedthrough', when using multiple antibodies, could give the appearance of colocalisation without any colocalisation actually occurring, thus stringent precautions must be taken to eradicate this inherent problem. Monitoring of the aforementioned laser intensities and photomultiplier tube levels is of paramount importance, as high levels will induce 'photobleaching' of individual fluorophores during image acquisition. Individual red, green and blue images were analysed off-line using Corel Photopaint 6 and superimposed upon the

corresponding brightfield image. Summated confocal pictures, representative of multiple sections through the specimen, were acquired using a z-plane stage fitted to the fluorescence microscope. Each z-plane section was set at 0.3-0.5μm apart with the total number of sections ranging from 1-25 depending upon specimen size/depth.

2.9. Off-line data analysis and statistical analysis

Electrophysiological data recorded in Clampex 8 and saved as axon binary files (.abf), were opened directly into Mini Analysis program 5.01 (Synaptosoft) for off-line analysis of mIPSCs, as shown in Fig. 2.5.

Fig. 2.5. Analysis and event detection window of Mini Analysis program

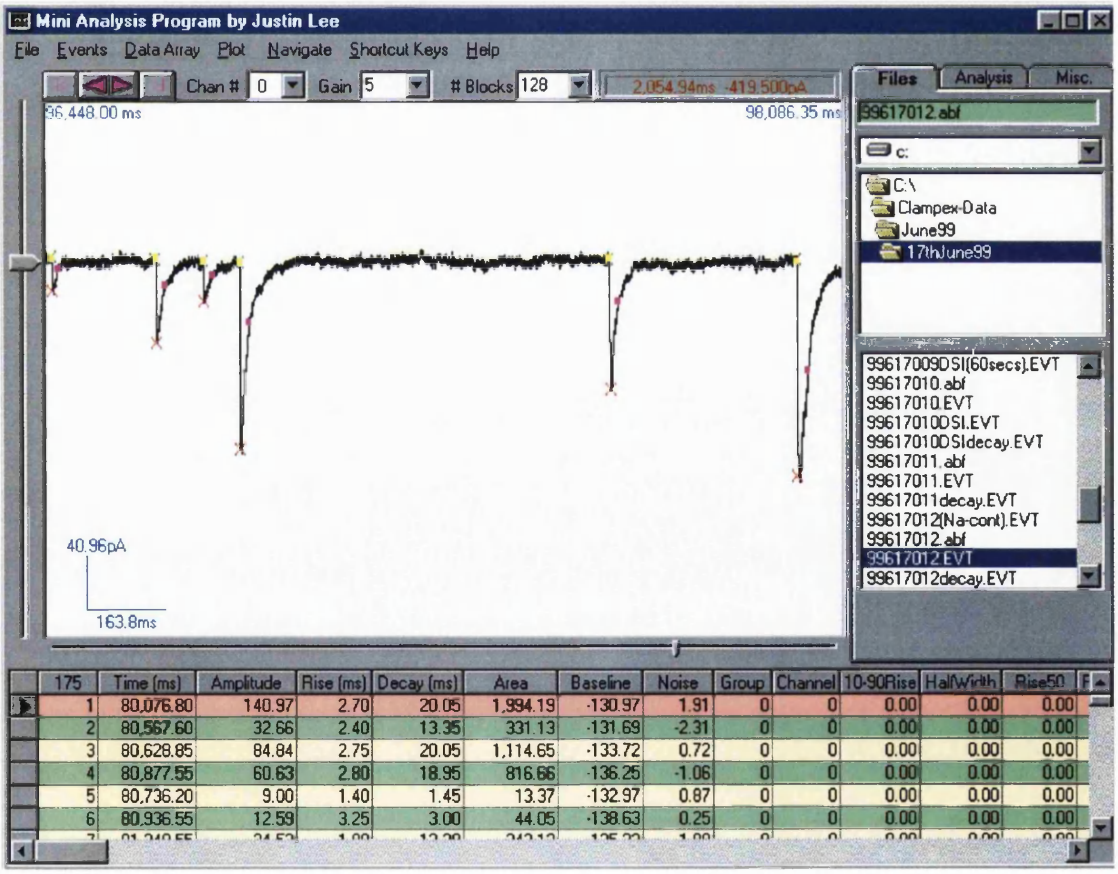

Fig. 2.5. – Key

X - displays the maximum amplitude and time point of the peak event

X - displays the amplitude of half-point of average baseline

■ - displays the time for initialisation of the event

■ - displays the time taken for the event to decay to 1/e of its maximum amplitude (i.e 67% decay of maximum amplitude)

Individual mIPSC peaks were always selected manually, as opposed to batch processing, in order to ensure correct identification of 'real' events throughout the varying time periods of data capture. Individual mIPSC peaks, after selection, were stored as .EVT (event file) for later use in statistical analysis. Event file statistics were displayed as means ± s.e. After optimisation the analysis parameters routinely used during mIPSC detection are summarised in Table. 2.3.

Table. 2.3. Mini analysis program event detection parameters

Analysis parameter	Value
Threshold Amplitude (pA)	**4**
Period to search a local maximum (μs)	**10000**
Time before a peak for baseline (μs)	**5000**
Period to search a decay time (μs)	**20000**
Fraction of peak to find a decay time (peak = 1)	**0.32**
Period to average a baseline (μs)	**2000**
Number of points to average for peak	**1**
Direction of Peak	**Negative**

Clampfit 8 was used to analyse currents induced by fast drug application. Peak amplitude (pA) and drug onset times (ms) were measured and expressed as means ± s.e.

2.9.1 Statistical Analysis

Grouped mIPSC events from periods prior to and after stimulus induction were analysed using the Kolmogorov-Smirnov two-sample test (K-S test). Data (either amplitudes or inter-event intervals) were entered in two arrays compared during the K-S test to identify any significant differences. This statistical test was used due to the ability to compare two populations of data where the population distribution is unknown and the data sets are unequal in size. In each case a two-tailed test was used. An example of the K-S test is shown in Fig. 2.6.

Fig. 2.6. Kolmogorov-Smirnov two-sample test (K-S test)

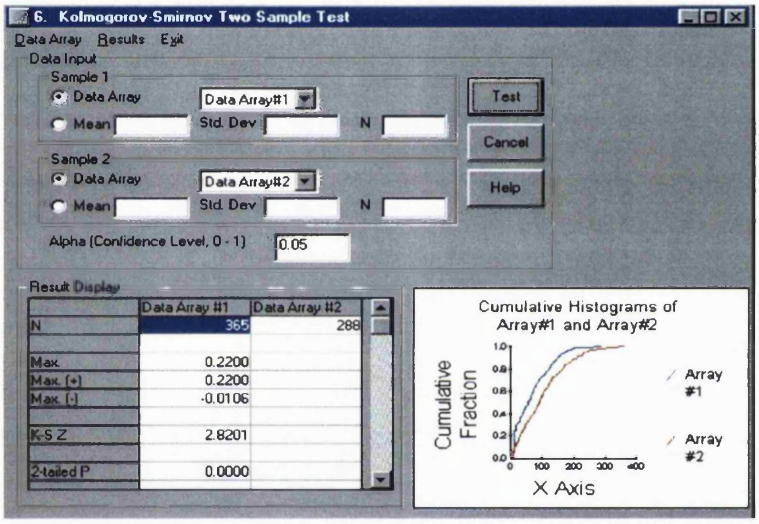

Statistical significance was calculated using a Paired t-test for cells within a group ($P<0.05$) and a one-way ANOVA with bonferroni post test between groups (GraphPad InStat version 3.01, GraphPad Software, USA). All histograms, bar charts and graphs were plotted using Origin 6.0 (Microcal software Inc., USA).

2.10. Drugs and their application

All drug stock solutions were made up in distilled water (concentrations ranging from 200nM to 600μM) with one or two exceptions requiring to be dissolved in 1M

NaOH. Drugs stock solutions were freshly diluted in Krebs solution when applied via superfusion (total volume 30-50mls). The recording chamber volume was approximately 1.5ml with a constant bath flow rate of 10.5 ± 0.3ml/min. Drug application, via bath superfusion, required a delay of 15 seconds before equilibrium in the recording chamber had been reached. All experimental situations utilised Krebs solution containing 10μM CNQX and 500nM TTX in order to block AMPA/Kainate receptor activity and action potential generation, respectively.

Drugs used during fast application via the U-Tube were freshly diluted in Krebs from stocks prepared with distilled water. Drugs applied using this method included, γ-aminobutyric acid (GABA, 1&10μM), NMDA (100μM), D-(2)-amino-5-phosphovalerate (D-APV, 50μM) and L-Serine-O-Sulphate (L-SOS, 300 & 600μM). Each drug dilution and wash-off solution contained CNQX and TTX in order to maintain their superfusing drug concentrations during drug application.

Metabotropic glutamate receptor antagonists, (s)-α-methyl-4-carboxy-phenylglycine ((S)-MCPG) and (αS) -α-amino-α- [(1S,2S) -2-carboxycyclopropyl] -9-H-xanthine-9-propanoic acid (LY341495) were supplied by Tocris.

NMDA and the NMDA receptor antagonist, D-APV, were supplied by Sigma and Tocris respectively.

N-methyl-D-glucamine ($NMDG^+$), mannitol and all other reagents used in formulating Krebs solutions were of 'Analar' grade and supplied by BDH.

Tetrodotoxin, picrotoxin , 1,2,bis(2-aminophenoxy)ethane-N,N,N',N'-tetraacetic acid (BAPTA), L-SOS, glycine, strychnine and Adenosine Triphosphate (ATP) were supplied by Sigma.

CNQX and QX-314 were supplied by Tocris.

FCS was supplied by Gibco.

t-octylphenoxypolyethoxyethanol (Triton X), paraformaldehyde, ammonium chloride (NH_4Cl), PBS, BSA and glycerol were all obtained from Sigma. Antibodies used during immunocytochemistry and their suppliers are listed in the Table. 2.4.

Table. 2.4. Antibody nomenclature and suppliers

Primary antibodies	**Supplier**
Rabbit anti-NR1	**Prof. R. Huganir (Baltimore)**
Mouse anti-Calbindin D_{28k}	**Sigma**
Rabbit anti-Calbindin D_{28k}	**Swant, Switzerland**
Mouse anti-Synaptophysin	**Biomeda Corporation, U.S.A**
Goat anti-Glutamic acid decarboxylase (GAD)	**Roche, U.K**
Rabbit anti-Metabotropic glutamate receptor 2/3 ($mGluR_{2/3}$)	**Upstate Biotechnology, U.S.A**
Mouse anti-Parvalbumin (PV)	**Sigma**
Secondary Antibodies	
Goat anti-mouse tetramethyl rhodamine isothyocyante (TRITC)$^{+}$	
Goat anti-mouse fluorescene isothyocyante (FITC)$^{+}$	**Sigma^{+}**
Donkey anti-rabbit fluorescene isothyiocyanate (FITC)*	
Donkey anti mouse Cyanine Dye 5 (Cy5)*	***Stratech Scientific Ltd, U.K**
Donkey anti-goat tetramethyl rhodamine isothyocyante (TRITC)*	
Donkey anti-goat Cy5*	
Donkey anti-mouse TRITC*	

Chapter 3

MORPHOLOGICAL CHANGES DURING DEVELOPMENT OF PURKINJE NEURONES IN CULTURE

INTRODUCTION

Purkinje neurone development *in vivo* can be segregated into four major stages. Initially, during midgestation, the PNs have smooth round cell bodies with only a few minor processes 'sprouting' from the soma. This period is when PNs begin to migrate to a position beneath the external granular layer, meanwhile juvenile climbing fibres, which have not yet arbourised, begin to make synaptic contact with the PN soma. Secondly, PNs in the early neonatal stage of development lose their primitive processes and develop more substantial perisomatic extensions. At this point climbing fibres develop to form a nest of terminals covering the entirety of the PN soma. Thirdly, flat apical dendrites emerge forming the basis for the dense dendritic tree observed in adult PNs. Elongation of the climbing fibre axons allow the development of synapses with the ascending apical dendrite. At this stage the second excitatory afferent input, parallel fibres (T-shaped axons of granule cells), extend orthogonal to the dendrites. Finally, as the dendritic arbour of the PN develops both climbing and parallel fibres synapse with specific subsets of synaptic spines in order to provide complete excitatory afferent input (Ramon Y Cajal, 1960; Altman, 1972; Altman & Bayer., 1978; Berry & Bradley., 1976; Hendelman & Aggerwal, 1980; Laxson & King, 1983; Mason *et al.*, 1990). Inhibitory afferent input to PNs arises from two types of molecular layer interneurones, basket cells (BC) and stellate cells (SC). These cells originate from dividing progenitor cells in the white matter between P1 and P14 (Zhang & Goldman, 1996) and reach their final destination in the molecular layer, between P7 and P21 (Altman, 1972, Zhang & Goldman, 1996). Functional studies have reported PN inhibition as early as P10 (Crepel, 1974) where, in mature rats, interneurones outnumber PNs by 10:1 (Korbo *et al.*, 1993).

Interestingly, *in vitro*, PN development can mimic the *in vivo* situation depending upon which cell types are present and the neurotrophic factors derived from

such innervation. Coculture of PNs with a monolayer of granule cells can aid their survival and support more pronounced dendritic differentiation of mature PNs (Baptista *et al.*, 1994; Morrison & Mason., 1998; Hirai & Launey., 2000). Neurotrophins, a family of structurally and functionally related peptide growth factors, including neurotrophin-3 (NT-3), NT-4/5, nerve growth factor (NGF) and brain-derived neurotrophic factor (BDNF), are produced in abundance in cerebellar granule cells (Rocamora *et al.*, 1993). Neurotrophins also exert their action on granule cells as they possess Trk receptors (receptors activated by neurotrophins) and are therefore responsive to neurotrophins (Schwartz *et al.*, 1997; Segal *et al.*, 1992, 1995; Gao *et al.*, 1995). Moreover, the stimulation of NMDA receptors, present on granule cells, induces the synthesis and release of BDNF having a twofold effect. Firstly, this promotes the survival and differentiation of granule cells. Secondly, BDNF aids in the differentiation of PN dendrites, the site of granule cell afferent input (Moran & Patel, 1989; Burgoyne *et al.*, 1993; Marini *et al.*, 1998). Therefore, activation of NMDA receptors (NMDAR) on granule cells may play a pivotal role in the differentiation of PNs via an indirect increase in trophic factor release. Hirai & Launey (2000) identified a link between BDNF-TrkB signalling pathway in granule cells and enhanced PN differentiation. Overwhelming evidence suggests that granule cell NMDAR-mediated release of neurotrophins is a pivotal step in the maturation of PNs in culture. Interestingly, a recent report by Mertz and colleagues (2000) identified BDNF as promoting basket/stellate cell differentiation and thus enhancing synaptic connectivity with PNs in culture. Therefore, the production of mixed cerebellar cultures, which mimic *in vivo* cell maturation due to sufficient neurotrophin levels, requires a high cell density ($5.0x10^6$ cell/ml) where granule cells constitute >70% of the neuronal cells present.

RESULTS

Identification of the morphological changes occurring during development of PNs was achieved using a monoclonal antibody recognising an epitope on the primary PN calcium binding protein, Calbindin D_{28K} (Celio, 1990; De Talamoni *et al.*, 1993). Titration of the antibody concentrations identified 1:1600 (primary) and 1:50 (secondary) as the optimal working concentrations in order to identify PN morphology without creating high levels of background astroglia staining.

Mixed cerebellar cultures maintained in Eagles Basal Medium (BME) solution showed early development consistent with that of *in vivo* PN development. The production of minor processes emanating from the smooth round soma occurred directly after plating continuing through to 3 DIV (Fig. 3.1 A&B). Subsequently, substantial perisomatic extensions replaced the primitive processes (Fig. 3.1 C&D) while the PN axon (Fig. 3.1D, white arrow) extended >100μm through the culture, bifurcating several times. The emergence of the apical dendrite occurred at approximately 8 DIV (Fig. 3.1 D, yellow arrow). At this morphological stage a single primary dendrite existed of limited length forming the basis of the PN dendritic tree. Elongation of the primary dendrite persisted from 8-14 DIV with the emergence of secondary and tertiary dendrite branchlets (Fig. 3.2 A&B, yellow arrows). During the dendrite elongation phase, synaptogenesis occurred forming synapses with both excitatory (granule cell-parallel fibres) and inhibitory (basket and stellate cells) afferent inputs, forming the basis for electrical control of the mature PN. Extensive dendrite branching occurred in cultures maintained for ≥ 21 DIV (Fig. 3.2 C&D, Fig. 3.4 & Fig. 3.6, yellow arrows) where upon synaptogenesis continued to occur, providing the mature PN with a multitude of synaptic inputs. Close examination of mature PN dendrites revealed the existence of fully formed spines (Fig. 3.3, Fig 3.5 & Fig 3.7) on the proximal and distal dendrites thus identifying the existence of excitatory afferent input and general survivability of the neurones. Application of 20mM K^+ to the BME based culture medium increased the survival rate of granule cells in the mixed cerebellar culture. However, this did not alter the survival rate of the PNs after plating but induced an increase in the morphological level of synaptogenesis such that the PN dendrite adopted an intense 'feathery'. Electrophysiological recordings from cells maintained in high K^+ displayed similar

GABAergic activity when compared to cells maintained in low K^+ medium. In conjunction with the formation of functionally mature PNs, depicted by the level of dendritic differentiation and spine formation, this study required the production of mature basket/stellate cells, constituting the main PN inhibitory afferent input, in order to examine PN inhibitory synaptic plasticity. Identification of mature cerebellar basket/stellate cells was achieved using a monoclonal antibody recognising an epitope on the second major calcium binding protein present in the cerebellum, parvalbumin (Celio, 1990; De Talamoni *et al.*, 1993). The mixed cerebellar cultures utilised within this study (18-21 DIV) contained a multitude of mature basket cells (BC) and stellate cells (SC) possessing fully differentiated dendrites and elongated, varicosity rich axons (Fig. 3.8 A, B, C & D). Passive observations of immunocytochemically stained cultures identified relatively few cerebellar Golgi cells (GC) and PNs in comparison to PV positive basket/stellate cells with the ratio of PN : BC/SC : GC approximately 1 : 20 : 1.

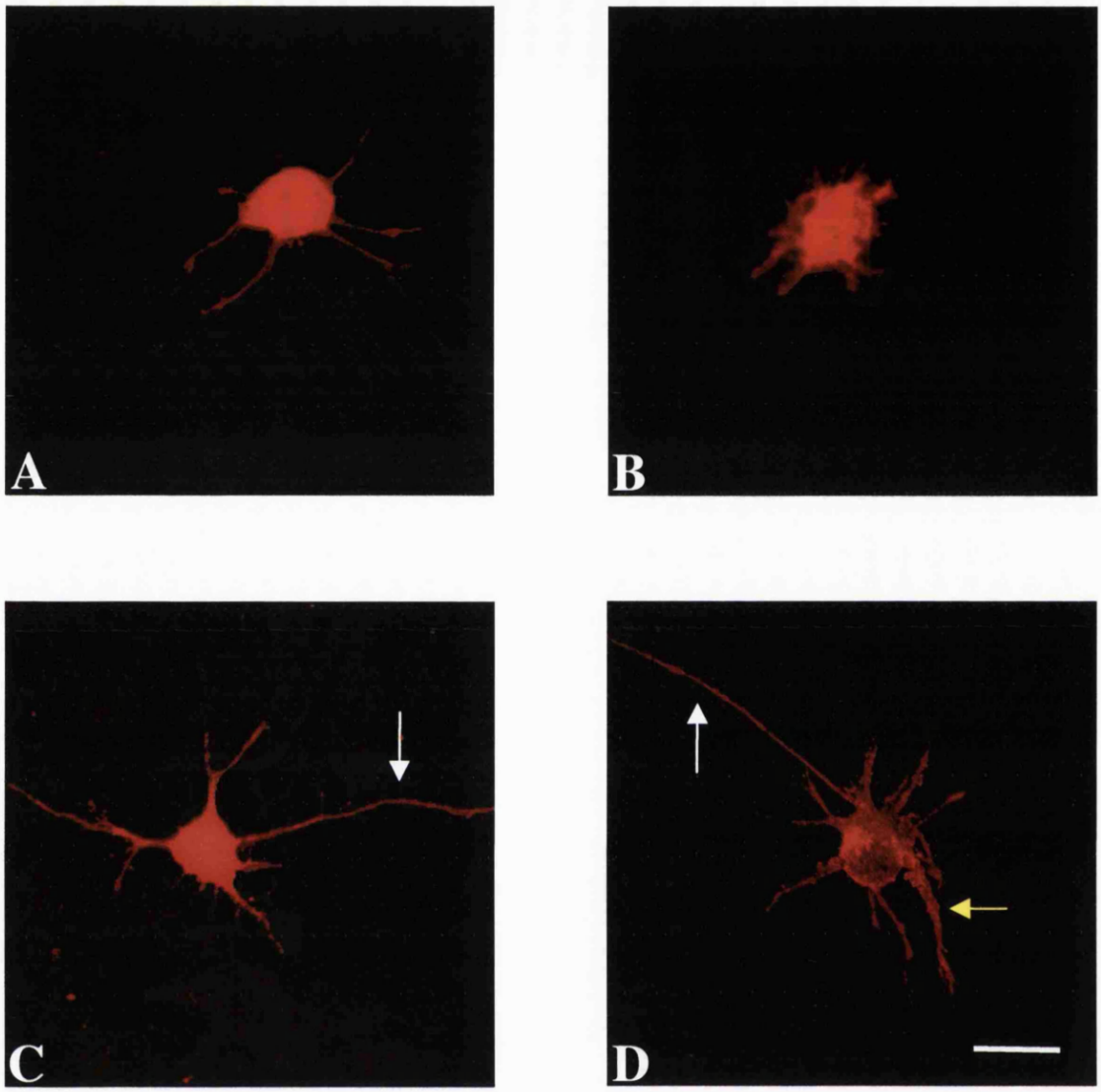

Fig. 3.1. Morphological development of cerebellar Purkinje neurones *in vitro*. Immunocytochemical staining using an anti-Calbindin D_{28K} antibody with an anti-mouse TRITC conjugate to identify developmental changes in Purkinje neuronal differentiation at 2 (A), 3 (B), 5 (C) and 8 (D) days *in vitro* using confocal microscopy. Arrows depict bifurcating axon (white arrow) and primary dendrite (yellow arrow). Images were acquired at X40 magnification with 25% zoom (scale bar = 15μm).

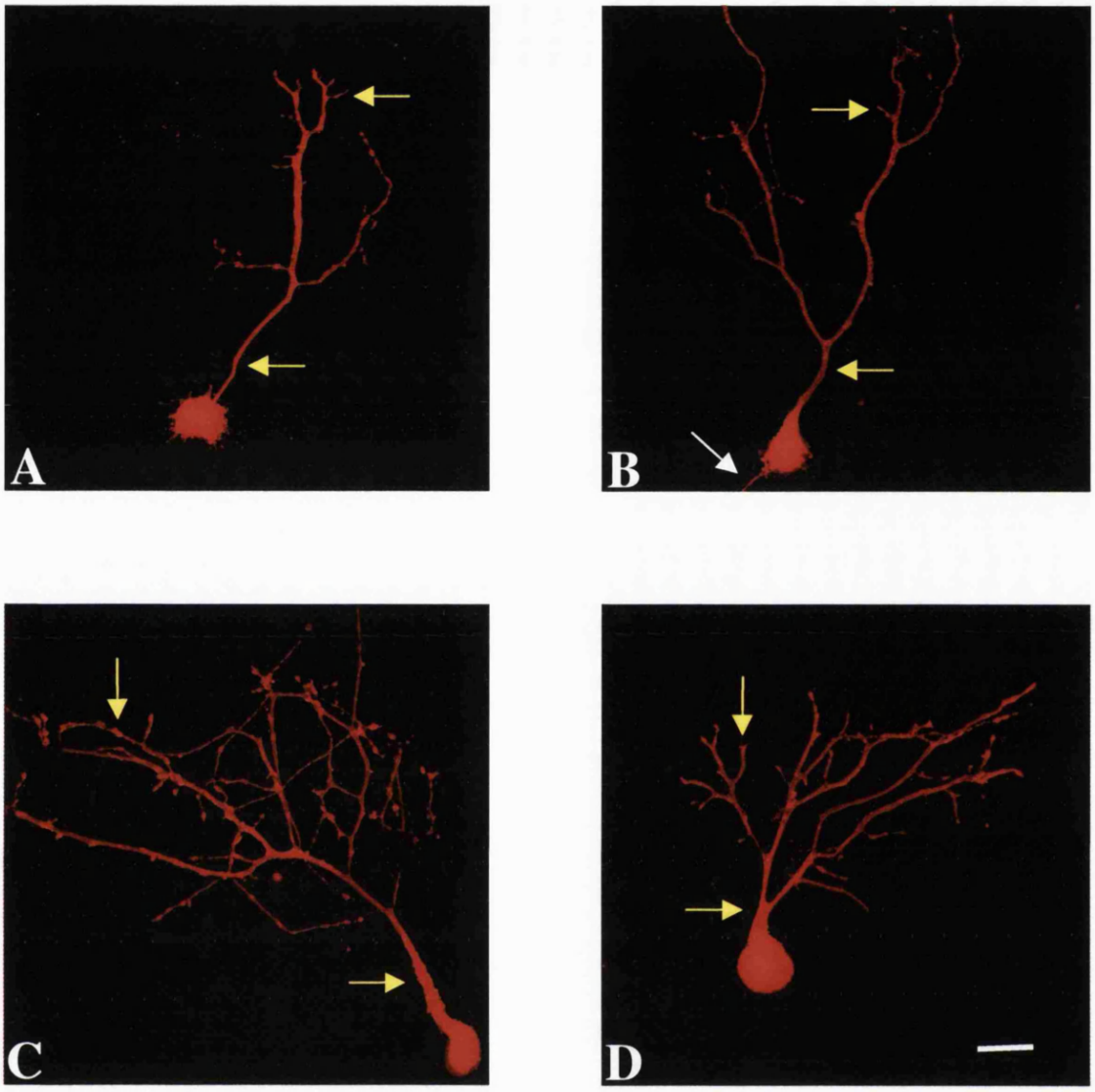

Fig. 3.2. Morphological development of cerebellar Purkinje neurones *in vitro*. Immunocytochemical staining using an anti-Calbindin D_{28K} antibody with an anti-mouse TRITC conjugate to identify developmental changes in Purkinje neuronal differentiation at 14 (A&B) and 21 (C&D) days *in vitro* using confocal microscopy. Arrows depict bifurcating axon (white arrow) and primary and tertiary dendrites (yellow arrows). Images were acquired at X40 magnification with zero zoom (scale bar = 20μm).

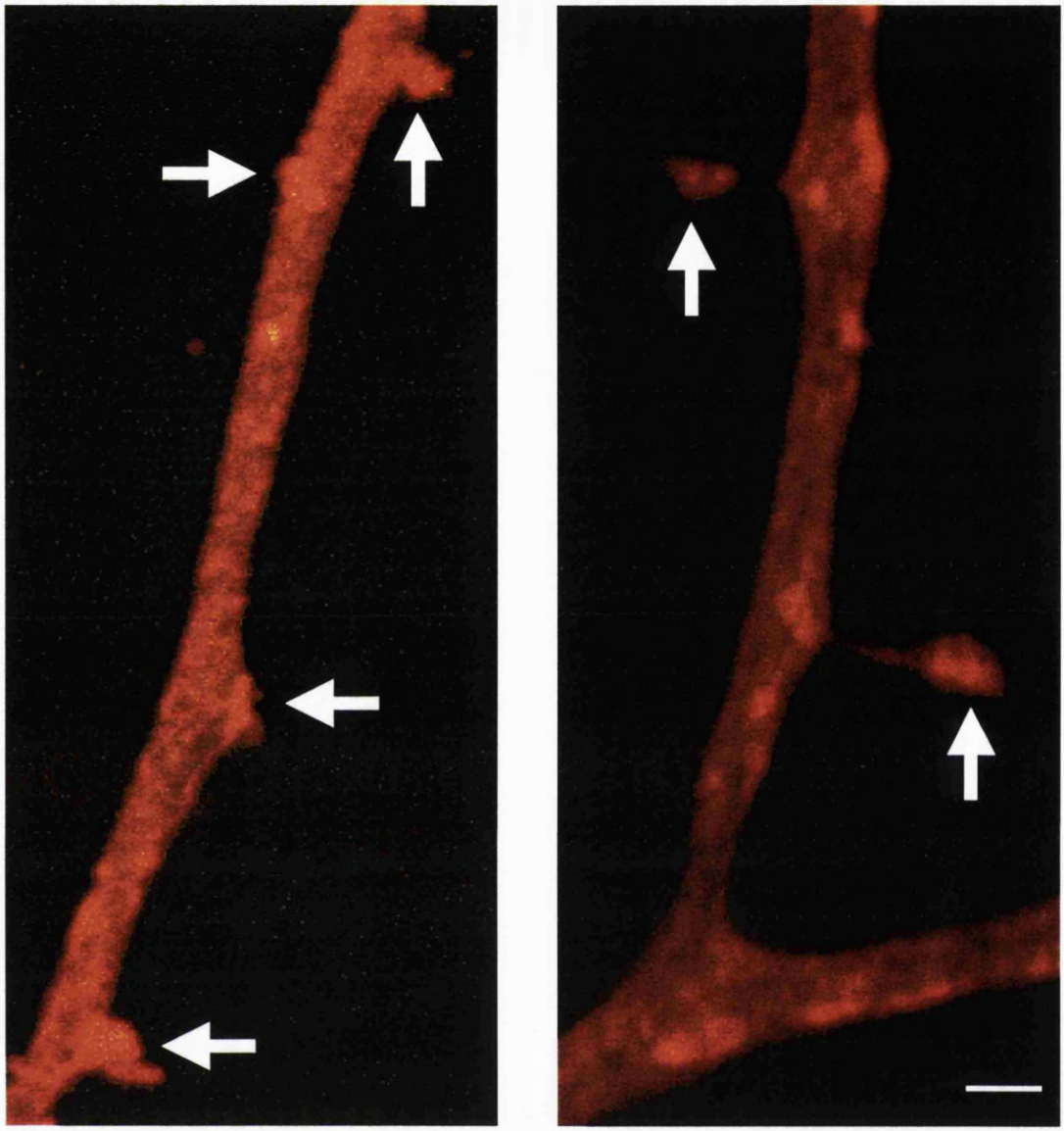

Fig. 3.3. Spine formation on mature cerebellar Purkinje neurones *in vitro*. Immunocytochemical staining using an anti-Calbindin D_{28K} antibody with an anti-mouse TRITC conjugate to identify single spines on mature Purkinje neurone dendrites (21 days *in vitro*) using confocal microscopy. Arrows depict mature spine head formation on secondary and tertiary PN dendrites. Images were acquired at X63 magnification with 75-100% zoom (scale bar = 1μm).

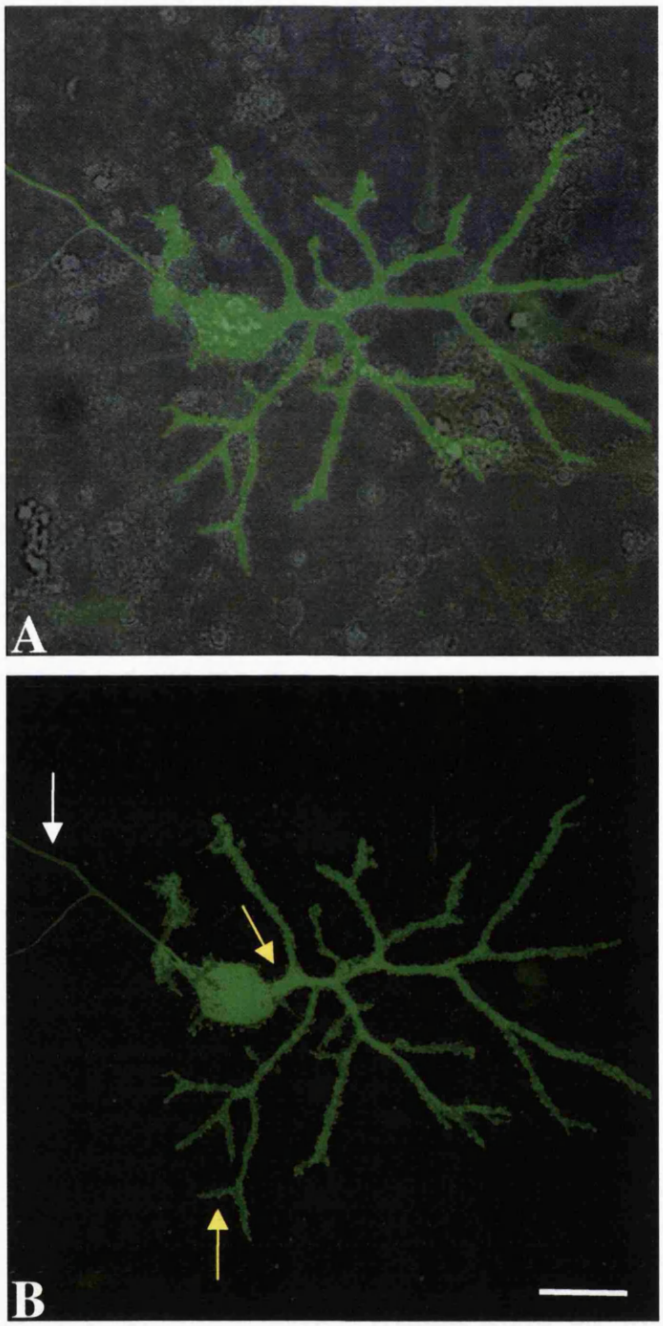

Fig. 3.4. Morphological development of cerebellar Purkinje neurones *in vitro*. A & B, Immunocytochemical staining using an anti-Calbindin D_{28K} antibody with an anti-mouse FITC conjugate to identify the morphology of mature Purkinje neurones at 21 days *in vitro* (A, Purkinje neurone morphology superimposed on corresponding brightfield image) using confocal microscopy. Arrows depict bifurcating axon (white arrow) and primary and tertiary dendrites (yellow arrows). Images were acquired at X40 magnification with 50% zoom (scale bar = 25μm).

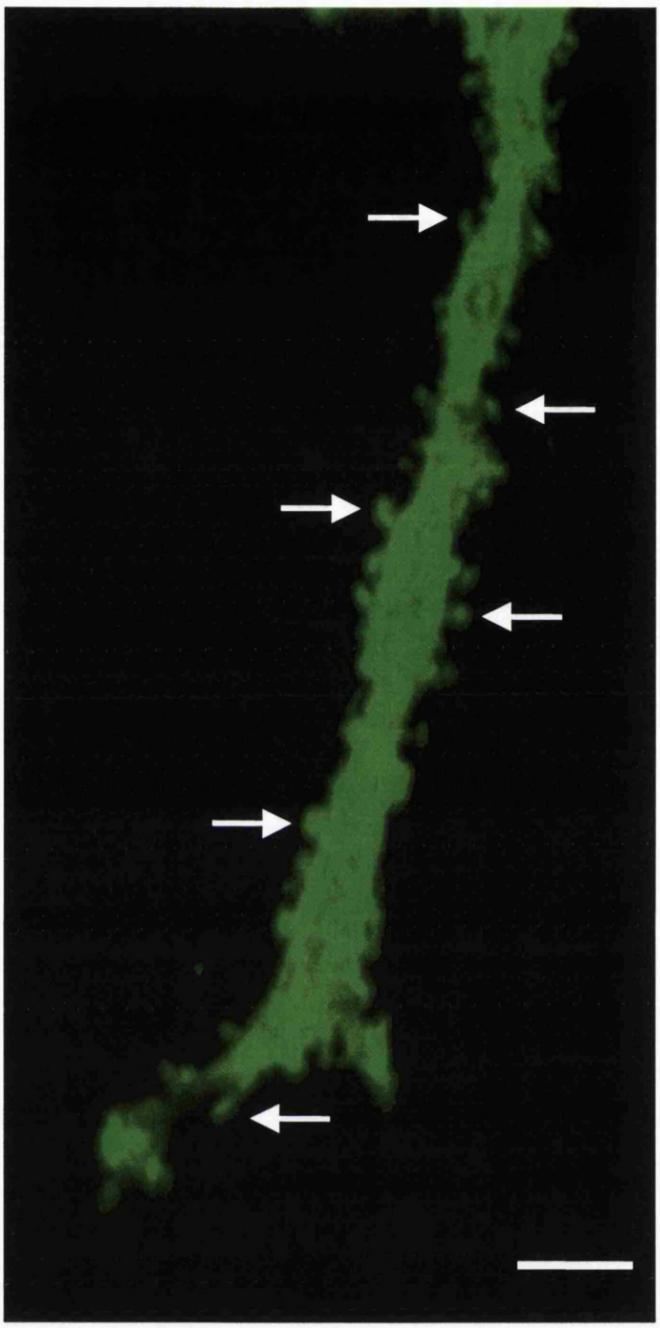

Fig. 3.5. Spine formation on mature cerebellar Purkinje neurones *in vitro*. Immunocytochemical staining using an anti-Calbindin D_{28K} antibody with an anti-mouse FITC conjugate to identify single spines on mature Purkinje neurone dendrites (21 days *in vitro*) using confocal microscopy. Arrows depict mature spine head formation on secondary and tertiary PN dendrites. Images were acquired at X63 magnification with 25% zoom (scale bar = 5μm).

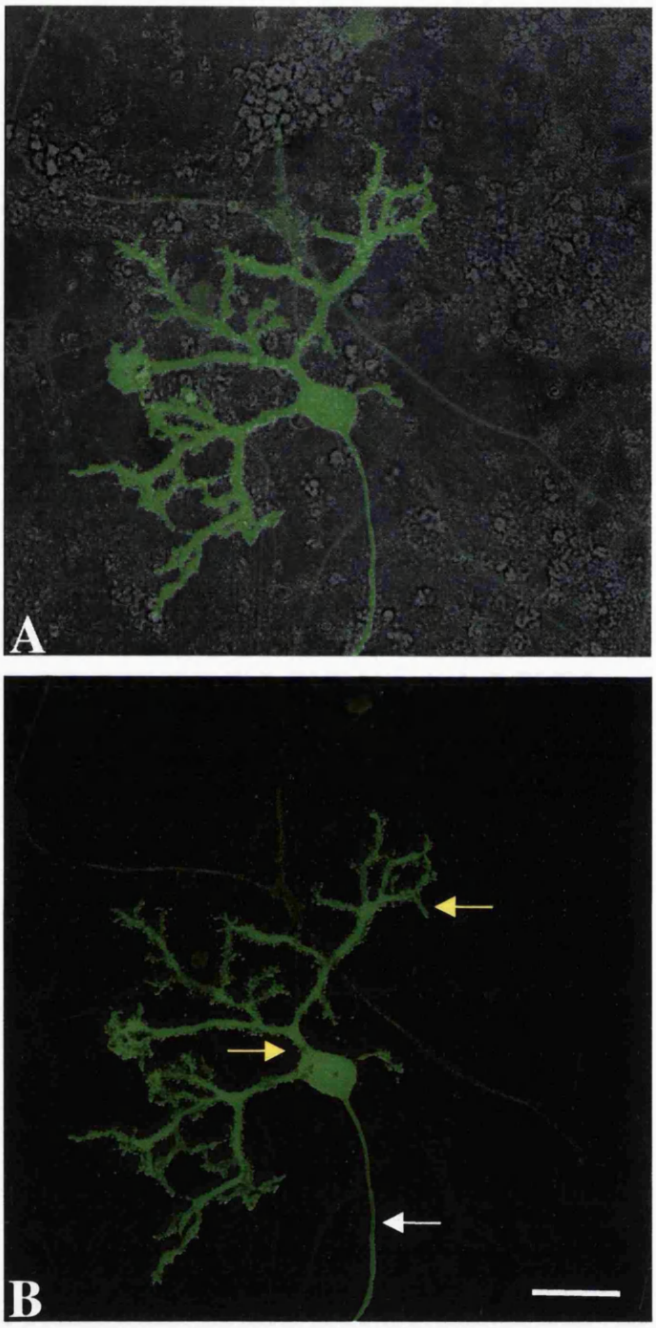

Fig. 3.6. Morphological development of cerebellar Purkinje neurones *in vitro*. A & B, Immunocytochemical staining using an anti-Calbindin D_{28K} antibody with an anti-mouse FITC conjugate to identify the morphology of mature Purkinje neurones at 21 days *in vitro* (A, Purkinje neurone morphology superimposed on corresponding brightfield image) using confocal microscopy. Arrows depict bifurcating axon (white arrow) and primary and tertiary dendrites (yellow arrows). Images were acquired at X40 magnification with 50% zoom (scale bar = 25μm).

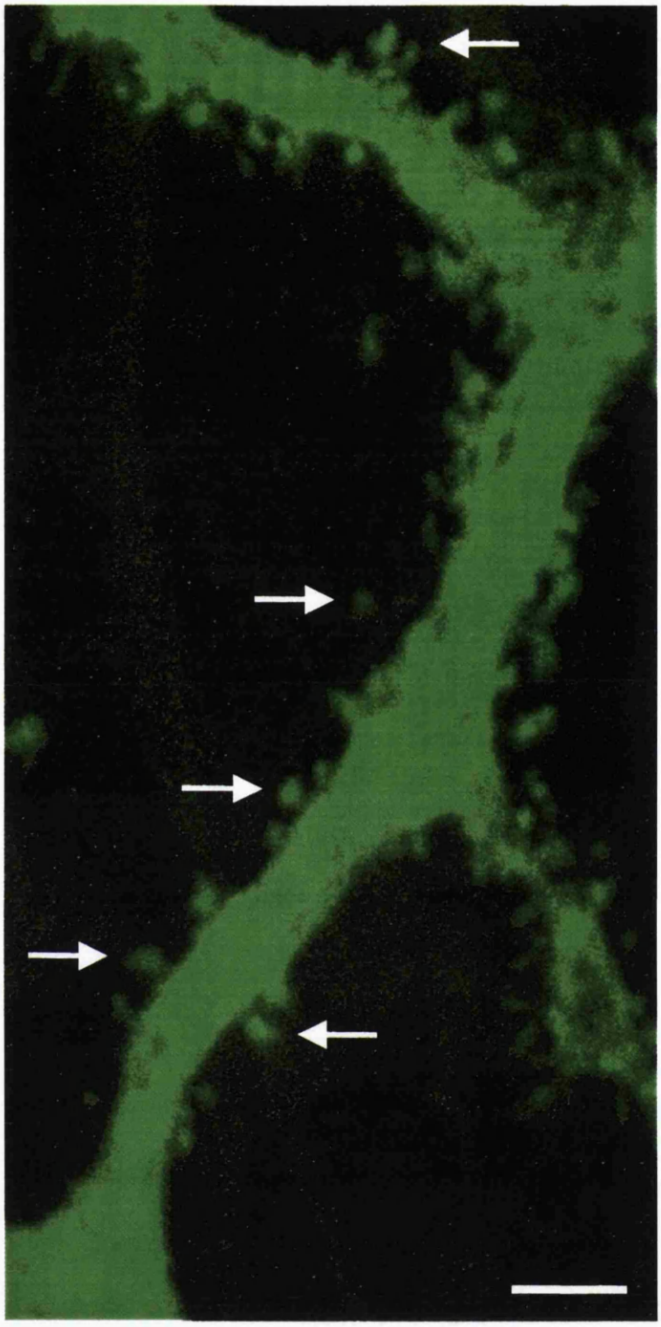

Fig. 3.7. Spine formation on mature cerebellar Purkinje neurones *in vitro*. Immunocytochemical staining using an anti-Calbindin D_{28K} antibody with an anti-mouse FITC conjugate to identify single spines on mature Purkinje neurone dendrites (21 days *in vitro*) using confocal microscopy. Arrows depict mature spine head formation on secondary and tertiary PN dendrites. Images were acquired at X63 magnification with 25% zoom (scale bar = 5μm).

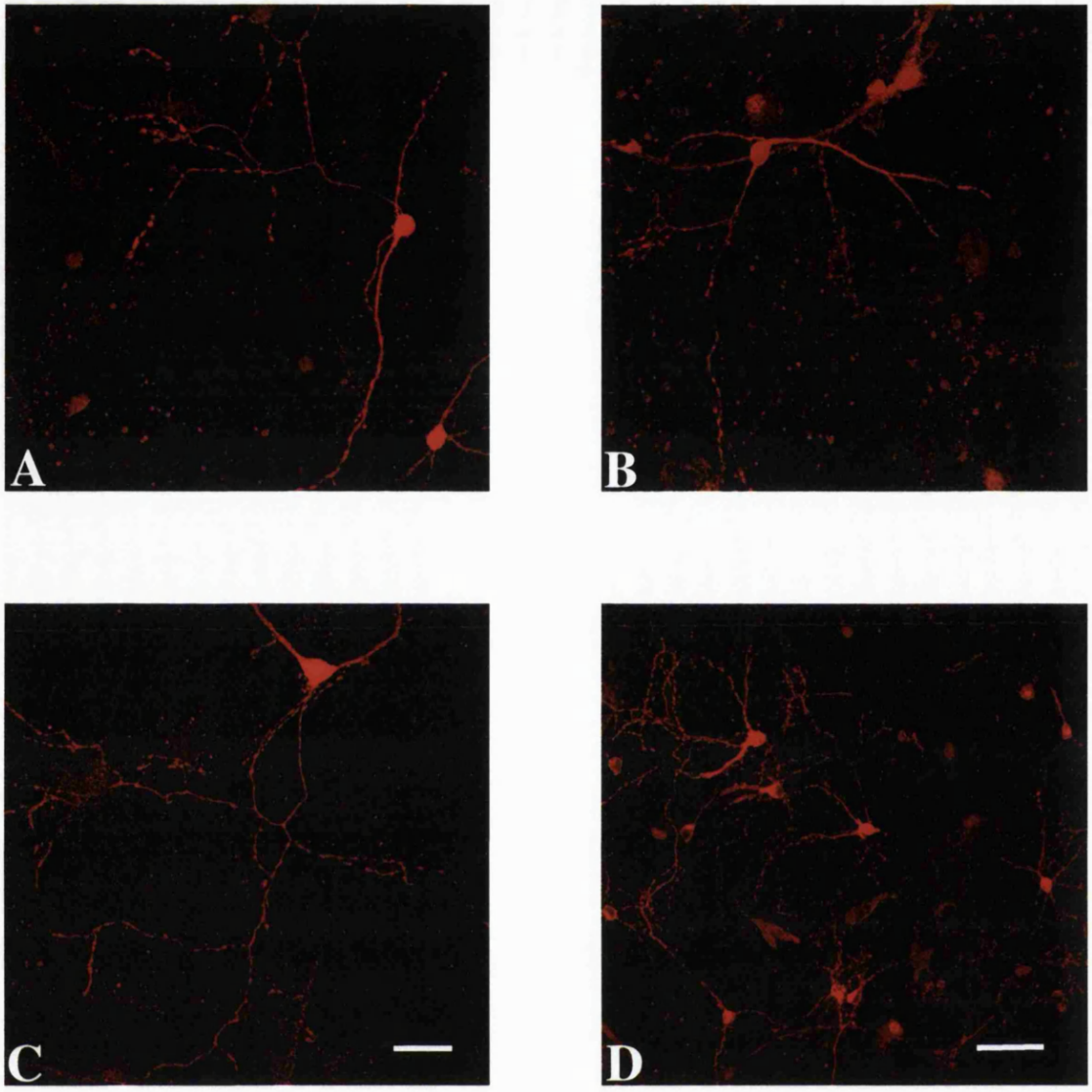

Fig. 3.8. Mature cerebellar basket and stellate cells *in vitro*. Immunocytochemical staining using an anti-parvalbumin antibody with an anti-mouse TRITC conjugate to identify the morphology of mature cerebellar basket/stellate cells (A-D, 21 days *in vitro*) using confocal microscopy. A-C, images were acquired at X40 magnification with 25% zoom (scale bar = 15μm). D, image was acquired at X25 magnification with 0% zoom (scale bar = 30μm).

DISCUSSION

The morphological changes occurring in the mixed cerebellar cultures used within this study concur well with those proposed for *in vivo* cerebellar cell maturation. Interestingly, the developmental changes are also consistent with previous findings in cultured cerebellar PNs (Baptista *et al.*, 1994; Morrison & Mason, 1998; Hirai & Launey, 2000) despite there being quite fundamental differences in culture media between these studies. There still remains much controversy as to the exact requirements, in terms of neurotrophic factors and afferent synaptic input, in order to produce sufficiently differentiated cerebellar PNs displaying electrical activity similar to that of their *in vivo* counterparts. The work carried out here has identified a protocol which consistently produced mixed cerebellar cultures of high quality and survival rate. Mature cultures provided PNs with an array of excitatory and inhibitory afferent inputs in order to maximise neuronal maturation and differentiation. Immunocytochemical staining provides evidence to support this as the Calbindin D_{28K} staining identified robust, healthy neurones while electrophysiological data identified PNs as having membrane properties (see Table 3.1. below) similar to that of PNs in cerebellar slice preparations (Llinas & Sugimori, 1980).

Table. 3.1. Cell membrane properties of PNs (>18DIV) in whole-cell configuration (n=12).

Cell membrane properties	Mean ± s.e
Resting potential	-56.1 ± 1.97 mV
Membrane capacity	40.5 ± 3.7ρF

The most compelling evidence as to the similarities between *in vivo* and *in vitro* PN cell differentiation arose at 8 DIV. At this timepoint *in vivo*, the emergence of electrical activity in PNs (7-9DIV) occurs coincident with the initiation of dendritic branching (7-9 DIV) (Schilling *et al.*, 1991). This coincidence induces further dendritic differentiation resulting in the dense dendritic arbour stereotypical of the mature PN. In the present study the emergence of the proximal dendrite at 8 DIV is consistent with this hypothesis and results, at 14 and 21 DIV, in the existence of PNs with highly branched

dendritic arbours. The coincident formation, during synaptogenesis, of fully formed spines indicates the level of excitatory afferent input to the mature PN. Early light microscopic studies of Golgi-stained cerebellar tissue identified an abundance of 'spines' on mature PNs. Each mature PN is estimated to possess ~200,000 spines, each one representative of a single excitatory input from a single granule cell axon. Interestingly, spines are not uniform in shape or size, ranging from short and stubby to the more stereotypical 'mushroom-shaped' spines (see Fig. 3.3, Fig. 3.5 & Fig. 3.7) (McKinney *et al.*, 1999). Although the PNs used in this study are not as fully differentiated as *in vivo*, they still possess an abundance of fully formed spines indicating a level of differentiation comparable to that of PNs in cerebellar slice preparations.

Granule cell survivability is of paramount importance in the maintenance and development of the PN dendritic arbour due to their ability to release trophic factors required for PN growth. Raising the K^+ concentration of the culture media has been shown to increase the survival rate of cerebellar granule cells (Lasher & Zagon, 1972; Balazs *et al.*, 1988) and should subsequently increase the survival rate of PNs in mixed cerebellar cultures. Our findings identified a marked increase in granule cell survival upon raising the K^+ concentration with no substantial change in PN survival (~20-50 PNs per coverslip counted at 21 DIV). The major morphological change was a 'feathery' appearance due to an increase in spine density. Transection of the Schaffer collateral afferent input to hippocampal CA1 neurones results in the loss of ~60% of spines on the dendrites innervated by the lesioned fibres (McKinney *et al.*, 1999). Interestingly, this study identified a role played by AMPA receptor (AMPAR) activation in the maturation and maintenance of dendritic spines where previously the determinants of spine morphology were unknown. This AMPAR-mediated effect persisted in the presence of TTX thus negating any effects of Ca^{2+} entry via postsynaptic VACCs. The AMPAR-mediated regulation of spine maturation may be stimulated by either direct Ca^{2+} entry via AMPARs or via a direct 'metabotropic' effect (Wang *et al.*, 1997) upon receptor activation. Therefore, due to the presence of AMPARs and not NMDARs on mature PN dendrites, it seems plausible that AMPAR activation might also control the maturation of cerebellar PN dendritic spines, although this remains to be evaluated. Granule cells are of paramount importance in the

differentiation of PNs due to their ability to release necessary trophic factors and in providing glutamate for stimulation of postsynaptic AMPARs. However, even though the granule cell density and subsequent PN spine formation was increased in the presence of high K^+ (Hirai & Launey, 2000; present study), no significant difference in the level of inhibitory afferent input was observed. Therefore, mixed cerebellar cultures were maintained in low K^+ media in order to minimise any adverse effects of perpetual depolarisation on the morphological changes of neurones during development.

In order to examine the process of PN inhibitory synaptic plasticity, mixed cerebellar cultures required the presence of a multitude of fully differentiated basket cells (BC) and stellate cells (SC), providing a level of inhibitory afferent input comparable to that of *in vivo*. Passive observations from mature cerebellar cultures, immunocytochemically stained for PV, GAD and Calbindin D_{28K} identified an approximate ratio of 1PN : 20BC/SC : 1GC (PN = Calbindin D_{28K}, GAD & PV positive; BC/SC = Calbindin D_{28K} negative, PV positive & GAD positive; GC = Calbindin D_{28K} negative, PV negative & GAD positive). The quantitative estimation of the ratio of PN : BS/SC : GC in the mixed cerebellar cultures used within the present study compare with those calculated, using a stereological method, for the intact rat cerebellar cortex, where PNs were calculated to be outnumbered 10 : 1 by interneurones of the molecular layer, 419 : 1 by granule cells of the granular layer and equal in number with cerebellar Golgi cells (1 : 1) (Korbo *et al.*, 1993). Therefore, the number of molecular layer interneurones present in the mixed cerebellar cultures used within the present study has the potential to provide mature PNs with a level of inhibitory afferent input comparable to that experienced by PNs *in vivo*. Recent evidence has suggested that the release, from granule cells, of the neurotrophin BDNF aids in both the maturation and differentiation of BC/SCs in culture (Mertz *et al.*, 2000). Interestingly, the release of BDNF also augments the dendrite proliferation of mouse PNs in mixed cerebellar culture preparations (Morrison & Mason, 1998). Therefore, the level of granule cell axon afferent input to both BC/SCs and PNs will denote the overall level of maturation of mixed cerebellar cultures used within previous studies and in the present study (Baptista *et al.*, 1994; Morrison & Mason, 1998; Hirai & Launey, 2000; Kawaguchi & Hirano, 2000).

The level of PN dendritic differentiation and mature spine formation obtained within this study identified a sufficient level of granule cell afferent excitatory input, further exemplified by the presence of a multitude of mature, differentiated molecular layer interneurones providing conjunctive inhibitory afferent input. Cultured interneurones possessed many branched dendrites in conjunction with an elongated, bifurcating axon which contained many varicosities, presumed to be both immature and mature presynaptic neurotransmitter release sites (Llano *et al.*, 2000). The overall morphology of the molecular layer interneurones in the present study compare with dye filled neurones from cerebellar slice preparations (Mitgaard, 1992; Pouzat & Hestrin, 1997; Pouzat & Marty, 1999) and thus constitute the major inhibitory afferent input to the mature PNs in culture.

The present study was undertaken with mature PNs (>18 DIV), whose morphological and electrophysiological properties mimicked their *in vivo* counterparts throughout all stages of neuronal development, thus providing a simplistic system in which to pharmacologically examine the process of PN inhibitory synaptic plasticity.

Chapter 4

DEPOLARISATION-INDUCED SUPPRESSION OF INHIBITION

&

REBOUND POTENTIATION

INTRODUCTION

Long lasting, activity dependent changes in synaptic transmission are thought to underlie learning and memory within the cerebellum (Levenes *et al.*, 1998). Long-term depression (LTD), established to occur at synapses between parallel fibres (PF) and Purkinje neurones (PNs), is one such example of a long-term change in synaptic efficacy. Climbing fibre (CF) activation induces a fast depolarisation of the PN due to activation of ionotropic AMPA receptors. Subsequently, all voltage-activated calcium channels (P-type channels constitute 90% of PN VACCs, the residual 10% consists of L, N and R-type channels (Llinas *et al.*, 1992)) open causing a rapid rise in the cytosolic calcium concentration. Coincident parallel fibre stimulation results in the activation of PN $mGluR_1$ thus activating the PLCβ-$InsP_3$ pathway (Ellisman *et al.*, 1990; Walton *et al.*, 1991; Kuwajima *et al.*, 1992; Nakanishi *et al.*, 1992; Ross *et al.*, 1992). Binding of $InsP_3$ to $InsP_3Rs$ induces the 'wave-like' release of calcium from intracellular stores in order to reinforce the calcium rise mediated by the initial CF induced depolarisation. This rise in cytosolic Ca^{2+} facilitates the activation of downstream protein kinases, such as protein kinase C (PKC) (Hidaka *et al.*, 1988; Nishizuka, 1986), resulting in a long term desensitisation of PN AMPA receptors, manifest as a reduced sensitivity to presynaptically released glutamate (Ito *et al.*, 1982; Crepel & Krupa, 1988; Linden & Connor, 1991). This prerequisite increase in cytosolic Ca^{2+}, similar in both depolarisation-induced suppression of inhibition (DSI) and rebound potentiation (RP), is the crucial precursor event to the induction of cerebellar synaptic plasticity. Interestingly, the same depolarisation-induced Ca^{2+} influx is required to induce LTD and DSI/RP in the cerebellum, irrespective of the fact that LTD concerns the depression of excitatory afferent input while DSI/RP concern modulation of inhibitory afferent

input. Therefore, it remains clear that there is a distinct commonality between the signal transduction cascade(s) activated during the induction of cerebellar LTD and RP. Activation of downstream protein kinases has been implicated in both forms of synaptic plasticity (Crepel & Krupa, 1988; Hartell, 2001; Kano & Konnerth, 1992; Kano *et al.*, 1996; Kawaguchi & Hirano, 2000) although to date there is no evidence to support a role for protein kinases in the induction of cerebellar DSI.

Depolarisation-induced suppression of inhibition is a transient form of inhibitory synaptic plasticity. A train of 8 depolarising pulses (+70mV from –70mV holding potential) is required to induce the prerequisite rise in cytosolic Ca^{2+} enabling DSI onset (Glitsch *et al.*, 1996). The main feature of DSI is a robust but transient (<1min) decrease in the frequency of PN mIPSCs, occurring immediately after stimulus cessation. Studies have identified DSI as having a purely presynaptic loci of expression (Llano *et al.*, 1991; Vincent *et al.*, 1992; Alger *et al.*, 1996), where presynaptic $mGluR_{2/3}$ are proposed to mediate the reduction in transmitter release via a block of the adenylate cyclase pathway (Glitsch *et al.*, 1996). Depolarisation of the PN is thought to induce the release of a calcium-dependent retrograde transmitter, possibly glutamate or a 'glutamate-like' substance (Glitsch *et al.*, 1996; Glitsch *et al.*, 2000). To date, minimal data exists as to the signal transduction cascades leading to the eventual release of a retrograde transmitter from the PN. Two mechanisms have been proposed to underlie the release of transmitter. Firstly, depolarisation may induce the reversal of an excitatory amino acid transporter thus releasing sequestered glutamate from the postsynaptic neurone or nearby glia. Secondly, calcium entry may induce the fusion of a novel form of postsynaptic vesicle to the PN membrane, thus releasing glutamate back into the cleft. Comparable to LTD and RP, the rise in cytosolic calcium is a prerequisite step in the retrograde neurotransmitter release process but still the release mechanism remains largely unclear.

In contrast, rebound potentiation is manifest as a steady-state increase in the mean amplitude of GABA mediated IPSCs in PNs, occurring subsequent to depolarisation. A single depolarising step is sufficient to induce a transient increase in IPSC amplitude (Vincent *et al.*, 1992) while a train of 8 depolarising pulses induces a robust, maintained (>40mins) increase in the mean IPSC amplitude. This stimulus protocol induced no discernible change in the frequency of IPSCs and was therefore

deemed to be an entirely postsynaptic phenomenon (Kano *et al.*, 1992; Hashimoto *et al.*, 1996, Kawaguchi & Hirano, 2000). To date, protein kinase A (PKA) and Ca^{2+}/calmodulin-dependent protein kinase II (CaMKII) are the only protein kinases putatively identified as having a role in the induction and maintenance of RP (Kano & Konnerth, 1992; Kano *et al.*, 1996; Kawaguchi & Hirano, 2000). At the molecular level there exists a void of understanding as to the specific phosphorylation sites on the different neuronal $GABA_A$ receptor subunits that may underlie this form of inhibitory synaptic plasticity.

RESULTS

4.1. Membrane and synaptic properties of cultured PNs

Prior to assessing the properties of mIPSCs in mature PNs it was important to examine the extent (if any) of dendritic cabling of mIPSCs by analysing the relationship between amplitude and rise time of individual mIPSCs. Examination of the relationship between amplitude (pA) and rise time (ms) found there to be no correlation between the two properties. Analysis of 500 consecutive mIPSCs using linear regression resulted in a correlation coefficient of 0.09917 and a standard deviation of ± 31.55 (Fig. 4.1)

Examination of the stability of PN mIPSC amplitude and frequency during a representative control recording identified minimal 'run-up' or 'run-down' throughout the duration of the recording (1000s) ($P>0.05$, one-way ANOVA with Bonferroni post test). A 15 min time period, analysed in 2 min epochs identified a mean amplitude of 97.8 ± 2.9 pA and a mean frequency of 3.7 ± 0.3 Hz (Fig. 4.2). The mean amplitude and frequency values for each epoch are displayed in Table 4.1 and are typical of n=7 controls.

Table 4.1 Mean PN mIPSC amplitude and frequency values during control recording period.

Epoch	1	2	3	4	5	6	7
Amplitude (pA)	94.5	91.1	93.7	103.1	101.1	89.7	111.2
Frequency (Hz)	3.2	3.25	3.5	2.9	3.8	3.8	5.4

Overall, cultured cerebellar Purkinje neurones had a mean mIPSC amplitude of 56.7 ± 13.7pA and a mean frequency of 3.1 ± 0.9 Hz during control recordings (n=7) which were completely blocked by the application of 50μM Picrotoxin.

Depolarisation of cultured Purkinje neurones, from a holding potential of -70mV to 0mV (100ms duration), resulted in a net outward current even though the cells were dialysed with a Cs^+ based pipette solution to minimise the size of outward K^+ currents. Cessation of the depolarising pulse and hyperpolarisation of the cell to –70mV resulted

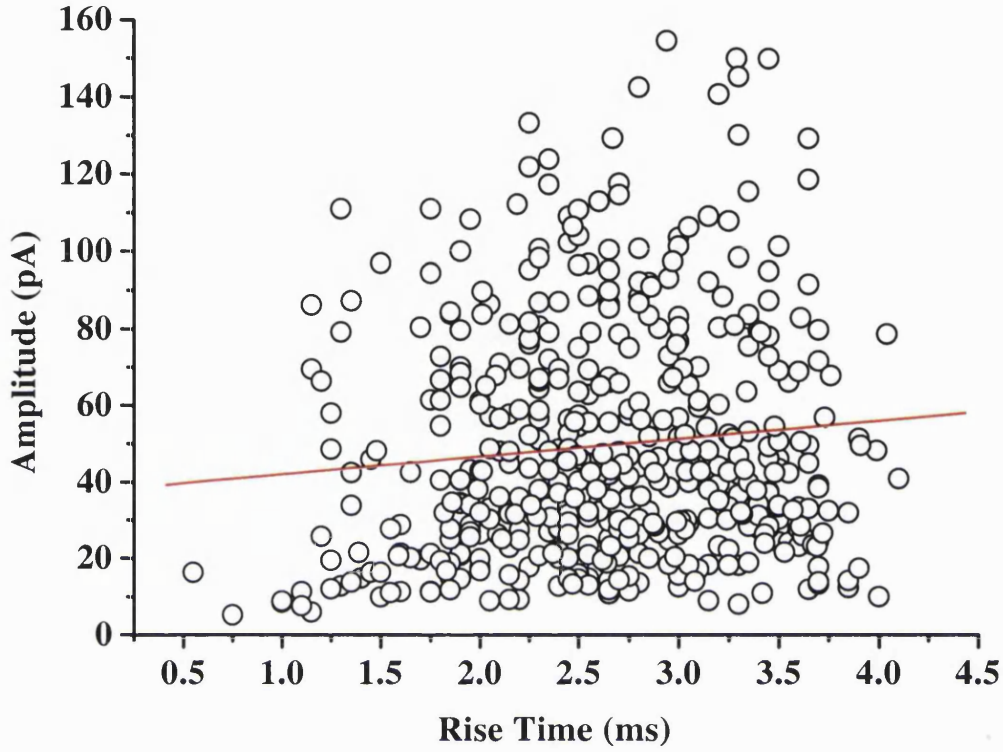

Fig. 4.1. Evaluation of dendritic cabling in mature cerebellar Purkinje neurones. The amplitude of individual mIPSCs (ordinate) are plotted against their respective rise times (abscissa). Linear regression analysis of 500 individual mIPSCs resulted in a correlation coefficient of 0.09917, SD±31.55. Each point represents a single mIPSC.

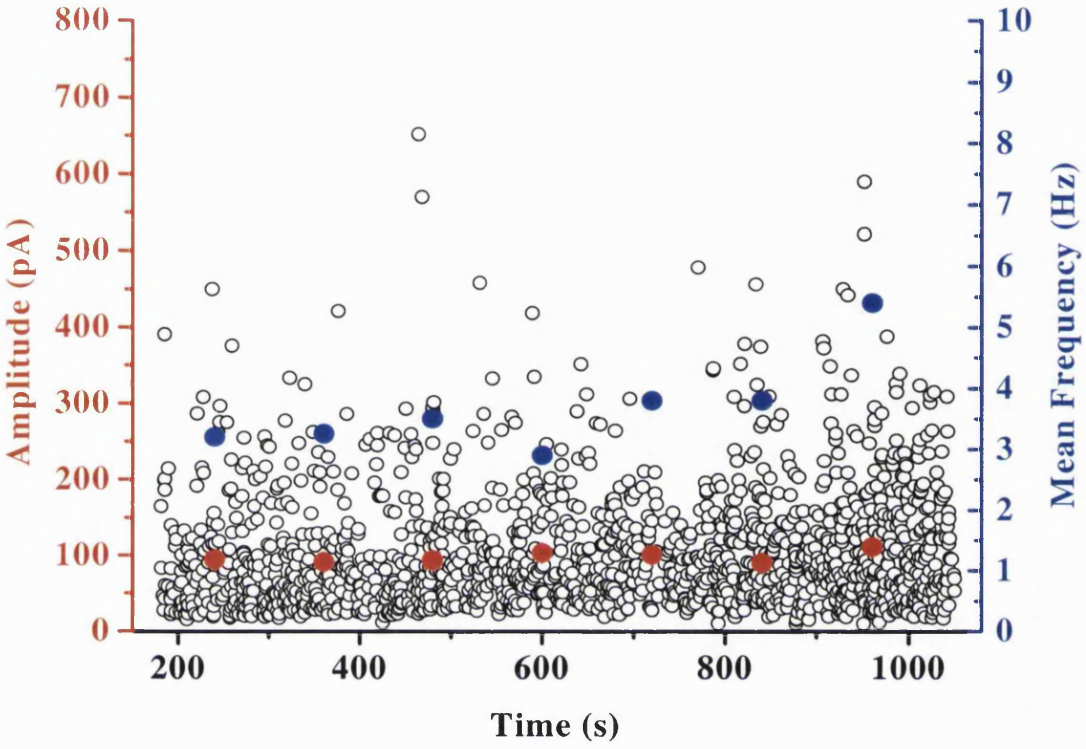

Fig. 4.2. Mean mIPSC amplitude and frequency during a control recording period. A representative cell displays a mean mIPSC amplitude of 97.8 ± 2.9 pA (●) and a mean frequency of 3.7Hz (●) during a 15 min recording period. Recording commenced 3 min after attaining whole-cell configuration at a holding potential of –70mV. Each point represents a single mIPSC.

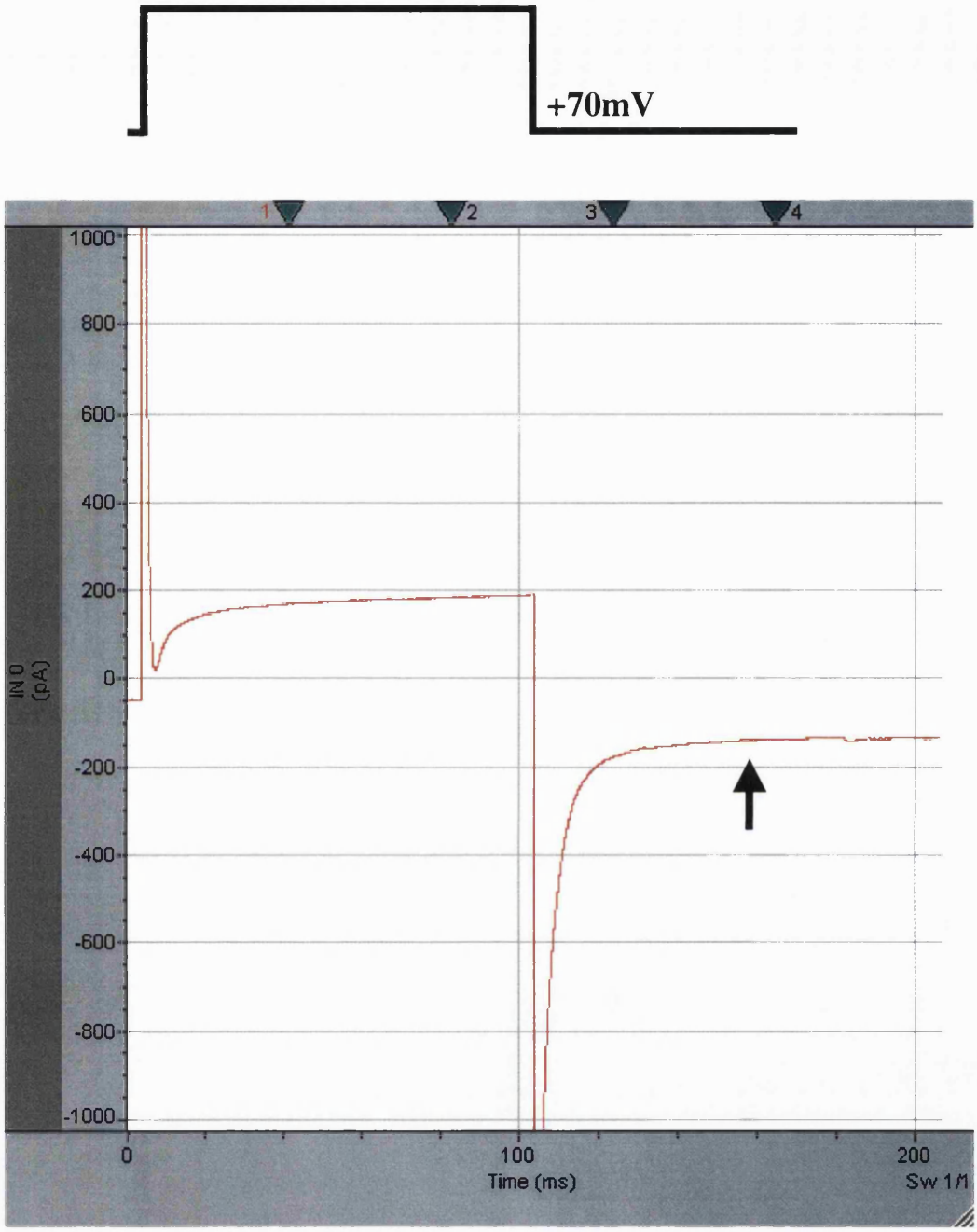

Fig. 4.3. Current trace depicting brief PN depolarisation. Depolarisation of PNs (above trace) from a holding potential of –70mV to 0mV (100ms duration) resulted in a net outward current due to ion flux through unblocked K^+ channels. Cessation of the depolarising pulse results in the activation of a delayed inward Ca^{2+}-activated Cl^- current persisting for the duration of the recording (>100ms) (arrow).

in the activation of a current likely to be a delayed inward Ca^{2+}-activated Cl^- tail current ($I_{Cl(Ca)}$) (Mayer, 1985; Owen *et al.*, 1986; Scott *et al.*, 1988). The tail current persisted for the duration of the recording (>100ms) without returning to the original holding current level (Fig. 4.3).

4.2. Depolarisation-induced suppression of inhibition (DSI)

Application of an 8 pulse depolarising protocol (8 pulses, +70mV step, 100ms duration at 2s intervals, Kano *et al.*, 1992; Hashimoto *et al.*, 1996), 5 min after achieving whole-cell configuration, caused a significant increase in mIPSC amplitude and a robust decrease in mIPSC frequency during the initial 20s after stimulus cessation (Fig. 4.4B, a & b). The mean mIPSC amplitude increased to 125.2 ± 10.2% ($P<0.05$) and the mean mIPSC frequency decreased to 77.7 ± 6.3% ($P<0.02$) of control (Fig. 4.7A & B) (n=7). A representative cell (Fig. 4.5A) illustrates the rapid increase in the mean amplitude of mIPSCs after stimulus cessation. In parallel to the increase in mean mIPSC amplitude was a robust decrease in the mean mIPSC frequency, persisting for ~40s after stimulus cessation (Fig. 4.5B). Therefore, application of a single depolarising protocol induces distinct opposing modulatory effects on both the amplitude and frequency of mIPSCs recorded in mature cultured cerebellar Purkinje neurones. These findings are similar to that found in cerebellar slice preparations after applying the same depolarising protocol (Llano *et al.*, 1991).

4.3. Rebound potentiation (RP)

Analysis of mIPSC modulation at 3 min after stimulus cessation (RP_{t3}), in the same cells in which DSI had been previously induced, identified a profound increase in the mean mIPSC amplitude and a 'rebound' increase in the mean mIPSC frequency (Fig. 4.4B, a & c). The mean mIPSC amplitude increased to 143.4 ± 6.6% of control ($P<0.001$) and the mean mIPSC frequency increased to 152.2 ± 11.7%

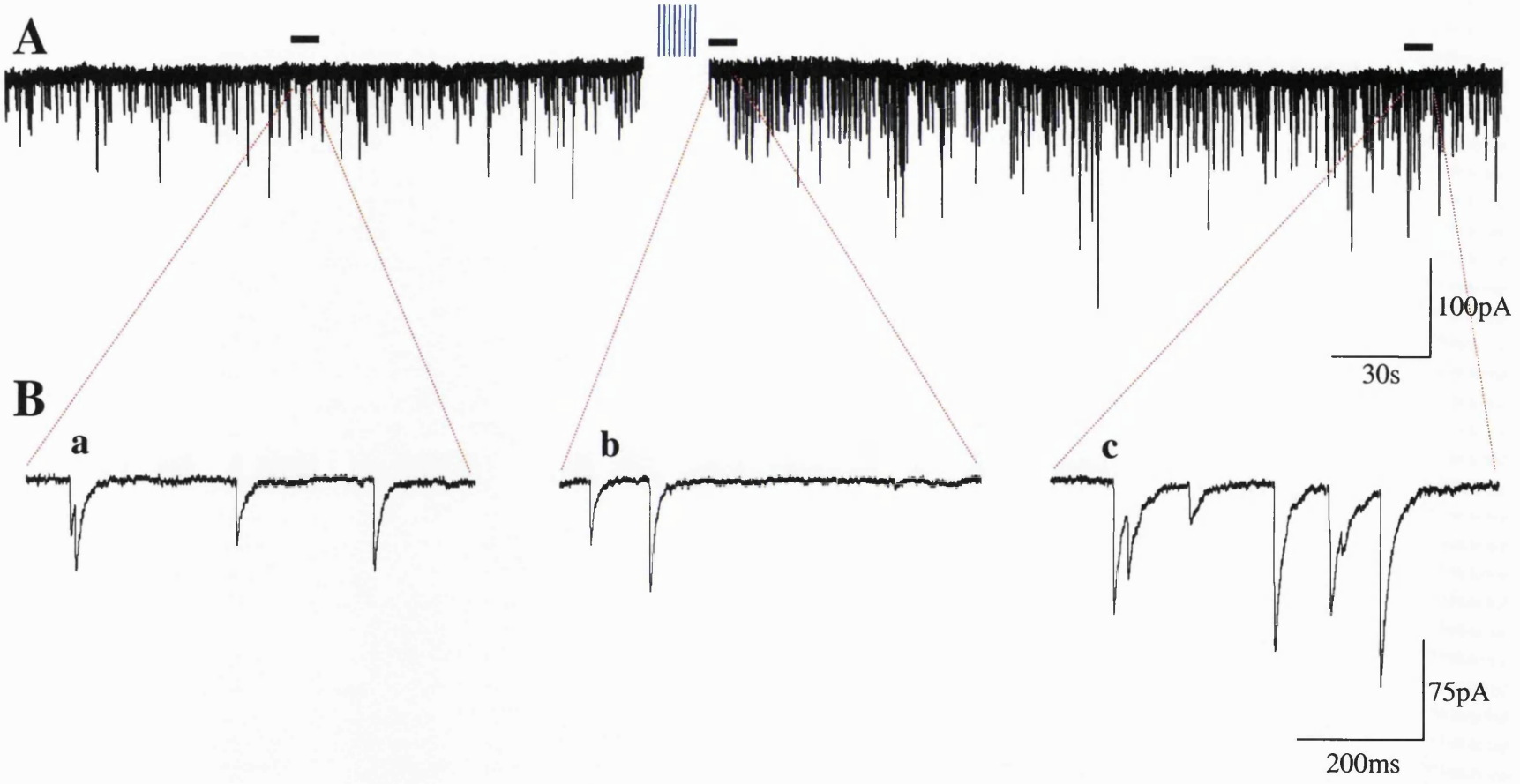

Fig. 4.4. Induction of DSI/RP in normal superfusing Krebs. A, summated mIPSCs recorded during control (upper left trace) and after (upper right trace) a train of depolarising pulses (▥) (8 pulses of 70mV amplitude, 100ms duration at 2s intervals) applied from a holding potential of –70mV at 3 min from the start of whole-cell recording. B, Insets show expanded time-base examples of mIPSCs recorded during control (a), initial 20s after stimulus (DSI) (b) and 3min after stimulus cessation (rebound potentiation (RP_{t3})) (c).

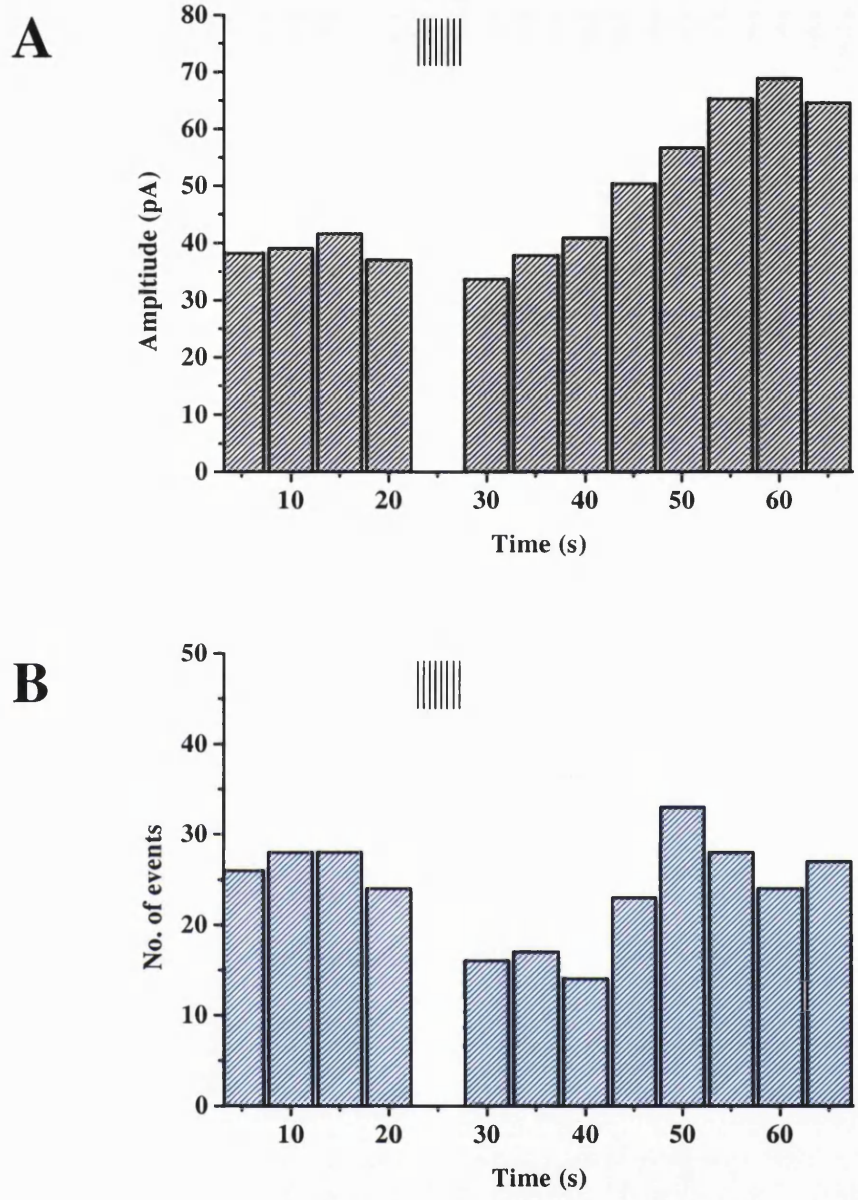

Fig. 4.5. Induction of DSI in normal superfusing Krebs. Representative cell displaying changes in mIPSC amplitude (A) and frequency (B) following stimulus induction (||||||||) in a PN voltage clamped at –70mV. Depolarisation induced a rapid rise in mIPSC amplitude, while inducing a longer lasting decrease in mIPSC frequency persisting for ~40s.

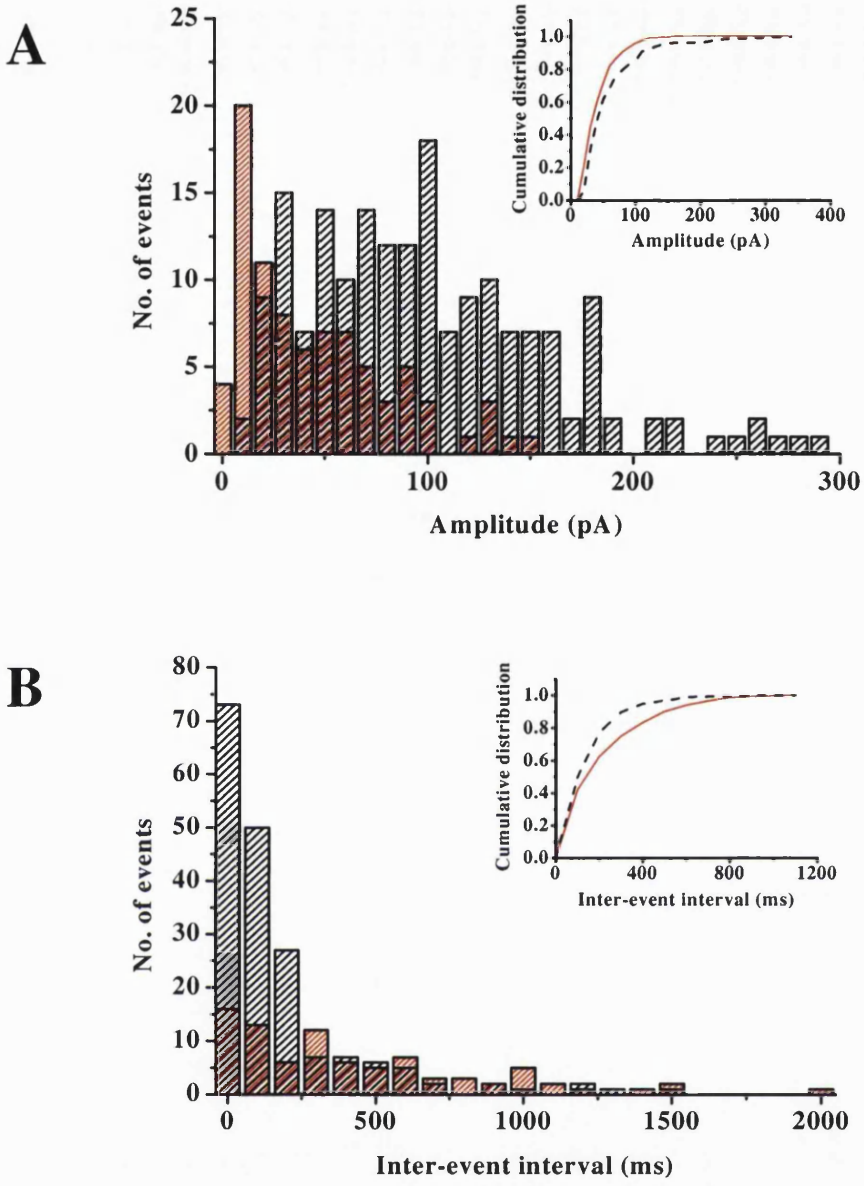

Fig. 4.6. RP in normal superfusing Kerbs. A, amplitude distribution of mIPSCs measured during control recording (dense red hatching) and at 3 min after stimulus cessation (RP_{t3}, medium black hatching) in a single PN. The cumulative distributions from both histograms are illustrated in A, inset (red line = control, black dash = RP_{t3}). B, frequency distribution of mIPSCs measured during control recording (dense red hatching) and at 3 min after stimulus cessation (RP_{t3}, medium black hatching). The cumulative distributions from both histograms are illustrated in B, inset (red line = control, black dash = RP_{t3}).

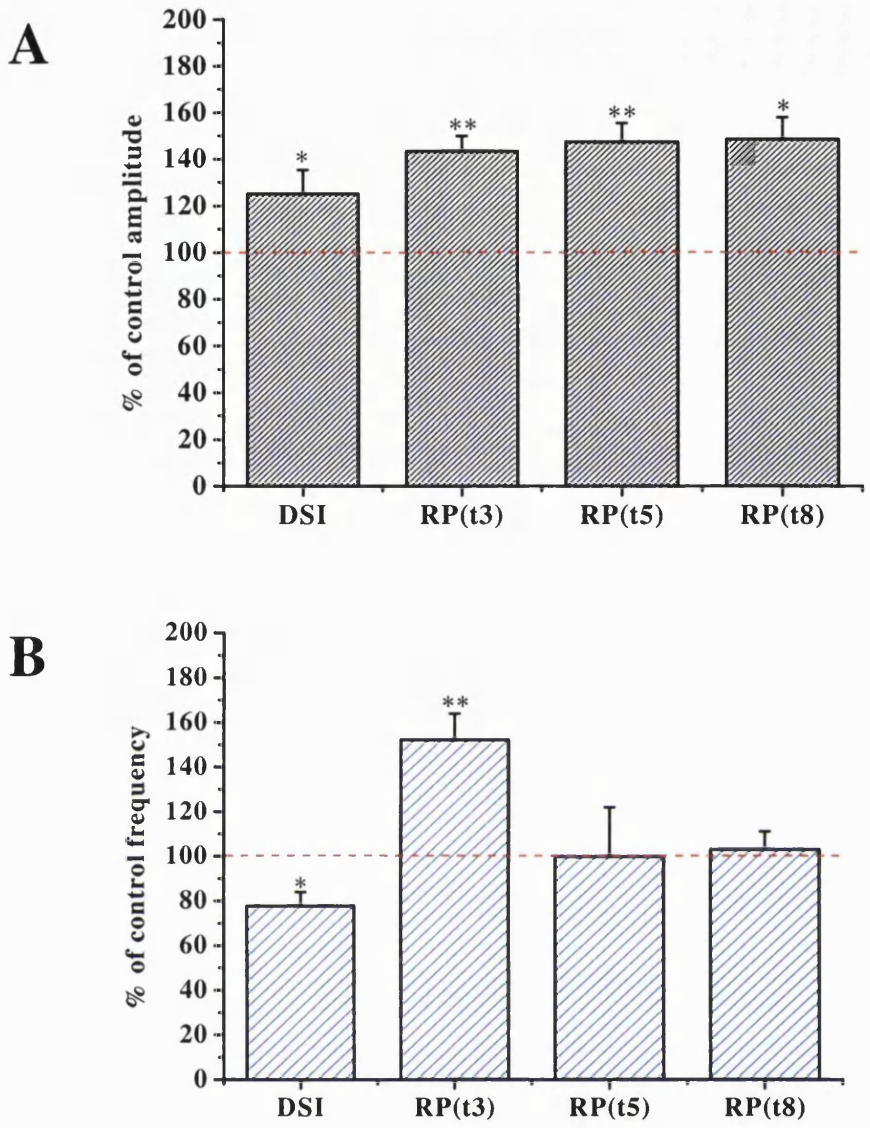

Fig. 4.7. Effects of depolarisation on the amplitude and frequency of PN mIPSCs. Average changes in mIPSC amplitude (A) and frequency (B) following stimulus induction in PNs voltage clamped at –70mV that are representative of cells (n=7/9) showing recovery from frequency potentiation at RP_{t5}. Bars represent average values (± s.e) normalised to control values taken in the same cells 2 min after the beginning of the whole-cell recording. Values for DSI were calculated from the initial 20s following stimulus cessation (n=7), $RP_{t3\ \&\ t5}$ were calculated at 3 & 5 min respectively (n=7) and RP_{t8} was calculated at 8 min after stimulus cessation (RP_{t8} n=3, * denotes $P<0.05$ and ** denotes $p<0.01$, Students t-test).

(P<0.005) of control (Fig. 4.7A & B) (n=7). A representative cell displaying the change in amplitude distribution at RP_{t3} (Fig. 4.6A) had a mean amplitude value of 62.4 ± 1.2pA during control and a mean value of 104.9 ± 1.1pA at RP_{t3}. The cumulative amplitude distributions calculated from control and RP_{t3} histograms (Fig. 4.6A, inset) are significantly different (P<0.01, K-S test). The same cell had a mean frequency value of 2.9Hz during control and a mean value of 4.6Hz during RP_{t3} (Fig. 4.6B). The cumulative frequency distributions calculated from control and RP_{t3} histograms (Fig. 4.6B, inset) are also significantly different (P<0.01, K-S test).

At 5 min after stimulus cessation (RP_{t5}) 78% of cells displayed an amplitude potentiation of 147.5 ± 8.1% of control (P<0.002, n=7) while the frequency potentiation diminished to 99.8 ± 22.2% (P=0.99, n=7) of control (Fig. 4.7A & B). Further recording (RP_{t8}) identified a maintained amplitude potentiation (148.7 ± 9.3% of control, n=3) and the absence of any further frequency modulation (103.0 ± 8.0% of control, n=3) compared to control values (Fig. 4.7A & B). Therefore, mIPSC frequency modulation was not examined after RP_{t5} in future experiments.

The persistent amplitude potentiation is consistent with that seen during RP in cerebellar slice preparations. Application of the same depolarising pulse protocol induced a long lasting RP which has been reported to exist for ~40 min (Kano & Konnerth, 1992; Hashimoto *et al.*, 1996). However, the transient frequency potentiation seen during RP_{t3} is a novel finding and has never been reported before. All previous work identified no discernible change in mIPSC frequency during RP (Kano & Konnerth, 1992; Hashimoto *et al.*, 1996).

4.4. Timecourse of PN mIPSC amplitude and frequency modulation after stimulus cessation

Previous studies have focussed on either the phenomenon of DSI (Llano *et al.*, 1991; Glitsch *et al.*, 1996) or RP (Kano *et al.*, 1992; Vincent *et al.*, 1992; Hashimoto *et al.*, 1996; Kano *et al.*, 1996; Kawaguchi & Hirano, 2000) without extensively studying both concurrently. While our amplitude potentiation is comparable to previous studies,

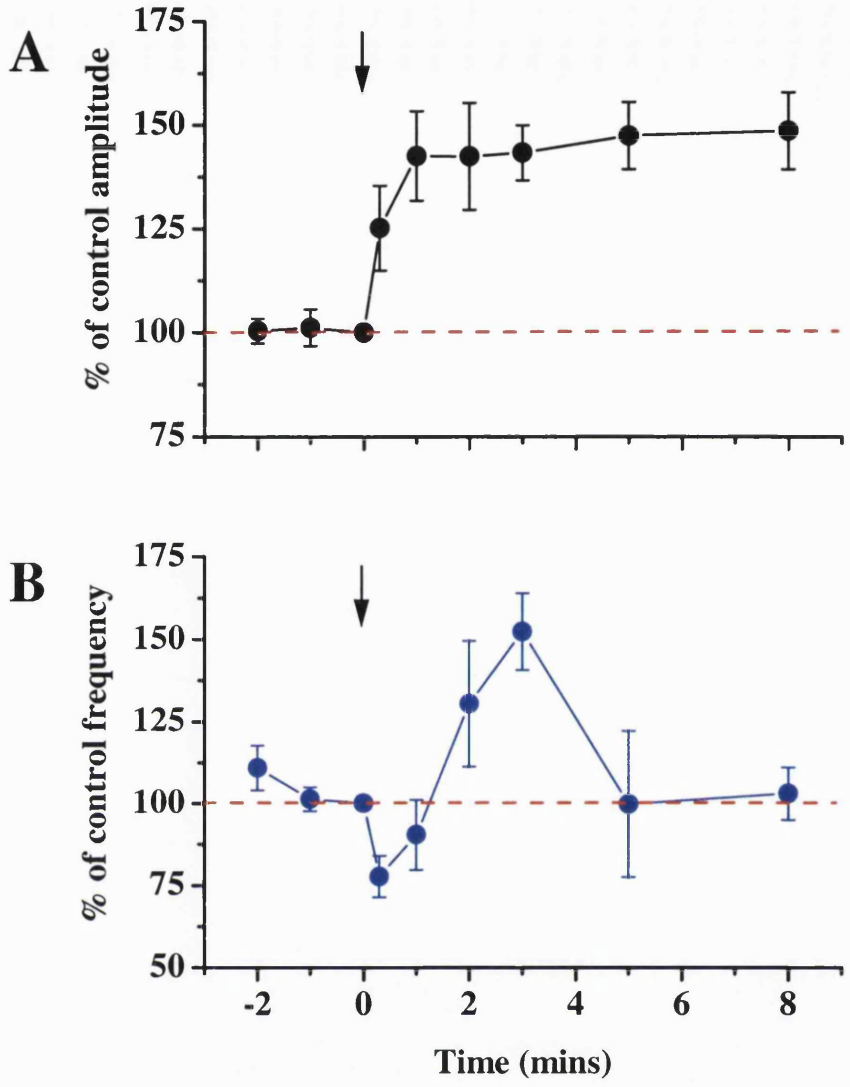

Fig. 4.8. Time-dependent changes in PN mIPSC amplitude and frequency after stimulus induction. A, changes in mean mIPSC amplitude during control period and after stimulus induction (amplitudes were measured throughout DSI and RP period). Current amplitudes were normalised with respect to the mean value recorded directly preceding the point of stimulus induction (depicted by the arrow). B, changes in mean mIPSC frequency during control and after stimulus induction (frequencies was measured throughout DSI and RP period). Mean mIPSC frequencies were normalised with respect to the mean value recorded directly preceding the point of stimulus induction (depicted by the arrow). All data are shown as mean ± s.e (DSI n=7, $RP_{t1\text{-}5}$ n=7 & RP_{t8} n=3).

the timecourse of frequency potentiation, derived from a single train of stimuli, has never been previously addressed. Initially, depolarisation induced a net decrease in mIPSC frequency persisting for ~40s, followed by a transient rebound increase in mIPSC frequency returning to baseline within 5 min of stimulus cessation (Fig. 4.8B). During the whole timecourse of PN mIPSC frequency modulation the amplitude remained potentiated, rising steadily before reaching a plateau at $RP_{t3\text{-}t8}$ (Fig. 4.8A). The mean values during control and after depolarisation are summarised in Table 4.2 below.

Table 4.2. Timecourse of PN mIPSC amplitude and frequency modulation after stimulus cessation.

Time (min)	Amplitude ± s.e	Frequency ± s.e	n
-2	**100.4** ± 3.0	**110.8** ± 6.8	7
-1	**101.2** ± 4.4	**101.3** ± 3.7	7
0	**100**	**100**	7
0.3	125.2 ± 10.2	77.7 ± 6.3	7
1	142.6 ± 10.8	**90.4** ± 10.7	7
2	142.5 ± 12.9	**130.3** ± 19.1	7
3	143.4 ± 6.6	152.2 ± 11.7	7
5	147.5 ± 8.1	**99.8** ± 22.2	7
8	148.7 ± 9.3	**103.0** ± 8.0	3

*Data in red depicts statistically significant values compared to control (Paired t-test, $P<0.05$). Time 0 is defined as the point of stimulus induction, all other times are referenced to time 0 min. All values of amplitude/frequency potentiation are normalised to values calculated at time 0 min (set to 100%).

4.5. mIPSC kinetic changes during DSI and RP

Comparison of the 'rise-time' and 'half-width' of mIPSCs during DSI and RP identified no significant change with respect to control values (Table 4.3). Superimposed average traces accrued from 30 consecutive mIPSC recorded during control, DSI and RP display the relative amplitude potentiation in a representative cell

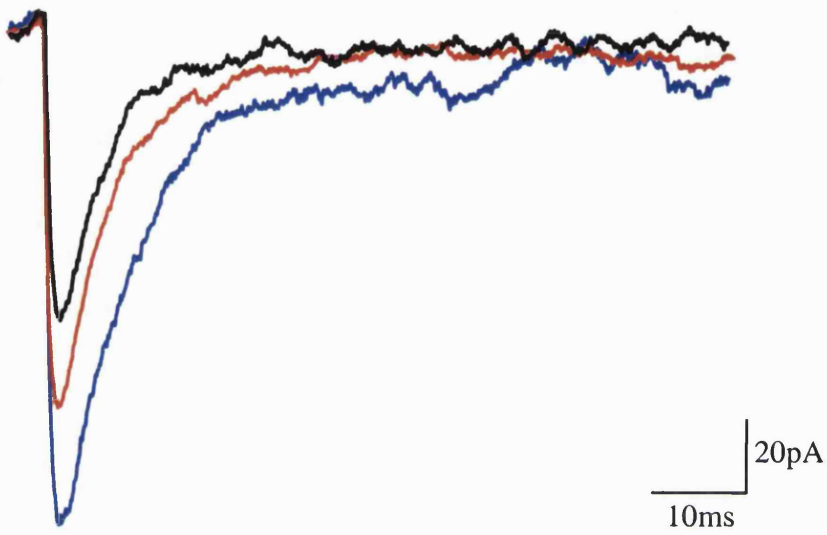

Fig. 4.9. Superimposed averaged traces from all mIPSCs recorded in a single control cell at designated times in normal superfusing Krebs. Traces were averaged from all mIPSCs recorded in a single control cell during control (black line), immediately after stimulus cessation (DSI) (red line) & 3 min after stimulus cessation (RP_{t3}) (blue line).

with respect to control values. Control mIPSCs have a mean amplitude value of 92.2 ± 4.8pA compared with 118.5 ± 8.2pA (DSI) and 126.9 ± 10.6pA (RP_{t3}) (Fig. 4.9).

Table 4.3. Analysis of PN mIPSC kinetic parameters during control, DSI and at 3 min (RP_{t3}) after stimulus cessation. All data are mean values ± s.e (n=7).

Kinetic Parameters	**control ± s.e.m**	**DSI ± s.e.m**	**RP ± s.e.m**
Rise-Time (ms)	3.1 ± 0.3	3.0 ± 0.2	2.8 ± 0.2
Half-Width (ms)	11.0 ± 0.4	10.9 ± 0.6	10.8 ± 0.3

DISCUSSION

4.1. Membrane and synaptic properties of cultured PNs

One inherent problem with mature PNs is the relatively limited electronic compactness of the neurone due to its extensive dendritic arbour and large membrane surface area (Rapp *et al.*, 1994). The limited compactness of the neurone creates a problem when attempting to attain sufficient voltage clamp of the cell during recording phases (space clamp). Events arising from distal dendritic regions of the neurone have to travel long distances in order to be detected by the recording electrode positioned on the soma. Therefore, if R_m (membrane resistance determined by the level of spontaneous channel activity) is low and R_a (resistance of the dendrite to current propagation) is high then the resultant space constant (λ) is small ($\lambda=\sqrt{R_m/R_a}$) (Kandel *et al.*, 1991). The space constant depicts the length of dendrite (μm) along which a current can pass before its amplitude passively decreases to 37% of its original size. Insufficient voltage clamp fidelity would manifest itself as a decrease in the amplitude and an increase in the rise-time of events originating from distal synapses, termed 'dendritic cabling'. Analysis of the amplitude and rise times of events during a control recording period found no correlation between the two mIPSC properties. Therefore, on the assumption that inhibitory synapses occur on sites proximal and distal to the PN soma, 'dendritic cabling' did not underestimate the mean amplitude potentiation observed during the phenomenon of inhibitory synaptic plasticity and thus all mIPSCs recorded are a true reflection of the level of individual synapse activation.

A single train of depolarising pulses induces a net outward current persisting for the duration (100ms) of each pulse. All cells were dialysed with an internal solution based on CsCl and although Cs^+ is a potent blocker of the majority of K^+ channels (Rudy, 1988) there still remains the prospect of some unblocked K^+ channels or non-specific cation channels in PNs (De Schutter & Bower, 1994). Therefore, depolarisation induces the efflux of K^+ or more likely, Cs^+ from the cytosol to the extracellular space and it is this efflux which 'masks' the inward Ca^{2+} current occurring during each depolarisation. In order to 'unmask' the underlying Ca^{2+} current 5-10mM

tetraethylammonium chloride (TEA-Cl) could be included in the perfusion medium to block the remainder of the K^+ channels producing an inward I_{Ca} (not shown). These findings concur with previous work where examination of the depolarisation-induced Ca^{2+}-activated Cl^- tail currents indicated the extent of Ca^{2+} entry. Although the net current on depolarisation was outward the underlying Ca^{2+} current was sufficient to induce inhibitory synaptic plasticity (Llano *et al.*, 1991; present study).

The presence of a long lasting calcium-activated repolarisation in neurones following action potential generation has been established for over a decade (Mayer, 1985; Owen *et al.*, 1986; Scott *et al.*, 1988). This current (whose principal charge carrying ion is Cl^-) manifests as a slow afterhyperpolarisation occurring post stimulus cessation (Owen *et al.*, 1986). The normal effect of $I_{Cl(Ca)}$ in neurones would be to repolarise the cell subsequent to Ca^{2+} entry. In cerebellar PNs it is probable, under physiological conditions, that this current may play a role in repolarisation of the dendritic membrane following Ca^{2+} spike generation (Llinas and Sigimori, 1980). The depolarising pulse protocol used in this study resulted in the net efflux of Cl^- that could change E_{Cl} from a value of 0mV, determined by the high Cl^- pipette solution, to a more negative value. The change in E_{Cl} would result in a net decrease in the driving force for Cl^- and could subsequently reduce the mIPSC current amplitudes recorded at –70mV. However, this is contradictory to the net increase in mIPSC amplitude observed immediately after stimulus cessation (see later discussion). Identification (in this case by physiological activation parameters) of the existence of the Ca^{2+}-activated Cl^- tail current provides a good indication that sufficient Ca^{2+} enters the cell during each depolarising pulse train to initiate inhibitory synaptic plasticity.

The action potential independent release of a single quantum of neurotransmitter, the minimal component of synaptic transmission, is thought to underlie mIPSCs. The stability of mIPSCs throughout the duration of experimental recording is of paramount importance when examining amplitude and frequency changes during the induction of inhibitory synaptic plasticity. The analysis of mIPSCs over a 15 minute control recording period displayed no 'run-up' or 'run-down' of the synaptic $GABA_A$ receptor-mediated currents. Therefore, the cultured cerebellar PNs used within this study provide a good basis in which to examine subtle changes in amplitude and frequency following depolarisation. Evaluation of spontaneous mIPSCs

provides a good model in which to study the specific effects of repetitive depolarisation on synaptic transmission, as opposed to the previously used exogenous application of GABA that will undoubtedly incorporate effects on extrasynaptic $GABA_A$ receptors (Kano *et al.*, 1996; Hashimoto *et al.*, 1996). Activation of both synaptic and extrasynaptic receptors would serve to overestimate the level of inhibitory synaptic plasticity observed subsequent to PN depolarisation. After achieving the whole-cell configuration cells were left for 3 minutes to allow sufficient Cl^- loading to occur before administering a depolarising pulse protocol. Induction of RP is maximal when induced 3 minutes after forming the whole-cell mode, whereas at 9 minutes, the level of RP is greatly reduced (Boxall & Marty, 1997). Therefore, the magnitude of RP will presumably reflect the level of 'wash-out' of necessary intracellular messengers crucial for the induction phase. In this study particular attention was taken to minimise the disruption of the intracellular milieu by Cl^- loading the cell for a limited period of time before initiating the depolarising pulse protocol, therefore allowing the examination of RP under 'normal' physiological conditions.

4.2. Depolarisation-induced suppression of inhibition (DSI)

Application of a train of depolarising pulses induced a potentiation of the mean amplitude of $GABA_A$ receptor-mediated mIPSCs while simultaneously initiating a transient decrease in the mean frequency. Early work by Llano and colleagues (1991) described the same magnitude of amplitude potentiation in response to local GABA (10μM) applications (144 ± 24% of control). Initiation of the potentiation occurred immediately after stimulus cessation. Interestingly, the same study identified differential effects of depolarisation on spontaneous IPSCs (action-potential dependent transmitter release) and miniature IPSCs (action potential-independent transmitter release). Depolarisation in normal saline induced a depression of IPSC amplitude (70 ± 12% of control) and frequency (72 ± 11% of control) lasting ≥ 30s after stimulus cessation. In comparison, the same depolarising pulse protocol applied in the presence of TTX caused a small increase in amplitude (112 ± 21% of control) and a significant decrease

in mIPSC frequency (53 ± 22% of control). Recent studies, examining DSI of PN mIPSCs, apply trains of depolarising pulses every 4 minutes (Glitsch *et al.*, 1996). The results from the first stimulation are excluded from the analysis to minimise contamination with long-lasting postsynaptic potentiation (Llano *et al.*, 1991; Kano *et al.*, 1992). However, this means that DSI is subsequently measured on a pre-existing amplitude potentiated plateau (caused by underlying RP). The question therefore exists as to the physiological relevance of DSI induction subsequent to the initiation of RP. One tentative explanation incorporates the idea that the initial induction of DSI is a subsidiary part of the induction phase of RP. Kawaguchi and Hirano (2000) recently identified the suppression of RP induction at individual synapses, via activation of postsynaptic PN $GABA_BRs$, where the presynaptic release of GABA was coincident with the RP induction stimulus. In the context of the present study, depolarisation induced the release of a retrograde messenger, possibly glutamate, causing a transient decrease in the presynaptic release of GABA from cerebellar interneurones while concurrently enhancing postsynaptic $GABA_A$ receptor responsiveness to GABA. Therefore, the process of DSI may only serve to reduce the possibility of coincident GABA release during PN depolarisation thus facilitating the induction of a robust RP by avoiding the possibility of a $GABA_BR$-mediated suppression of RP (Kawaguchi & Hirano, 2000). In this situation one plausible hypothesis would be that the retrograde transmitter release and subsequent presynaptic effects are part of the induction phase of RP and are not components of a separable phenomenon. Depolarising stimuli applied subsequent to attaining the amplitude potentiated plateau observed during RP would serve only to transiently decrease the presynaptic release of GABA without inducing any further effect on the mean mIPSC amplitude. In the present study we have attempted to examine the effects of a *single* train of depolarising pulses on mIPSC amplitude and frequency, without first reaching a potentiated amplitude plateau. Disregarding the initial results after a primary depolarisation will effectively separate DSI from the long-lasting effects of RP but would negate the possibility that DSI is a component part of the RP induction phase. As shown in this study 'both' phenomena can be effectively examined after the cessation of a single train of stimuli. Although the DSI induced in this study displays the same rate of onset and duration, the magnitude of the mIPSC frequency depression is ~30% less than that of previous studies (Llano *et al.*,

1991; Glitsch *et al.*, 1996). One reason for this discrepancy may be due to insufficient Ca^{2+} entry during depolarisation, resulting in the sub-maximal release of the presumed retrograde transmitter. However, the mIPSC amplitude enhancement during both DSI and RP is comparable to that in previous studies (Llano *et al.*, 1991; Kano *et al.*, 1992; Hashimoto *et al.*, 1996; Kawaguchi & Hirano, 2000). Glitsch and colleagues (2000) examined the Ca^{2+} dependence of the retrograde transmitter release process and found it to be more sensitive to Ca^{2+} entry than initiating presumed $GABA_AR$ phosphorylation during RP. The induction of RP had previously been shown to require a Ca^{2+} rise between 900nM (Kano *et al.*, 1992) and 5μM (Hashimoto *et al.*, 1996) in cerebellar slice and culture preparations, respectively. However, the release of the retrograde transmitter during cerebellar DSI requires a rise in the cytosolic Ca^{2+} concentration of only ~200nM (Glitsch *et al.*, 2000). Therefore, it seems unlikely that the reduced magnitude of DSI observed within this study reflects sub-maximal entry of Ca^{2+} during depolarisation. The possibility remains that there may be differences in presynaptic receptor density between cerebellar slice and cerebellar culture preparations. This remains to be addressed.

The amplitude potentiation observed during DSI is postulated to result from the phosphorylation of postsynaptic $GABA_A$ receptors, activated as a result of the rise in cytosolic Ca^{2+} upon repetitive depolarisation (Kano & Konnerth, 1992; Kano *et al.*, 1996; Kawaguchi & Hirano, 2000). There now exists overwhelming evidence that the frequency depression during DSI results from the Ca^{2+}-dependent release of a retrograde transmitter, postulated to be glutamate or a 'glutamate-like' substance. Efflux of 'glutamate' from the PN is postulated to diffuse back to the presynaptic terminal, activating $mGluR_{2/3}$ and thus reduces transmitter release via a block of the adenylate cyclase pathway (Glitsch *et al.*, 1996; Glitsch *et al.*, 2000). Activation of presynaptic $mGluR_{2/3}$ would result in an overall decrease in the release probability (P) thus lowering the release rate of single quanta (thought to underlie miniature synaptic events). Therefore, in this study, the phenomenon of DSI exists as an increase in the mean mIPSC amplitude while simultaneously displaying a decrease in the mean mIPSC frequency.

4.3. Rebound Potentiation (RP)

Rebound potentiation has previously been established as a sustained increase in the mean amplitude of PN $GABA_AR$-mediated currents. Depolarisation of PNs via CF activation or application of a stimulating protocol results in a ~50% increase in the mean mIPSC current amplitude. Interestingly, the level of amplitude potentiation remains constant irrespective of whether the cells are cultured (Hashimoto *et al.*, 1996; Kawaguchi & Hirano, 2000; present study) or in a slice preparation (Llano *et al.*, 1991; Vincent *et al.*, 1992; Kano *et al.*, 1992; Kano & Konnerth, 1992; Kano *et al.*, 1996) suggesting activation of equivalent signal transduction cascade(s). The present results, consistent with that of previous work, illustrate the immediate onset of mIPSC amplitude potentiation, reaching a plateau at >1min and lasting for the duration of the recording. Phosphorylation of PN $GABA_A$ receptors is postulated to underlie the mean amplitude increase observed during RP (Kano & Konnerth, 1992; Kano *et al.*, 1996; Kawaguchi & Hirano, 2000). Entry of Ca^{2+} during each depolarising pulse is thought to activate downstream protein kinases, resulting in eventual $GABA_AR$ subunit phosphorylation and subsequent amplitude potentiation. Identification of the specific kinases involved in RP was outwith the scope of this study. The similarity between the magnitude of PN RP in slice preparations and in this study implies that common signal transduction cascades are involved in RP induction in both preparations.

Depolarisation of the PN induced a previously undocumented transient increase in the mean frequency of mIPSCs recorded at RP_{t3}. Initially, during DSI, the frequency significantly decreased before recovering and developing into a 'rebound' frequency increase during RP_{t3}. The release of a retrograde messenger (possibly glutamate) is thought to underlie the phenomenon of DSI, therefore, it is also likely that stimulation of the presynaptic vesicle release machinery may underlie the increase in frequency observed during RP_{t3}. Alternatively, the co-release of a second type of retrograde messenger, activating a population of non-glutamatergic receptors, may underlie the increase in mIPSC frequency observed during RP_{t3}. This latter concept is unlikely however (see chapter 6). Electrical separation of the neuronal culture network exists due to all recordings being made in TTX, thus eliminating any potential effects of PN axon

retrograde innervation of presynaptic elements. Previous studies on RP utilised the brief pulse application of GABA (Kano & Konnerth, 1992; Kano *et al.*, 1996) or the analysis of a specific number of mIPSCs (Kano & Konnerth, 1992; Kano *et al.*, 1996) to examine the level of amplitude potentiation after stimulus induction. The former approach does not account for changes in presynaptic GABA release rates as the application of GABA is entirely exogenous. The latter case analyses an exact number of mIPSCs thus overlooking any potential change in mIPSC frequency subsequent to depolarisation. In either situation the frequency change of synaptic events would be entirely missed in favour of solely examining the change in responsiveness of postsynaptic $GABA_A$Rs to GABA. One previous study analysed both the amplitude and frequency of sIPSCs after depolarisation, and found a significant increase in the mean amplitude but no discernible change in the frequency, analysed at RP_{t3} (Hashimoto *et al.*, 1996). One possible explanation for the lack of change in sIPSC frequency could be due to this group 'holding' their cells for a period of 10 min before applying any stimulation protocol. This duration of Cl^- loading will also inevitably lead to 'wash-out' of soluble cytosolic components, possibly involved in the release of a retrograde messenger, and as a result, modulation of the sIPSC frequency may not be observed at RP_{t3}. The original work on RP by Kano and colleagues (1992) analysed a timepoint 20 minutes (RP_{t20}) after stimulus cessation finding a robust, maintained increase in sIPSC amplitude with no change in frequency. Analysis at RP_{t20} would also entirely miss a possible transient increase in IPSC frequency, observed at RP_{t3} (which would have returned to baseline at RP_{t5}), resulting in the incorrect conclusion that no frequency changes occur during the phenomenon of RP. Alternatively, the two aforementioned studies examined the changes in sIPSC amplitude and frequency during the induction and maintenance of RP. The spontaneous release of GABA is dependent upon the action potential-dependent release of neurotransmitter from the presynaptic terminal, governed by the influx of Ca^{2+} via presynaptic VACCs. Evidently, both spontaneous AP-dependent release (sIPSCs) and spontaneous, AP-independent miniature release (mIPSCs) may be regulated by differing presynaptic signal transduction cascade(s) (Bouron, 2001). Therefore, the discrepancy between previous studies and the present one may illustrate the differential signal transduction pathways regulating the two alternative neurotransmitter release pathways.

Results from the present study intimate the activation of a secondary receptor type, also activated by the release of a retrograde messenger (possibly glutamate, see chapter 6 & 7), in mediating the increase in frequency observed subsequent to the termination of DSI. The physical location or affinity for 'glutamate' of the different glutamate receptor types may play a pivotal role in the time dependent frequency changes observed during DSI and RP.

4.4. mIPSC kinetic changes during DSI and RP

One major drawback of PNs in culture is the ability to produce fully differentiated neurones receiving a level of synaptic input comparable to their *in vivo* counterparts. Comparison of the frequency and amplitude of mIPSCs in cerebellar slice preparations and the mixed cerebellar cultures used in this study provides the best indication as to their level of differentiation. The amplitude of mIPSCs recorded in the present study is comparable to that of the early work on RP in cerebellar slice preparations (Kano *et al.*, 1992), thus implying that the PN GABAergic synapses in the cultures are fully formed and vary sufficiently in size. Basal mIPSC frequency levels are also comparable to a variety of previous studies in both slice and culture preparations (Llano *et al.*, 1991; Hashimoto *et al.*, 1996; Glitsch *et al.*, 2000; Boxall, 2000; Llano *et al.*, 2000).

In this study, phosphorylation of PN $GABA_AR$s, thought to underlie the phenomenon of RP, does not interfere with either the rise-time or half-width decay times of individual PN mIPSCs. It has been postulated that $GABA_AR$ phosphorylation underlies the phenomenon of RP but to date no conclusive evidence exists as to the exact mechanism. Examination of the specific effects of $GABA_AR$ phosphorylation requires analysis of the single channel properties of recombinant and/or native $GABA_AR$s. The PN provides a simplistic system in which to examine $GABA_AR$ phosphorylation due to the expression of a limited number of subunits (Wisden *et al.*, 1996). Previous work on the single channel properties of recombinant $GABA_A$ receptors ($\alpha_1/\beta_1/\gamma_{2L}$) identified a significant increase in the open probability of channels after tyrosine phosphorylation (Moss *et al.*, 1995). Although the mean open time (τ_0) of

$GABA_A$ channels increased, the individual open times τ_1 and τ_2 did not change subsequent to tyrosine phosphorylation. Therefore, the increase in τ_0 underlies an increase in the open probability (P_o) of channels possibly reflecting an increased frequency of opening. In the present study the comparable half-width decay times during control, DSI and RP can only approximately be attributed to an increase in the open probability of $GABA_AR$ channels, subsequent to receptor phosphorylation. A recent study examining the modulatory effects of tyrosine phosphorylation on PN mIPSCs described an ~30% increase in the mean amplitude with no discernible change in half-width decay times (Boxall, 2000). Therefore, $GABA_AR$ subunits, possessing candidate sites for phosphorylation, may serve to increase the mean open probability of $GABA_ARs$, manifest as an increase in the mean PN mIPSC amplitude during DSI and RP, however this remains to be evaluated, particularly since phosphorylation by some other protein kinases, e.g. PKC, can inhibit $GABA_A$ receptor function (Moss & Smart, 1995).

Chapter 5

PRESYNAPTIC mGluR-MEDIATED CONTROL OF INHIBITORY SYNAPTIC TRANSMISSION AT THE INTERNEURONE-PN SYNAPSE

Introduction

In the past decade an abundance of electrophysiological and biochemical evidence has identified a predominant role for mGluRs in the regulation of neurotransmission in the mammalian brain (Cartmell & Schoepp, 2000). Although a wealth of information exists as to the regulation of glutamate release by presynaptic mGluRs, the area of mGluR regulation of GABA release still remains relatively unexplored. Interestingly, activation of presynaptic mGluRs can have both positive and negative modulatory effects on GABA release dependent upon both tissue type and receptor subtype expression. Facilitation of KCl-evoked endogenous GABA release, by activation of presynaptic $mGluR_1$, has been identified in the rat striatum (Wang and Johnson, 1995). This effect was enhanced by the costimulation of dopamine D1 receptors. Activation of both presynaptic mGluRs and dopamine D1 receptors serves to induce rises in both intracellular Ca^{2+} and cAMP levels, respectively, thus inducing an enhancement of the release of GABA (Wang & Johnson, 1995). Similarly, application of quisqualate evoked the release of [^{3}H]GABA from rat coronal hippocampal slices which could be abolished by the application of L-AP3 (Janaky *et al.*, 1994). Conversely, electrophysiological reports have identified a negative modulation of GABA release, on activation of presynaptic mGluRs by the non-selective agonist t-ACPD, in both the hippocampus (Liu *et al.*, 1993; Jouvenceau *et al.*, 1995) and the cerebellum (Llano & Marty, 1995). Subsequent work, in the same preparations, identified a predominant role for this G-protein coupled receptor in the induction of short-term inhibitory synaptic plasticity, termed DSI. Hippocampal DSI is proposed to be induced by the activation of group I mGluRs, while cerebellar DSI is thought to be

mediated via group II mGluRs (Morishita & Alger, 1999; Glitsch *et al.*, 1996). Although group I mGluR activation induces phospholipid hydrolysis to produce DAG and $InsP_3$, the overall effect upon receptor activation in the hippocampus, contrary to that expected, is negative modulation of transmitter release thus raising the possibility of a secondary G-protein mediated effect (Morishita & Alger, 1999). However, cerebellar DSI is thought to be attributed to the $mGluR_{2/3}$-mediated inhibition of the adenylate cyclase pathway, thus restricting the release of GABA (Glitsch *et al.*, 1996). Although the specific pharmacological block of $mGluR_{2/3}$, during DSI, has never been achieved, the application of the specific group II agonist DCG-IV mimics the induction of cerebellar DSI (Glitsch *et al.*, 1996). Therefore, the possibility remains that the differential effects of mGluR receptor activation on neurotransmitter release is entirely dependent upon subtype specific receptor expression at the axon terminals of interneurones in both the hippocampus and cerebellum.

Purkinje neurones possess an abundance of $mGluR_{1a/1b}$ (Baude *et al.*, 1993; Fotuhi *et al.*, 1993; Hampson *et al.*, 1994; Martin *et al.*, 1992; Nusser *et al.*, 1994; Shigemoto *et al.*1994; Mateos *et al.*, 2000), positively coupled to the PLC-$InsP_3$ pathway, which on activation serves to increase the cytosolic Ca^{2+} level (Netzeband *et al.*, 1997). This rise in Ca^{2+}, the prerequisite step in LTD, DSI and RP induction, activates downstream signalling cascades resulting in differential receptor phosphorylation and induction of transient and long-term changes in synaptic efficacy (Daniel *et al.*, 1998; Glitsch *et al.*, 1996; Kano & Konnerth, 1992). Application of the agonist t-ACPD, has been shown to have conflicting effects in both cerebellar slice and mixed cerebellar culture preparations. Early studies revealed a reduction in the frequency of PN mIPSCs/sIPSCs on application of t-ACPD to cerebellar slice preparations (Llano & Marty, 1995) while application of the same agonist, to PNs in mixed cerebellar cultures, resulted in a marked enhancement of PN sIPSC amplitude and frequency (Hashimoto *et al.*, 1996). The anomalies that exist create a problem when trying to evaluate the effects of presynaptic and postsynaptic mGluR activation at the interneurone-PN synapse. The conflicting effects of t-ACPD application on the rate of GABA release makes identification of the mGluR subtype and associated presynaptic signal transduction cascade(s) difficult. The presynaptic activation of the PKC

(Capogna *et al.*, 1995; Jarolimek & Misgeld, 1997) and PKA (Capogna *et al.*, 1995; Jarolimek & Misgeld, 1997; Chavais *et al.*, 1998; Trudeau *et al.*, 1998) signalling cascades have been established to enhance the spontaneous TTX-resistant release of neurotransmitter. Interestingly, PKA and PKC have additive effects on the rate of spontaneous neurotransmitter release (Capogna *et al.*, 1995; Bouron & Reuter, 1999), indicating that these two kinases recruit independent vesicle recycling proteins.

Although there remains a void of understanding as to the exact mechanisms underlying the presynaptic mGluR-mediated modulation of transmitter release it seems likely that there are both separable and overlapping pathways. The advent of novel pharmacological agents specific for individual mGluR subtypes will aid in the dissection of mGluR-mediated changes in synaptic efficacy in the mammalian brain.

RESULTS

5.1. Effects of the non-specific mGluR antagonist (S)-MCPG on DSI & RP induction

5.1.1. Control DSI/RP *vs* DSI/RP$_{((S)\text{-MCPG})}$

Application of the non-specific group I/II mGluR antagonist (S)-MCPG (100μM: a concentration known to induce significant block of group I and group II mGluRs) failed to alter the basal mIPSC amplitude (107 ± 5.6% of control, P=0.26) or basal mIPSC frequency (113 ± 8.0%, P=0.18) (n=5). A comparison between the induction of DSI and RP in control conditions and in the presence of 100μM (S)-MCPG is displayed in Table 5.1 & Table 5.2.

Table 5.1. Comparison between PN mIPSC amplitude modulation (DSI & RP) in control (n=7) and in the presence of 100μM (S)-MCPG (n=4).

Time	Control ± s.e.m	100μM (S)-MCPG ± s.e.m
Control	100	100
DSI	125.2 ± 10.2	130.2 ± 8.2
RP_{t3}	143.4 ± 6.6	165.7 ± 34.5
RP_{t5}	147.5 ± 8.1	157.9 ± 9.5

Table 5.2. Comparison between PN mIPSC frequency modulation (DSI & RP) in control (n=7) and in the presence of 100μM (S)-MCPG (n=4).

Time	Control ± s.e.m	100μM (S)-MCPG ± s.e.m
Control	100	100
DSI	77.7 ± 6.3	77.6 ± 5.1
RP_{t3}	152.2 ± 11.7	168.2 ± 10.3
RP_{t5}	99.8 ± 22.2	111.4 ± 10.7

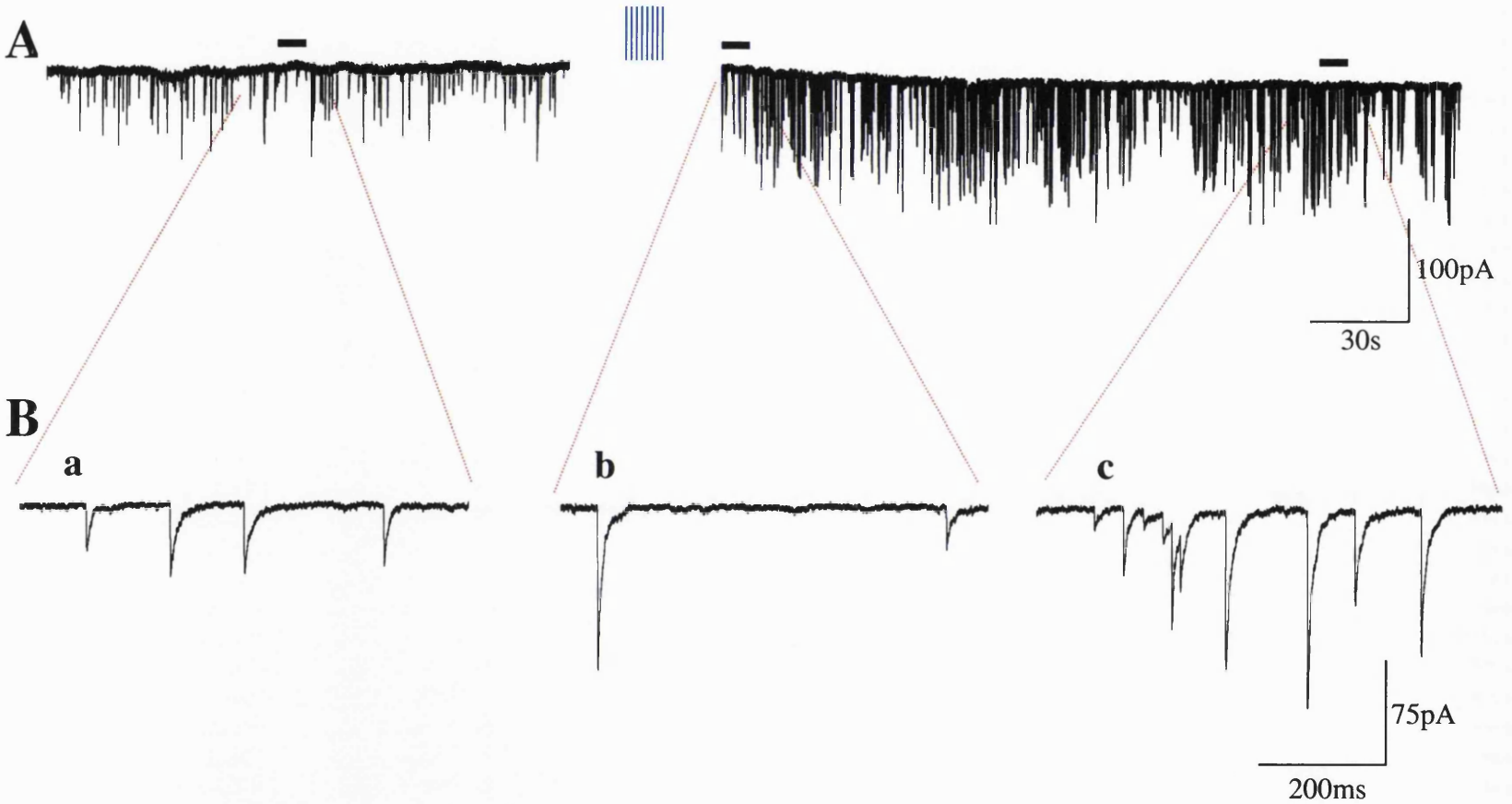

Fig. 5.1. Effects of (S)-MCPG on the induction of DSI/RP. A, summated mIPSCs recorded during control (upper left trace) and after (upper right trace) a train of depolarising pulses (▥) (8 pulses of 70mV amplitude, 100ms duration at 2s intervals) applied from a holding potential of –70mV at 3 min from the start of whole-cell recording. All recordings were made with 100μM (S)-MCPG in the perfusion media. B, Insets show expanded time-base examples of mIPSCs recorded during control (a), initial 20s after stimulus (DSI) (b) and 3min after stimulus cessation (rebound potentiation (RP_{t3})) (c).

Due to there being no statistical difference between DSI and RP induction/maintenance in control and in the presence of 100μM (S)-MCPG ($P>0.05$ one-way ANOVA with Bonferroni post-test) all subsequent data were therefore pooled (n=11).

5.1.2. Depolarisation-induced suppression of inhibition - DSI

Application of the same depolarising protocol as in control, 5 min after achieving whole-cell configuration, caused a significant increase in mIPSC amplitude and a significant decrease in mIPSC frequency during the initial 20s after stimulus cessation (Fig. 5.1B, a & b). The mean mIPSC amplitude increased to 129.8 ± 7.4% ($P<0.002$) (Fig. 5.4A) and the mean mIPSC frequency decreased to 77.7 ± 4.8% ($P<0.001$) (Fig. 5.4B) of control (n=11). A representative cell illustrates the rise in the mean amplitude of mIPSCs after stimulus cessation (Fig. 5.2A). In parallel with the increase in mIPSC amplitude is a robust decrease in mIPSC frequency, persisting ~40s after stimulus cessation (Fig. 5.2B). Therefore, the application of 100μM (S)-MCPG does not affect the induction or magnitude of DSI when compared to DSI in normal Krebs.

5.1.3. Rebound potentiation - RP

Analysis of mIPSC modulation at 3 min after stimulus cessation (RP_{t3}), in the same cells in which DSI had been previously induced, identified a maintained increase in the mean mIPSC amplitude and a 'rebound' increase in the mean mIPSC frequency (Fig. 5.1B, a & c). The mean mIPSC amplitude increased to 151.5 ± 12.6% ($P<0.003$) of control (Fig. 5.4A) and the mean mIPSC frequency increased to 158.0 ± 8.3% ($P<0.0001$) of control (Fig. 5.4B) (n=11). A representative cell displaying the change in amplitude distribution at RP_{t3} had a mean amplitude value of 41.3 ± 1.9pA during control and a mean value of 57.0 ± 2.8pA at RP_{t3} (Fig. 5.3A). The

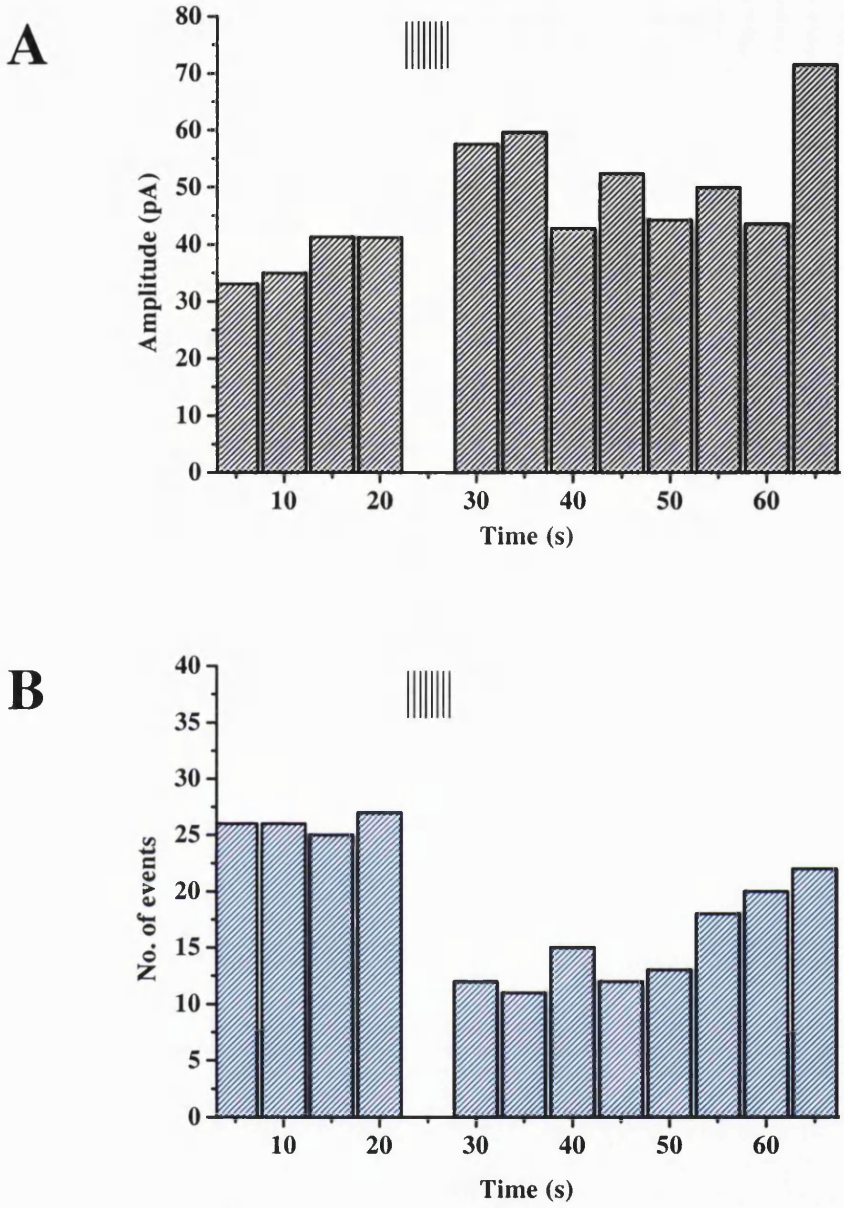

Fig. 5.2. Induction of DSI in the presence of 100μM (S)-MCPG. Representative cell displaying changes in mIPSC amplitude (A) and frequency (B) following stimulus induction (||||||||) in a PN voltage clamped at –70mV. Depolarisation induced a rapid rise in mIPSC amplitude, while inducing a longer lasting decrease in mIPSC frequency persisting for ~40s.

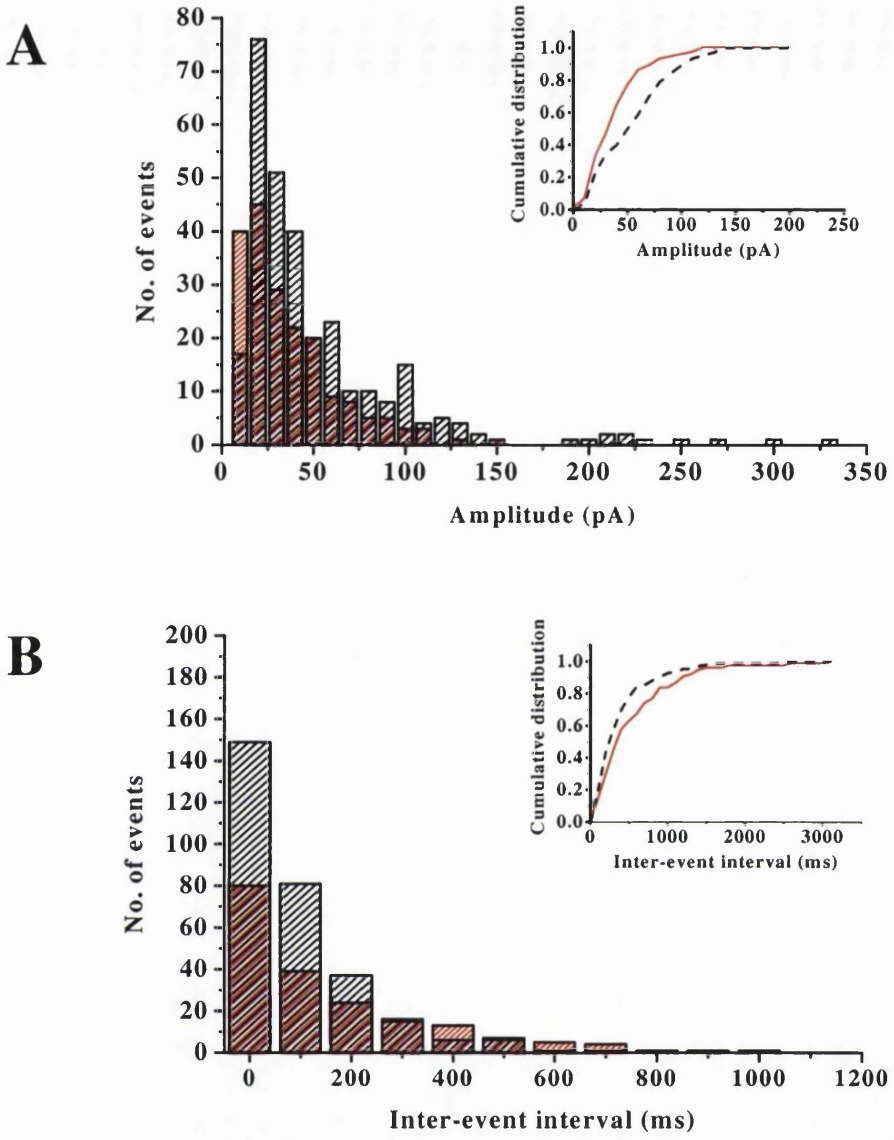

Fig. 5.3. RP in the presence of 100μM (S)-MCPG. A, amplitude distribution of mIPSCs measured from a 40s period during control recording (dense red hatching) and at 3 min after stimulus cessation (RP_{t3}, medium black hatching) in a single PN. The cumulative distributions from both histograms are illustrated in the inset of A, inset (red line = control, black dash = RP_{t3}). B, frequency distribution of mIPSCs measured from a 40s period during control recording (dense red hatching) and at 3 min after stimulus cessation (RP_{t3}, medium black hatching). The cumulative distributions from both histograms are illustrated in the inset of B, inset (red line = control, black dash = RP_{t3}).

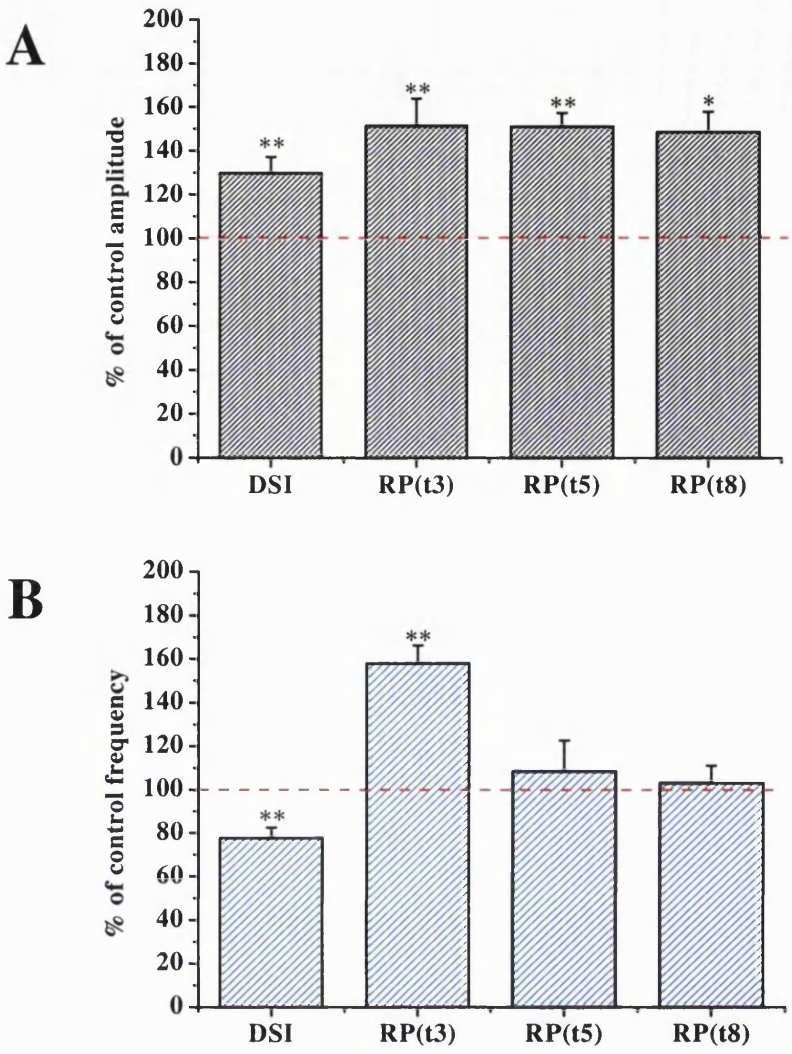

Fig. 5.4. (S)-MCPG does not affect DSI/RP induction. Average changes in mIPSC amplitude (A) and frequency (B) following stimulus induction in PNs voltage clamped at –70mV. Data represents mean values from control data combined with data acquired in the presence of 100μM (S)-MCPG. Representative of cells (n=11/13) showing recovery from frequency potentiation at RP_{t5}. Bars represent average values (± s.e) normalised to control values taken in the same cells 2 min after the beginning of the whole-cell recording. Values for DSI were calculated from the initial 20s following stimulus cessation (n=11), $RP_{t3\ \&\ t5}$ were calculated at 3 & 5 min respectively (n=11) and RP_{t8} was calculated at 8 min after stimulus cessation, respectively (RP_{t8} n=3, * denotes $P<0.05$ and ** denotes $p<0.01$, Students t-test).

cumulative amplitude distributions calculated from control and RP_{t3} histograms (Fig. 5.3A, inset) are significantly different ($P<0.002$, K-S test). The same cell had a mean frequency of 4.8Hz in control and 7.4Hz during RP_{t3} (Fig. 5.3B). The cumulative frequency distributions calculated from control and RP_{t3} histograms (Fig. 5.3B, inset) are also significantly different ($P<0.001$, K-S test).

At 5 min after stimulus cessation (RP_{t5}) 85% of cells displayed an amplitude potentiation of 151.3 ± 6.1% ($P<0.0001$) of control while the frequency potentiation diminished to 108.5 ± 14.2% ($P=0.6$) of control (Fig. 5.4A & B) ($n=11$). Further recording (RP_{t8}) identified a maintained amplitude potentiation (148.7 ± 9.3% of control, $P<0.05$) and the absence of any further frequency modulation (103.0 ± 8.0% of control, $P=0.7$) compared to control values (Fig. 5.4A & B) ($n=3$). Therefore, mIPSC frequency modulation was not examined after RP_{t5} in future experiments.

Application of 100μM (S)-MCPG does not antagonise the induction or maintenance of a robust RP when compared to control data.

5.1.4. Timecourse of PN mIPSC amplitude and frequency modulation after stimulus cessation

Initially, depolarisation induced a net decrease in mIPSC frequency persisting for ~40s, followed by a transient rebound increase in mIPSC frequency which returned to baseline within 5 min of stimulus cessation (Fig. 5.5B). During the whole timecourse of frequency modulation the amplitude remained potentiated, rising steadily before reaching a plateau at $RP_{t3\text{-}t8}$ (Fig. 5.5A). The mean values during control and after depolarisation are summarised in Table 5.3 below.

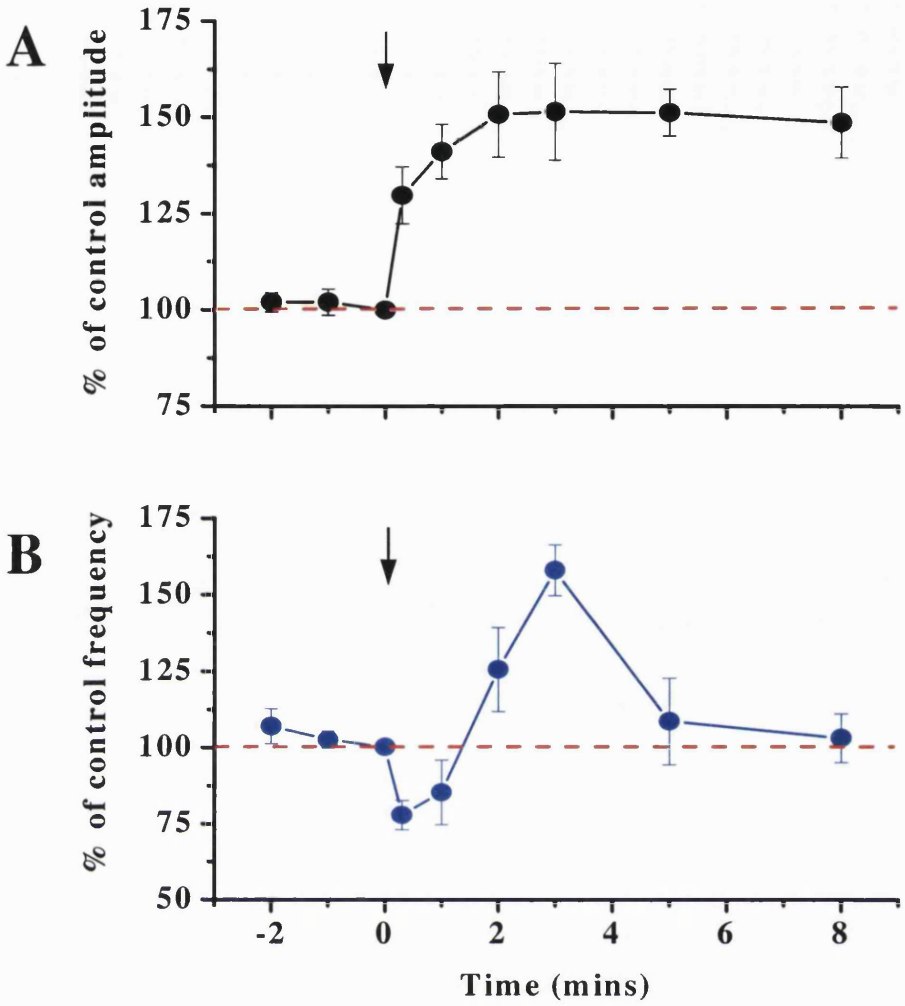

Fig. 5.5. Effects of 100μM (S)-MCPG on the time-dependent changes in PN mIPSC amplitude and frequency after stimulus induction. A, changes in mean mIPSC amplitude during control period and after stimulus induction (amplitudes were measured throughout DSI & RP). Data represents mean values from control data combined with data acquired in the presence of 100μM (S)-MCPG. Current amplitudes were normalised with respect to the mean value recorded directly preceding the point of stimulus induction (depicted by the arrow). B, changes in mean mIPSC frequency during control and after stimulus induction (frequencies were measured throughout DSI & RP). Data represents mean values from control data combined with data acquired in the presence of 100μM (S)-MCPG. Mean mIPSC frequencies were normalised with respect to the mean value recorded directly preceding the point of stimulus induction (depicted by the arrow). All data are shown as mean ± s.e. (DSI n=11, $RP_{t1\text{-}5}$ n=11 & RP_{t8} n=3).

Table 5.3. Timecourse of PN mIPSC amplitude and frequency modulation after stimulus cessation.

Time (min)	Amplitude ± s.e	Frequency ± s.e	n
-2	**102.0** ± 2.5	**106.9** ± 5.7	11
-1	**102.0** ± 3.4	**102.5** ± 2.9	11
0	**100**	**100**	11
0.3	**129.8** ± 7.4	**77.7** ± 4.8	11
1	**141.1** ± 7.1	**85.2** ± 10.6	11
2	**150.8** ± 11.1	**125.5** ± 13.8	11
3	**151.5** ± 12.6	**158.0** ± 8.3	11
5	**151.3** ± 6.1	**108.5** ± 14.2	11
8	**148.7** ± 9.3	**103.0** ± 8.0	3

*Data in red depicts statistically significant values compared to control (Paired t-test, $P<0.05$). Time 0 is defined as the point of stimulus induction, all other times are referenced to time 0 min. All values of amplitude/frequency potentiation are normalised to values calculated at time 0 min (set to 100%).

5.1.5. mIPSC kinetic changes during DSI& RP

Comparison of the 'rise-time' and 'half-width' of mIPSCs recorded in the presence of 100μM (S)-MCPG, during DSI and RP, identified no significant change with respect to control values (Table 5.4). Superimposed average traces accrued from 30 consecutive mIPSCs recorded during control, DSI and RP display the relative amplitude potentiation in a representative cell with respect to control values. Control mIPSCs had a mean amplitude value of 61.5 ± 4.0pA compared with 76.2 ± 4.5pA (DSI) and 84.7 ± 5.0pA (RP_{t3}) (Fig. 5.6).

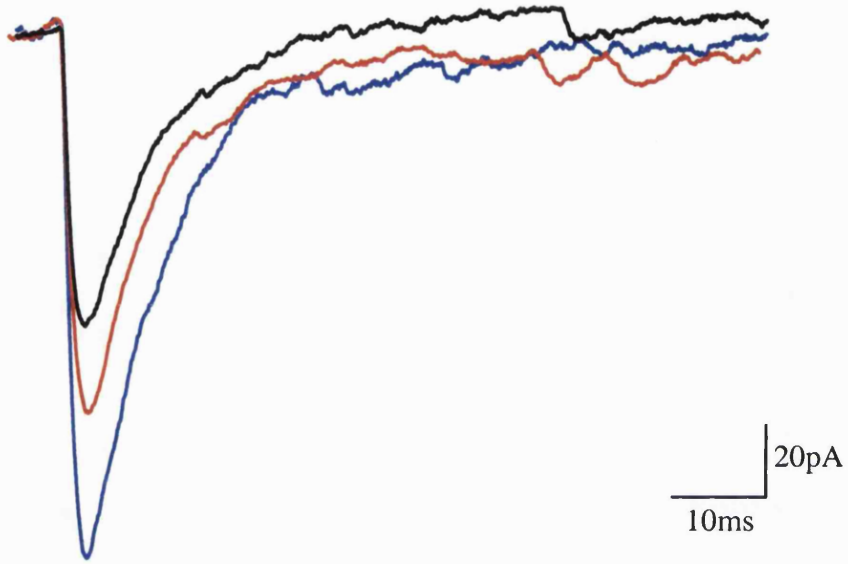

Fig. 5.6. Effect of 100μM (S)-MCPG on PN mIPSC kinetics. Superimposed averaged traces from all mIPSCs recorded in a single control cell at designated times. Traces were averaged from all mIPSCs recorded in a single control cell during control (black line), immediately after stimulus cessation (DSI) (red line) & 3 min after stimulus cessation (RP_{t3}) (blue line).

Table 5.4. Analysis of PN mIPSC kinetic parameters during control, DSI and at 3 min (RP_{t3}) after stimulus cessation. All data are mean values ± s.e. (n=4).

Kinetic Parameters	Control ± s.e.m	DSI ± s.e.m	rebound ± s.e.m
Rise-Time (ms)	2.4 ± 0.2	2.4 ± 0.1	2.4 ± 0.06
Half-Width (ms)	10.1 ± 0.4	10.5 ± 1.6	10.2 ± 0.3

5.2. Effects of the specific group II mGluR antagonist LY 341495 on DSI & RP induction

Application of the specific group II mGluR antagonist LY 341495 (200nM: a concentration known to induce selective block of group II mGluRs) failed to alter the basal mIPSC amplitude (100.49 ± 3.0% of control, P=0.9) or basal mIPSC frequency by (105.9 ± 7.2%, P=0.0.5) (n=4).

5.2.1. Depolarisation-induced suppression of inhibition – $DSI_{(LY\ 341495)}$

Application of a train of depolarising stimuli, in the presence of the specific $mGluR_{2/3}$ antagonist, LY 341495 (200nM), induced a significant increase in mIPSC amplitude and a complete abolition of the frequency decrease observed during DSI in normal Krebs (Fig. 5.7B, a & b). The mean mIPSC amplitude increased to 136 ± 9.9% (P<0.02) (Fig. 5.10A) of control while the mean mIPSC frequency remained unchanged (101.3 ± 10.6% of control, P=0.9) (Fig. 5.10B) (n=5). A representative cell (Fig. 5.9A) illustrates the rise in the mean amplitude of mIPSCs after stimulus cessation while the mIPSC frequency remains constant, with respect to control, for the duration of DSI (~20s) (Fig. 5.8 A&B). Therefore, the application of 200nM LY 341495 completely abolished the frequency modulation observed during DSI.

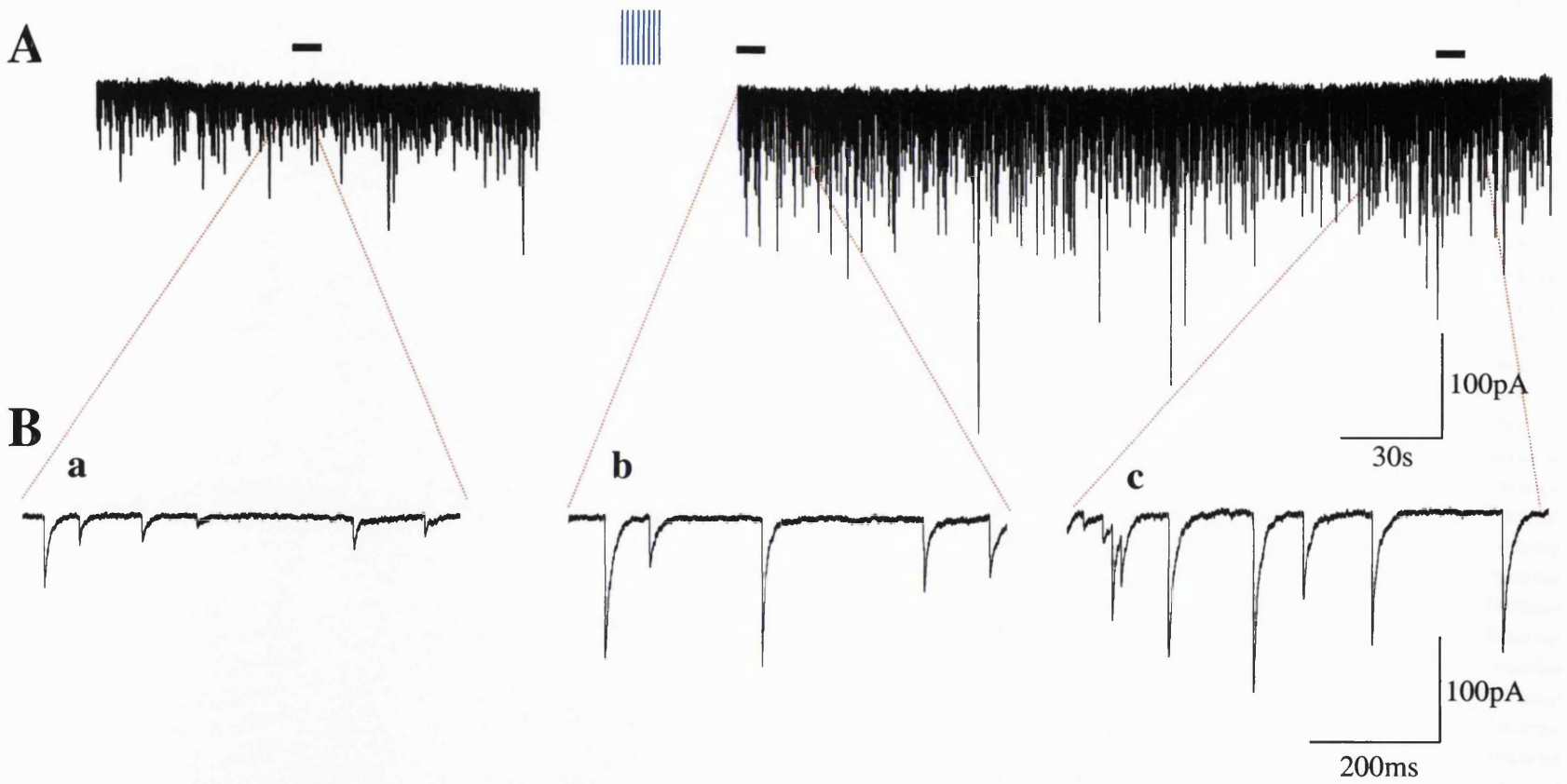

Fig. 5.7. Effects of LY 341495 on the induction of DSI/RP. A, summated mIPSCs recorded during control (upper left trace) and after (upper right trace) a train of depolarising pulses (▥) (8 pulses of 70mV amplitude, 100ms duration at 2s intervals) applied from a holding potential of –70mV at 3 min from the start of whole-cell recording. All recordings were made with 200nM LY 341495 in the perfusion media. B, Insets show expanded time-base examples of mIPSCs recorded during control (a), initial 20s after stimulus (DSI) (b) and 3min after stimulus cessation (rebound potentiation (RP_{t3})) (c).

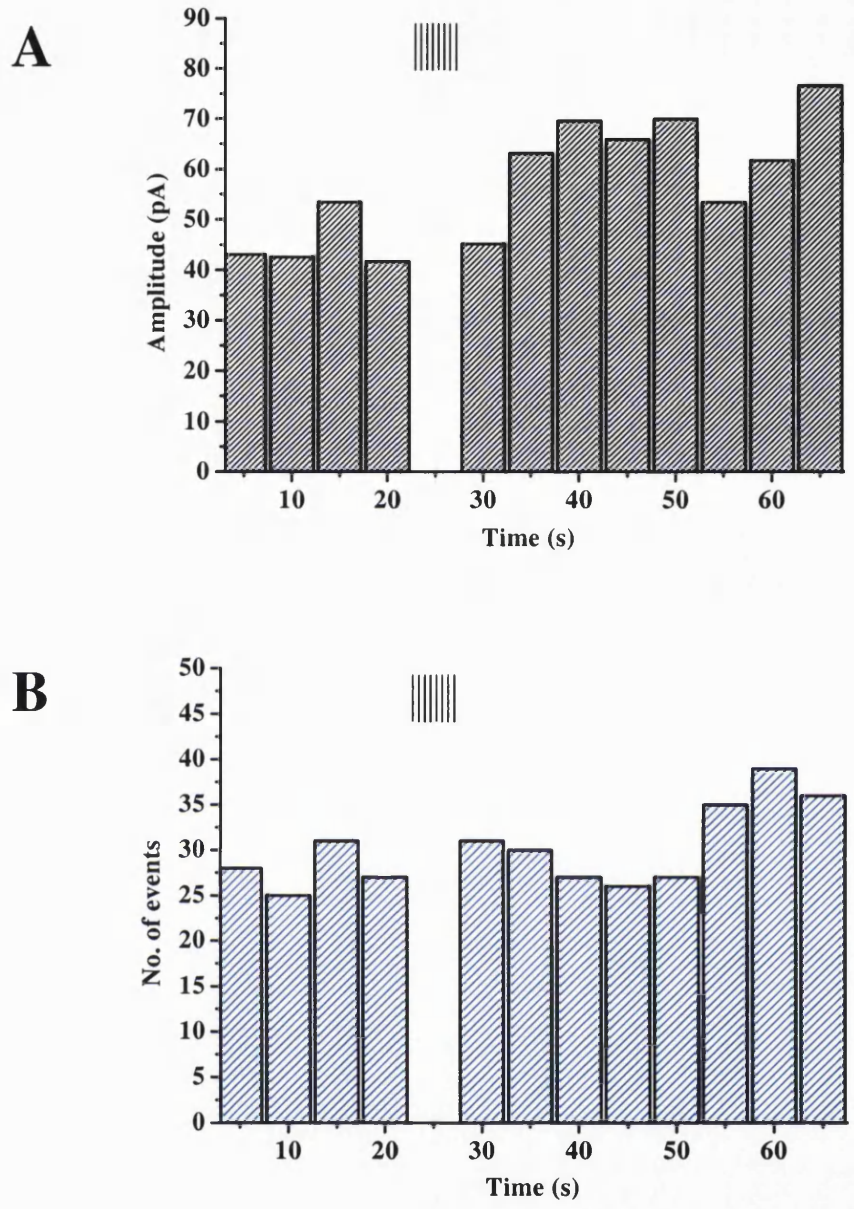

Fig. 5.8. Induction of DSI in the presence of 200nM LY 341495. Representative cell displaying changes in mIPSC amplitude (A) and frequency (B) following stimulus induction (||||||||) in a PN voltage clamped at –70mV. Depolarisation induced a rapid rise in mIPSC amplitude, while producing no discernible change in mIPSC frequency when compared to control.

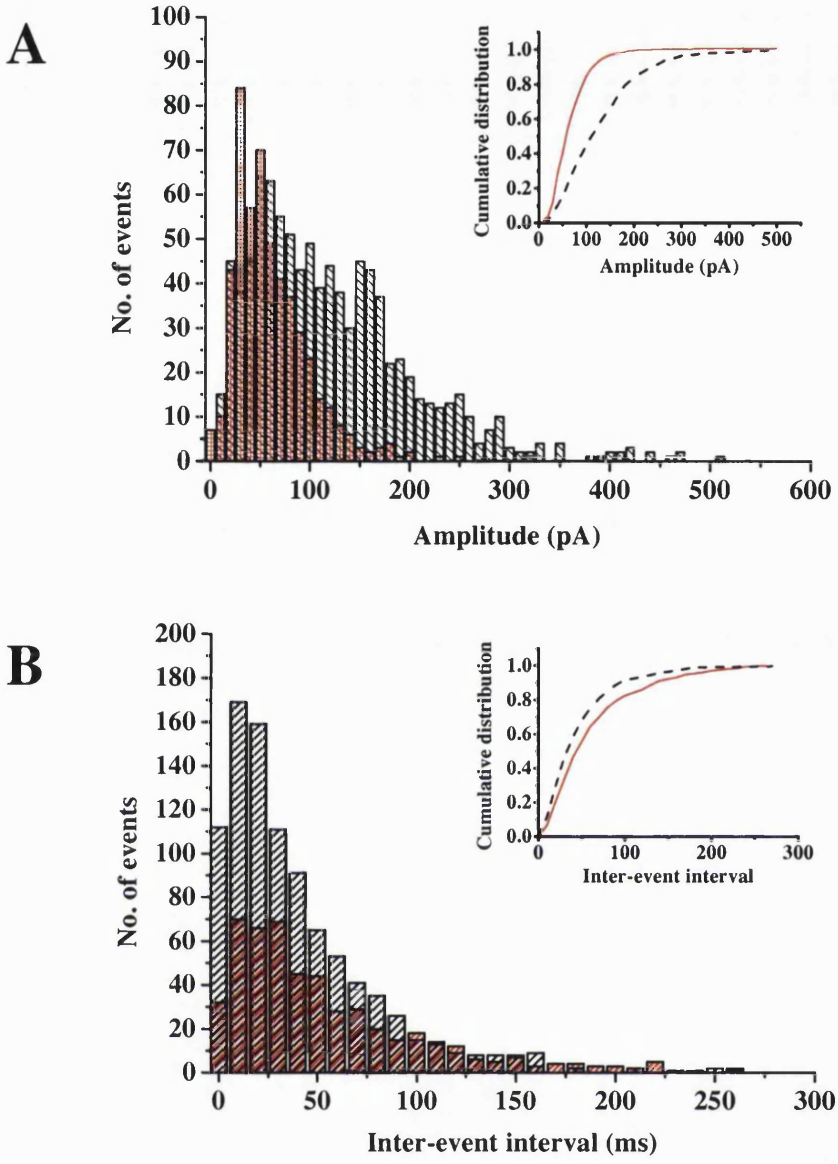

Fig. 5.9. RP in the presence of 200nM LY 341495. A, amplitude distribution of mIPSCs measured from a 40s period during control recording (dense red hatching) and at 3 min after stimulus cessation (RP_{t3}, medium black hatching) in a single PN superfused with Krebs solution containing 200nM LY 341495. The cumulative distributions from both histograms are illustrated in the inset of A, inset (red line = control, black dash = RP_{t3}). B, frequency distribution of mIPSCs measured from a 40s period during control recording (dense red hatching) and at 3 min after stimulus cessation (RP_{t3}, medium black hatching). The cumulative distributions from both histograms are illustrated in the inset of B, inset (red line = control, black dash = RP_{t3}).

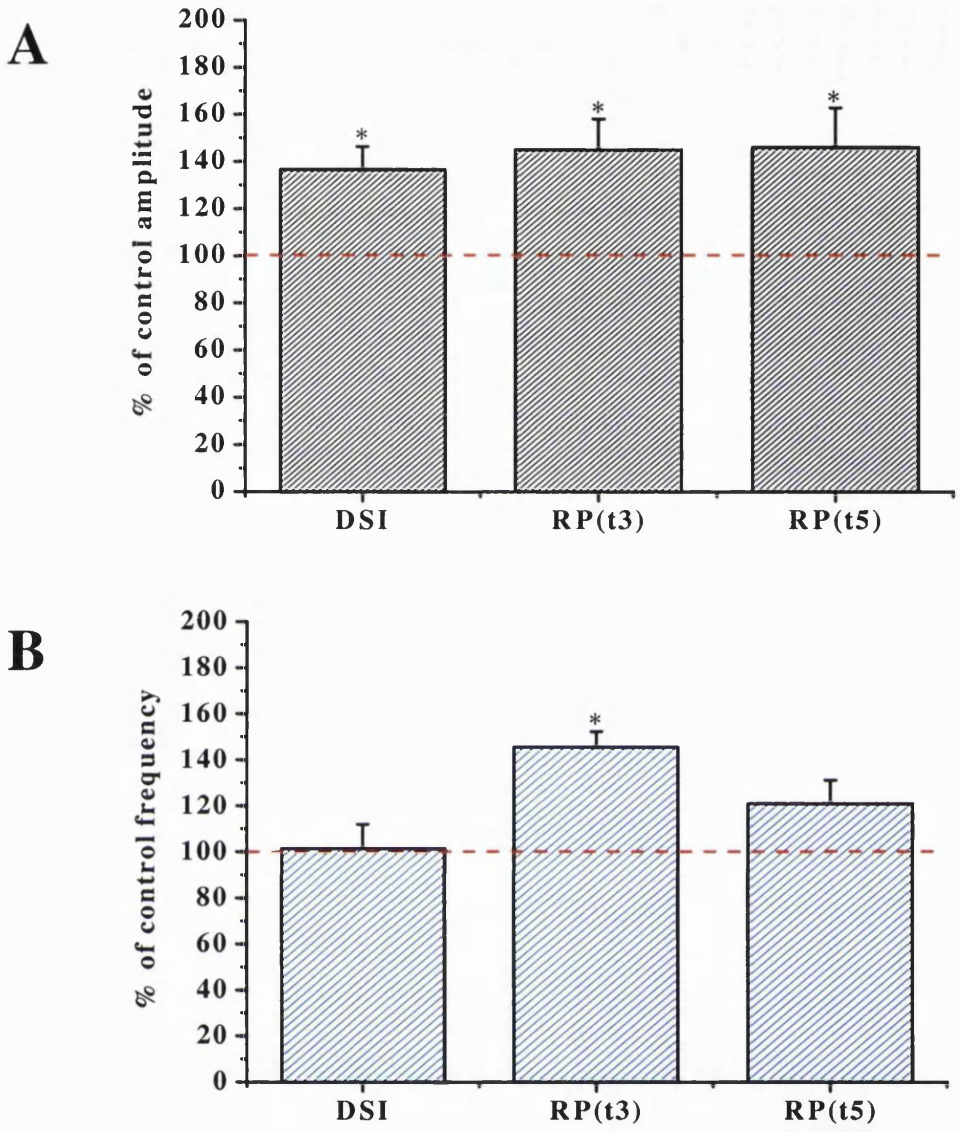

Fig. 5.10. Comparison of the effects of LY 341495 on DSI and RP. Average changes in mIPSC amplitude (A) and frequency (B) following stimulus induction in PNs voltage clamped at –70mV. Data represents mean values from data acquired in the presence of 200nM LY 341495. Bars represent average values (± s.e) normalised to control values taken in the same cells 2 min after the beginning of the whole-cell recording. Values for DSI were calculated from the initial 20s following stimulus cessation (n=5), $RP_{t3\ \&\ t5}$ were calculated at 3 & 5 min respectively (n=5) (* denotes $P<0.05$, Students t-test).

5.2.2. Rebound potentiation - $RP_{(LY\ 341495)}$

Analysis of mIPSC modulation at 3 min after stimulus cessation (RP_{t3}), in the same cells in which DSI had been abolished, identified a maintained increase in the mean mIPSC amplitude and the onset of a 'rebound' increase in the mean mIPSC frequency (Fig. 5.7B, a & c). The mean mIPSC amplitude increased to 145.0 ± 13.2% ($P<0.03$) (Fig. 5.10A) and the mean mIPSC frequency increased to 145.6 ± 6.8% ($P<0.03$) (Fig. 5.10B) of control (n=5). A representative cell displaying the change in amplitude distribution at RP_{t3} (Fig. 5.9A) had a mean amplitude value of 66.4 ± 1.7pA during control and a mean value of 128.1 ± 5.0pA during RP_{t3}. The cumulative amplitude distributions calculated from control and RP_{t3} histograms (Fig. 5.9A, inset) are significantly different ($P <0.0001$, K-S test). The same cell had a mean frequency of 16.9Hz in control and 21.5Hz during RP_{t3} (Fig. 5.9B). The cumulative frequency distributions calculated from control and RP_{t3} histograms (Fig. 5.9B, inset) are significantly different ($P<0.0001$, K-S test). At 5 min after stimulus cessation (RP_{t5}) the amplitude potentiation remained at 146.2 ± 16.7% of control ($P<0.05$) while the frequency potentiation diminished to 121.0 ± 10.2% ($P=0.1$) of control (Fig. 5.10A & B) (n=5). Therefore, the application of 200nM LY 341495 does not antagonise the 'rebound' frequency increase observed during RP.

5.2.3. Timecourse of PN mIPSC amplitude and frequency modulation after stimulus cessation in the presence of LY 341495

Depolarisation induced no change in the mean mIPSC frequency during the initial 20s after stimulus cessation. However, approximately 20s after depolarisation the mIPSC frequency began to gradually increase until reaching a plateau of potentiation at RP_{t3}, similar in magnitude to the frequency potentiation observed during RP_{t3} in normal Krebs (Fig. 5.11B). During the whole timecourse of frequency modulation the amplitude remained potentiated, rising steadily before reaching a plateau at $RP_{t1\text{-}5}$ (Fig.

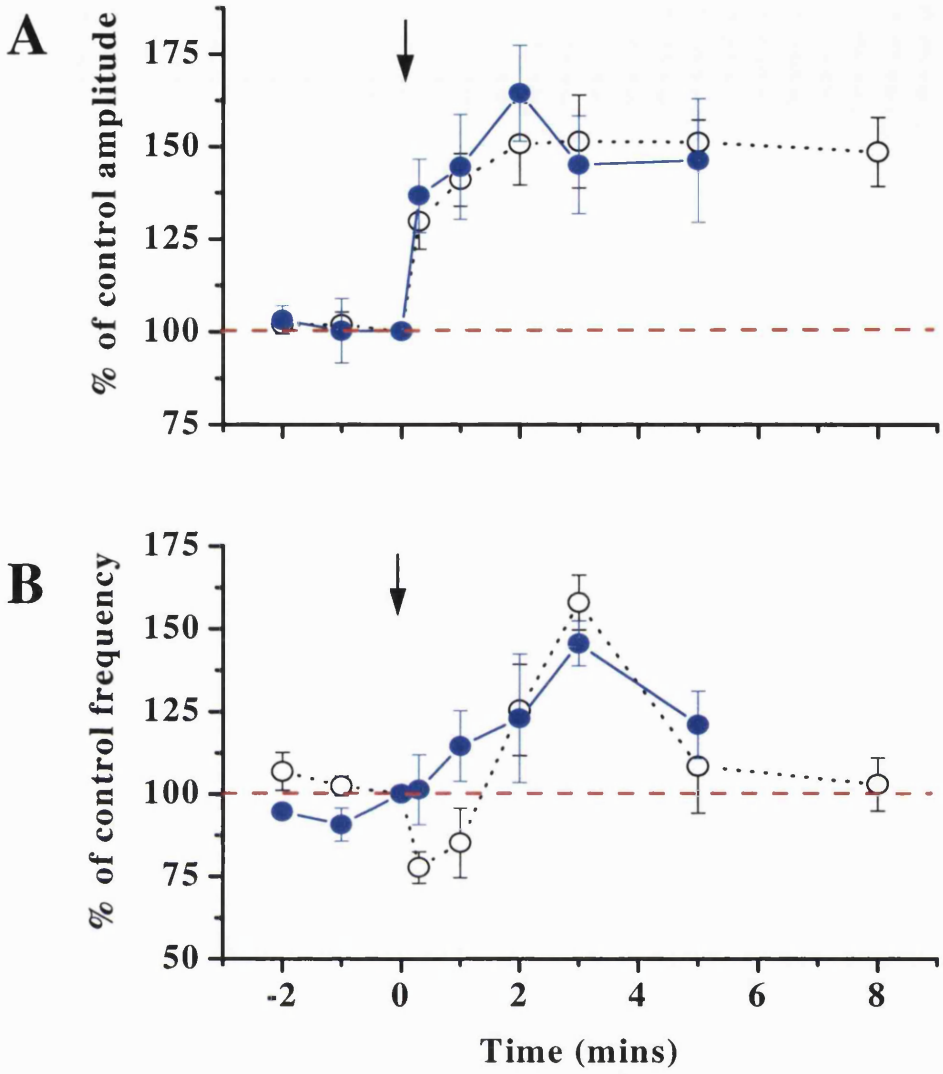

Fig. 5.11. Comparison between the time-dependent changes in PN mIPSC amplitude and frequency, following stimulus induction, in normal Krebs (empty black circles) and in the presence of 200nM LY 341495 (filled blue circles). A, changes in mean mIPSC amplitude during control period and after stimulus induction (amplitudes were measured throughout DSI & RP). Current amplitudes were normalised with respect to the mean value recorded directly preceding the point of stimulus induction (depicted by the arrow). B, changes in mean mIPSC frequency during control and after stimulus induction (frequencies were measured throughout DSI & RP). Mean mIPSC frequencies were normalised with respect to the mean value recorded directly preceding the point of stimulus induction (depicted by the arrow). All data are shown as mean ± s.e (Control n=11, LY 341495 n=5).

5.11A). The mean values during control and after depolarisation are summarised in Table 5.5.

Table 5.5. Timecourse of PN mIPSC amplitude and frequency modulation after stimulus cessation in the presence of LY 341495.

Time (m)	Amplitude ± s.e	Frequency ± s.e	n
-2	103.1 ± 3.8	94.6 ± 1.7	5
-1	100.2 ± 8.7	90.7 ± 5.0	5
0	100	100	5
0.3	136.6 ± 9.9	101.3 ± 10.6	5
1	144.4 ± 14.2	114.5 ± 10.7	5
2	164.3 ± 13.0	122.9 ± 19.4	5
3	145.0 ± 13.2	145.6 ± 6.8	5
5	146.2 ± 16.7	121.0 ± 10.2	5

*Data in red depicts statistically significant values compared to control (Paired t-test, $P<0.05$). Time 0 is defined as the point of stimulus induction, all other times are referenced to time 0 min. All values of amplitude/frequency potentiation are normalised to values calculated at time 0 min (set to 100%).

5.2.4. mIPSC kinetic changes during $DSI_{(LY\ 341495)}$ & $RP_{(LY\ 341495)}$

Comparison of the 'rise-time' and 'half-width' of mIPSCs recorded in the presence of 200nM LY 341495, during DSI and RP, identified no significant change with respect to control values (Table 5.6). Superimposed average traces accrued from 30 consecutive mIPSCs recorded during control, DSI and RP display the relative amplitude potentiation in a representative cell with respect to control values. Control mIPSCs had a mean amplitude value of 50.9 ± 2.3pA compared with 59.4 ± 2.3pA (DSI) and 84.1 ± 4.5pA (RP_{t3}) (Fig. 5.12).

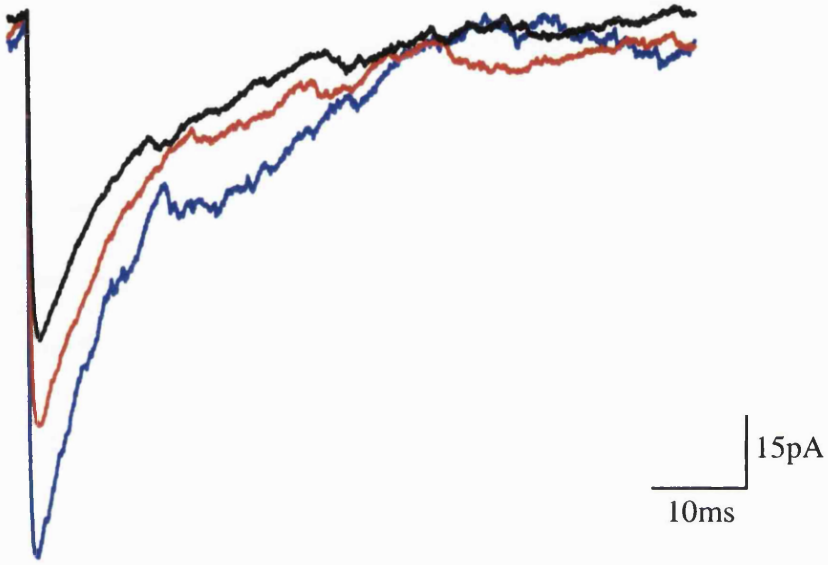

Fig. 5.12. Effect of 200nM LY 341495 on PN mIPSC kinetics. Superimposed averaged traces from all mIPSCs recorded in a single control cell at designated times. Traces were averaged from all mIPSCs recorded in a single control cell during control (black line), immediately after stimulus cessation (DSI) (red line) & 3 min after stimulus cessation (RP_{t3}) (blue line).

Table 5.6. Analysis of PN mIPSC kinetic parameters recorded in the presence of 200nM LY 341495 during control, DSI and at 3 min (RP_{t3}) after stimulus cessation. All data are mean values ± s.e. (n=5).

Kinetic Parameters	control ± s.e.m	DSI ± s.e.m	rebound ± s.e.m
Rise-Time (ms)	2.4 ± 0.1	2.4 ± 0.1	2.3 ± 0.1
Half-Width (ms)	8.9 ± 0.5	9.6 ± 0.7	9.4 ± 0.4

5.2.5. Immunocytochemical evidence for the existence of presynaptic $mGluR_{2/3}$

The presence of presynaptic $mGluR_{2/3}$ at release sites has long been established within the mammalian brain (Ohishi *et al.*, 1993; Ohishi *et al.*, 1994; Lujan *et al.*, 1997; Shigemoto *et al.*, 1997). A previous study in the cerebellum intimated a role for presynaptic $mGluR_{2/3}$ in the reduction of sIPSC and mIPSC amplitude and frequency during DSI, using the specific $mGluR_{2/3}$ agonist DCG-IV (Glitsch *et al.*, 1996; Satake *et al.*, 2000). In the present study the electrophysiological data unequivocally supports the role of presynaptic group II-like mGluR in the induction of cerebellar DSI. However, in order to compound this theory, immunocytochemical studies were undertaken in order to examine the possibility of $mGluR_{2/3}$ being present on putative release sites on cerebellar interneurones. An antibody directed against a common epitope on both $mGluR_2$ and $mGluR_3$ (amino acids 853-872 of human $mGluR_2$, identical to rat $mGluR_2$ and 89% identical to human & rat $mGluR_3$) was used to identify the presence all group II mGluRs and their cellular location (Fig. 5.13B & Fig. 5.14B). Simultaneous staining with an anti-glutamic acid decarboxylase (GAD) antibody identified all interneurones within the mixed cerebellar culture (Fig. 5.13A & Fig. 5.14A). To examine the hypothesis of a presynaptic location for $mGluR_{2/3}$, an antibody directed against the protein synaptophysin, a component of the presynaptic vesicle docking process, was used in order to identify putative release sites (Fig. 5.13C & Fig. 5.14C). Analysing the existence of presynaptic mGluRs required locating an interneurone within a relatively cell sparse area of the mixed cerebellar culture. This maximised the identification of specific structures on the axon without contamination from surrounding cell bodies,

axons or dendrites. Triple immunocytochemical staining identified only a subset of large (10-15μm) cerebellar interneurones displaying immunoreactivity for $mGluR_{2/3}$. Subsequent observations from mixed cerebellar cultures stained with antibodies recognising both $mGluR_{2/3}$ and parvalbumin identified only cerebellar Golgi cells displaying $mGluR_{2/3}$ immunoreactivity. Immunocytochemical staining for $mGluR_{2/3}$ could be seen throughout the cell body, beaded dendrites and axons of cultured cerebellar Golgi cells with more punctate staining in the distal cell processes (Fig. 5.13D & Fig. 5.14D).

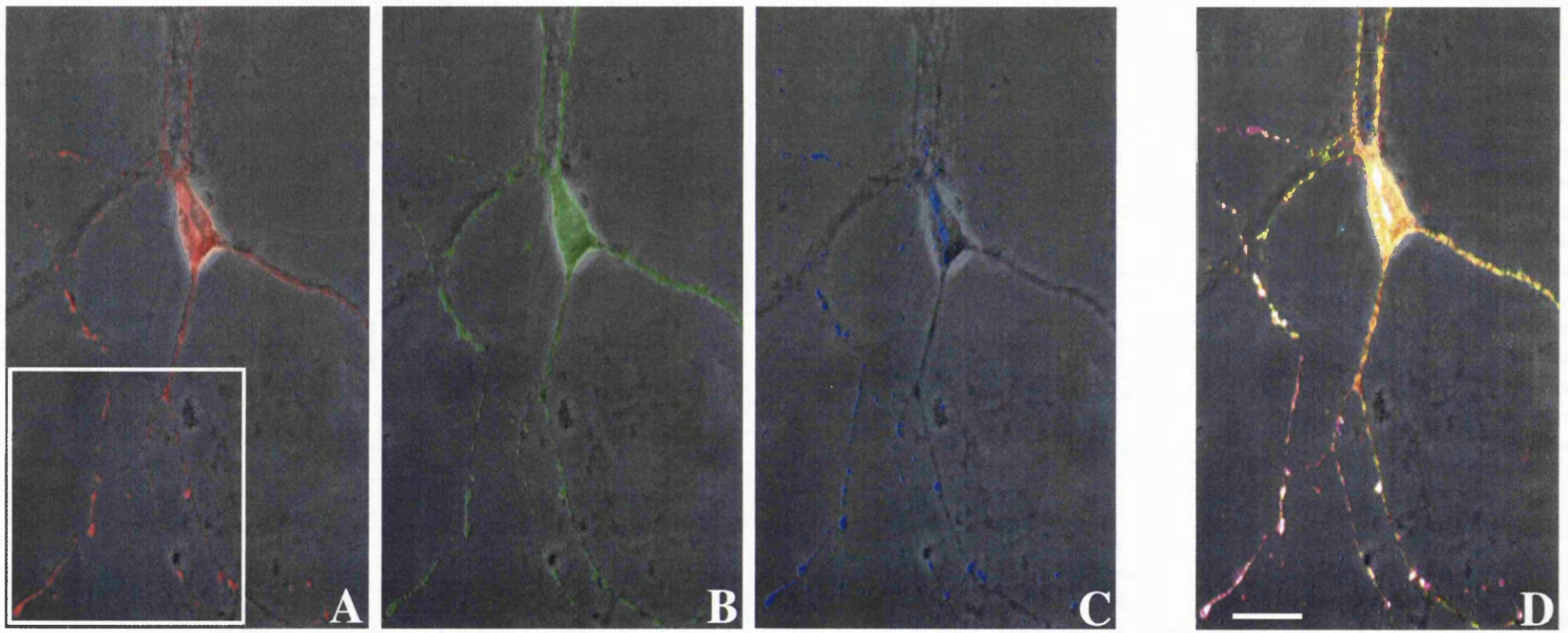

Fig. 5.13. Triple immunocytochemical staining of a putative cerebellar Golgi cell in a relatively cell sparse mixed cerebellar culture. A, anti-glutamic acid decarboxylase (GAD) – TRITC conjugate stain identifying GABAergic interneurones. B, anti-$mGluR_{2/3}$ – FITC conjugate stain displaying $mGluR_{2/3}$ distribution. C, anti-synaptophysin – Cy5 conjugate stain identifying putative release sites. D, triple overlay of RGB images identifying high percentage of GAD-Cy5 colocalisation and the presence of $mGluR_{2/3}$ subunits at release sites on a putative cerebellar Golgi cell. A-D, all images were superimposed on the corresponding brightfield image after acquisition. Images were acquired at X40 (oil immersion) at 10% zoom. Scale bar represents 15μm.

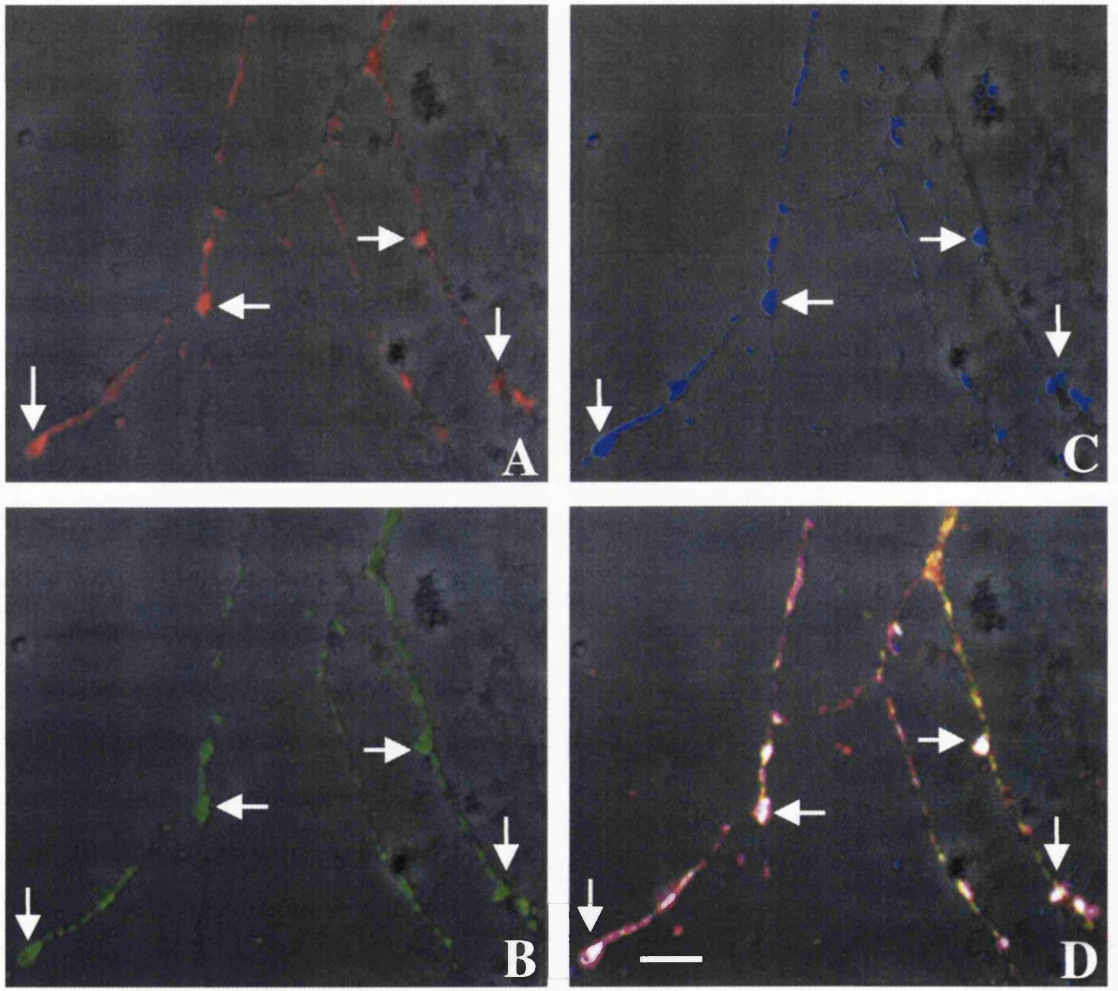

Fig. 5.14. Triple immunocytochemical staining of a putative cerebellar Golgi cell axon at high magnification (depicted in Fig. 5.13 A, inset). A, anti-glutamic acid decarboxylase (GAD) – TRITC conjugate stain identifying GABAergic interneurones. B, anti-mGluR$_{2/3}$ – FITC conjugate stain displaying mGluR$_{2/3}$ distribution. C, anti-synaptophysin – Cy5 conjugate stain identifying putative release sites. D, triple overlay of RGB images identifying high percentage of GAD-Cy5 colocalisation and the presence of mGluR$_{2/3}$ at release sites on a putative cerebellar Golgi cell. A-D, all images were superimposed on the corresponding brightfield image after acqusition. Images were acquired at X63 (oil immersion) at 0% zoom. Scale bar represents 5μm.

DISCUSSION

5.1. Effects of the non-specific mGluR antagonist (S)-MCPG on DSI & RP induction

The regulation of neurotransmitter release by presynaptic mGluRs has been the focus of many studies over the last decade. In the cerebellum presynaptic mGluRs, present on the axon terminals of interneurones in the molecular layer, have been implicated in the modulation of GABA release. Application of the broad spectrum agonist t-ACPD facilitated a decrease in the amplitude of evoked IPSCs and a decrease in the frequency of mIPSCs. Interestingly, application of the broad spectrum mGluR antagonist (s)-MCPG failed to block the t-ACPD induced changes in GABA release (Llano & Marty, 1995). The unusual pharmacology of the presynaptic mGluRs present on the axon terminals of cerebellar basket and stellate cells made it difficult for the authors to precisely specify the mGluR subtype(s) involved in the modulation of GABA release. Investigation into the phenomenon of cerebellar DSI confirmed previous findings where the application of (S)-MCPG (1mM), at a concentration which fully blocked $mGluR_1$-mediated inward currents in PNs, failed to block the depolarisation-induced reduction of GABA release (Glitsch *et al.*, 1996). The work in the present study confirms that of Llano and Marty (1995) and Glitsch and colleagues (1996) in that the application of (S)-MCPG, at a somewhat lower concentration (100μM), produced no significant change in the magnitude of DSI nor the basal rate of spontaneous AP-independent miniature release. However, exogenous application of the specific $mGluR_{2/3}$ agonist DCG-IV induced a reduction in the mIPSC frequency equal in magnitude to that induced during cerebellar DSI (Glitsch *et al.*, 1996). A similar study by Satake and colleagues (2000) induced a 60% reduction in sIPSC, recorded in mature cerebellar PNs, upon exogenous application of DCG-IV and this 'DCG-IV-sensitive DSI' could be abolished by the application of the specific $mGluR_{2/3}$ antagonist CPPG. Therefore, the work presented in this and previous studies seems to intimate that the regulation of GABA release by presynaptic mGluRs occurs via a $mGluR_{2/3}$-like receptor negatively linked to adenylate cyclase although the use of (S)-MCPG, as a

pharmacological tool to examine the role played by presynaptic mGluRs in the regulation of GABA release from basket and stellate cells in the cerebellum, is entirely ineffective. Coincident activation of PFs and CFs, *in vivo*, leads to the activation of $mGluR_1$ on the postsynaptic membrane of PNs. This leads to activation of the PLC pathway and a subsequent increase in the cytosolic calcium level, the pre-requisite step in the induction of both DSI and RP (Llano *et al.*, 1991). Since mixed cerebellar cultures are largely devoid of co-ordinated CF and PF inputs to PNs, a depolarising protocol is used to mimic the overall effect of PF and CF stimulation, thus inducing the mIPSC amplitude potentiation observed during DSI and RP. The application of 100μM (S)-MCPG has been demonstrated to sufficiently block PN $mGluR_1$-mediated inward currents, irrespective of the lack of presynaptic antagonism (Llano & Marty, 1995; Glitsch *et al.*, 1996). Stimulation of the PN $mGluR_1$-PLC pathway has been illustrated to mimic the depolarisation-induced enhancement of $GABA_AR$-mediated currents during RP and induce a large increase in the frequency of mIPSCs (Hashimoto *et al.*, 1996), although this was contrary to the findings of two previous studies (Llano & Marty, 1995; Glitsch *et al.*, 1996). Therefore, the release of 'glutamate', on depolarisation, back into the synaptic cleft should serve to facilitate the further release of Ca^{2+} from intracellular stores due to stimulation of the PN $mGluR_1$-PLC pathway. The application of (S)-MCPG did not alter the magnitude of mIPSC amplitude potentiation during both DSI and RP with respect to control. Therefore, repetitive depolarisation must serve to maximally activate the signal transduction cascade(s) leading to PN $GABA_AR$ phosphorylation, such that the possible further release of Ca^{2+} from intracellular stores would not result in a further enhancement of PN mIPSC amplitude.

5.2. Effects of the specific group II mGluR antagonist LY 341495 on DSI and RP induction

The mGluR antagonist LY 341495 is a novel and potent group II antagonist, displaying a unique range of selectivities across the mGluR receptor subtypes. The IC_{50}

values for $mGluR_{1/4/5/7\&8}$ range from 1-22μM as calculated from functional and binding studies (Ornstein *et al.*, 1998; Kingston *et al.*, 1998a; Fitzjohn *et al.*, 1998; Johnson *et al.*, 1999). However, this compound shows nanomolar affinity (IC_{50} 10-30nM) for $mGluR_{2/3}$ thus providing a selective pharmacological tool to dissect the role played by group II mGluRs in the phenomena termed DSI and RP. The use of the high affinity, specific $mGluR_{2/3}$ antagonist LY 341495 induced a complete abolition of the mIPSC frequency decrease observed during DSI without affecting the retrograde transmitter release process and subsequent frequency potentiation during RP. Application of LY 341495 had no effect on the magnitude of mIPSC amplitude potentiation during either DSI or RP nor on the timecourse of the amplitude potentiation (such that it reached a potentiated plateau at an equivalent point to control) when compared to DSI/RP in normal Krebs. Therefore, it can be assumed that LY 341495 does not have any adverse effects upon PN $GABA_A$Rs, VACCs or the phosphorylation process thought to underlie the mIPSC amplitude potentiation (Kano & Konnerth, 1992; Kano *et al.*, 1996; Kawaguchi *et al.*, 2000). Interestingly, during the initial 20s after stimulus cessation, in the presence of LY 341495, the mIPSC frequency remained comparable to that in control, only after ~20s does the mIPSC frequency begin to increase to a level comparable to that observed during RP_{t3} in normal Krebs. Although there is an almost immediate increase in the mIPSC frequency in the presence of a $mGluR_{2/3}$ antagonist there still remains a short time-lag, suggesting that the mIPSC frequency changes during DSI and RP are mediated via different receptor types and are not entirely overlapping. Therefore, the mIPSC frequency changes observed during DSI and RP are most likely to be part of the same phenomenon. The possible reasons for this time-dependent lag will be discussed fully in Chapter 6. The results from the present study and that of previous studies unequivocally identified a role for presynaptic $mGluR_{2/3}$-like activation in the reduction of GABA release from the axon terminals of cerebellar basket and stellate cells during DSI (Llano & Marty, 1995; Glitsch *et al.*, 1996; Satake *et al.*, 2000). However, some discrepancies still exist, such as the inability of (S)-MCPG to antagonise the putative $mGluR_{2/3}$-mediated effects, making the precise identification of the specific mGluR subtype involved in this transient form of synaptic plasticity difficult.

5.3. Immunohistochemistry & pharmacology: The anomalies that exist

Although the electrophysiological and pharmacological evidence for the involvement of $mGluR_{2/3}$ in the mIPSC frequency depression during DSI is somewhat overwhelming (Glitsch *et al.*, 1996; Satake *et al.*, 2000; present study) there exists no immunohistochemical or immunocytochemical evidence to support the presence of this mGluR subtype on the axon terminals of basket and stellate cells in cerebellar slice (Ohishi *et al.*, 1994; Lujan *et al.*, 1997; Meguro *et al.*, 1999) or mixed cerebellar culture preparations (present study). Early immunohistochemical studies in the cerebellum identified strong $mGluR_{2/3}$ staining of Golgi cells and moderate to light staining in the molecular layer proposed to be stellate cells (Ohishi *et al.*, 1993). However, a subsequent paper, by the same author, identified that the only neuronal type to show immunoreactivity for $mGluR_{2/3}$ were Golgi cells present in the PN layer. The majority of the staining was present in the granular layer where the bifurcating axons of the Golgi cells terminate, forming part of the cerebellar glomerulus. The beaded dendrites of the Golgi cells ascended into the molecular layer where they acquired inhibitory synaptic input from stellate and basket cells and excitatory synaptic input from PFs. Therefore, the light $mGluR_{2/3}$ staining in the molecular layer observed in the former study was deemed to be either the beaded dendrites of Golgi cells or immunoreactive glial cells and not basket or stellate cells. In the present study it was pertinent to ascertain whether basket and/or stellate cells in culture expressed $mGluR_{2/3}$ on their axon terminals and could therefore underlie the mIPSC frequency decrease observed during cerebellar DSI. In accordance with previous studies, only cerebellar Golgi cells were immunopositive for $mGluR_{2/3}$ and immunonegative for parvalbumin while basket and stellate cells were immunonegative for $mGluR_{2/3}$ and immunopositive for parvalbumin. One inherent problem with mixed cerebellar cultures is the loss of coordinated afferent inputs, although it is possible that Golgi cells may form synaptic inputs with mature PNs it is most unlikely that they would provide the majority of the inhibitory synaptic inputs to PNs as they are outnumbered 20:1 by basket and stellate cells (see chapter 3). Therefore, there are major anomalies which exist between the pharmacological profile of the presynaptic mGluR subtype involved in the mIPSC frequency decrease observed during cerebellar DSI and the immunohistochemical

evidence supporting mGluR expression in cerebellar interneurones. A summary of mGluR subtype pharmacology and the evidence supporting a role for presynaptic mGluRs in the induction of DSI are displayed in table 5.7 and table 5.8.

Table 5.7 mGluR subtype pharmacology and localisation in the cerebellum

mGluR subtype	Transduction mechanism	Cerebellar cell type	Selective agonist	EC_{50} (μM)	Selective antagonist	IC_{50} (μM)
$mGluR_1$	+PLC	PN,BC/SC,GC[1]	t-ACPD &	(5-200)	MCPG &	(40-500)
$mGluR_5$	+PLC	GC[2]	DHPG	(1-60)	LY 341495	(7-10)
$mGluR_2$	-A.C	GC[3,4,5,6]	t-ACPD &	(5-900)	MCPG	(15-300)
$mGluR_3$	-A.C	GC[3,4,5,6]	DCG-IV	(0.1-0.3)	LY 341495	(0.002)
					CPPG	(~400)
$mGluR_4$	-A.C	-				
$mGluR_6$	-A.C	-	t-ACPD &	(20-1000)	MPPG	(4-500)
$mGluR_7$	-A.C	PN,BC/SC[7]	L-AP4	(0.06-1)	LY 341495	(1-22)
$mGluR_8$	-A.C	BC/SC[8]				

[1]Shigemoto *et al.*, 1992, [2]Neki *et al.*, 1996, [3]Ohishi *et al.*, 1993, [4]Ohishi *et al.*, 1994, [5]Lujan *et al.*, 1997, [6]Meguro *et al.*, 1999, [7]Philips *et al.*, 1998, [8]Berthele *et al.*, 1999. EC_{50} and IC_{50}s refer to the selective ligands respectively.

Table 5.8 Evidence supporting mGluR involvement in the induction of cerebellar DSI

Agonist applied	Ability to mimic DSI	Antagonist Applied	Ability to block DSI	mGluR affected	Immunoreactivity on BC/SCs
t-ACPD[9]	Yes	-	-	Grp I,II,III	Grp I,III
-	-	MCPG[9,10]	No	Grp I,II	Grp I
DCG-IV[10,11]	Yes	-	-	Grp II	n/a
-	-	L-AP3[10]	Yes	Grp II	n/a
-	-	CPPG[11]	Yes	Grp II	n/a
Retrograde	Yes	-	-	Grp I,II,III*	Grp I,III
messenger[10,12]	-	-	-		
-	-	LY 341495	Yes	Grp II+	n/a

[9]Llano *et al.*, 1995, [10]Glitsch *et al.*, 1996, [11]Satake *et al.*, 2000, [12]present study
(*on the assumption that glutamate or a 'glutamate like' substance is the retrograde messenger)
(+at the concentration used in this study)

Therefore, it can clearly be seen that the there are discrepancies between the pharmacological and immunohistochemical results of this study and previous studies thus proposing that $mGluR_{2/3}$ may not play a predominant role in the induction of cerebellar DSI. The work carried out on cerebellar DSI by Glitsch and colleagues (1996) assumed that previous immunohistochemical data, identifying weak $mGluR_{2/3}$ staining in the molecular layer, unequivocally identified the presence of $mGluR_{2/3}$ on stellate cells (Ohishi *et al.*, 1993). Unfortunately, Glitsch and colleagues completely neglected the findings of a subsequent more detailed immunohistochemical study by the same group, identifying no $mGluR_{2/3}$ on stellate or basket cells (Ohishi *et al.*, 1994).

The results of the present study, when considered with the results of previous studies on cerebellar DSI, support the theory that presynaptic mGluRs do underlie the induction of DSI although it now seems evident that $mGluR_{2/3}$ are not the subtypes mediating the depolarisation-induced reduction in mIPSC frequency. Therefore, two possibilities exist as to the nature of the mGluR subtype involved. Firstly, the pharmacology seems consistent with the presence of a group II mGluR raising the possibility that an alternative splice variant may exist. This splice variant may have an N-terminal sequence, the epitope site for the antibody used in this study, or C-terminal sequence, the epitope site for the antibody used by Ohishi and colleagues (1994), dissimilar to that required to attain sufficient antibody binding for $mGluR_{2/3}$. Secondly, the possibility exists that cerebellar DSI is mediated by a novel mGluR subtype displaying some pharmacological similarities to group II mGluRs but possessing sufficiently different N-/C-terminal sequences such that existing mGluR antibodies would not recognise the required epitope. Obviously this is only a very tentative hypothesis and remains to be evaluated in future experiments.

Chapter 6

PRESYNAPTIC NMDAR-MEDIATED CONTROL OF INHIBITORY SYNAPTIC TRANSMISSION AT THE INTERNEURONE-PN SYNAPSE

INTRODUCTION

The phenomenon of DSI, extensively studied over the past decade, has identified the predominant role of presynaptic mGluRs in the modulation of mIPSC amplitude and frequency in both the hippocampus and cerebellum (Morishita *et al.*, 1998; Glitsch *et al.*, 1996). Pharmacological dissection of DSI in the cerebellum identified an increase in the frequency of spontaneous or miniature IPSCs on application of L-AP3, a broad-spectrum agonist acting on several glutamate receptor subtypes (Glitsch *et al.*, 1996). This increase in transmitter release could be completely abolished by the application of the competitive NMDAR antagonist, D-APV, therefore suggesting mediation via presynaptic NMDA receptors. Complimentary work, utilising bath application of NMDA, induced a marked potentiation of mIPSC frequency persisting even in the presence of physiological levels of Mg^{2+} (Glitsch & Marty, 1999). Similarly, these effects could be abolished by the application of D-APV thus supporting the theory of presynaptic NMDARs at the interneurone-PN synapse. The existence of presynaptic NMDARs is by no means a novel concept, although in physiological terms, the roles and functions played by these receptors still remains largely unclear.

The presence of NMDARs on the terminals of glutamatergic and GABAergic fibres has been established both immunohistochemically (Liu *et al.*, 1994; DeBiasi *et al.*, 1996; Paquet & Smith, 2000) and electrophysiologically (Berretta & Jones, 1996; Glitsch & Marty, 1999; Pouzat & Marty, 1999; Casado *et al.*, 2000). Interestingly, in the cerebellum the effect of presynaptic NMDAR activation is input dependent. At PF-PN synapses presynaptic autoreceptor activation, upon PF stimulation, induced a reduction in amplitude of EPSCs recorded in PNs. This is postulated to arise due to a NMDAR-mediated release of nitric oxide (NO) which diffused from the CF terminal to

the PN, where upon it caused a decrease in the postsynaptic glutamate sensitivity (Casado *et al.*, 2000). Interestingly, this study develops the idea that Ca^{2+} entry via NMDARs and VACCs produce two spatially distinct Ca^{2+} microdomains inducing differential effects on both the liberation of NO and neurotransmitter release process. Persistent application of NMDA at the interneurone-PN synapse caused a marked enhancement of neurotransmitter release (Glitsch & Marty, 1999), preferentially increasing release at small synapses, thus intimating a role for presynaptic NMDARs in the developmental regulation of cerebellar interneurones and/or developmental inhibitory synaptic plasticity. The downstream signalling cascade(s) involved in the NMDAR-mediated modulation of GABA release from cerebellar interneurones has as yet, not been elucidated. Therefore, it is pertinent to ascertain the possible role for presynaptic NMDARs in the modulation of synaptic efficacy observed during cerebellar DSI and RP.

RESULTS

6.1. Effects of the specific NMDAR antagonist D-APV on DSI and RP induction

Application of the specific NMDAR antagonist D-APV (50μM) produced no change in the mean amplitude (105.8 ± 7.5% of control,P=0.5) but reduced the basal frequency of PN mIPSCs (75.9 ± 5.2% of control, P<0.01), indicating the likelihood of tonic activation of NMDARs by background glutamate.

6.1.1. $DSI/RP_{(D\text{-}APV)}$ *vs* $DSI/RP_{(D\text{-}APV + (S)\text{-}MCPG)}$

A comparison between the induction of DSI and RP in the presence of 50μM D-APV and in the presence of 50μM D-APV + 100μM (S)-MCPG reiterated the findings of chapter 5 in that (S)-MCPG does not affect synaptic transmission at the interneurone-PN synapse. The results from the comparison are displayed in Table 6.1 & Table 6.2.

Table 6.1. Comparison between mIPSC amplitude modulation (DSI & RP) in the presence of 50μM D-APV (n=5) and in the presence of 50μM D-APV + 100μM (S)-MCPG (n=5).

Time	Control ± s.e.m	50μM D-APV ± s.e.m	50μM D-APV + 100μM (S)-MCPG ± s.e.m
Control	100	100	100
DSI	**129.8** ± 7.4	130.1 ± 8.7	118.8 ± 6.7
RP_{t3}	**151.5** ± 12.6	147.4 ± 13.5	135.6 ± 8.0
RP_{t5}	**151.3** ± 6.1	150.9 ± 7.7	148.3 ± 10.0

Table 6.2. Comparison between mIPSC frequency modulation (DSI & RP) in the presence of 50μM D-APV (n=5) and in the presence of 50μM D-APV + 100μM (S)-MCPG (n=5).

Time	Control ± s.e.m	50μM D-APV ± s.e.m	50μM D-APV + 100μM (S)-MCPG ± s.e.m
Control	100	100	100
DSI	**77.7** ± 4.8	79.1 ± 1.2	80.4 ± 5.2
RP_{t3}	**158.0** ± 8.3	115.6 ± 19.1	92.7± 7.1
RP_{t5}	**108.5** ± 14.2	83.3 ± 17.3	89.8 ± 6.8

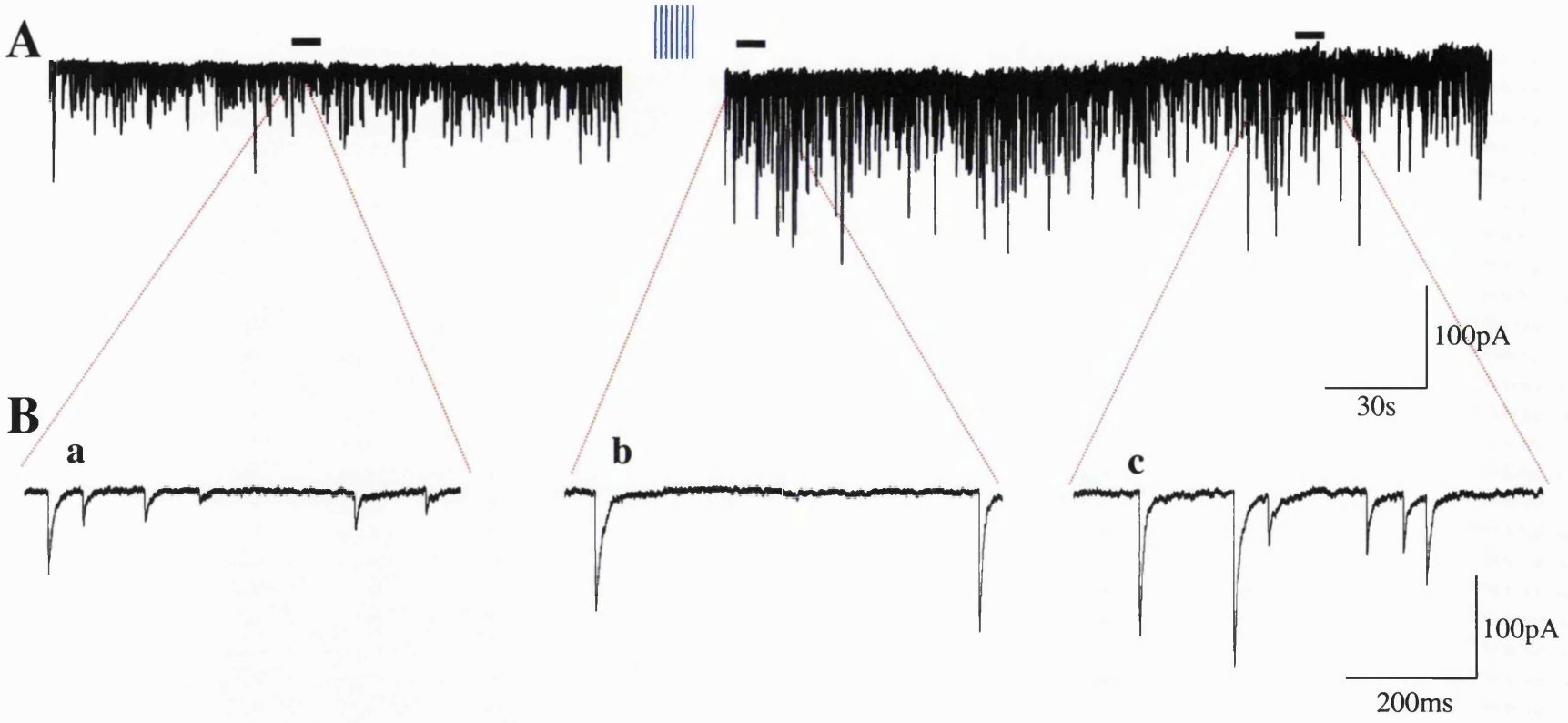

Fig. 6.1. Effects of D-APV on the induction of DSI/RP. A, summated mIPSCs recorded during control (upper left trace) and after (upper right trace) a train of depolarising pulses (▮) (8 pulses of 70mV amplitude, 100ms duration at 2s intervals) applied from a holding potential of –70mV at 3 min from the start of whole-cell recording. All recordings were made in perfusion media containing 50μM D-APV. B, Insets show expanded time-base examples of mIPSCs recorded during control (a), initial 20s after stimulus (DSI) (b) and 3min after stimulus cessation (rebound potentiation (RP_{t3})) (c).

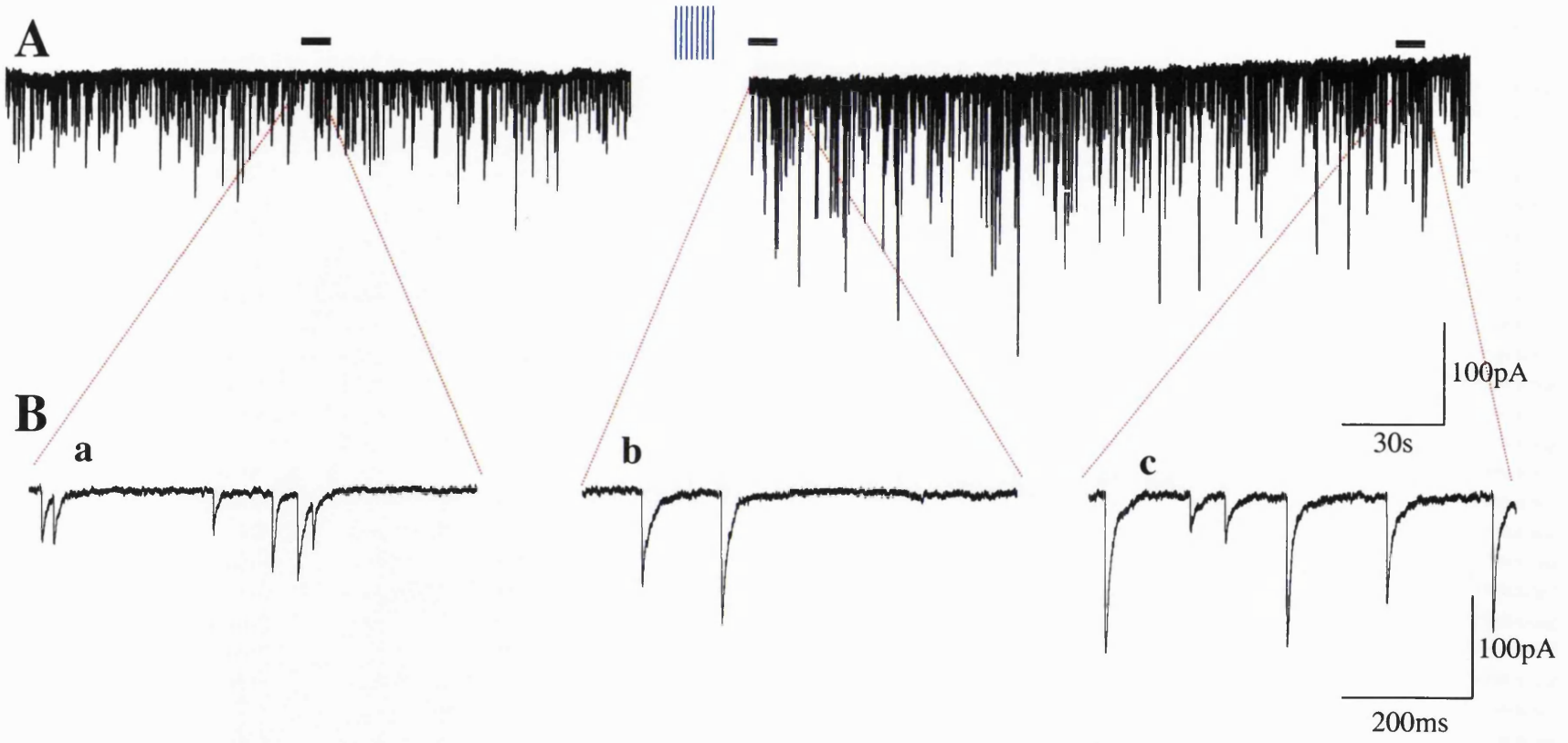

Fig. 6.2. Effects of D-APV + (S)-MCPG on the induction of DSI/RP. A, summated mIPSCs recorded during control (upper left trace) and after (upper right trace) a train of depolarising pulses (▥) (8 pulses of 70mV amplitude, 100ms duration at 2s intervals) applied from a holding potential of –70mV at 3 min from the start of whole-cell recording. All recordings were made in perfusion media containing 50μM D-APV & 100μM (S)-MCPG. B, Insets show expanded time-base examples of mIPSCs recorded during control (a), initial 20s after stimulus (DSI) (b) and 3min after stimulus cessation (rebound potentiation (RP_{t3})) (c).

Due to there being no statistical difference between DSI and RP induction/maintenance in the presence of 50μM D-APV and in the presence of 50μM D-APV + 100μM (S)-MCPG ($P>0.05$ one-way ANOVA with Bonferroni post-test) all subsequent data with these antagonists were therefore pooled (n=10) (Fig 6.1B, a, b & c & Fig 6.2B, a, b & c). Data termed D-APV (alone) and D-APV + (S)-MCPG will be referred to as D-APV hereafter.

6.1.2. Depolarisation-induced suppression of inhibition - $DSI_{D\text{-}APV}$

Application of a train of depolarising pulses, in the presence of 50μM D-APV induced no change in the magnitude of amplitude or frequency modulation when compared to DSI in control conditions (Fig 6.1B, a & b & Fig. 6.2B, a & b). The mean mIPSC amplitude increased to 124.5 ± 5.5 % ($P<0.002$) of control and the mean mIPSC frequency decreased to 79.7 ± 9.6% ($P<0.0001$) of control (n=10) (Fig. 6.5A & B). A representative cell (Fig. 6.3A) illustrates the rapid onset of amplitude potentiation after stimulus cessation while simultaneously displaying a sustained (~40s) reduction in the mean frequency of mIPSCs (Fig. 6.3B). Pharmacological block of NMDARs does not interfere with the induction of a robust DSI when compared to DSI in normal Krebs.

6.1.3. Rebound potentiation - $RP_{D\text{-}APV}$

Analysis of mIPSC modulation at 3 min after stimulus cessation (RP_{t3}), in the same cells in which DSI had been previously induced, identified a maintained increase in the mean mIPSC amplitude. However, application of 50μM D-APV completely abolished the increase in the mean mIPSC frequency observed during RP_{t3} in normal Krebs (Fig. 6.1B, a & c & 6.2B, a & c). The mean mIPSC amplitude increased to 141.5 ± 7.7% ($P<0.0004$) of control with no discernible change in mIPSC frequency (104.2 ± 10.3%, $P=0.7$) (Fig. 6.5A & B) (n=10). A representative cell

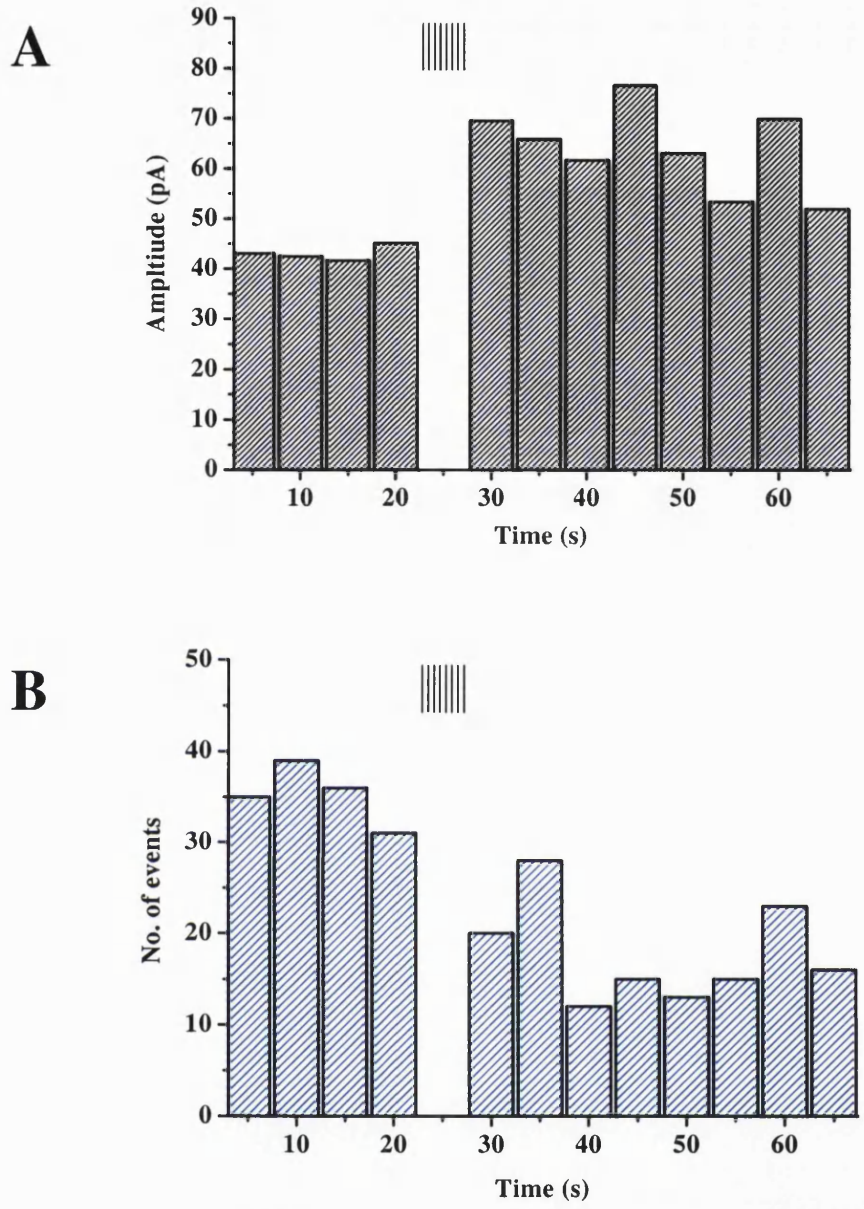

Fig. 6.3. Induction of DSI in the presence of 50μM D-APV. Representative cell displaying changes in mIPSC amplitude (A) and frequency (B) following stimulus induction (||||||||) in a PN voltage clamped at –70mV. Depolarisation induced a rapid rise in mIPSC amplitude, while inducing a longer lasting decrease in mIPSC frequency persisting for ≥ 40s.

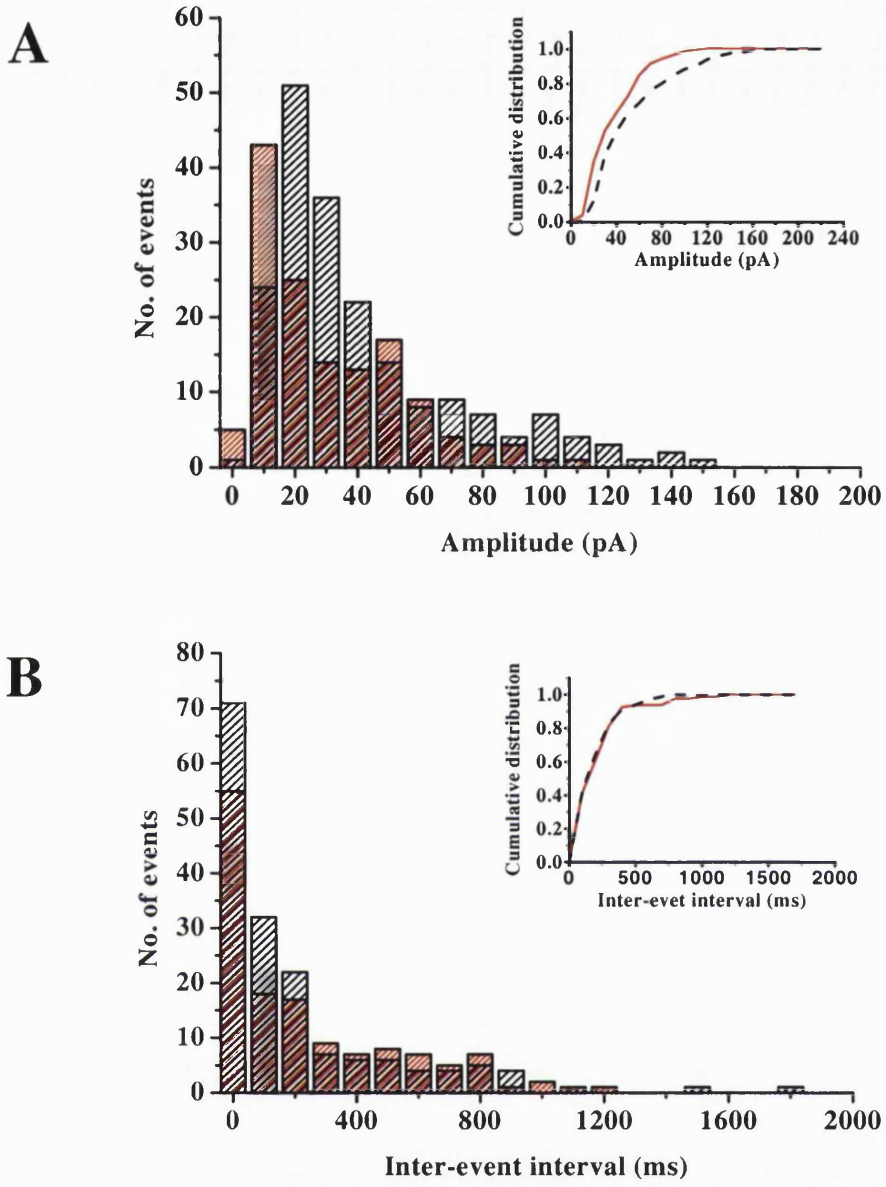

Fig. 6.4. RP in the presence of 50μM D-APV. A, amplitude distribution of mIPSCs measured during control recording (dense red hatching) and at 3 min after stimulus cessation (RP_{t3}, medium black hatching), in a single PN superfused with Krebs solution containing 50μM D-APV. The cumulative distributions from both histograms are illustrated in A, inset (red line = control, black dash = RP_{t3}). B, frequency distribution of mIPSCs measured during control recording (dense red hatching) and at 3 min after stimulus cessation (RP_{t3}, medium black hatching). The cumulative distributions from both histograms are illustrated in B, inset (red line = control, black dash = RP_{t3}).

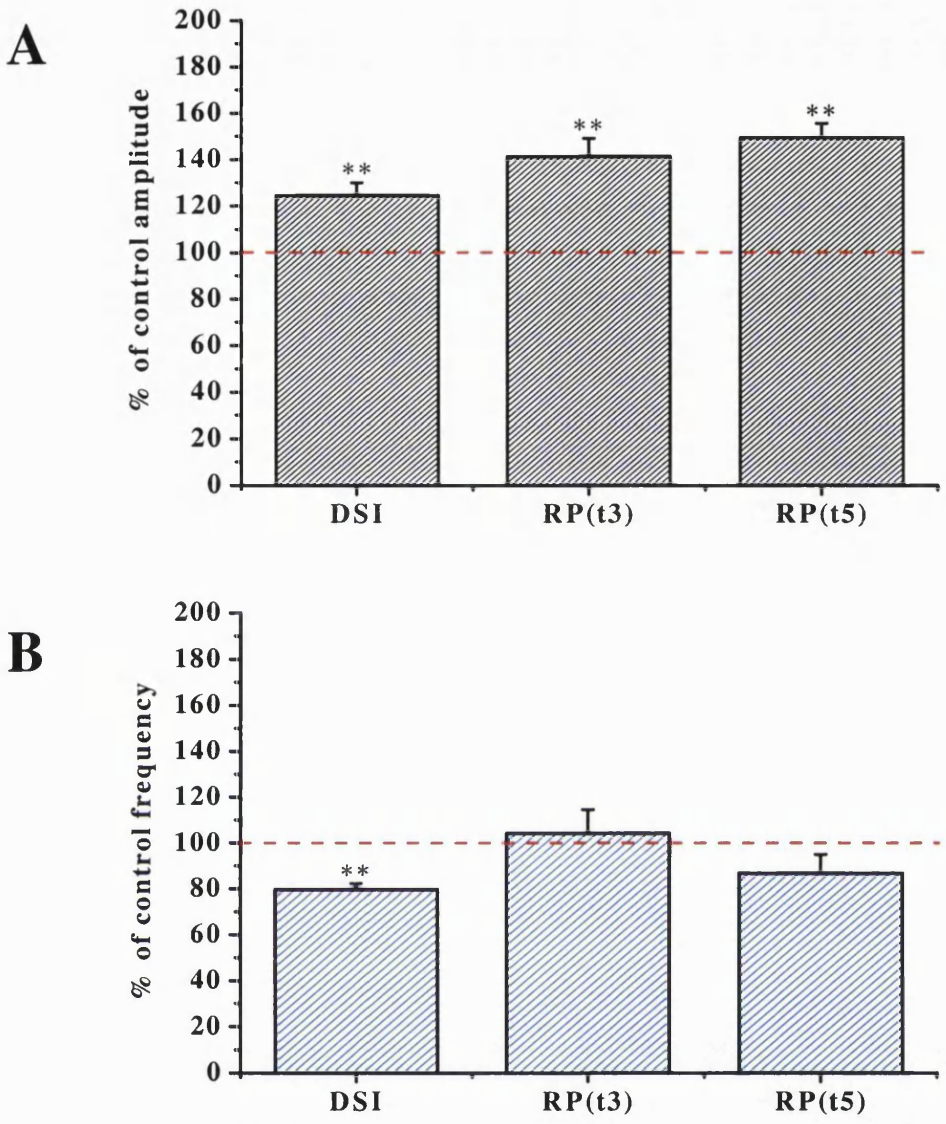

Fig. 6.5. Comparison of the effects of D-APV on DSI and RP. Average changes of mIPSC amplitude (A) and frequency (B) following stimulus induction in PNs voltage clamped at –70mV. Bars represent mean values from data acquired in the presence of 50μM D-APV normalised to control values taken in the same cells 2 min after the beginning of whole-cell recording. Values for DSI were calculated from the initial 20s following stimulus cessation (n=10), $RP_{t3\ \&\ t5}$ were calculated at 3 & 5 min respectively (n=10) (** denotes $p<0.01$, Students t-test).

displaying the change in amplitude distribution at RP_{t3} (Fig. 6.4A) had a mean amplitude value of 37.9 ± 5.2pA during control and a mean value of 47.2 ± 5.0pA during RP_{t3}. The cumulative amplitude distributions calculated from control and RP_{t3} histograms (Fig. 6.4A, inset) are significantly different ($P<0.01$, K-S test). The same cell had a mean frequency of 3.4Hz in control and 3.5Hz during RP_{t3} (Fig. 6.4B). The cumulative frequency distributions calculated from control and RP_{t3} histograms (Fig. 6.4B, inset) are not significantly different ($P>0.05$, K-S test).

At 5 min after stimulus cessation (RP_{t5}) all cells displayed an amplitude potentiation of 149.5 ± 6.2% ($P<0.0001$) of control while the frequency remained at 86.9 ± 8.0% ($P=0.1$) of control (Fig. 6.5A & B) (n=10). Due to there being an absence of any 'rebound' frequency modulation after DSI cessation the mIPSC frequency modulation was not examined after RP_{t5}.

6.1.4. Timecourse of PN mIPSC amplitude and frequency modulation after stimulus cessation in the presence of D-APV

Table 6.3. Timecourse of PN mIPSC amplitude and frequency modulation after stimulus cessation in the presence of D-APV.

Time (min)	Amplitude ± s.e	Frequency ± s.e	n
-2	**103.7** ± 5.8	**93.6** ± 6.4	10
-1	**102.5** ± 2.9	**94.0** ± 4.9	10
0	**100**	**100**	10
0.3	**124.5** ± 5.5	**79.7** ± 2.6	10
1	**127.1** ± 4.2	**96.6** ± 8.6	10
2	**152.0** ± 8.0	**96.3** ± 9.0	10
3	**141.5** ± 7.7	**104.2** ± 10.3	10
5	**149.5** ± 6.2	**86.9** ± 8.0	10

*Data in red depicts statistically significant values compared to control (Paired t-test, $P<0.05$). Time 0 is defined as the point of stimulus induction, all other times are referenced to time 0 min. All values of amplitude/frequency potentiation are normalised to values calculated at time 0 min (set to 100%).

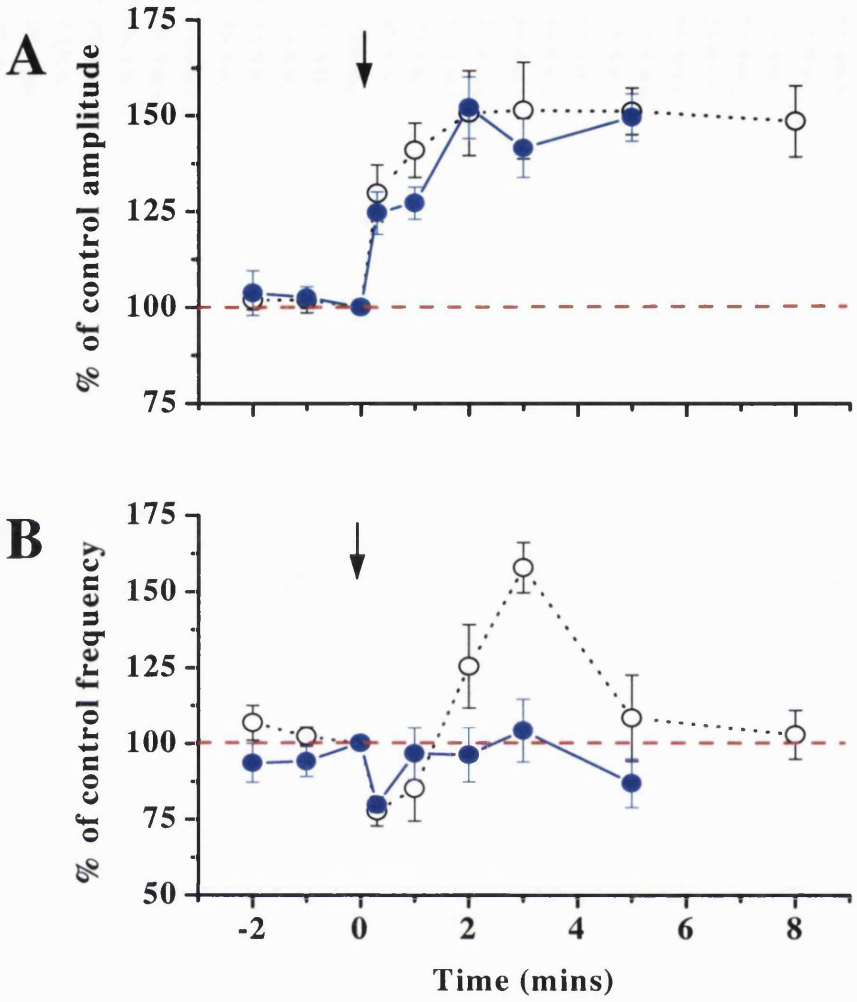

Fig. 6.6. Comparison between the time-dependent changes in PN mIPSC amplitude and frequency, following stimulus induction, in normal Krebs (empty black circles) and in the presence of 50μM D-APV (filled blue circles). A, changes in mean mIPSC amplitude during control period and after stimulus induction (amplitude was measured throughout DSI and RP period). Current amplitudes were normalised with respect to the mean value recorded directly preceding the point of stimulus induction (depicted by the arrow). B, changes in mean mIPSC frequency during control and after stimulus induction (frequency was measured throughout DSI and RP period). Mean mIPSC frequencies were normalised with respect to the mean value recorded directly preceding the point of stimulus induction (depicted by the arrow). All data are shown as mean ± s.e.m (Control n=11, D-APV n=10).

Application of 50μM D-APV was without effect on the magnitude and time course of frequency modulation during DSI (initial 0-20s) while completely abolishing the subsequent 'rebound' frequency increase during RP_{t3} (Fig. 6.6B). The mean mIPSC amplitude remained potentiated throughout DSI and RP_{t1-5}, rising steadily before reaching a plateau at RP_{t2} (Fig. 6.6A). The mean values during control and after depolarisation are summarised in Table 6.3 above.

6.1.5. mIPSC kinetic changes during $DSI_{D\text{-}APV}$ & $RP_{D\text{-}APV}$

Comparison of the 'rise-time' and 'half-width' of mIPSCs recorded in the presence of 50μM D-APV, during DSI and RP, identified no significant change with respect to control values (Table 6.4). Superimposed average traces accrued from 30 consecutive mIPSCs recorded during control, DSI and RP display the relative amplitude potentiation in a representative cell with respect to control values. Control mIPSCs had a mean amplitude value of 45.4 ± 4.1pA compared with 49.0 ± 3.9pA (DSI) and 73.4 ± 6.5pA (RP_{t3}) (Fig. 6.7).

Table 6.4. Analysis of PN mIPSC kinetic parameters in the presence of 50μM D-APV during control, DSI and at 3 min (RP_{t3}) after stimulus cessation. All data are mean values ± s.e. (n=10).

Rise-Time (ms)	2.8 ± 0.2	2.7 ± 0.1	2.8 ± 0.2
Half-Width (ms)	10.3 ± 0.3	10.8 ± 0.7	10.3 ± 0.2

6.2. Effects of extracellular Na^+ removal on the induction/maintenance of DSI & RP

Removal of Na^+ from the superfusing Krebs solution and substitution by NMDG produced no change in the mean amplitude (105.6 ± 13.7% of control, P=0.9) of PN mIPSCs while reducing the basal mIPSC frequency (72.8 ± 8.8% of control, P<0.02)

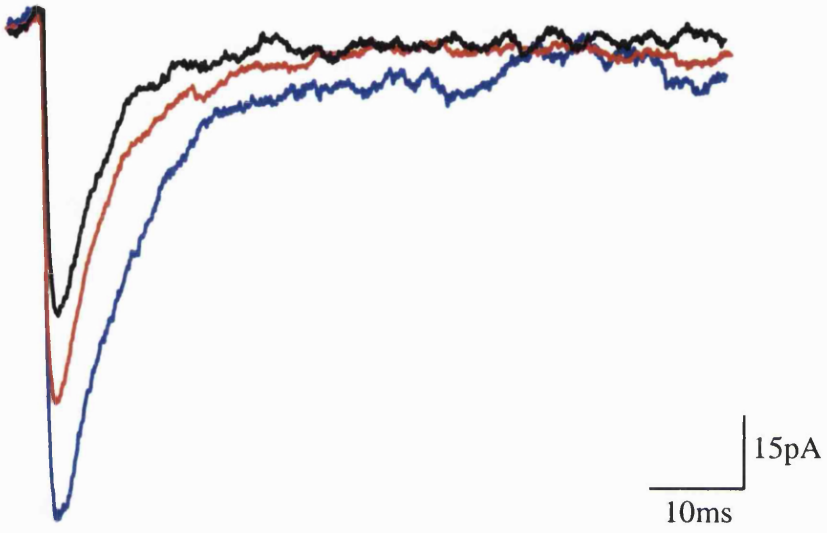

Fig. 6.7. Effect of 50μM D-APV on PN mIPSC kinetics. Superimposed averaged traces from all mIPSCs recorded in a single control cell at designated times. Traces were averaged from all mIPSCs recorded in a single control cell during control (black line), immediately after stimulus cessation (DSI) (red line) & 3 min after stimulus cessation (RP_{t3}) (blue line).

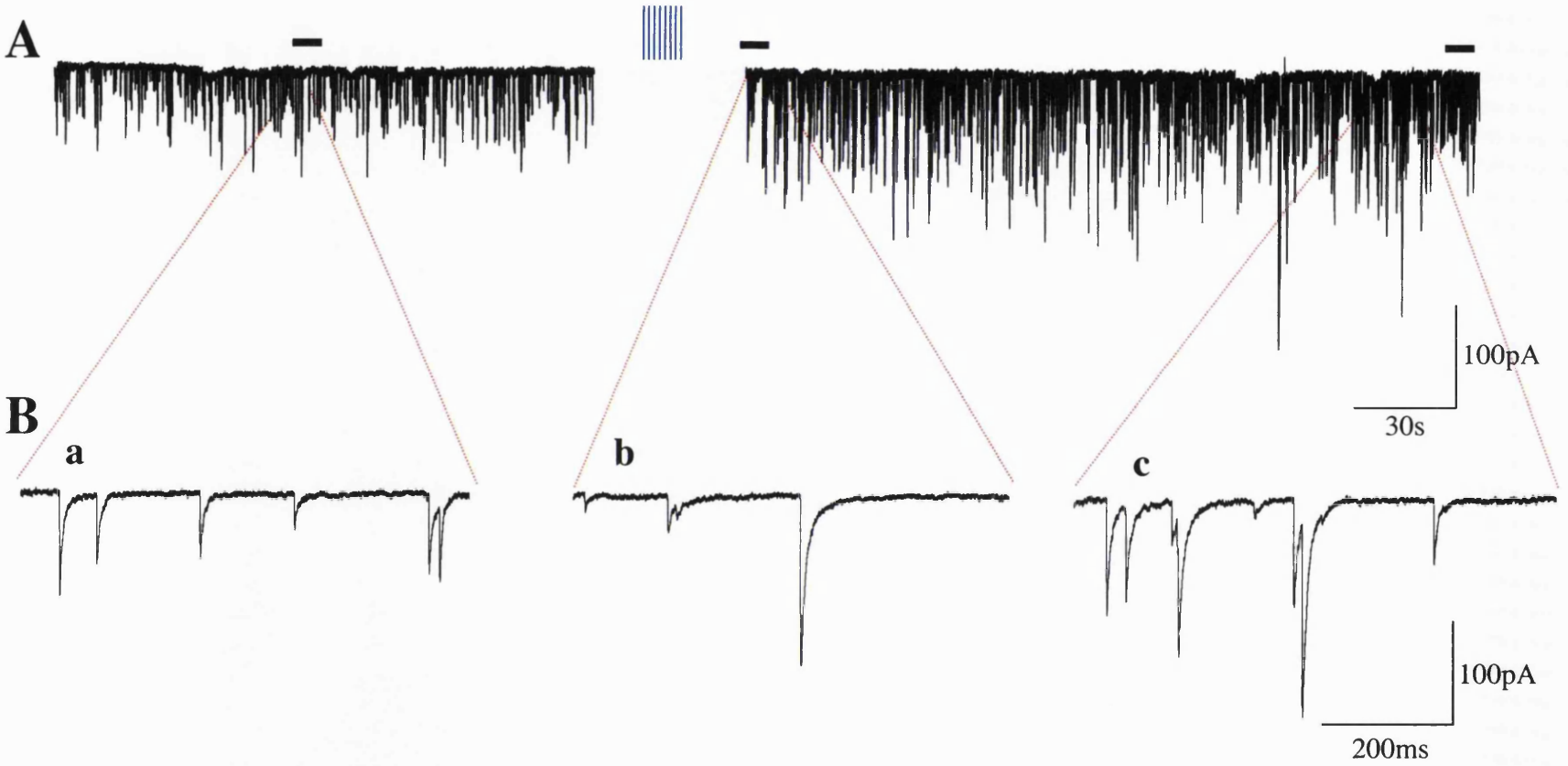

Fig. 6.8. Effects of a nominally Na^+ free Krebs solution on the induction of DSI/RP. A, summated mIPSCs recorded during control (upper left trace) and after (upper right trace) a train of depolarising pulses (▥) (8 pulses of 70mV amplitude, 100ms duration at 2s intervals) applied from a holding potential of –70mV at 3 min from the start of whole-cell recording. All recordings were made in a nominally Na^+ free perfusion media. B, Insets show expanded time-base examples of mIPSCs recorded during control (a), initial 20s after stimulus (DSI) (b) and 3min after stimulus cessation (rebound potentiation (RP_{t3})) (c).

(n=4). This could be interpreted as indicating that the tonic activation of NMDARs by background glutamate was reduced.

6.2.1. Depolarisation-induced suppression of inhibition - $DSI_{(Na^+ free)}$

Application of a train of depolarising pulses, in the absence of any extracellular Na^+ (replaced by $NMDG^+$), induced a slight increase in the magnitude of amplitude and frequency modulation when compared to DSI in control conditions (Fig. 6.8B, a & b). The mean mIPSC amplitude increased to 145.7 ± 11.3% ($P<0.03$) of control and the mean mIPSC frequency decreased to 65.1 ± 1.7% ($P<0.0003$) of control (n=4) (Fig. 6.11A & B). The removal of extracellular Na^+ also induced a profound increase in the duration of the mIPSC frequency decrease during DSI. In normal Krebs the mIPSC frequency decrease returned to control levels after <1min while in Na^+ free Krebs the frequency decrease persisted for >2min (see below). A representative cell (Fig. 6.9A) illustrates the rapid onset of amplitude potentiation after stimulus cessation while simultaneously displaying a sustained (>40s) reduction in the mean frequency of mIPSCs (Fig. 6.9B). Removal of the main charge-carrying ion through NMDARs induced a small but non-significant change in the magnitude but significantly increased the duration of DSI when compared to DSI in the presence of D-APV or in normal Krebs.

6.2.2. Rebound potentiation - $RP_{(Na^+ free)}$

Analysis of mIPSC modulation at 3 min after stimulus cessation (RP_{t3}), in the same cells in which DSI had been previously induced, identified a maintained increase in the mean mIPSC amplitude. However, the removal of all Na^+ from the superfusing Krebs solution completely abolished the increase in the mean mIPSC frequency observed during RP_{t3} in normal Krebs (Fig. 6.8B, a & c). The mean mIPSC amplitude increased to 142.3 ± 2.1% ($P<0.0003$) of control while the mean mIPSC frequency displayed no discernible change (96.2 ± 17.2%, $P=0.8$) (Fig. 6.11A &

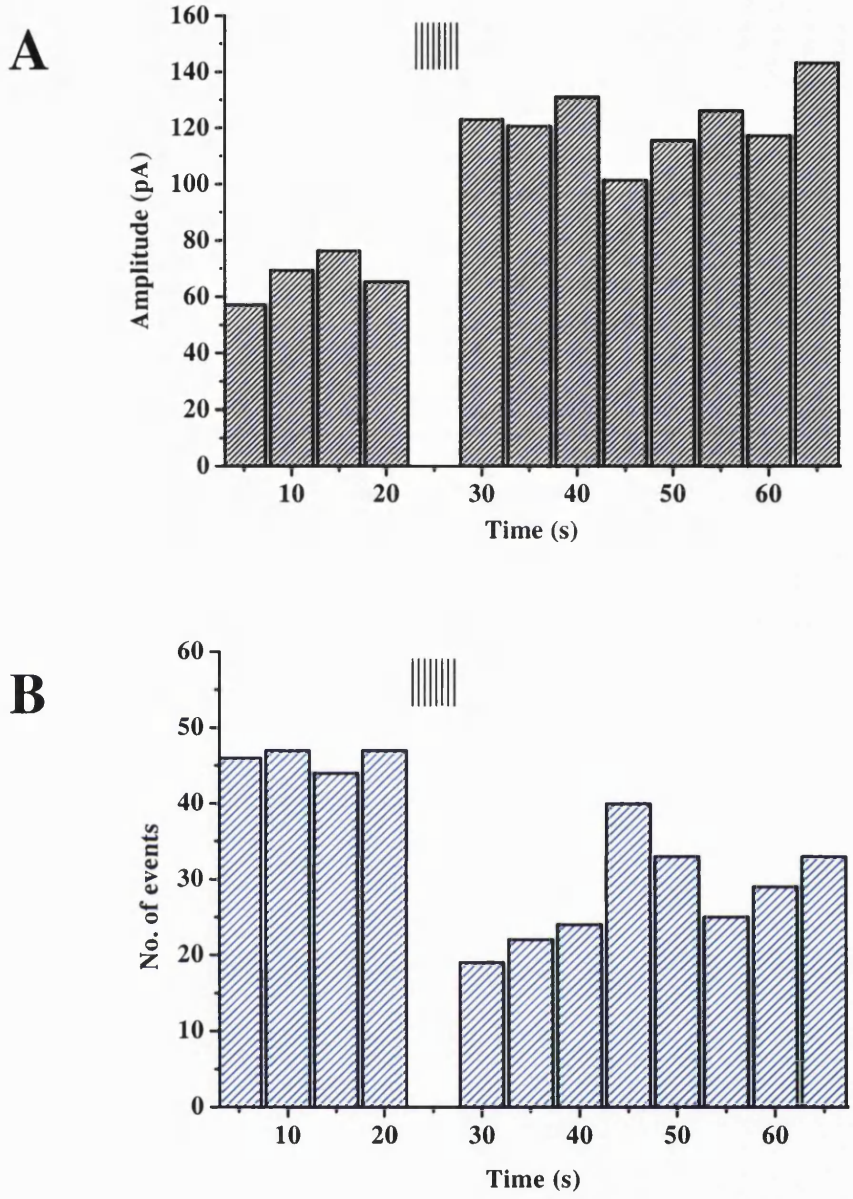

Fig. 6.9. Induction of DSI in the presence of a nominally Na^+ free Krebs solution. Representative cell displaying changes in mIPSC amplitude (A) and frequency (B) following stimulus induction (|||||||) in a PN voltage clamped at –70mV. Depolarisation induced a rapid rise in mIPSC amplitude, while inducing a longer lasting decrease in mIPSC frequency persisting for ≥ 40s.

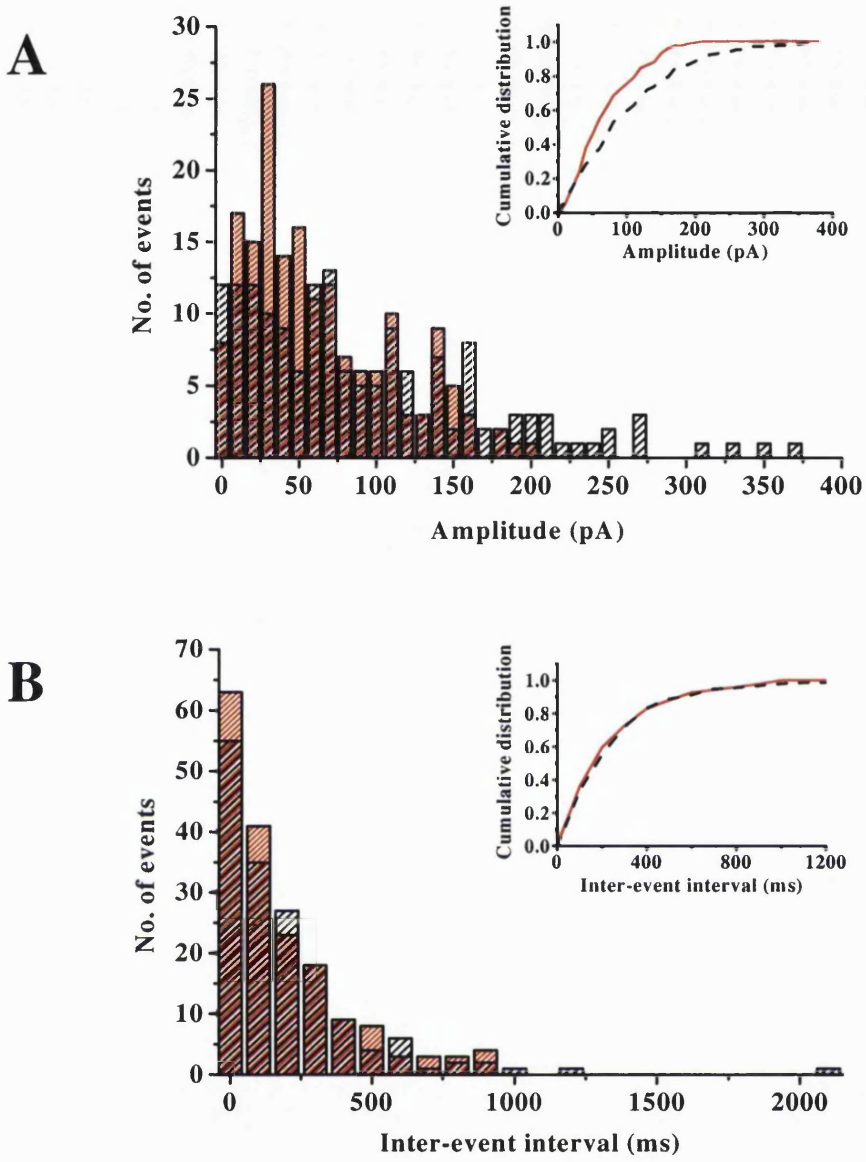

Fig. 6.10. RP in the presence of a nominally Na^+ free Krebs solution. A, amplitude distribution of mIPSCs measured during control recording (dense red hatching) and at 3 min after stimulus cessation (RP_{t3}, medium black hatching), in a single PN superfused with a nominally Na^+-free Krebs solution. The cumulative distributions from both histograms are illustrated in A, inset (red line = control, black dash = RP_{t3}). B, frequency distribution of mIPSCs measured during control recording (dense red hatching) and at 3 min after stimulus cessation (RP_{t3}, medium black hatching). The cumulative distributions from both histograms are illustrated in B, inset (red line = control, black dash = RP_{t3}).

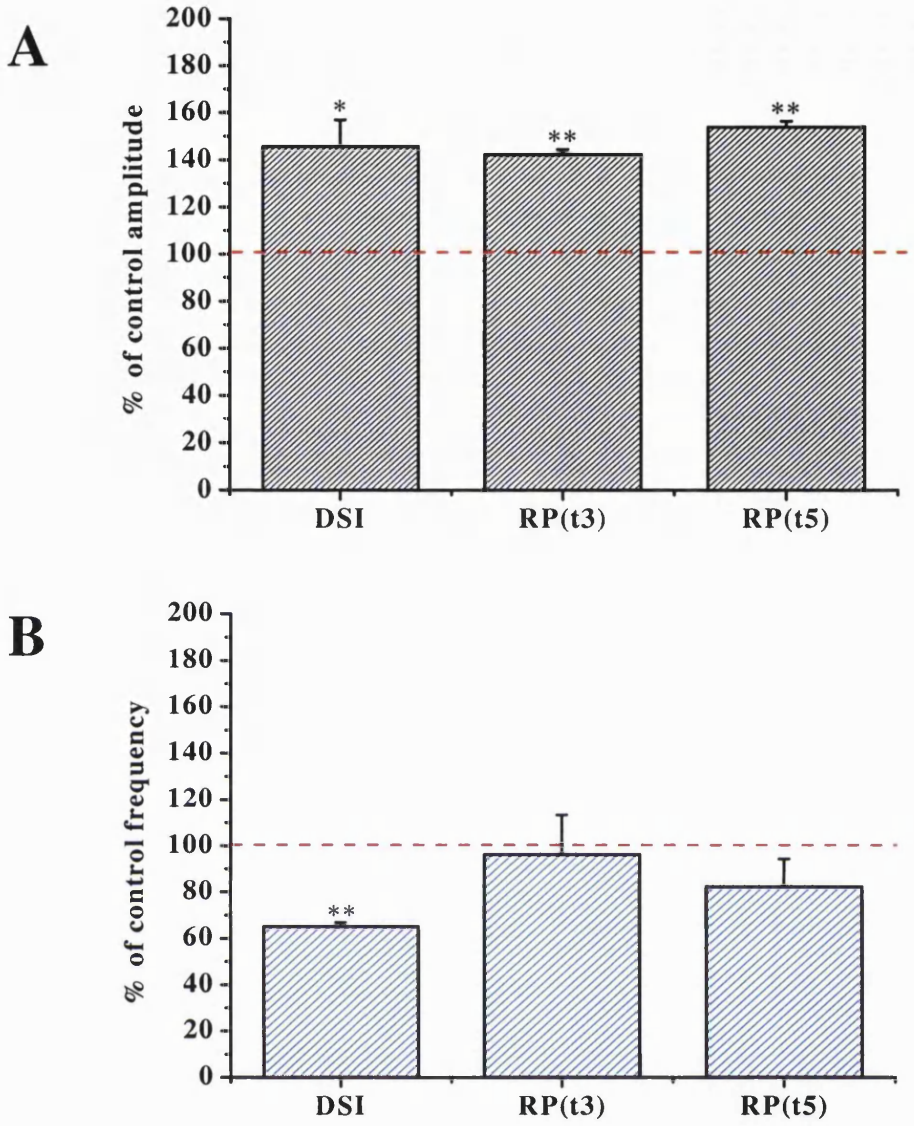

Fig. 6.11. Comparison of the effects of a nominally Na^+ free Krebs solution on DSI and RP. Average changes of mIPSC amplitude (A) and frequency (B) following stimulus induction in PNs voltage clamped at –70mV. Bars represent mean values (± s.e) normalised to control values taken in the same cells 2 min after the beginning of the whole-cell recording. All data were acquired in a nominally Na^+ free Krebs solution. Values for DSI were calculated from the initial 20s following stimulus cessation (n=4), $RP_{t3\ \&\ t5}$ were calculated at 3 & 5 min respectively (n=4) (* denotes $P<0.05$ and ** denotes $p<0.01$, Students t-test).

B) compared to control (n=4). A representative cell displaying the change in amplitude distribution at RP_{t3} (Fig. 6.10A) had a mean amplitude value of 69.1 ± 2.9pA during control and a mean value of 102.6 ± 4.4pA during RP_{t3}. The cumulative amplitude distributions calculated from control and RP_{t3} histograms (Fig. 6.10A, inset) are significantly different (P<0.0002, K-S test). The same cell had a mean frequency of 9.1Hz in control and 10.2Hz during RP_{t3} (Fig. 6.10B). The cumulative frequency distributions calculated from control and RP_{t3} histograms (Fig. 6.10B, inset) are not significantly different (P >0.05, K-S test).

At 5 min after stimulus cessation (RP_{t5}) all cells displayed an amplitude potentiation of 154 ± 2.5% (P<0.0002) of control while the frequency remained at 82.4 ± 12.0% (P=0.2) of control (Fig. 6.11A & B) (n=4). Due to there being an absence of any 'rebound' frequency modulation after DSI cessation, mIPSC frequency modulation was not examined after RP_{t5}. Removal of the main charge-carrying ion through NMDARs abolished the 'rebound' frequency potentiation seen during RP_{t3} in normal Krebs.

6.2.3. Timecourse of PN mIPSC amplitude and frequency modulation after stimulus cessation in the presence of nominally Na^+ free Krebs

The removal of all Na^+ from the superfusing Krebs solution increased the duration of the mIPSC frequency decrease during DSI when compared to control values. The removal of Na^+ mimicked the application of 50μM D-APV by completely abolishing the subsequent 'rebound' frequency increase during RP_{t3} (Fig. 6.12B). The mean mIPSC amplitude remained potentiated throughout DSI and RP_{t1-5} (Fig. 6.12A). The mean values during control and after depolarisation are summarised in Table 6.5 below.

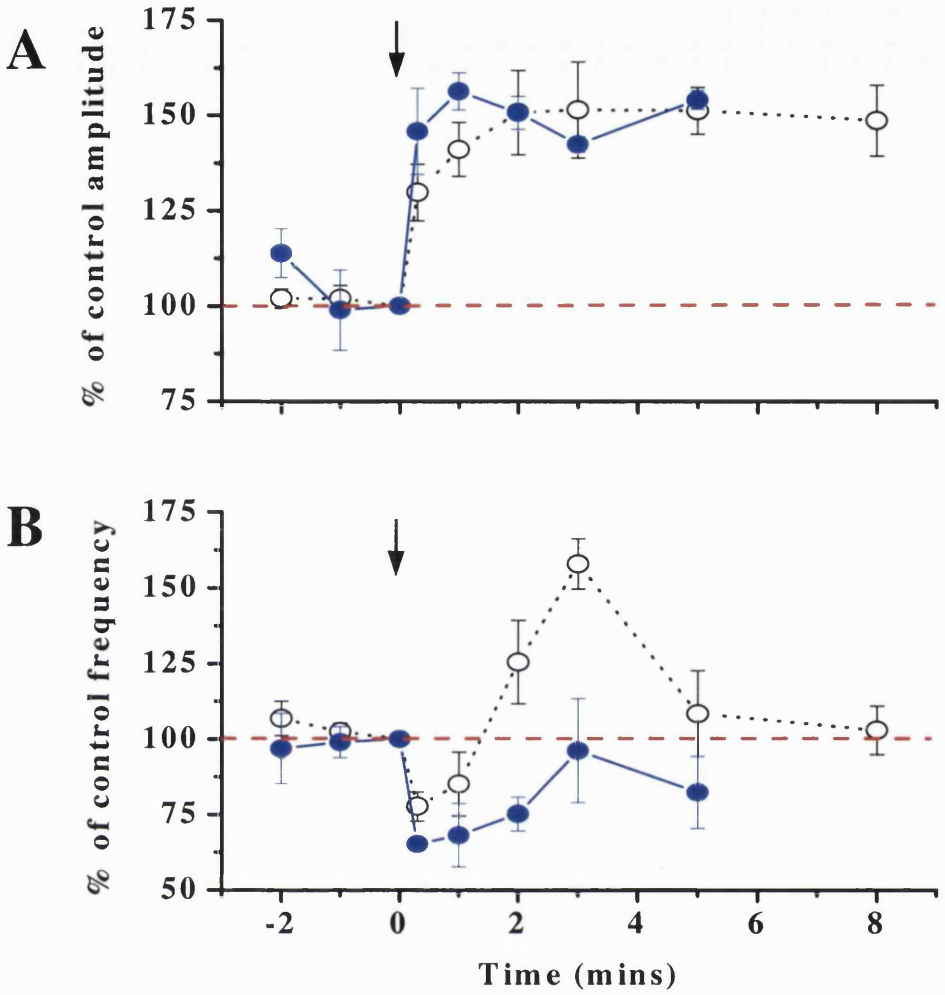

Fig. 6.12. Comparison between the time-dependent changes in PN mIPSC amplitude and frequency, following stimulus induction, in normal Krebs (empty black circles) and in the presence of nominally Na^+ free Krebs (filled blue circles). A, changes in mean mIPSC amplitude during control period and after stimulus induction (amplitude was measured throughout DSI & RP). Current amplitudes were normalised with respect to the mean value recorded directly preceding the point of stimulus induction (depicted by the arrow). B, changes in mean mIPSC frequency during control and after stimulus induction (frequency was measured throughout DSI & RP). Mean mIPSC frequencies were normalised with respect to the mean value recorded directly preceding the point of stimulus induction (depicted by the arrow). All data are shown as mean ± s.e (Control n=11, Na^+ free n=4).

Table 6.5. Timecourse of PN mIPSC amplitude and frequency modulation after stimulus cessation in the presence of nominally Na^+ free Krebs.

Time (m)	Amplitude ± s.e	Frequency ± s.e	n
-2	113.8 ± 6.4	96.9 ± 11.6	4
-1	98.9 ± 10.5	99.0 ± 5.2	4
0	100	100	4
0.3	145.7 ± 11.3	65.1 ± 1.7	4
1	156.2 ± 4.9	68.1 ± 10.5	4
2	150.6 ± 4.3	75.1 ± 5.7	4
3	142.3 ± 2.1	96.2 ± 17.2	4
5	154.0 ± 2.5	82.4 ± 12.0	4

*Data in red depicts statistically significant values compared to control (Paired t-test, $P<0.05$). Time 0 is defined as the point of stimulus induction, all other times are referenced to time 0 min. All values of amplitude/frequency potentiation are normalised to values calculated at time 0 min (set to 100%).

6.2.4. mIPSC kinetic changes during $DSI_{(Na^+ free)}$ & $RP_{(Na^+ free)}$

Comparison of the 'rise-time' and 'half-width' of mIPSCs recorded in Na^+-free Krebs solution, during DSI and RP, identified no significant change with respect to control values (Table 6.6). Superimposed average traces from 30 consecutive mIPSCs recorded during control, DSI and RP display the relative amplitude potentiation in a representative cell with respect to control values (Fig. 6.13). Control mIPSCs have a mean amplitude value of 41.1 ± 5.4pA compared with 51.1 ± 4.2pA (DSI) and 68.3 ± 5.0pA (RP_{t3}) (Fig. 6.13).

Table 6.6. Analysis of PN mIPSC kinetic parameters recorded in nominally Na^+ free Krebs during control, DSI and at 3 min (RP_{t3}) after stimulus cessation. All data are mean values ± s.e. (n=4).

Kinetic Parameters	control ± s.e.m	DSI ± s.e.m	rebound ± s.e.m
Rise-Time (ms)	2.6 ± 0.1	2.7 ± 0.1	2.6 ± 0.1
Half-Width (ms)	10.5 ± 0.4	12.1 ± 0.4	12.2 ± 0.5

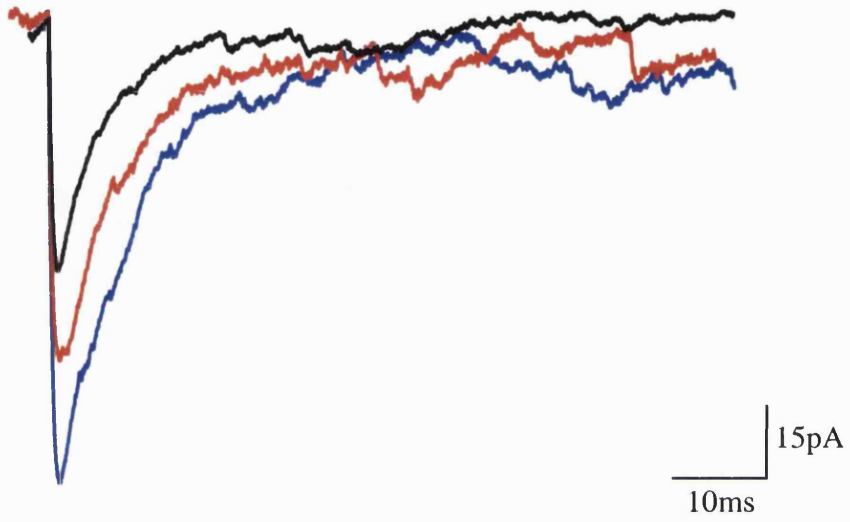

Fig. 6.13. Effect of a nominally Na^+ free Krebs solution on PN mIPSC kinetics. Superimposed averaged traces from all mIPSCs recorded in a single control cell at designated times. Traces were averaged from all mIPSCs recorded in a single control cell during control (black line), immediately after stimulus cessation (DSI) (red line) & 3 min after stimulus cessation (RP_{t3}) (blue line).

6.3. Effects of Na^+ removal on NMDAR-mediated currents in interneurones

Removal of Na^+ from the superfusing Krebs solution induced an almost complete abolition of NMDA-induced currents in cerebellar interneurones, while the application of 100μM NMDA, applied in normal Krebs, induced large NMDAR-mediated inward currents. A summary of the effects of Na^+ removal on NMDA induced currents is displayed in Table 6.7.

Table 6.7. Na^+ free effects on NMDAR-mediated currents in cerebellar interneurones

Krebs	Mean Amplitude (pA) (100μM NMDA)	Mean rise-time (ms)	n
Normal (control)	1596.7 ± 259.4	348.1 ± 32.7	10
Na^+ free	121.0 ± 14.9	396.7 ± 27.3	10
% Change	-92.4%	+14.0%	

*Data in red depicts statistically significant value (Students t-test, P<0.0005).

Removal of Na^+ from the superfusing Krebs resulted in a fully reversible reduction of NMDAR-mediated currents in cerebellar interneurones (Fig. 6.14A, B & C). A small residual current persists on application of NMDA in the presence of Na^+ free Krebs but is negligible in comparison to NMDA-induced currents in normal Krebs (Fig. 6.14B). Application of 50μM D-APV completely blocked the NMDAR-mediated currents in interneurones when co-applied with 100μM NMDA (Fig. 6.14D).

6.4. Immunocytochemical identification of presynaptic NMDARs

The pharmacological dissection of presynaptic NMDARs on cerebellar interneurones led to the requirement for complimentary immunocytochemical evidence. Development of a triple antibody staining protocol aided in evaluating the presence of one of the NMDAR subunits (NR1) at putative release sites present on the axon terminals of interneuornes. The NR1 subunit is required for the assembly of functional NMDA receptors (Moriyoshi *et al.*, 1991) and thus is a useful target for

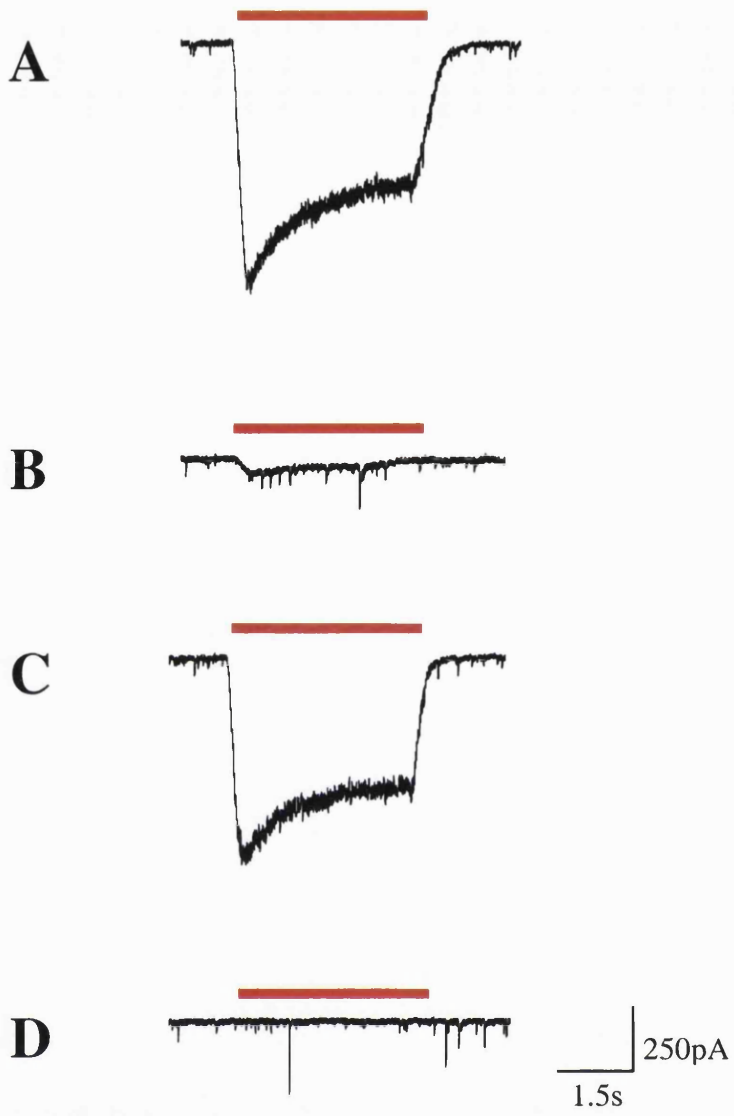

Fig. 6.14. Effects of the removal of Na^+ on NMDAR-mediated currents in cerebellar interneurones. A, Application of 100μM NMDA (red bar) for a duration of 4s produced large NMDAR-mediated inward currents when applied to mature cerebellar interneurones. B, Removal of extracellular Na^+ resulted in an almost complete abolition of NMDA-induced currents, leaving only a small residual current. C, Converting back to Na^+ containing Krebs resulted in the production of large NMDAR-mediated inward currents. D, Application of the specific NMDAR antagonist, D-APV (50μM), resulted in the complete abolition of all NMDAR-mediated currents. Experiments were conducted in nominally Mg^{2+} free Krebs solution containing 1μM Strychnine, 10μM glycine, 500nM TTX and 10μM CNQX (n=10).

immunocytochemical analysis. An antibody directed against an epitope on the intracellular carboxy-terminus of the NR1 subunit was used to identify the presence of all splice variants of the NR1 subunit and their cellular location (Fig. 6.15B, Fig. 6.16B, Fig. 6.18B & Fig. 6.19B) while an anti-glutamic acid decarboxylase (GAD) antibody identified all interneurones within the mixed cerebellar culture (Fig. 6.15A, Fig. 6.16A, Fig. 6.18A & Fig. 6.19A). To substantiate the theory of presynaptic NMDARs an antibody directed against the protein synaptophysin, a component of the presynaptic vesicle docking process, was used in order to identify putative release sites (Fig. 6.15C, Fig. 6.16C, Fig. 6.18C & Fig. 6.19C). Analysis of presynaptic NMDARs required locating an interneurone within a relatively cell sparse area of the mixed cerebellar culture. This maximised the identification of specific structures on the axon without contamination from surrounding cell bodies, axons or dendrites. Immunocytochemical staining identified the co-localisation of the NR1 subunit, specifically at putative release sites on cerebellar interneurones. Staining for NR1 could be seen throughout the cell body and main dendrite/axon with more punctate staining in the distal cell processes (Fig. 6.15D, Fig. 6.16D, Fig. 6.18D & Fig. 6.19D). Identification of BC/SC morphology using an anti-parvalbumin antibody displayed morphology consistent with that identified using the triple immunocytochemical staining in accordance with NR1 at putative release sites on cerebellar BC/SCs (Fig. 6.17 & Fig. 6.20).

6.5. NMDA enhancement of GABA release from cerebellar interneurones

Mature PNs, identified by immunocytochemical staining for Calbindin D_{28K} (Fig. 6.21A), displayed robust $GABA_AR$-mediated inward currents on application of 10μM GABA (963.4 ± 239.9pA, n=5) (Fig. 6.21a). Counter-staining of the same neurone for the presence of the NMDA receptor subunit NR1 displayed diffuse staining throughout the soma and dendrites (Fig. 6.21B). Brief application of 100μM NMDA, while producing no NMDAR-mediated current in mature PNs (Fig. 6.21b), induced a significant rise in the frequency of PN mIPSCs in all cells tested (n=5). A single 4s pulse of NMDA (100μM) increased PN mIPSC frequency by 156.8 ± 50.8% ($P<0.04$)

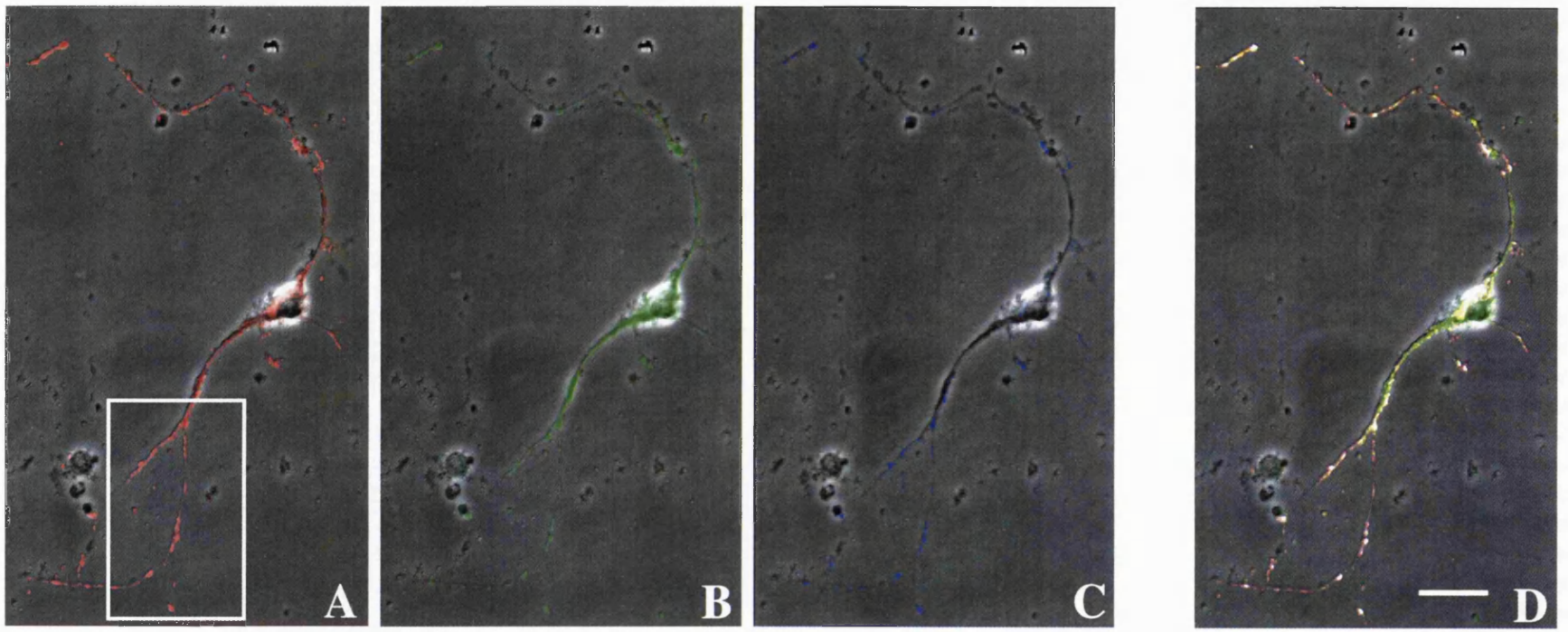

Fig. 6.15. Triple immunocytochemical staining of a single cerebellar interneurone in a relatively cell sparse mixed cerebellar culture. A, anti-glutamic acid decarboxylase (GAD) – TRITC conjugate stain identifying GABAergic interneurones. B, anti-NR1 – FITC conjugate stain displaying NMDAR (NR1) subunit distribution. C, anti-synaptophysin – Cy5 conjugate stain identifying putative release sites. D, triple overlay of RGB images identifying high percentage of GAD-Cy5 colocalisation and the presence of NR1 subunits at putative release sites on cerebellar interneurones. A-D, all images were superimposed on the corresponding brightfield image after acqusition. Images were acquired at X40 (oil immersion) at 15% zoom. Scale bar represents 10μm.

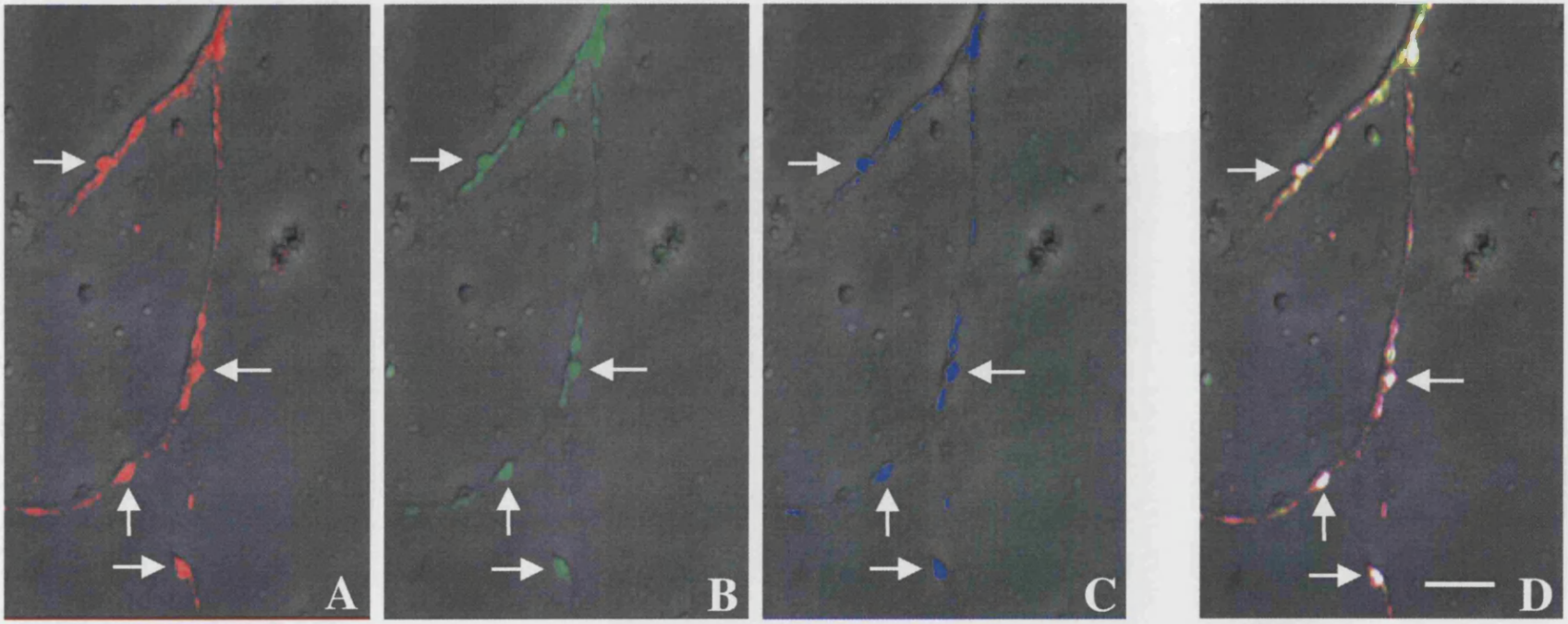

Fig. 6.16. Triple immunocytochemical staining of a GABAergic interneurone axon at high magnification (depicted in Fig. 6.15A, inset). A, anti-glutamic acid decarboxylase (GAD) – TRITC conjugate stain identifying GABAergic interneurone. B, anti-NR1 – FITC conjugate stain displaying NMDAR (NR1) subunit distribution. C, anti-synaptophysin – Cy5 conjugate stain identifying putative release sites. D, triple overlay of RGB images identifying high percentage of GAD-Cy5 colocalisation and the presence of NR1 subunits at putative release sites on cerebellar interneurones. A-D, all images were superimposed on the corresponding brightfield image after acqusition. Images were acquired at X63 (oil immersion) at 0% zoom. Scale bar represents 5μm.

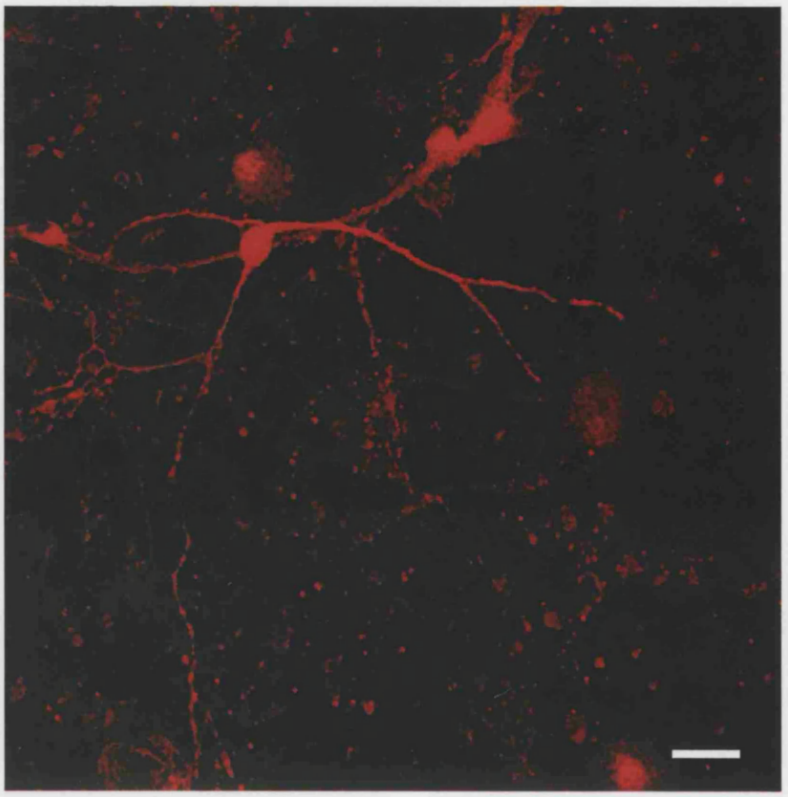

Fig. 6.17. Mature cerebellar basket/stellate cell *in vitro*. Immunocytochemical staining using an anti-parvalbumin antibody with an anti-mouse TRITC conjugate to identify the morphology of mature cerebellar basket/stellate cells (21 days *in vitro*). Images were acquired at X40 magnification with 15% zoom (scale bar = 10μm).

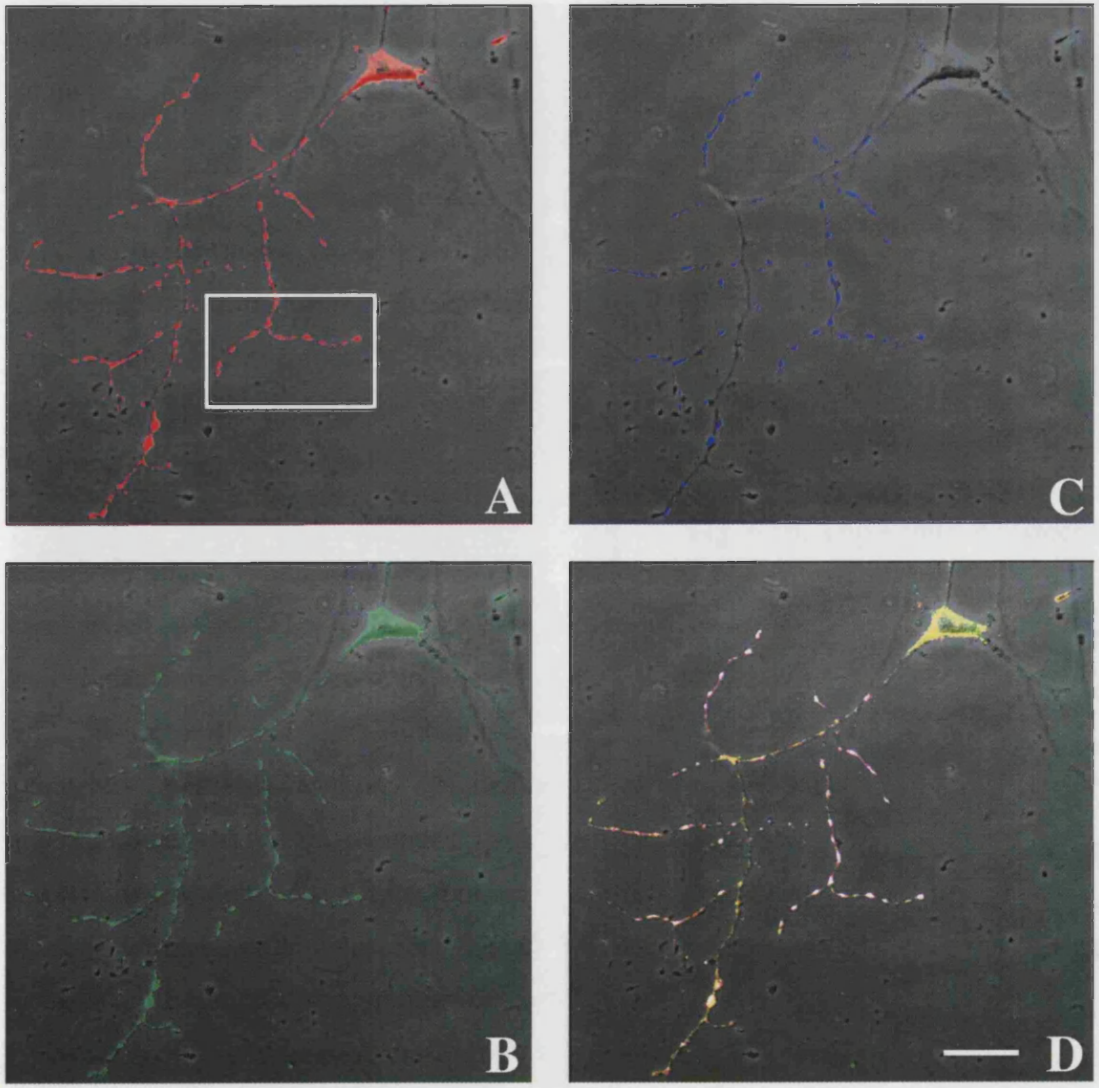

Fig. 6.18. Triple immunocytochemical staining of a single cerebellar interneurone in a relatively cell sparse mixed cerebellar culture. A, anti-glutamic acid decarboxylase (GAD) – TRITC conjugate stain identifying GABAergic interneurones. B, anti-NR1 – FITC conjugate stain displaying NMDAR (NR1) subunit distribution. C, anti-synaptophysin – Cy5 conjugate stain identifying putative release sites. D, triple overlay of RGB images identifying high percentage of GAD-Cy5 colocalisation and the presence of NR1 subunits at putative release sites on cerebellar interneurones. A-D, all images were superimposed on the corresponding brightfield image after acqusition. Images were acquired at X40 (oil immersion) at 15% zoom. Scale bar represents 10μm.

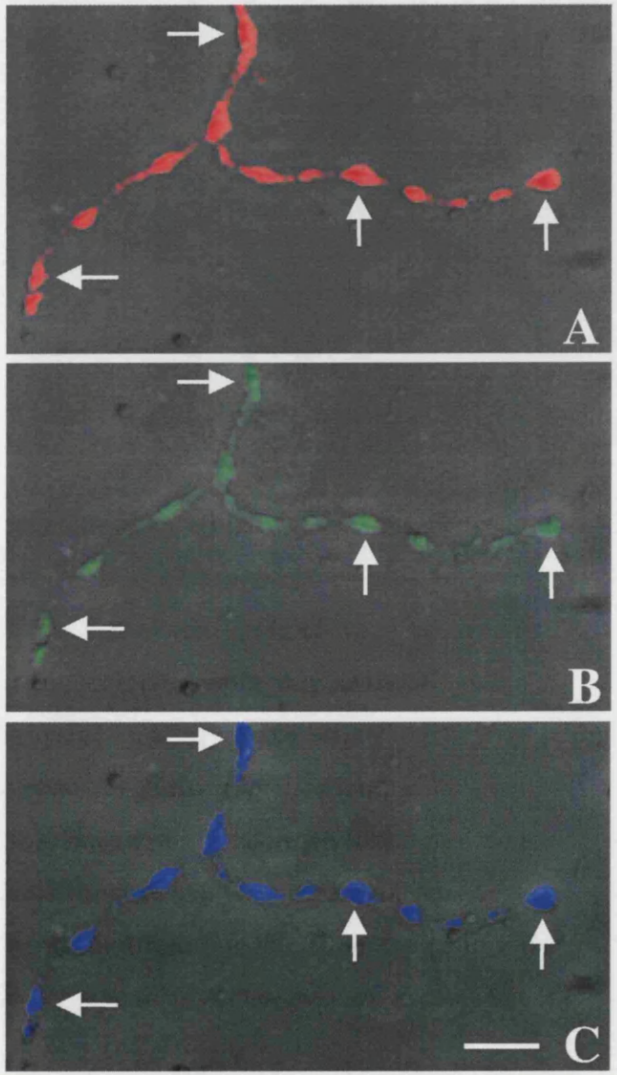

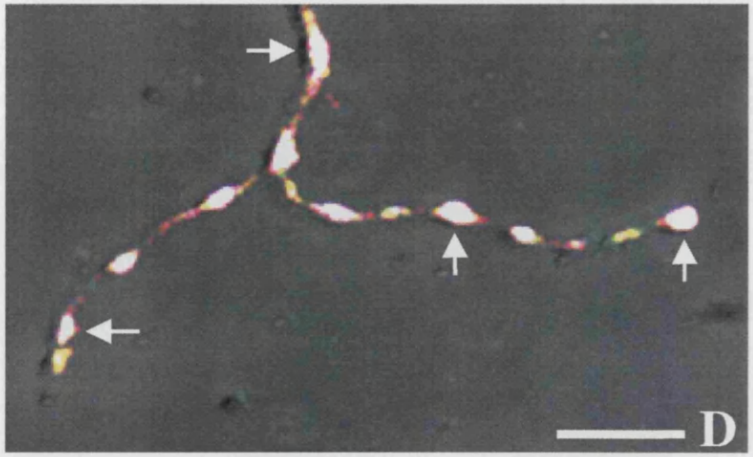

Fig. 6.19. Triple immunocytochemical staining of a GABAergic interneurone axon at high magnification (depicted in Fig. 6.17A, inset). A, anti-glutamic acid decarboxylase (GAD) – TRITC conjugate stain identifying GABAergic interneurone. B, anti-NR1 – FITC conjugate stain displaying NMDAR (NR1) subunit distribution. C, anti-synaptophysin – Cy5 conjugate stain identifying putative release sites. D, triple overlay of RGB images identifying high percentage of GAD-Cy5 colocalisation and the presence of NR1 subunits at putative release sites on cerebellar interneurones. A-D, all images were superimposed on the corresponding brightfield image after acqusition. Images were acquired at X63 (oil immersion) at 0% zoom. Scale bar represents 5μm.

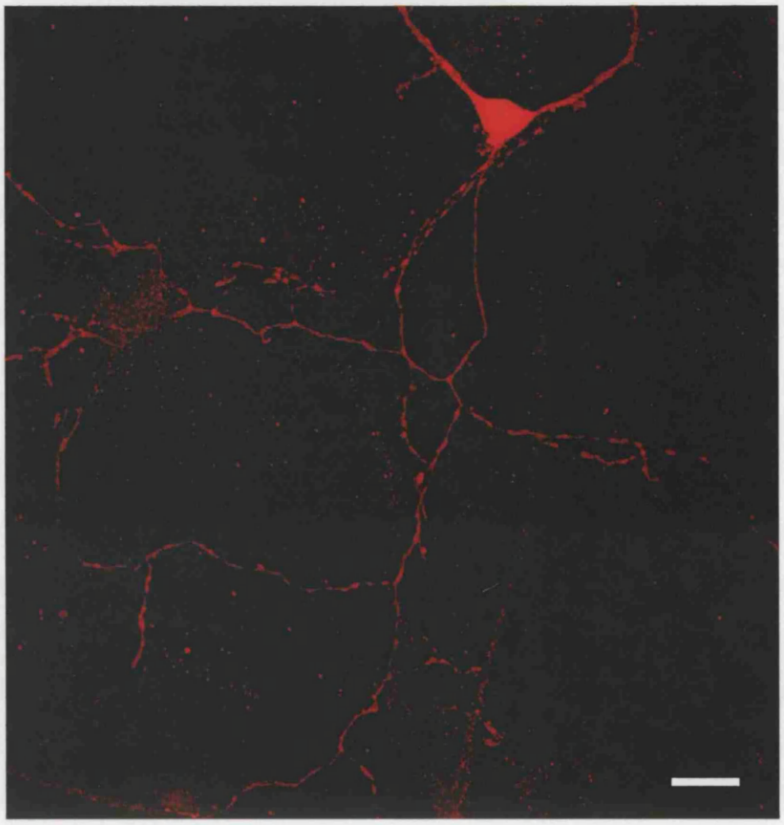

Fig. 6.20. Mature cerebellar basket/stellate cell *in vitro*. Immunocytochemical staining using an anti-parvalbumin antibody with an anti-mouse TRITC conjugate to identify the morphology of mature cerebellar basket/stellate cells (21 days *in vitro*). Images were acquired at X40 magnification with 15% zoom (scale bar = 10μm).

during NMDA application, by 41.9 ± 8.3% ($P<0.01$) 1 min after pulse cessation and by 70.0 ± 24.9% ($P<0.05$) 3 min after pulse cessation (Fig. 6.22B).

Interestingly, in 4 out of 5 cells, application of NMDA caused a decrease in the mean PN mIPSC amplitude. During NMDA application the mean amplitude decreased to 86.8 ± 6.7% ($P=0.14$) of control while at 2 and 3 min after NMDA pulse cessation the mean mIPSC amplitudes were 76.1 ± 5.4% ($P<0.03$) and 76.3 ± 4.7% ($P<0.02$) respectively, of control (n=4) (Fig. 6.23A). Analysis of the pooled amplitude distribution histograms from all cells (at 3 min after NMDA pulse cessation) identified a preferential NMDA-induced increase in small amplitude events (Fig. 6.24A). Subtraction of the amplitude distribution in NMDA from the amplitude distribution in control identified the NMDA-induced events (Fig. 6.24B), which had a smaller average amplitude when compared to control events. The NMDA-enhancement of PN mIPSC frequency, measured in normal 1mM Mg^{+} Krebs, persisted for the duration of the recording (3min, n=5) (Fig. 6.22A & Fig. 6.22B, a, b & c). Ionophoretic application of NMDA specifically activates NMDARs, inducing the enhanced release of neurotransmitter from cerebellar interneurones. Unfortunately, this method ignores the coincident activation of presynaptic mGluRs, possibly having a modulatory role on the activity of NMDARs, during DSI and RP. Therefore, only the induction and maintenance (until an equivalent time corresponding to RP_{t3}) of the NMDA-mediated increase in mIPSC frequency was examined, so as to avoid an overestimation of the NMDAR-mediated enhancement of PN mIPSC frequency during RP.

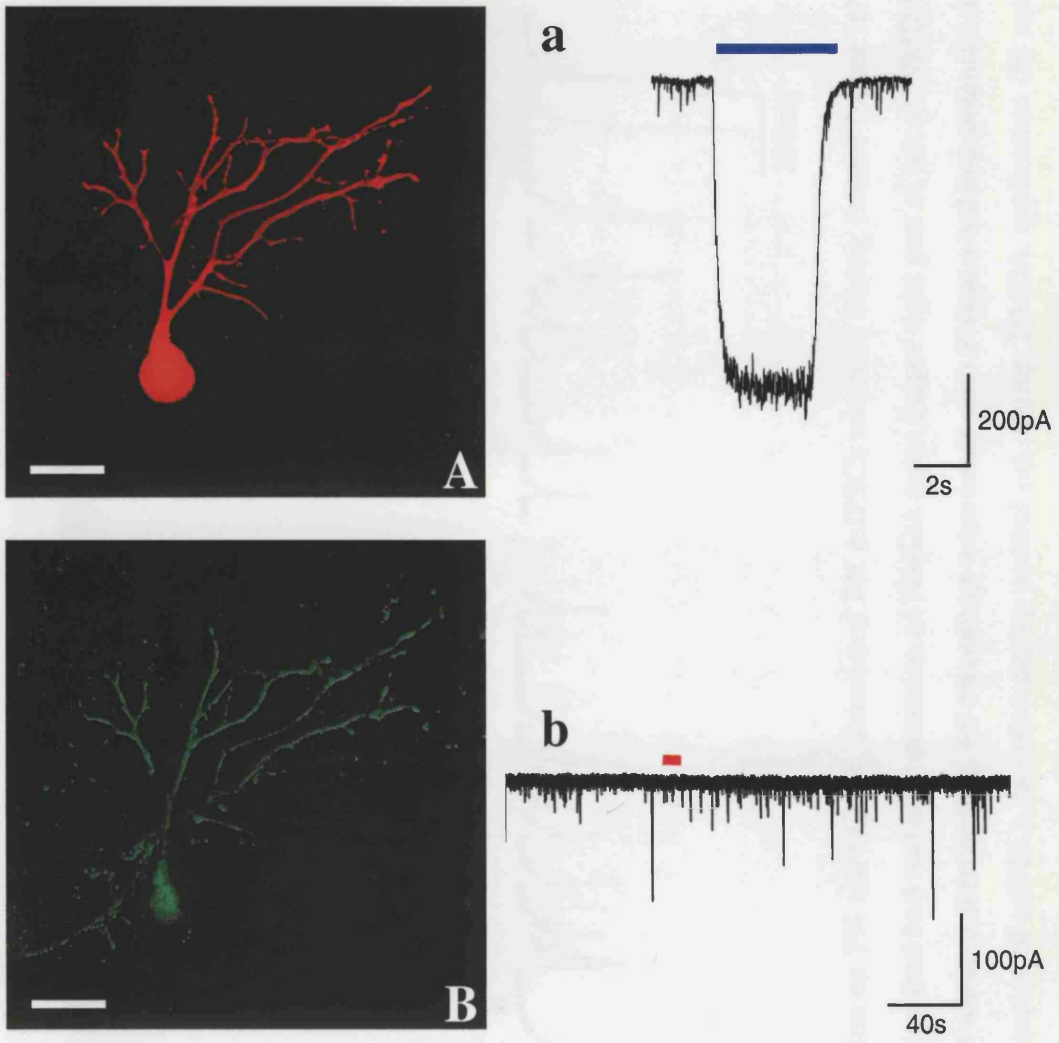

Fig. 6.21. Mature PNs possess functional $GABA_ARs$ but no functional NMDARs. Immunocytochemical staining using an anti-Calbindin D_{28K} antibody with an anti-mouse TRITC conjugate (A) and an anti-NR1 antibody with an anti-rabbit FITC conjugate (B) to identify the distribution of the NMDA receptor NR1 subunit in a mature, 21 days *in vitro*, Purkinje neurone (A). Images were acquired at X40 magnification with zero zoom (scale bar = 20μm). Application of 10μM GABA for a duration of 4s (a, blue bar) induces a large inward current on activation of Purkinje neurone $GABA_ARs$ (n=5). Application of 100μM NMDA for a duration of 4s (b, red bar) produces no inward current when applied to mature Purkinje neurones (n=5). All experiments were conducted in nominally Mg^{2+} free Krebs solution containing 1μM Strychnine, 10μM glycine, 500nM TTX and 10μM CNQX.

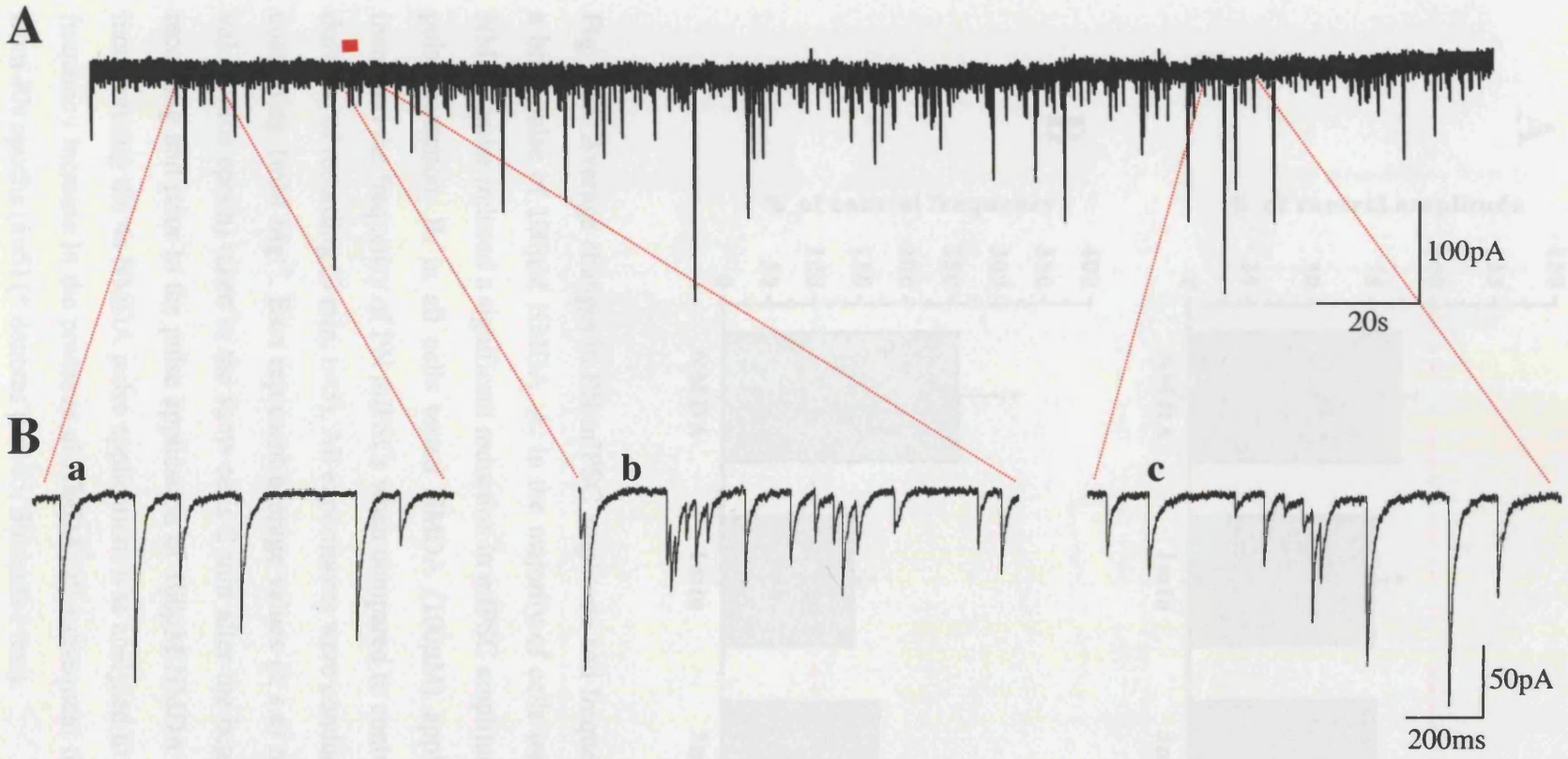

Fig. 6.22. Effects of exogenous NMDA application on PN mIPSCs. A, summated PN mIPSCs recorded during control (upper left part of trace) during 100μM NMDA (4s) application (red bar) and after cessation of NMDA pulse (upper right part of trace). NMDA pulses (4s) were applied at 3 min from the start of whole-cell recording. All recordings were made with PNs at a holding potential of –70mV. B, Insets show expanded time-base examples of mIPSCs recorded during control (a), during NMDA application (b) and 3min after cessation of the NMDA pulse (c).

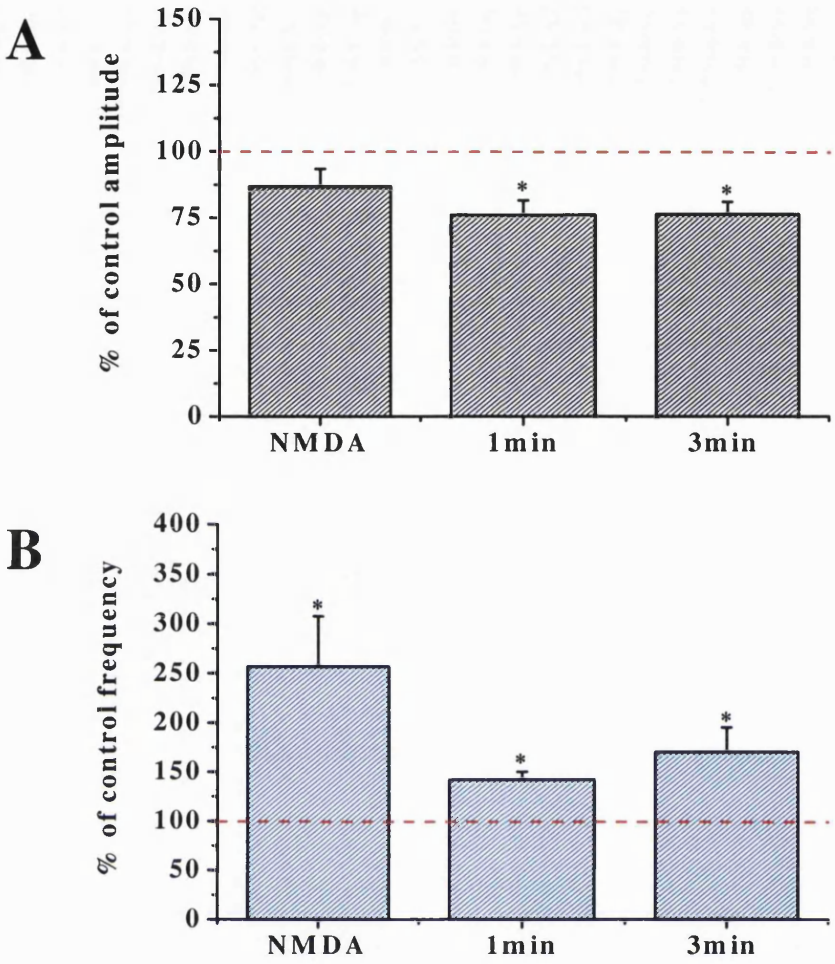

Fig. 6.23. Average changes in PN mIPSC amplitude and frequency during and after a brief pulse of 100μM NMDA. A, in the majority of cells tested (n=4/5) a single NMDA pulse induced a significant reduction in mIPSC amplitude at 1 & 3 min after pulse cessation. B, in all cells tested NMDA (100μM) application significantly increased the frequency of PN mIPSCs when compared to control, persisting for the duration of recording (3 min, n=5). All experiments were conducted in normal Krebs containing 1mM Mg^{2+}. Bars represent average values (± s.e) normalised to control values (40s epoch) taken in the same cells 2 min after the beginning of whole-cell recording and prior to the pulse application of 100μM NMDA (n=5). A 10s epoch, incorporating the 4s NMDA pulse application, was analysed to examine the mIPSC frequency increase in the presence of NMDA, all subsequent times were calculated from 40s epochs (n=5) (* denotes $p<0.05$, Students t-test).

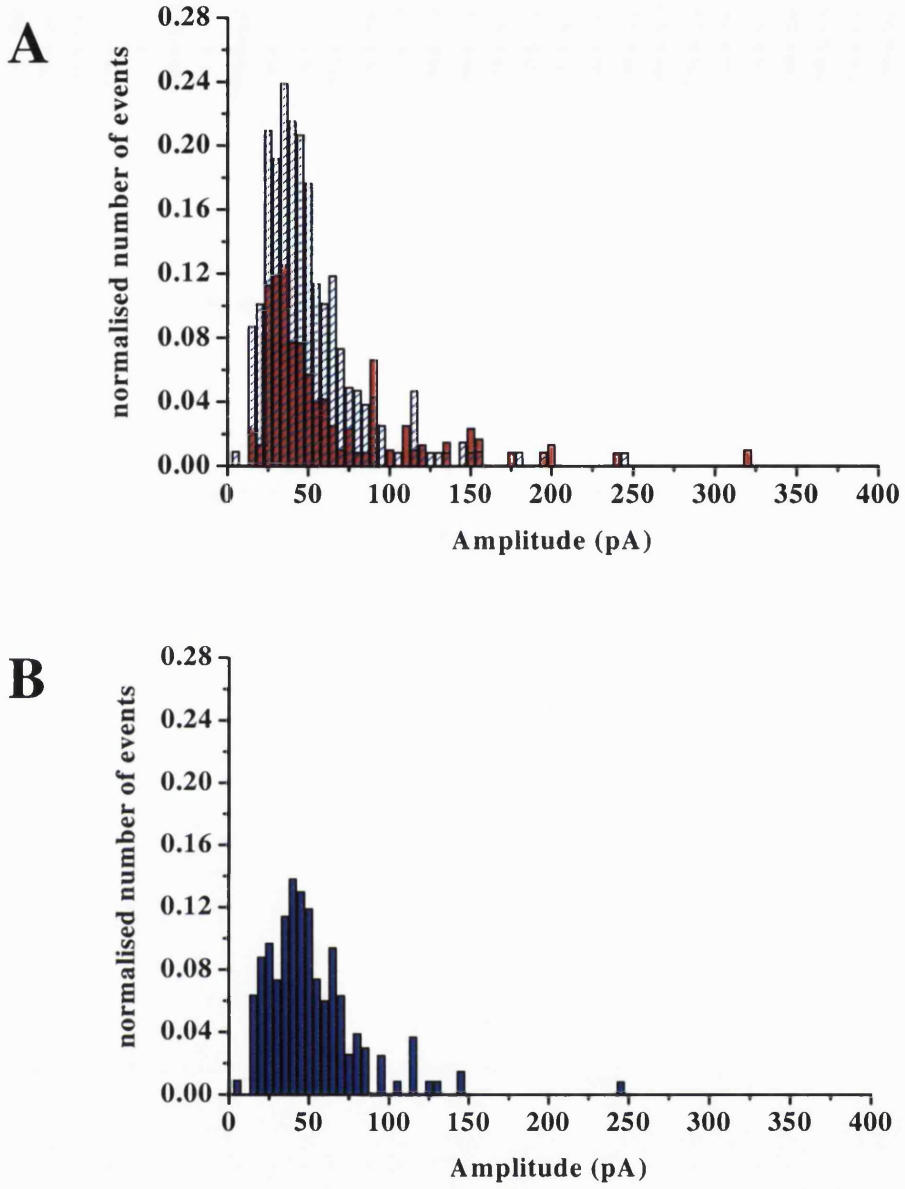

Fig. 6.24. NMDA application enhances the frequency of small amplitude mIPSCs. A, average normalised PN mIPSC amplitude distributions recorded during control (red bars) and 3 min after application of a 4s pulse of 100μM NMDA (blue hatching). Histogram bins were normalised to the total number of events (n=4). B, average normalised PN mIPSC amplitude distribution of NMDA-induced events obtained by subtracting the distributions in NMDA from that of control (n=4). All experiments were conducted in Krebs solution containing 1mM Mg^{2+}.

DISCUSSION

6.1. NMDA receptors: Involvement in DSI & RP

The inclusion of the competitive NMDA receptor antagonist, D-APV, in the bathing Krebs solution induced a significant reduction to the basal rate of PN mIPSCs, which is in agreement with earlier studies on NMDA receptor activation in cerebellar interneurones (Glitsch & Marty, 1999). This compounds the theory of a tonic regulation of transmitter release as a result of background glutamate levels. Activation of postsynaptic PN NMDARs can be discounted due to the absence of functional NMDA receptors on mature PNs (Farrant & Cull-Candy, 1991; Llano *et al.*, 1991; Rosemund *et al.*, 1992; present study). All experiments were conducted in the presence of TTX and CNQX eliminating spontaneous AP-dependent release and non-NMDA receptor activity. Previous evidence has described an interaction of CNQX with the NMDAR strychnine-insensitive glycine binding site (Lester *et al.*, 1989) where CNQX induced a concentration dependent reduction in NMDAR-mediated currents, that could be entirely reversed by increasing the concentration of glycine in the superfusing Krebs. Although there is minimal evidence as to the level of glycinergic afferent input to the cerebellum the existence of glycine can be inferred by the abundant presence of two types of glycine uptake transporters, GLYT1 and GLYT2 (Zafra *et al.*, 1995; Poyatos *et al.*, 1997) coupled with the NMDAR-mediated increase in mIPSC frequency observed in PNs upon application of NMDA (Glitsch & Marty, 1999; present study). The spontaneous release of glycine, even in the presence of TTX, must provide a sufficient background level of glycine to facilitate the basal activation of presynaptic NMDARs. There is a possibility that the use of CNQX may potentially underestimate the level of NMDAR activation although in this study a minimal concentration of CNQX (10μM) was used to minimise any potential inhibitory effects. The use of TTX creates a situation where in order to influence the release of neurotransmitter, NMDA receptors must be in the locality of the interneurone axon terminals, proximal to the active zone. The block of all Na^+ channels and subsequent block of action potential generation/propagation allows the production of a completely electrically isolated

system in which to examine the effects of differential receptor activation on neurotransmitter release.

Application of a single depolarising protocol and subsequent release of glutamate or a 'glutamate-like' substance should therefore activate presynaptic and postsynaptic mGluRs and presynaptic NMDARs (if present) during both DSI and RP. The present study shows that NMDARs play no role in the induction of DSI, as the magnitude in the presence of D-APV and in control is comparable. This is in accord with the work of Glitsch and colleagues (1996), as they found no significant difference between DSI in control conditions and DSI in the presence of D-APV or NBQX. Therefore, it has now become the standard protocol to apply NBQX and D-APV to the superfusing Krebs in order to solely look at hippocampal and cerebellar 'mGluR-mediated' DSI (Morishita & Alger, 1999; Glitsch *et al.*, 2000). The phenomenon of DSI began to wane at ~1min after stimulus cessation, consistent with the transient nature of cerebellar DSI. The PN mIPSC frequency after returning to control levels displayed no 'rebound' frequency increase during $RP_{t1\text{-}5}$ in the presence of D-APV. Therefore, the possibility exists that the blockade of presynaptic interneurone NMDARs abolishes the mIPSC frequency increase observed during RP.

Application of D-APV did not alter the rise-time, half-width or basal amplitudes of PN mIPSCs nor did it alter the magnitude of mIPSC amplitude potentiation during DSI and RP. This is entirely consistent with the theory that NMDARs do not exist on mature PNs (Farrant & Cull-Candy, 1991; Llano *et al.*, 1991; Rosemund *et al.*, 1992). If glutamate, on release from PN dendrites during depolarisation, were to act on PN NMDARs then an increase in cytosolic Ca^{2+}, $GABA_A$ receptor phosphorylation and eventual enhanced mIPSC amplitude potentiation may occur. Also, if NMDARs were present on PNs then the depolarisation-induced release of 'glutamate' would induce an NMDAR-mediated EPSC. However, no inward currents were recorded after cessation of the stimulus protocol. Alternatively, if the level of Ca^{2+} increase is maximal during repetitive depolarisation, then a further increase in cytosolic Ca^{2+}, via NMDARs, would not serve to increase the already maximal mIPSC amplitude potentiation. Therefore, it seems unlikely, due to the comparable levels of potentiation in control and in the presence of D-APV and the absence of any NMDAR-mediated EPSCs, that NMDARs exist in mature cultured cerebellar PNs (see later for verification).

Therefore, a single depolarising pulse protocol seems likely to induce the release of a retrograde messenger facilitating a mGluR-mediated reduction in PN mIPSC frequency during the initial period (<1min) after stimulus cessation, similar to previous findings (Glitsch *et al.*, 1996; Glitsch *et al.*, 2000). Subsequently, this decrease gives way to a novel, transient (~5min) 'rebound' NMDAR-mediated increase in PN mIPSC frequency during RP. These findings would suggest the presence of functional NMDARs on the axon terminals of cerebellar interneurones and their activation playing a pivotal role in mIPSC frequency changes during RP.

6.2. Removal of extracellular Na^+: Effects on Ca^{2+} sequestration and EAATs

The magnitude of the frequency decrease during DSI, an entirely 'group II-like' mGluR-mediated phenomenon, is slightly, but not significantly, increased by the removal of extracellular Na^+. This could be accounted for in terms of a change in the Ca^{2+} homeostatic mechanisms in the PN. Previous work has identified the extremely high Ca^{2+} buffering capacity of the mature PN due to the abundance of calcium extrusion/sequestration mechanisms. It has been established that mature PNs have a Ca^{2+} binding ratio of 2000, thus for every 1 free Ca^{2+}, 2000 are immediately sequestered on entry (Fierro & Llano, 1996). This produces a neurone where only slight, focal changes in the Ca^{2+} concentration are required in order to initiate downstream signalling cascades. Rapid sequestration is achieved via uptake in the intracellular stores or binding to the abundant Ca^{2+}-binding proteins, parvalbumin and calbindin D_{28K}. Clearance of calcium occurs through plasma membrane Ca^{2+} pumps (PMCA), sarco-endoplasmic reticulum Ca^{2+} pumps (SERCA) and via the cell surface Na^+-Ca^{2+} exchanger. During repetitive depolarisation the $[Ca^{2+}]_i$ may rise in excess of 2μM from a resting level of 25-35nM and at this level of Ca^{2+} entry the Na^+-Ca^{2+} exchanger contributes to ~20% of the total Ca^{2+} removal (Fierro *et al.*, 1998). Removal of extracellular Na^+ results in the collapse of the electromotive force for the forward reaction of the exchanger. This effectively eliminates, at a holding potential of –70mV, one of the PN Ca^{2+} extrusion mechanisms which manifests as a slowing of the depolarisation-induced Ca^{2+} transient decay phase (Fierro *et al.*, 1998). Therefore, in

this study a net increase in the duration of the cytosolic Ca^{2+} rise could eventually lead to an enhancement in the level of retrograde transmitter release leading to a more pronounced mGluR-mediated mIPSC frequency decrease and an increase in the duration of DSI. An increase in duration of the postsynaptic Ca^{2+} rise may also induce maximal activation of postsynaptic protein kinases thus leading to an increased level of $GABA_AR$ phosphorylation and the mIPSC amplitude potentiation reaching a plateau at earlier times compared to control. The aforementioned changes in DSI on Na^+ removal, although not significantly different, could be accounted for by the 'removal' of the PN Na^+-Ca^{2+} exchanger.

One major difference on removal of extracellular Na^+ is that the duration of DSI is prolonged. Glutamate when released into the synaptic cleft, from CFs or PFs, is rapidly sequestered into presynaptic neurones, glia and PNs via excitatory amino acid transporters (EAATs). Removal of extracellular Na^+ will result in an abolition of the transmembrane ion gradients such that the Na^+-dependent EAAT transporters will cease to function and may in some extreme situations (severe hypoxia or ischaemia inducing rapid rise in $[H^+]_o$) reverse (Takahashi *et al.*, 1997). Therefore, depolarisation will result in the release of glutamate or a 'glutamate-like' substance from the PN into the synaptic cleft where upon it will elicit its effect on presynaptic 'group II-like' mGluRs. However, due to the inability of the EAATs to function, the retrograde transmitter will not be sequestered from the cleft and may saturate the presynaptic mGluRs. Inhibition of glutamate transporters will have the equivalent effect of increasing the ligand concentration available for receptor binding (Fitzsimonds & Dichter, 1996). This will continue until, via diffusion in the superfusing Krebs, the glutamate concentration in the synaptic cleft becomes low enough to minimise presynaptic mGluR activation, therefore, allowing the mIPSC frequency to return to control levels. The increase in duration of DSI in Na^+ free medium could be accounted for by the recruitment of presynaptic mGluRs distal to the site of retrograde transmitter release. Under normal physiological conditions the released transmitter would activate a subset of mGluRs initiating DSI, thus causing a reduction in transmitter release for ~1min. The block of EAAT-mediated glutamate uptake will result in the activation of mGluRs distal to the site of release, which may, under normal circumstances, not be activated. This would result in a sequential activation of mGluRs, first proximal then distal to the site of

release, resulting in a prolonged activation of the presynaptic signal transduction mechanisms underlying DSI, manifest as an increase in the duration of DSI. Interestingly, blockade of EAATs in the hippocampus serves to markedly increase the level of DSI without altering the time constant of recovery (τ) (Morishita & Alger, 1999). This group also states that the total duration of DSI is enhanced due to the level of IPSC suppression being larger at each measured interval. However, if the duration of DSI is enhanced then the time constant of recovery (τ) should be increased to allow the IPSC suppression to return to the baseline at differing times. Morishita and Alger (1999) did not elude to this fact and presented data which was apparently conflicting. Interestingly, the timecourse of recovery during hippocampal and cerebellar DSI appears to be enhanced upon increasing the cleft glutamate concentration when compared to DSI in control conditions. These findings would intimate the sequential recruitment of mGluRs proximal, then distal to the site of retrograde transmitter release, manifest as a slowing of the timecourse of recovery. Under normal physiological conditions the cleft glutamate concentration would be stringently controlled by cerebellar EAATs such that only a subset of presynaptic mGluRs would be activated upon initiation of cerebellar DSI. Alternatively, the maintained postsynaptic calcium rise, due to block of the Na^+-Ca^{2+} exchangers in nominally Na^+ free Krebs, may induce the Ca^{2+}-mediated release of transmitter persisting after cessation of the depolarising stimuli. On the assumption that not all presynaptic mGluRs are saturated on release of 'glutamate' then the prolonged transmitter release would sequentially activate receptors proximal and then distal to the site of release. This would also manifest as a subtle increase in the magnitude of DSI, as the immediate concentration of transmitter in the cleft increased, and a significant increase in the duration of DSI, due to sequential mGluR activation.

6.3. Removal of extracellular Na^+: Effects on resting membrane potential

The removal of Na^+ from the superfusing Krebs solution will have a twofold effect on both the resting membrane potential (E_m) of cells which are not under voltage-clamp and on the reversal potential ($E_{rev(NMDA)}$) of the presynaptic NMDARs. The

resting membrane potential of a neurone is defined as the potential difference between inside the neurone and outside the neurone, set by the relative transmembrane gradients of both Na^+ and K^+. Neurones in the CNS possess negative resting membrane potentials which is representative of a resting membrane primarily permeable to K^+ (Hille, 1992). In order to examine the effects of Na^+ removal on the resting membrane potentials of presynaptic interneurones, which are not under voltage-clamp, the Goldman-Hodgkin-Katz (GHK) *voltage* equation was used to predict E_m in the presence of differing extracellular solutions. The permeability ratio for Na^+ and K^+ ions in PNs (P_{Na+}/P_{K+}) of 0.08 has been assumed in order to attain the mean value of E_m recorded from cells within this study (E_m = -56.1 ± 1.97mV). This value falls within the range of P_{Na+}/P_{K+} values calculated from experimental data obtained from a range of different tissues (P_{Na+}/P_{K+} ranges from 0.01 – 0.09) (Hille, 1992). The values used to calculate E_m (all experiments were conducted at 30°C) were gas constant (R) = 8312.3, absolute temperature (K) 303 and Faraday's constant (F) 96,500.

Normal Krebs

$$E_m = \frac{RT}{F}\ln\left\{\frac{[K^+]_o + \frac{P_{Na+}}{P_{K+}}[Na^+]_o}{[K^+]_i + \frac{P_{Na+}}{P_{K+}}[Na^+]_i}\right\}$$

$$E_m = \frac{8312.3X303}{96{,}500}\ln\left[\frac{[4.7]_o + 0.08[140]_o}{[140]_i + 0.08[2]_i}\right]$$

$$E_m = 26.1\ln\left[\frac{4.7+11.2}{140+0.16}\right]$$

$$E_m = -56.8mV$$

Na^+ Free Krebs

$$E_m = \frac{RT}{F}\ln\left\{\frac{[K^+]_o + \frac{P_{Na+}}{P_{K+}}[Na^+]_o}{[K^+]_i + \frac{P_{Na+}}{P_{K+}}[Na^+]_i}\right\}$$

$$E_m = \frac{8312.3X303}{96{,}500}\ln\left[\frac{[3]_o + 0.08[0]_o}{[140]_i + 0.08[2]_i}\right]$$

$$E_m = 26.1\ln\left[\frac{3}{140+0.16}\right]$$

$$E_m = -100.3mV$$

Therefore, using the permeability ratio P_{Na+}/P_{K+} = 0.08 the value of E_m shifts quite considerably in the negative direction inducing a strong hyperpolarisation of the non

voltage-clamped neurones upon removal of extracellular Na^+ assuming the permeability to other ions is negligible. In reality cerebellar interneurones will have a resting membrane potential of approximately -65 to -70mV (Midtgaard, 1992; De Schutter & Bower, 1994; Pouzat & Marty, 1999). In order to ascertain the changes in E_m subsequent to Na^+ removal, in neurones possessing a resting membrane potential of approximately -68mV, the permeability ratio $P_{Na+}/P_{K+} = 0.04$ was used. The values used to calculate E_m (all experiments were conducted at 30°C) were gas constant (R) = 8312.3, absolute temperature (K) 303 and Faraday's constant (F) 96,500.

Normal Krebs

$$E_m = \frac{RT}{F}\ln\left\{\frac{[K^+]_o + \frac{P_{Na+}}{P_{K+}}[Na^+]_o}{[K^+]_i + \frac{P_{Na+}}{P_{K+}}[Na^+]_i}\right\}$$

$$E_m = \frac{8312.3 X 303}{96{,}500}\ln\left[\frac{[4.7]_o + 0.04[140]_o}{[140]_i + 0.04[2]_i}\right]$$

$$E_m = 26.1\ln\left[\frac{4.7 + 5.6}{140 + 0.8}\right]$$

$$E_m = -68.1mV$$

Na^+ Free Krebs

$$E_m = \frac{RT}{F}\ln\left\{\frac{[K^+]_o + \frac{P_{Na+}}{P_{K+}}[Na^+]_o}{[K^+]_i + \frac{P_{Na+}}{P_{K+}}[Na^+]_i}\right\}$$

$$E_m = \frac{8312.3 X 303}{96{,}500}\ln\left[\frac{[3]_o + 0.04[0]_o}{[140]_i + 0.04[2]_i}\right]$$

$$E_m = 26.1\ln\left[\frac{3}{140 + 0.08}\right]$$

$$E_m = -100.3mV$$

The negative shift in E_m, on removal of extracellular Na^+, is consistent irrespective of the starting value of E_m in normal Krebs thus illustrating the pivotal role played by Na^+ in the definition of E_m in neurones. Removal of extracellular Na^+ will result in the membrane attaining a value for E_m approximately = E_K (-100mV) since under these conditions the GHK equation simply reduces to the Nernst equation for K^+.

The secondary effect of removing extracellular Na^+ would be a shift in the reversal potential ($E_{rev(NMDA)}$) of presynaptic interneurone NMDARs. Mayer and Westbrook (1987) identified the $E_{rev(NMDA)}$ of cultured hippocampal neurones to be approximately +0.5mV in the presence of 140mM $[Na^+]_o$, 140mM $[K^+]_i$ and 2mM

$[Ca^{2+}]_o$. On replacement of extracellular Na^+ with the impermeant compound $NMDG^+$ the $E_{rev(NMDA)}$ shifted to a value of –20mV.

6.4. Removal of extracellular Na^+: Effects on presynaptic NMDARs

One distinctive property of the NMDA receptor is its dual dependence of function on agonist (+ co-agonist) binding and membrane potential due to the presence of a voltage-dependent block by Mg^{2+} at resting membrane potentials (Mayer *et al.*, 1984; Nowak *et al.*, 1984; Mayer & Westbrook, 1987; Alford *et al.*, 1993; Monyer *et al.*, 1994; Momiyama *et al.*, 1996; Glitsch & Marty, 1999). The physiological role of NMDARs is therefore constrained by the excitability of the neurone where at rest most (but not all; see below) NMDARs are blocked by Mg^{2+} although depolarisation of the neurone, through action potential generation/propagation or activation of colocalised AMPARs, will alleviate the strong voltage-dependent block permitting the influx of Na^+ and Ca^{2+} (Dingledine *et al.*, 1999). The marked change in E_m of non voltage-clamped presynaptic interneurones, upon removal of extracellular Na^+, may facilitate an *increase* in the voltage-dependent Mg^{2+} block of presynaptic NMDARs thus reducing or blocking the influx of Na^+/Ca^{2+} to presynaptic release sites. Interestingly, there are subtle differences in the strength of the voltage-dependent Mg^{2+} block over a range of physiological membrane potentials dependent entirely upon which NR2 subunit was co-expressed with the NR1 subunit. Monyer and colleagues (1994) expressed NR2A-D with NR1 in human embryonic kidney cells (HEK) and showed distinct differences in their pharmacology. Expression of both NR1-NR2A and NR1-NR2B displayed a stronger voltage sensitivity to the Mg^{2+} block when compared to both NR1-NR2C and NR1-NR2D. The glutamate-activated inward current in the presence of 1mM extracellular Mg^{2+} is largest at membrane potentials in the range of –25mV for the former two receptor channels, whereas it is around –45mV for the latter two. Therefore, at physiological resting membrane potentials it is plausible that activation of presynaptic NMDARs, consisting of either NR1-NR2C or NR1-NR2D, may induce an influx of Na^+/Ca^{2+} thus facilitating an increase in the spontaneous release of GABA, manifest as an increase in the frequency of mIPSCs recorded from mature PNs.

Immunohistochemical studies have identified a predominant expression of NR1, NR2C and NR2D in basket and stellate cells in the molecular layer of the adult cerebellum (Akazawa *et al.*, 1994; Thompson *et al.*, 2000). Interneurones of the molecular layer constitute the major inhibitory afferent input to mature PNs thus the activation of presynaptic NMDARs with a reduced voltage-dependent Mg^{2+} block may underlie the 'rebound' frequency potentiation observed during RP in this study. Glitsch and Marty (1999) postulated that presynaptic NMDARs, present on molecular layer interneurones of the cerebellum, contained NR1-NR2D subunits and were responsible for the NMDAR-mediated increase in mIPSC frequency recorded in PNs.

As previously mentioned, the removal of Na^+ from the extracellular perfusion medium will have a profound effect upon the activity of presynaptic NMDARs in the present study. If the membrane potential of non voltage-clamped presynaptic interneurones shifted from resting (-56.1 ± 1.97mV) to a value approximately –100mV then this may induce a significant increase in the level of Mg^{2+} block. Examination of the current-voltage relationship plots (I-V plots) for NMDAR receptors containing NR1-NR2C and NR1-NR2D subunits identified that at increasingly negative membrane potentials the voltage-dependent Mg^{2+} block significantly reduced the NMDAR-mediated currents (in the presence of 1mM Mg^{2+}) (Monyer *et al.*, 1994). Therefore, the possibility exists that removal of extracellular Na^+ will result in the block of presynaptic NMDARs present at putative release sites on interneurones innervating mature PNs. The resultant effect would be similar to applying the selective NMDAR antagonist, D-APV. Interestingly, application of D-APV and the removal of extracellular Na^+ resulted in an equivalent reduction in the basal frequency of mIPSCs (~20%) and both eliminated the 'rebound' frequency increase in mIPSCs observed during RP in normal Krebs.

Although removal of Na^+, the major charge-carrying ion through NMDARs, will result in a possible increase in the voltage-dependent Mg^{2+} block in non voltage-clamped neurones it does not negate the influx of Ca^{2+} through NMDARs present on interneurones voltage-clamped at –70mV. Whole-cell NMDAR currents are an amalgamation of somatic, dendritic and axonal NMDAR-mediated currents, activated by a short pulse of NMDA. Therefore, the assumption has to be made that all NMDARs throughout the interneurone will be affected in the same way during pharmacological

manipulation. Early work identifying the Ca^{2+} permeability of neuronal NMDA receptors found under normal physiological conditions (145mM $[Na^+]_o$, 2mM $[Ca^{2+}]_o$ and 140mM $[K^+]_i$), as predicted by the constant-field equation, Na^+ carried 87.8% and Ca^{2+} carried 12.2% of the NMDA-activated inward current at –60mV (Mayer & Westbrook, 1987). Work by Schneggenburger and colleagues (1993) used confocal imaging to examine changes in Ca^{2+}-sensitive fura-2-fluorescence in large forebrain neurones of medial septal slices to predict the fraction of Ca^{2+} entering via NMDARs upon activation. The results displayed a 2-fold lower Ca^{2+} permeability (6.8%) when compared to previously established values using reversal potential measurements. More recent studies on recombinant HEK 293 cells, overexpressing NR1-NR2A subunits, calculated the fractional calcium current (P_f) in these cells to be 13.3% (Wollmuth & Sakmann, 1998). The anomaly between the predicted P_f values within different studies may underlie the different methodologies used to obtain the values. The use of Ca^{2+} fluorescence imaging examines Ca^{2+} fluxes at physiological resting membrane potentials and extracellular ion gradients. The estimated Ca^{2+} flux under these conditions should provide a good indication of the relative ion flux upon NMDAR activation, without having to significantly alter the ionic gradients. Changes in one or more of the ion concentrations may lead to effects not observed under normal physiological conditions, and may result in an incorrect interpretation of the relative proportion of Ca^{2+} entering the cell through NMDARs. Interestingly, the replacement of Na^+ with N-methyl-D-glucamine ($NMDG^+$) does not inhibit the movement of Ca^{2+} through neuronal NMDA receptors voltage-clamped at –70mV. Brief applications of glutamate (50-200ms) in a nominally Na^+ free Krebs solution (5mM Ca^{2+}), at –60mV holding potential, still induced a net inward current in cultured hippocampal neurones. The amplitude of the Ca^{2+} current was entirely dependent upon $[Ca^{2+}]_o$ (Iino *et al.*, 1990). Confocal microscopic imaging of Ca^{2+} changes in rat hippocampal neurones further identified the persistence of NMDAR-mediated Ca^{2+} currents after NMDA application, in nominally Na^+ free Krebs (Segal & Manor, 1992). The removal of Na^+ from the superfusing medium resulted in a prolonged $[Ca^{2+}]_i$ rise in response to NMDA as a result of the inhibition of cell surface Na^+-Ca^{2+} exchangers. Interestingly, removal of Na^+ has the same effects on Ca^{2+} homeostatic mechanisms in hippocampal and cerebellar Purkinje neurones (Segal & Manor, 1992; Fierro *et al.*, 1998). Therefore, the

removal of Na^+ will neither negate the entry of Ca^{2+} via NMDARs on activation nor the subsequent Ca^{2+}-induced activation of downstream second messenger systems. For NMDA-dependent long-term potentiation (LTP), it is proposed that Ca^{2+} influx via NMDARs is a requirement for the induction of LTP either through direct activation of Ca^{2+}-sensitive substrates and/or subsequent release from intracellular stores (Madison *et al.*, 1991; Bliss & Collingridge, 1993). Similarly, local dendrodendritic feedback inhibition of GABA release in the olfactory bulb has been shown to be entirely due to Ca^{2+} influx via NMDA receptors with only minimal contribution from VACCs (Chen *et al.*, 2000). Therefore, removal of Na^+ in the present study will not oppose the entry of Ca^{2+} through presynaptic NMDARs providing that the voltage-dependent Mg^{2+} block is insufficient to inhibit receptor activation. Although, the evidence in this study supports the hypothesis that at highly negative membrane potentials the voltage-dependent Mg^{2+} block of presynaptic NMDARs is sufficient to block any influx and subsequent enhancement of transmitter release during RP.

Alternatively, the possibility remains that the NMDAR-mediated Ca^{2+} entry is sufficient to induce CICR in the presynaptic terminal although this does not occur due to the prolonged negative regulation of NMDARs upon presynaptic mGluR activation during DSI (Martin *et al.*, 1997; Haak, 1999). This negative regulation of NMDAR function may underlie the abolition of the NMDAR-induced increase in mIPSC frequency observed during RP in this study.

6.5. Cerebellar interneurone axon terminals: Putative sites for presynaptic NMDARs

In this study PNs were immunopositive for NR1 throughout the soma and proximal/distal dendrites, corroborating earlier early evidence as to the abundance of this subunit in adult rat cerebellum (Petralia *et al.*, 1994). However, brief applications of NMDA induced no inward currents in mature PNs due to the lack of NR2 subunits required to produce functional NMDARs (Moriyoshi *et al.*, 1991). Interestingly, recent immunohistochemical studies have identified differential staining of PNs with NR2A/B/C & D antibodies (Petralia *et al.*, 1994; Thompson *et al.*, 2000). These

findings pose an interesting question as to the reason why NMDAR subunits, capable of forming functional NMDARs, exist separately or as non-functional heteromers in mature PNs. The major inhibitory afferent input to PNs, stellate and basket cells, possess NR1 (Hafidi & Hillman, 1997), NR2A/C (Thompson *et al.*, 2000) and NR2D subunits (Akazawa *et al.*, 1994; Thompson *et al.*, 2000). Unfortunately, immunohistochemical studies in the cerebellum concentrate on the somatic and dendritic distribution of NMDAR subunits whereas this study examined the possibility of NMDARs located at putative presynaptic release sites on interneurone axon terminals. Previous work has identified the existence of presynaptic NMDARs on both excitatory and inhibitory axon terminals in the basal forebrain, midline thalamus and periventricular hypothalamus. However, these findings are not universal to all presynaptic release sites as very few NR1 labelled fibres are found in the midbrain, brainstem and cortical levels, thus demonstrating a degree of specificity in expression (Paquet & smith, 2000). The immunocytochemical results of this study confirm the presence of NR1 subunits at release sites on cerebellar interneurones, confirming earlier studies of NMDAR immunostaining in the pinceau region of basket cell terminals onto Purkinje neurones (Petralia *et al.*, 1994). Although the staining of NR1 does not confirm the presence of functional presynaptic NMDARs it does, when corroborated by the electrophysiological data, compound the theory of presynaptic NMDARs at release sites on interneurones of the cerebellum. Interestingly, there is significant staining for NR1 at sites juxtaposed to and distal to putative neurotransmitter release sites. Release of a retrograde transmitter from mature PNs may activate NMDARs both on and adjacent to release sites thus altering the neuronal excitability of the presynaptic interneurone. A large proportion of release sites on basket and stellate cells are present <100μm from the soma (Bishop, 1993; Pouzat & Kondo, 1996). Analysis of paired recordings of interneurone-PN synapses in the presence of TTX found that somatic depolarisation does influence the excitability of release sites (Glitsch & Marty, 1999). Therefore, there exists the possibility that NMDARs located close to but not at the release site may still influence the neurotransmitter release process. Although, the NMDARs involved in the increase in transmitter release during RP, would have to be located proximal to the retrograde release site due to the glutamate concentration diminishing rapidly as the distance of diffusion is increased. Interestingly, previous studies have shown multiple

putative release sites spanning the length of both basket and stellate cell axons (Pouzat & Kondo, 1996; Forti *et al.*, 2000; Llano *et al.*, 2000). In young animals (P12-P16) the level of Ca^{2+} fluorescence hot spots, indicating Ca^{2+} entry via P/Q type channels during action potential-dependent depolarisation, is ~10 times more abundant than morphologically mature presynaptic varicosities/release sites (Forti *et al.*, 2000). The sites of high Ca^{2+} entry, hot spots, were deemed to be functionally immature release sites undergoing maturation. Light-microscopy studies, of mature rat cerebella (21-34 days old), have reported estimates of the mean density of varicosities on axons of neurobiotin-filled rat interneurones to be 0.15 boutons μm^{-1} (Pouzat & Kondo, 1996). Therefore, the developmental maturation of cerebellar interneurones results in a high density of axon varicosities, each of which constitutes a functional release site. The staining of cerebellar interneurones within this study identified a high percentage of co-localisation between glutamic acid decarboxylase (GAD), identifying axon varicosities, and synaptophysin, depicting functionally mature presynaptic release sites. The triple immunocytochemical staining protocol achieved in this study identifies two major developmental points. Firstly, the high proportion of synaptophysin, present in axonal varicosities, indicates a high level of developmental maturity in the cultured interneurones used within this study each possessing a multitude of synaptic release sites. Secondly, the presence of NR1 subunits at these functionally mature release sites indicates a putative role for the regulation of vesicle release by NMDARs during the phenomenon of RP. One fundamental flaw in the neuronal connectivity in cerebellar culture preparations is the possibility that cerebellar Golgi cells, which do not make synaptic connections with cerebellar PNs *in vivo*, may potentially form synapses with mature PNs in culture. Passive observations, in cultures stained with GAD, PV and calbindin D_{28K}, identified the presence of a minimal number of Golgi cells (refer to Chapter 3) incapable of producing the majority of inhibitory afferent input to mature PNs in culture. Therefore, it would be advantageous to attain a quadruple immunocytochemical stain using GAD, PV, synaptophysin and NR1 to identify cerebellar interneurones, BC/SCs, putative presynaptic release sites and the distribution of the NMDAR NR1 subunit, respectively, in order to specifically identify if NMDARs were present on the axon terminals of the major inhibitory afferent input to PNs in culture (BC/SCs). Although it is not possible to use four separable conjugated

flurorophores, due to insufficient separation of the fluorophore emission spectra, comparative staining using PV identified BC/SCs possessing identical morphology to those identified by the triple immunocytochemical staining protocol. Therefore, it can be concluded that NMDARs are present at putative release sites on mature cerebellar BC/SCs.

Background application of NMDA has been shown to preferentially increase the frequency of 'small' mIPSCs recorded in mature PNs (Glitsch & Marty, 1999). Although this provides evidence to suggest the presence of presynaptic NMDARs it fails to evaluate the possible NMDA-induced enhancement of synaptic efficacy after only brief applications of NMDA. Results from this study identify an NMDAR-induced enhancement of mIPSC frequency, persisting for the duration of recording, after only a 4s pulse of 100μM NMDA in normal superfusing Krebs (1mM Mg^{2+}). Although Mg^{2+} induces a voltage-dependent block of native NMDARs, previous work has identified a 100% increase in mIPSC frequency on application of 15μM NMDA in normal Krebs (1mM Mg^{2+}) (Glitsch & Marty, 1999). However, the aforementioned study applied NMDA to the bath for 3 minutes prior to the onset of recording to allow a sufficient equilibrium to be attained. This method of estimating NMDAR-mediated enhancement of transmitter release is overestimated for two reasons. Firstly, bath applying an agonist will persistently saturate all presynaptic NMDARs inducing an almost pathophysiological state. This may lead to long-term changes such as receptor internalisation (Lissin *et al.*, 1999) and a disruption of the regulatory mechanisms underlying normal physiological NMDAR activity. Secondly, bath application of the agonist fails to emulate the minimal release of a retrograde transmitter subsequent to depolarisation, the presence of which would diminish rapidly due to uptake via EAATs and diffusion into the superfusing Krebs. Therefore, the persistent but minimal enhancement of mIPSC frequency, observed after brief NMDA application in this study, may reflect a more physiological NMDAR-mediated enhancement of transmitter release. Interestingly, during RP_{t3} the mIPSC frequency is enhanced by ~50% which is comparable to the ~70% enhancement of mIPSC frequency observed 3 minutes after the cessation of a brief pulse of NMDA. These findings allow an estimation of the maximal enhancement of transmitter release possible under normal physiological conditions. However, the results from the exogenous application of NMDA do not account for the

evident time-lag before the onset of mIPSC frequency potentiation observed during RP in chapters 4 and 5. The application of 100μM NMDA would saturate both somatic and axonal NMDARs inducing a supramaximal increase in $[Ca^{2+}]_i$ at interneurone axon terminals. The global NMDAR-mediated increase in $[Ca^{2+}]_i$ may account for the 156.8% increase in mIPSC frequency observed during NMDA application. Under 'normal' physiological conditions the presynaptic rise in $[Ca^{2+}]_i$, upon retrograde transmitter activation of presynaptic NMDARs, would be submaximal and may require the recruitment of only a subset of presynaptic NMDARs to induce the ~50% increase in mIPSC frequency observed during RP. The possibility remains that raising the cleft glutamate concentration may activate more presynaptic NMDARs thus enhancing the mIPSC frequency potentiation observed during RP although this hypothesis still has to be investigated.

One interesting aspect of the NMDA-induced enhancement of transmitter release is the preferential increase in release from small, possibly immature synapses. The data acquired in this study concurs with that of Glitsch and Marty (1999) identifying a seemingly developmental role for presynaptic NMDAR activation. This previous study utilised animals from 12-14 days old. As previously mentioned, animals from this age range show a multitude of immature and only minimal functionally mature release sites when compared to cerebella from 21-34 days old animals. The cells used in the present study were maintained in culture for 18-28 days allowing maximal maturation to occur. Although this is sufficient time to allow complete maturation of neurones in culture to occur, there still remains some doubt as to whether neurones in culture can attain the same level of 'functional' maturation as those in slice preparations. Therefore, the question as to whether NMDAR-mediated enhancement of neurotransmitter release from cerebellar interneurones is present at all stages in development still remains to be answered.

Chapter 7

PURKINJE NEURONAL GLUTAMATE TRANSPORTERS: PUTATIVE ROLE FOR EAAT3 IN THE RELEASE OF A RETROGRADE MESSENGER DURING CEREBELLAR DSI & RP

INTRODUCTION

Glutamate is the most important and widespread excitatory neurotransmitter in the mammalian CNS. Crucial to the use of glutamate as a neurotransmitter in the brain is the presence of a system which terminates its action. There is no extracellular enzyme capable of breaking down glutamate subsequent to release, unlike the situation for acetylcholine at the neuromuscular junction (Ginsborg & Jenkinson, 1976). Therefore, the synaptic action of glutamate is terminated by its removal from the extracellular space via a family of excitatory amino acid transporters (EAATs). Transmembrane ion gradients (Na^+, K^+ & OH^-/H^+) drive the uptake of glutamate into glial cells and neurones. Interestingly, PNs in the cerebellum possess an abundance of both EAAT3 (also referred to as EAAC1) and EAAT4 throughout the soma and dendritic tree even though they themselves are not glutamatergic neurones. The process of glutamate sequestration, by the PN EAATs, not only terminates the synaptic action of glutamate released from parallel and climbing fibres but also provides the precursor for the production of GABA. Immunohistochemical studies have identified the localisation of EAAT3 to be enriched in the somatodendritic region and EAAT4 to be prominent in both the soma and dendrites of cerebellar PNs (Furuta *et al.*, 1997). A wealth of evidence now exists indicating an extrajunctional localisation for EAAT4 in cerebellar PNs ideal for a role in both glutamate sequestration and/or restriction of glutamate spillover to adjacent synapses (Kanai *et al.*, 1995; Furuta *et al.*, 1997; Tanaka *et al.*, 1997; Dehnes *et al.*, 1998). Although the localisation of EAAT3 and EAAT4 only partly overlap (Furuta *et al.*, 1997), it could be predicted that EAAT3 would also

facilitate glutamate sequestration and the restriction of glutamate spillover. However, in hippocampal neurones staining for EAAC1 displayed no co-localisation with typical presynaptic or postsynaptic markers (Coco *et al.*, 1997). Therefore, in the hippocampus EAAC1 may play an unconventional non-synaptic role in glutamate uptake under normal physiological conditions.

Glutamate sequestration by PN EAATs serves to eliminate the possibility of glutamate induced excitotoxicity in the cerebellum (Takahashi *et al.*, 1997). However, if one or more of the transmembrane ion gradients fails then the normal uptake of glutamate may cease, and in the most severe of cases (hypoxia or ischaemia) may ultimately lead to the reversal of PN EAATs thus releasing glutamate back into the synaptic cleft (Takahashi *et al.*, 1996). Such a release of glutamate during ischaemia selectively destroys PNs despite the absence of functional NMDARs (Balchen & Diemer, 1992). Therefore, activation of non-NMDA and metabotropic receptors may induce a critical rise in postsynaptic Ca^{2+} leading to the excitotoxic death of the neurone. Although glutamate release via EAATs occurs in situations of severe ischaemia or hypoxia it still remains a possibility that, under normal physiological conditions, high frequency stimulation may induce a rise in the external K^+ concentration and reversal of EAAT uptake so as to release glutamate back into the synaptic cleft at physiological concentrations. Previous studies on the possible reversal of neuronal EAATs have mimicked the changes in transmembrane ionic gradients observed during a state of ischaemia or hypoxia (Roettger & Lipton, 1996; Takahashi *et al.*, 1996; Takahashi *et al.*, 1997; Katsumori *et al.*, 1999), however to date, no study has examined the possibility of glutamate efflux under normal physiological conditions.

RESULTS

To examine any potential role for EAATs in the induction of DSI and RP, a specific blocker of EAAT3, L-Serine-O-Sulphate (L-SOS), was included in the superfusing Krebs solution. Initially L-SOS was added at a concentration of 300μM and subsequently at 600μM as these concentrations have been shown to potently block (>80%), in a concentration-dependent manner, glutamate uptake in COS cells expressing EAAT3 (Arizza *et al.*, 1994).

7.1. Concentration-dependent effects of L-serine-O-sulphate on DSI and RP

Application of a depolarising pulse protocol in the presence of Krebs containing 300μM L-SOS, although not being significant, induced an increase in the amplitude and a slight reduction in the frequency of PN mIPSCs immediately after cessation of the stimuli, comparable to mIPSC changes during DSI in normal Krebs. The mean mIPSC amplitude increased to 125.6 ± 18.0% (P=0.3) of control and the mean mIPSC frequency decreased to 80.6 ± 17.6% (P=0.4) of control (Fig. 7.1 A & B) (n=3). Increasing the concentration of L-SOS to 600μM induced a significant increase in the mean mIPSC amplitude while the mIPSC frequency remained unchanged with respect to control. The mean mIPSC amplitude increased to 156.9 ± 14.2% (P<0.02) of control and the mean mIPSC frequency remained at 84.4 ± 11.4% (P=0.2) of control (Fig. 7.1 A & B) (n=5).

Analysis of mIPSC modulation at 3 min after stimulus cessation (RP_{t3}), in the same cells in which DSI induction had been attempted, identified a maintained increase in the mean mIPSC amplitude. However, application of L-SOS caused a concentration dependent reduction in the 'rebound' PN mIPSC frequency potentiation observed during RP_{t3} in normal Krebs. In the presence of 300μM L-SOS, depolarisation induced a rise in the mean mIPSC amplitude to 144.7 ± 4.7% (P<0.01) of control but no significant rise in the mean mIPSC frequency (139.2 ± 17.3% (P=0.2) of control) (Fig. 7.2 A & B) (n=3). In the presence of 600μM L-SOS, depolarisation induced a rise in the mean mIPSC amplitude to 139.7 ± 4.6% (P<0.001) of control

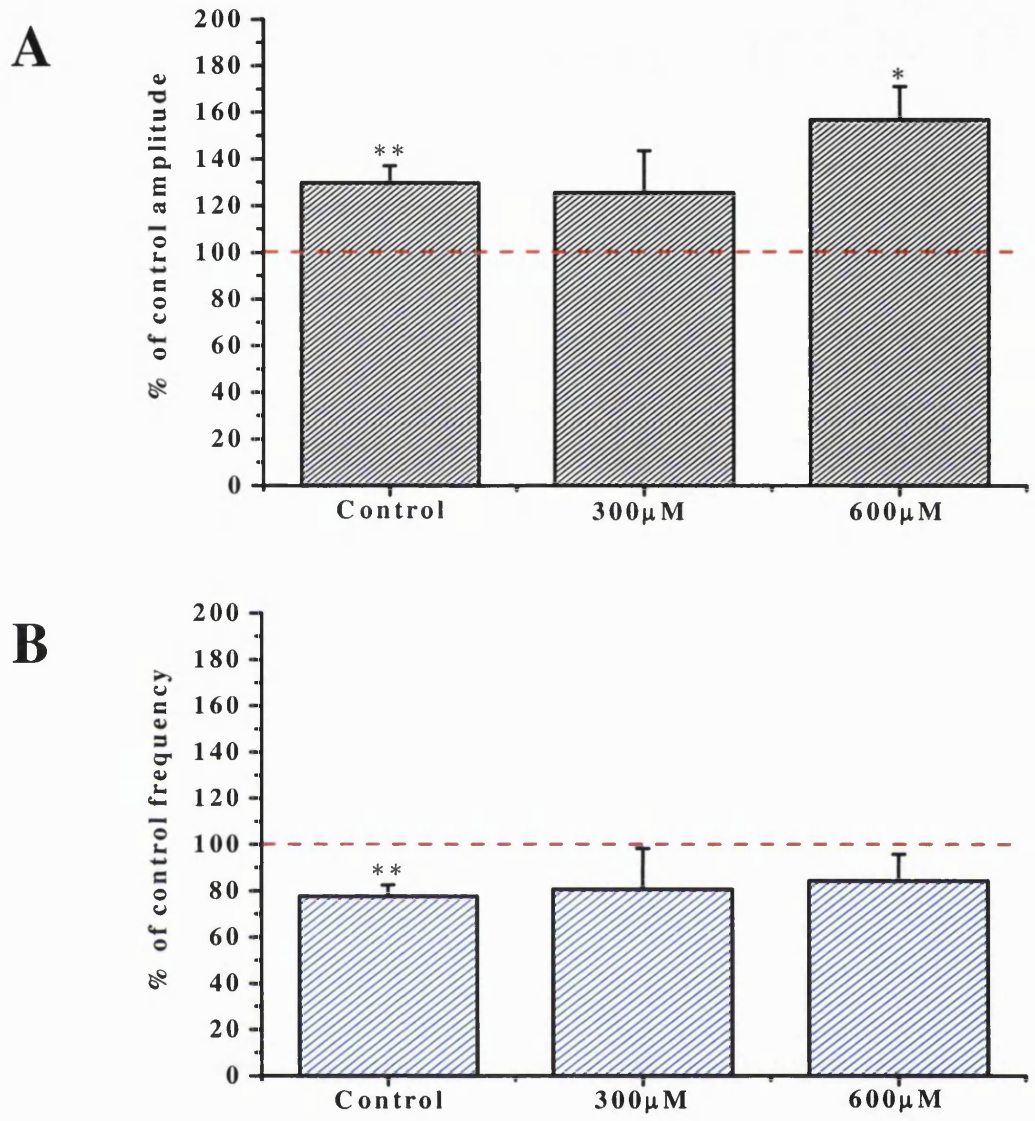

Fig. 7.1. Effects of L-SOS on the induction of DSI. Average changes of mIPSC amplitude (A) and frequency (B) during initial 20s following stimulus induction in PNs voltage clamped at –70mV. Data represents mean values from data acquired in normal Krebs (control) and in 300µM & 600µM L-serine-O-sulphate (L-SOS). Bars represent average values (± s.e) normalised to control values taken in the same cells 2 min after the beginning of the whole-cell recording (Control n=11, 300µM L-SOS n=3, 600µM L-SOS n=5).

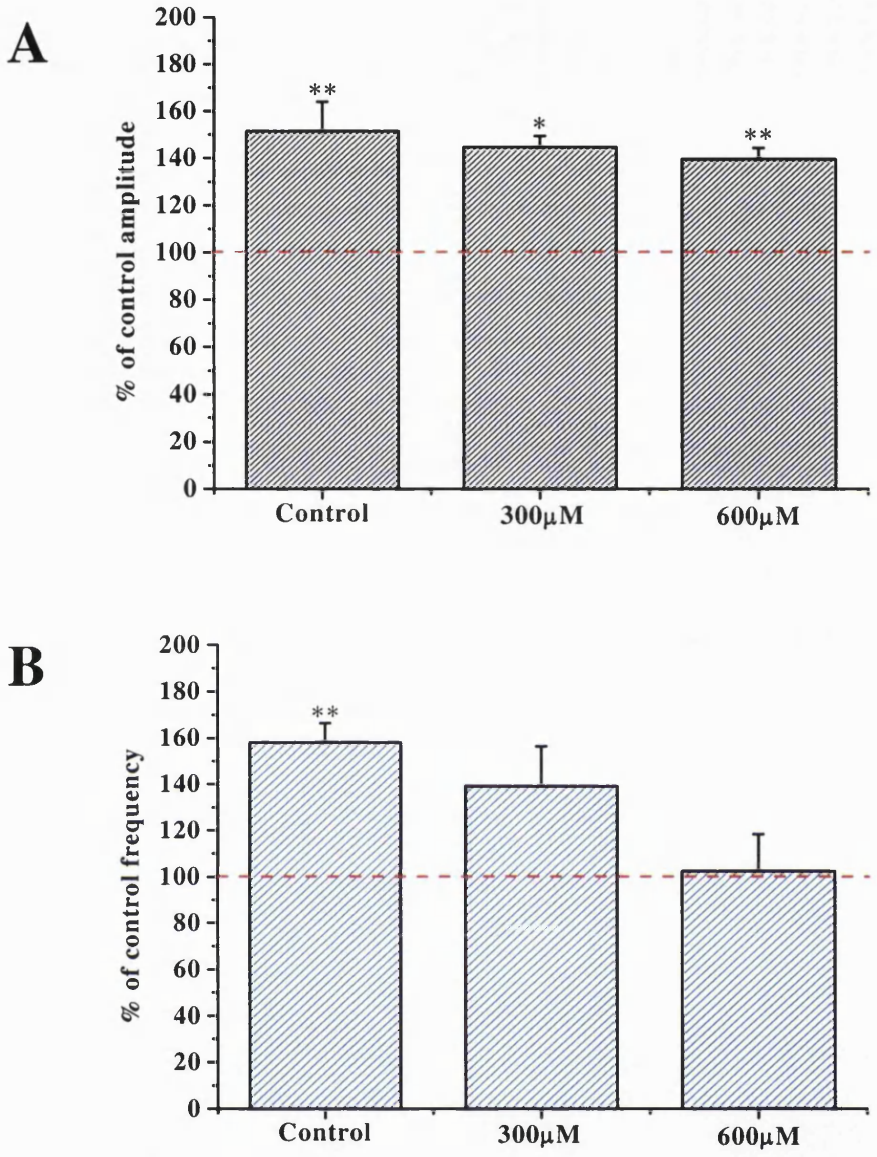

Fig. 7.2. Effects of L-SOS on RP. Average changes of mIPSC amplitude (A) and frequency (B) during RP_{t3} in PNs voltage clamped at –70mV. Data represents mean values from data acquired in normal Krebs (control) and in 300μM & 600μM L-serine-O-sulphate (L-SOS). Bars represent average values (± s.e) normalised to control values taken in the same cells 2 min after the beginning of the whole-cell recording (Control n=11, 300μM L-SOS n=3, 600μM L-SOS n=5).

while again not significantly altering the mIPSC frequency (102.6 ± 15.8% (P=0.9) of control) (Fig. 7.2 A & B) (n=5).

7.2. L-serine-O-sulphate: Effects on cerebellar interneurone NMDARs

Application of a brief 4s pulse of 300μM (Fig. 7.3 A) & 600μM (Fig. 7.3 B) L-SOS produced large inward currents in mature cerebellar interneurones which were partially blocked by co-application with 50μM D-APV (Fig. 7.3 C). After washout this partial block was reversed revealing large inward currents on application of 600μM L-SOS (Fig. 7.3 D). Brief application of 600μM L-SOS did not affect $GABA_AR$-mediated currents in mature cerebellar interneurones. The effects of L-SOS on $GABA_AR$ and NMDAR-mediated currents are summarised in Table 7.1 below.

Table 7.1. L-SOS effects on $GABA_AR$- and NMDAR-mediated currents in mature cerebellar interneurones.

Krebs	Mean Amplitude (pA)	n
L-SOS (300μM)	611.4 ± 81.5	5
L-SOS (600μM)	811.8 ± 105.7	5
L-SOS (600μM) + 50μM D-APV	158.5 ± 39.4	5
10μM GABA	3375.8 ± 546.1	5
L-SOS (600μM) + 10μM GABA	3469.2 ± 273.0	5

7.3. Intracellular L-SOS and the induction and maintenance of DSI & RP

The internal perfusion of 600μM L-SOS will act to block EAAT3 reversal as EAATs can bind/transport glutamate from both extracellular (normal, uptake mode) and intracellular (reversed, efflux mode) sources. The addition of L-SOS to the cytosol will

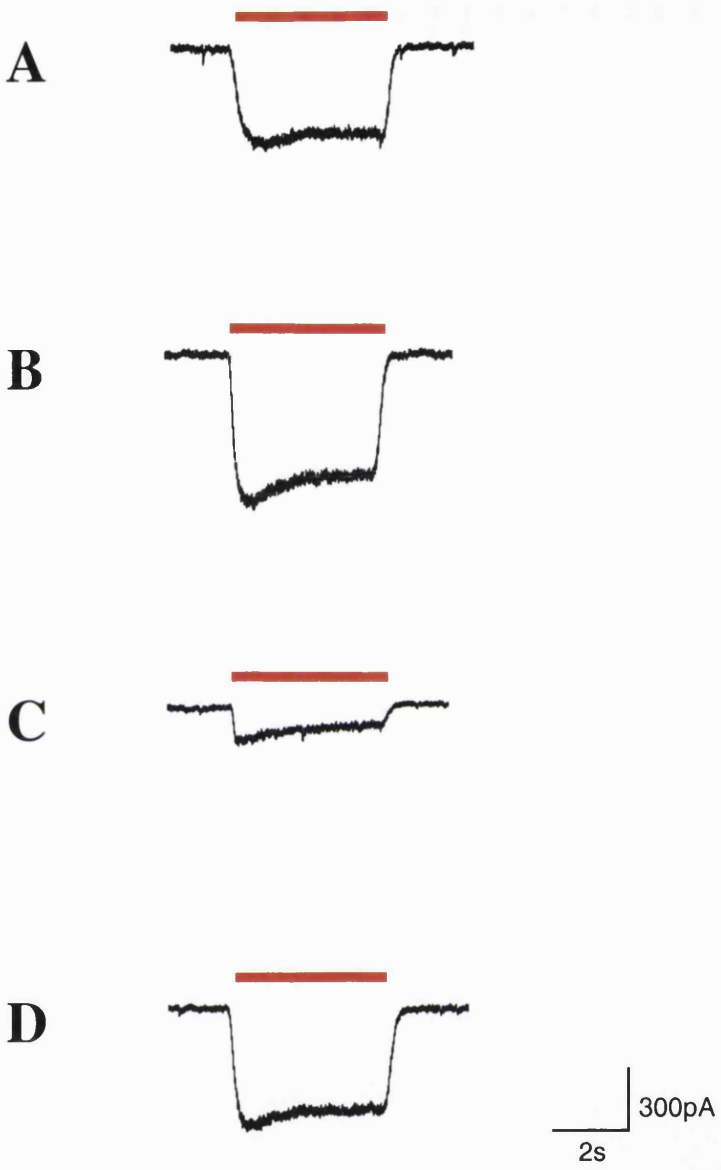

Fig. 7.3. Effects of applying a sulphate containing serine analogue, L-serine-O-sulphate (L-SOS) on mature cerebellar interneurones. A & B, Application (red bar) of 300μM (A) & 600μM (B) L-SOS resulted in the production of large inward currents when applied to mature cerebellar interneurones. C, Partial block of the L-SOS (600μM) induced current by the addition of the specific NMDAR antagonist, D-APV (50μM). D, Wash-out of D-APV resulted in the recurrence of a large inward current on application of 600μM L-SOS. All experiments were conducted in normal superfusing Krebs (n=5).

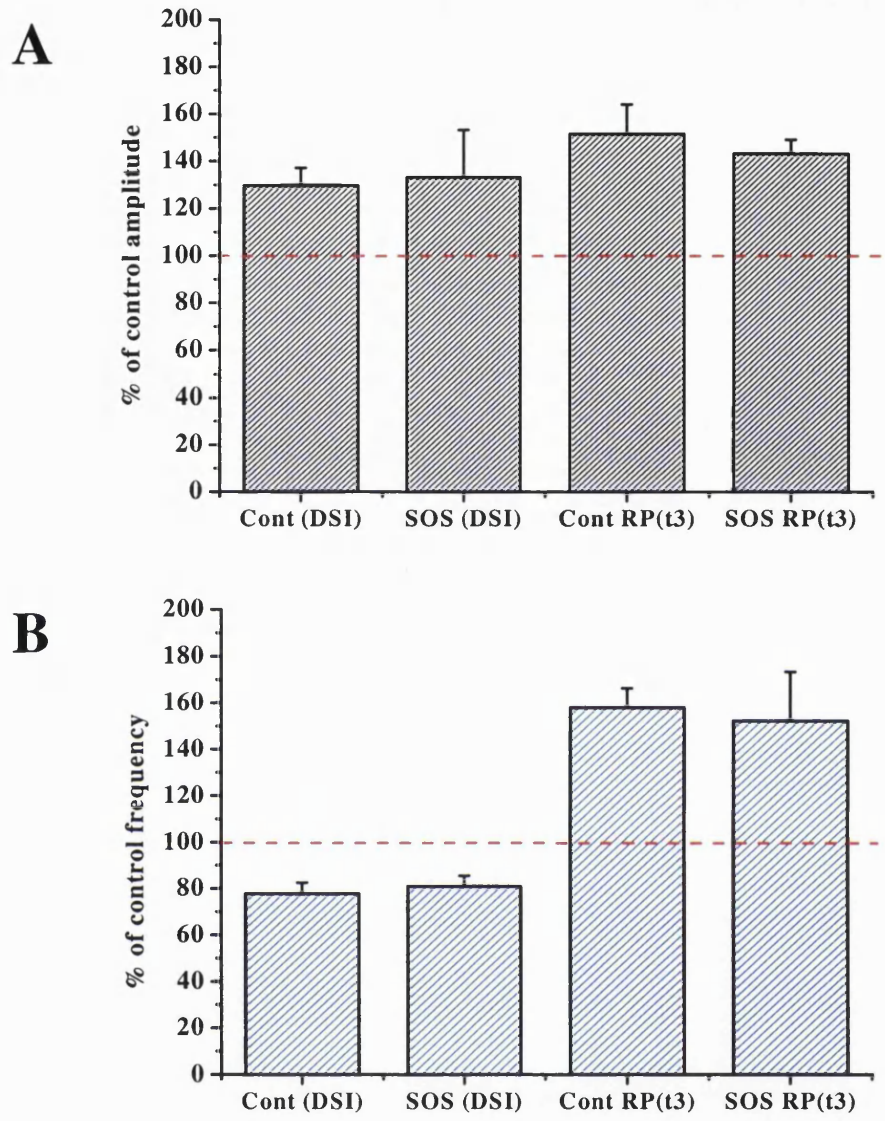

Fig. 7.4. Inclusion of L-SOS in the patch pipette solution does not inhibit DSI/RP induction. Comparison between the average changes in mIPSC amplitude (A) and frequency (B) during DSI and RP_{t3} in control conditions (n=11) and with 600μM L-SOS present in the internal patch pipette solution (n=3). Bars represent mean values (± s.e) normalised to control values taken in the same cells 2 min after the beginning of the whole-cell recording.

avoid the non-specific activation of presynaptic NMDARs which would potentially complicate the analysis.

Inclusion of 600μM L-SOS in the internal patch pipette solution did not alter the magnitude of DSI or RP when compared to control. During the initial 20s after stimulation (DSI) the mean mIPSC amplitude increased to 133.2 ± 20.1% of control and the mean mIPSC frequency decreased to 80.9 ± 4.6% of control (Fig. 7.4 A & B) (n=3). Analysis of mIPSC modulation at 3 min after stimulus cessation (RP_{t3}), in the same cells in which DSI had been previously induced, identified a maintained increase in the mean mIPSC amplitude and a concurrent 'rebound' increase in mIPSC frequency. During RP_{t3} the mean mIPSC amplitude increased to 144.7 ± 4.7% of control and the mean mIPSC frequency increased to 152.2 ± 4.7% of control (Fig. 7.4 A & B) (n=3). Therefore, inclusion, in the internal patch solution, of a specific blocker of EAAT3 does not block the induction or maintenance of DSI or RP.

7.4. Block of PN Na^+-dependent EAA transporters: Effects on the duration of DSI

Neuronal glutamate transporters are Na^+-dependent thus relying on the Na^+ concentration gradient across the plasma membrane in order to facilitate glutamate uptake from the synaptic cleft. Removal of extracellular Na^+ will result in the abolition of the electromotive force driving the glutamate uptake process and thus inhibiting EAAT function.

Complete removal of Na^+ from the extracellular medium (as shown in Chapter 6) resulted in a slight, but not significant, increase in the magnitude of mIPSC frequency modulation during DSI but a significant increase in the total duration of DSI. The mean mIPSC amplitude increased to 145.7 ± 11.3% ($P<0.03$) of control and the mean mIPSC frequency decreased to 65.1 ± 1.7% ($P<0.0003$) of control (n=4) (Fig. 7.5 A & B). A summary of the time-dependent changes in both mIPSC amplitude and

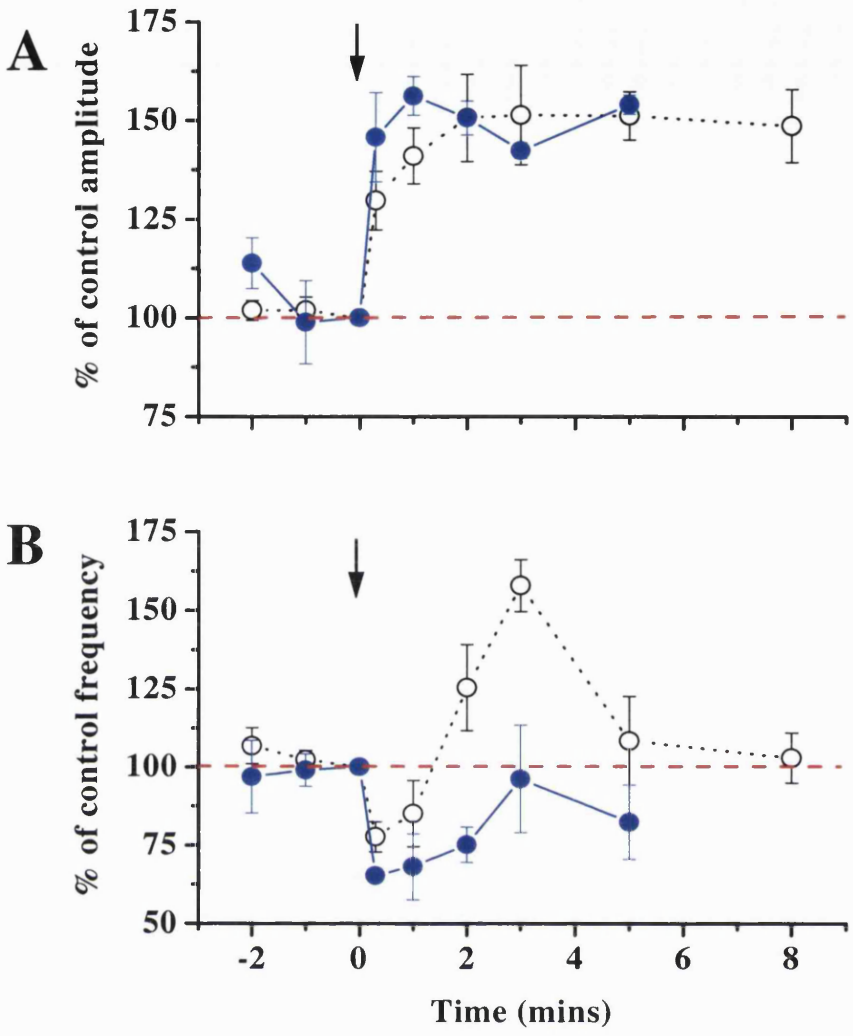

Fig. 7.5. (As previously shown in Chapter 6, Fig 6.12.) Comparison between the time-dependent changes in PN mIPSC amplitude and frequency, following stimulus induction, in normal Krebs (empty black circles) and in the presence of nominally Na^+ free Krebs (filled blue circles). A, changes in mean mIPSC amplitude during control period and after stimulus induction (amplitudes were measured throughout DSI & RP). Current amplitudes were normalised with respect to the mean value recorded directly preceding the point of stimulus induction (depicted by the arrow). B, changes in mean mIPSC frequency during control and after stimulus induction (frequencies were measured throughout DSI & RP). Mean mIPSC frequencies were normalised with respect to the mean value recorded directly preceding the point of stimulus induction (depicted by the arrow). All data are shown as mean ± s.e (Control n=11, Na^+ free n=4).

frequency during DSI in nominally Na^+ free Krebs is displayed in Table 7.2 below (as previously shown in Chapter 6, Table 6.5).

Table 7.2. Timecourse of PN mIPSC amplitude and frequency modulation after stimulus cessation in a nominally Na^+ free Krebs solution.

Time (m)	Amplitude ± s.e	Frequency ± s.e	n
-2	113.8 ± 6.4	96.9 ± 11.6	4
-1	98.9 ± 10.5	99.0 ± 5.2	4
0	100	100	4
0.3	145.7 ± 11.3	65.1 ± 1.7	4
1	156.2 ± 4.9	68.1 ± 10.5	4
2	150.6 ± 4.3	75.1 ± 5.7	4
3	142.3 ± 2.1	96.2 ± 17.2	4

*Data in red depicts statistically significant values compared to control (Paired t-test, $P<0.05$). Time 0 is defined as the point of stimulus induction, all other times are referenced to time 0 min. All values of amplitude/frequency potentiation are normalised to values calculated at time 0 min (set to 100%).

DISCUSSION

7.1 Concentration-dependent effects of L-serine-O-sulphate on PN EAATs

Excitatory amino acid transporters present on both cerebellar PNs and glial cells are believed to facilitate the processing of information at a relatively high rate in the mammalian CNS, such that they sequester glutamate from the synaptic cleft in order to 'sculpt' postsynaptic currents (Takahashi *et al.*, 1996). Selective inhibitors of the PN EAAT4 serve to prolong the synaptic input from cerebellar CFs and PFs therefore illustrating the putative role of EAATs in the termination of synaptic transmission (Barbour *et al.*, 1994). Similarly, uptake of glutamate, via the second PN transporter EAAT3, serves to reduce the cleft glutamate concentration and suppress synaptic transmission. The glutamate uptake current (depicted by the current derived from the co-transport of Na^+) can be slowed by increasing the intracellular glutamate concentration thus reducing the driving force for the uptake of glutamate (Takahashi *et al.*, 1996). Furthermore, distinct changes in the ion gradients which drive the uptake of glutamate into PNs, if significantly altered as in situations of hypoxia or ischaemia, can reverse the uptake of glutamate facilitating a rapid rise in the cleft glutamate concentration leading to eventual excitotoxicity of surrounding neurones (Choi *et al.*, 1987; Attwell *et al.*, 1993).

The question therefore remains as to whether under 'normal' physiological recording conditions PN EAATs may reverse to liberate glutamate, resulting in the activation of surrounding NMDA and non-NMDARs. Recent evidence suggesting the reversal of glutamate uptake in PNs utilised solutions whereby $[Na^+]_i$ and $[glutamate]_i$ were increased while $[K^+]_i$ was reduced to nominally 0mM (TEA-Cl was included to block K^+ channel activation) and $[Na^+]_o$ was maintained at physiological levels. Reversal of the PN EAATs was induced by the brief application of 30mM $[K^+]_o$ at +37mV and could be blocked by the co-application of 100μM D-aspartate (Takahashi *et al.*, 1996). In the present study cells were dialysed with CsCl to block the majority of PN K^+ channels although as previously mentioned a substantial number of PN K^+ channels remained unblocked (refer to Chapter 4). The inclusion of Cs^+ in the internal

solution improves voltage space clamp uniformity and can replace counter-transported K^+ on glutamate transporters (Barbour *et al.*, 1991). The $[Na^+]_i$ was provided in the form of Na^+-ATP (2mM) while the PN glutamate concentration remained at a concentration 10,000 fold higher than that present in the cleft (Takahashi *et al.*, 1997). Repetitive depolarisation (0mV) induced a net efflux of Cs^+/K^+ through unblocked K^+ channels thus moderately altering transmembrane ion gradients. Modelling the ionic fluxes during repetitive depolarisation, under conditions used to record PN inhibitory synaptic plasticity, calculated the concentration of Cs^+/K^+ efflux to be ~10-15mM (unpublished results). Although in reality this will be a gross underestimation of the total K^+ efflux as the majority of K^+ channels are blocked by the inclusion of Cs^+ in the patch pipette solution. Therefore the question exists as to whether this focal increase in extracellular Cs^+/K^+ is sufficient to induce the reversal of PN EAATs at depolarised membrane potentials (0mV) thus driving Na^+ and glutamate out of the PN. As previously mentioned Takahashi and colleagues (1996) induced reversed uptake by removing $[K^+]_i$ without replacing it with Cs^+, thus significantly altering the K^+ transmembrane gradient while in the present study the $[K^+/Cs^+]_i$ was maintained at 150mM CsCl inducing an efflux of ~10-15mM (gross underestimated of K^+ efflux under normal physiological conditions) upon depolarisation. Therefore, it seems unlikely that the transmembrane gradient of K^+ would alter sufficiently, under the conditions used for recording within this study, to induce the reversal and subsequent efflux of glutamate via PN EAATs. In comparison, Rossi and colleagues (2000) applied 30mM and 50mM K^+ to hippocampal CA1 cells (clamped at –30mV to relieve Mg^{2+} block of NMDARs), utilising intra- and extracellular solutions similar to the present study, finding that 30mM K^+ did not induce a significant release of glutamate while 50mM K^+ induced a large NMDA and non-NMDA receptor-mediated current activated subsequent to the release of glutamate via hippocampal neurone EAATs. Therefore, the level of K^+ efflux occurring during repetitive depolarisation of PNs may have to rise to a concentration of ~50mM in order to induce reversal of PN EAATs and the subsequent release of glutamate under 'normal' physiological conditions. The release of glutamate into the synaptic cleft upon depolarisation would have the potential to activate presynaptic non-NMDA and NMDA receptors therefore modulating neurotransmission.

In the present study we attempted to identify the possible role of the abundant glutamate transporter EAAT3 (EAAC1) in facilitating the release of the retrograde messenger postulated to underlie the changes in synaptic efficacy observed during DSI and RP. One inherent problem in the identification of the roles played by individual EAATs during synaptic transmission is the lack of subtype-specific pharmacological blockers that also do not interact with glutamate receptors. In order to make the distinction between the possible activity of EAAT3 and EAAT4 in the depolarisation-induced release of a retrograde transmitter the sulphur-containing amino acid L-serine-O-sulphate (L-SOS) provided a useful tool. Specificity of this compound allowed the preferential block of EAAT3 without having any effect on EAAT4 (Palacin *et al.*, 1998). The majority of EAAT blockers are structural analogues of glutamate or related amino acids such that they either block EAATs or are transported at reduced rates in comparison to glutamate. Interestingly, while L-SOS is a potent blocker of EAAT3 it is also a substrate for EAAT1 and EAAT2 (Arriza *et al.*, 1994; Vandenberg *et al.*, 1995; Vandenberg *et al.*, 1998) such is the inherent problem of using 'supposedly' subtype-specific EAAT blockers. Arriza and colleagues (1994) identified EAAT3-mediated glutamate uptake in COS cells by pharmacological block using L-SOS where the K_i was calculated to be ~150μM. In the present study, depolarisation of PNs in the presence of 300 and 600μM L-SOS induced an increase in the mean mIPSC amplitude, during the initial 20s after stimulus cessation, comparable to that observed during DSI in normal Krebs. However, the reduction in mIPSC frequency observed during DSI in normal Krebs was abolished at both concentrations of L-SOS. In concurrence, the 'rebound' frequency potentiation, observed during RP in normal Krebs, was abolished in a concentration dependent manner while the mIPSC amplitude potentiation remained unaffected throughout. Therefore, the application of L-SOS does inhibit the mIPSC frequency modulation during both DSI and RP in a concentration dependent manner without affecting the depolarisation-induced mIPSC amplitude potentiation. As previously mentioned one drawback of using EAAT blockers is their ability to act as agonists at other glutamatergic receptors. On detailed review of the literature it became apparent that L-SOS could potentially be a substrate at both mGluR and NMDARs. Sulphur-containing amino acids such as L-SOS were found to be full agonists at $mGluR_{1a}$, $mGluR_2$ and $mGluR_4$ receptors (Thomsen *et al.*, 1994; Kingston *et al.*, 1998b)

and NMDARs (Pullan *et al.*, 1987; O'Shea *et al.*, 1991). In this scenario the application of L-SOS may cause the persistent activation of presynaptic mGluRs, postulated to mediate cerebellar DSI (Glitsch *et al.*, 1996), NMDARs, identified in this study to underlie the 'rebound' frequency increase observed during RP, and PN $mGluR_{1a}$, identified as having a putative role in the induction of LTD and RP (Crepel and Krupa, 1988; Hashimoto *et al.*, 1996). Therefore, assuming that the depolarisation-induced release of a retrograde messenger is not inhibited by the application of L-SOS, then saturation of presynaptic mGluRs by L-SOS may result in the perpetual block of the adenylate cyclase pathway (assuming that the mGluR involved in cerebellar DSI is 'group II-like') and the inability of the retrograde transmitter to further reduce the mIPSC frequency during DSI. Similarly, persistent activation of presynaptic NMDARs by L-SOS may potentially induce one of two effects. Firstly, persistent NMDAR activation may result in an overall desensitisation of presynaptic NMDARs such that the release of a retrograde transmitter will not induce the 'rebound' increase in mIPSC frequency observed during RP in normal Krebs. Secondly, bath application of L-SOS may produce a persistent increase in the basal frequency of mIPSCs, similar to the mIPSC frequency increase observed upon bath application of NMDA in the study by Glitsch & Marty (1999). Therefore, all subsequent analysis will be calculated from an already fully potentiated mIPSC frequency plateau. The apparent concentration dependent reduction in the mIPSC frequency potentiation during RP could be accounted for by the competition between L-SOS and the retrograde transmitter for the glutamate binding site on NMDARs, however this remains to be evaluated.

Interestingly, L-SOS is a potent agonist at $mGluR_{1a}$ receptors which is known to be abundant on mature PNs (Baude *et al.*, 1993; Fotuhi *et al.*, 1993; Hampson *et al.*, 1994; Martin *et al.*, 1992; Nusser *et al.*, 1994; Shigemoto *et al.*1994). Application of L-SOS should therefore activate PN mGluRs resulting in the production of $InsP_3$ and subsequent 'wave-like' release of Ca^{2+} from intracellular $InsP_3$-sensitive stores. The resultant effect of a rise in $[Ca^{2+}]_i$ would be to induce DSI and RP before any postsynaptic depolarisation had been administered thus negating the possibility of being able to induce any further changes in mIPSC amplitude. However, even in the presence of 300 and 600μM L-SOS depolarisation induced an immediate and robust increase in mIPSC amplitude persisting for the duration of recording. One tentative conclusion

drawn form this is that the activation of PN mGluRs alone is insufficient to raise the $[Ca^{2+}]_i$ to such a level so as to activate the downstream signal cascade(s) required to induce both DSI and RP. The coincident depolarisation-induced opening of PN VACCs and mGluR activation, mediated by CF and PF activation respectively, may be required in order to attain a $[Ca^{2+}]_i$ sufficient to activate downstream signalling cascades and induce PN inhibitory synaptic plasticity. This conclusion contradicts the findings of Hashimoto and colleagues (1996) who mimicked the induction of RP on application of the non-specific mGluR agonist t-ACPD. Therefore, controversy still exists as to whether PN mGluR activation is alone sufficient to induce DSI/RP or whether the coincident influx of Ca^{2+} via VACCs is required.

7.2 L-serine-O-sulphate: Agonist action on cerebellar interneurone NMDARs & intracellular blockade of EAAT3 transport.

In order to confirm the agonist activity of L-SOS on NMDARs brief pulses were applied to mature cerebellar interneurones, due to there being no functional NMDARs present on mature PNs (Farrant and Cull-Candy, 1991; Llano *et al.*, 1991; Rosemund *et al.*, 1992). Application of both 300 and 600μM L-SOS induced large inward currents which could be substantially reduced by the application of D-APV (50μM) thus confirming the agonist action of L-SOS on NMDARs. Application of D-APV (50μM) is sufficient to block all interneurone NMDARs (refer to Chapter 6), therefore, it remains unclear which receptor type, other than NMDAR and AMPA/KA (blocked by the presence of CNQX in the perfusion media), underlies the residual D-APV/CNQX insensitive current. The effect of the extracellular application of L-SOS, to investigate the role played by EAAT3 in the release of a retrograde transmitter, would be masked by the non-specific effects on presynaptic mGluRs and NMDARs. The Na^+-dependent uptake of glutamate can in certain situations, such as ischaemia and hypoxia, reverse to facilitate the release of glutamate from neurones thus identifying the symmetrical nature of neuronal EAATs in allowing the transport of ions and glutamate in either direction. Therefore, the inclusion of L-SOS in the internal patch pipette solution should, in theory, block the reversal of PN EAAT3 without the possibility of activating PN mGluRs or

presynaptic interneurone NMDARs. Application of L-SOS was without effect on neuronal $GABA_A$ receptors thus providing a useful tool to examine the role of EAAT3 in the depolarisation-induced release of a retrograde transmitter during cerebellar DSI and RP. Depolarisation, in the presence of 600μM L-SOS in the patch pipette solution, induced a reduction in the mIPSC frequency during DSI and a 'rebound' increase in mIPSC frequency during RP, entirely comparable to that observed in normal Krebs. In conjunction with the mIPSC frequency changes was an increase in the mean mIPSC amplitude which occurred during DSI and persisted for the duration of recording, again comparable to that observed in normal Krebs. The inclusion of 600μM L-SOS in the internal patch pipette solution will only block EAAT glutamate efflux (during reversal) leaving EAAT glutamate uptake unaffected. Therefore, it can be concluded, on the assumption that EAAT efflux is blocked by L-SOS inclusion, that EAAT3 is unlikely to play a role in the depolarisation-induced release of a retrograde messenger during DSI/RP.

7.3. Block of PN Na^+-dependent EAA transporters: Effects on the duration of DSI

Although EAAT3 does not play a direct role in the release of the messenger which initiates cerebellar synaptic plasticity, it may provide a role in 'sculpting' the presynaptic effects on neurotransmission and resultant postsynaptic currents. As previously mentioned (see chapter 6 discussion) removal of extracellular Na^+ blocks glutamate transport through the Na^+-dependent EAAT3 and EAAT4 thus allowing the $[glutamate]_o$ to rise subsequent to release from CFs, PFs or PNs. In this study, depolarisation, after the removal of extracellular Na^+, resulted in a slight, but not significant increase in the magnitude but a significant increase in the duration of DSI. This increase can be entirely attributed to a rise in the synaptic cleft concentration of glutamate after release from PNs. The lack of glutamate sequestration results in the recruitment of an increased level of presynaptic mGluRs resulting in a more pronounced level of mIPSC frequency depression. The lack of glutamate sequestration also allows the released glutamate to persist in the synaptic cleft for a longer duration, thus possibly recruiting mGluRs both proximal and distal to the site of release manifest as an increase

in the duration of DSI, where glutamate levels only decrease with diffusion into the superfusing Krebs solution. Therefore, PN EAATs do play a prominent role during inhibitory synaptic plasticity within the cerebellum albeit as a background modulator of the time-dependent changes in cleft glutamate concentration. Further experimentation will be required to identify the proportion of glutamate uptake achieved by EAAT3 and EAAT4 subsequent to the depolarisation-induced release of 'glutamate'.

Chapter 8

GENERAL DISCUSSION

8.1 Presynaptic release of neurotransmitters

Nerve terminals are thought to be the archetypal sites of chemical neurotransmission in the mammalian CNS. Action potential (AP) generation in the cell soma propagates down the axon inducing an overall depolarisation of the axon terminals. This depolarisation serves to facilitate the opening of a plethora of VACCs (Catterall, 1998; Seagar *et al.*, 1999) inducing a rapid, brief influx of Ca^{2+} resulting in the AP-dependent release of neurotransmitter (Johnston & Wu, 1995). The depolarisation-induced influx of Ca^{2+} serves to increase the probability of fusion of the vesicular membrane to the presynaptic membrane subsequently ejecting neurotransmitter into the synaptic cleft. Downstream to the opening of VACCs, subsequent to invasion of the axon terminal by an AP, a signalling cascade consisting of Ca^{2+}, cytosolic factors, proteins of the vesicular and plasma membrane and cytoskeletal elements facilitates the final release of neurotransmitter (Bouron, 2001).

An alternative pathway exists for the vesicular release of neurotransmitter which is independent of presynaptic nerve terminal depolarisation. This form of AP-independent release is termed 'spontaneous' because the mechanisms governing the triggering and release are not known. The phenomenon of spontaneous release persists in the presence of the Na^+ channel blocker, TTX, which inhibits action potential generation and propagation. This form of AP-independent exocytosis occurs at both PNS and CNS synapses and generates both spontaneous excitatory and inhibitory postsynaptic currents of small amplitudes (Katz, 1969). The currents induced by the spontaneous release of neurotransmitters are often referred to as '*minis*' (Bekkers & Stevens, 1989). Spontaneous release occurs at relatively low frequency when compared to that of AP-dependent release which indicates the low probability of release in the absence of any presynaptic depolarisation. The AP-dependent or AP-independent

release of neurotransmitter occurs in small 'packets' termed quanta. Each quantum is proposed to represent the release of a single synaptic vesicle (SV), its contents giving rise to a miniature postsynaptic response. Therefore, large amplitude events are representative of the release of a multitude of SVs upon presynaptic depolarisation. Alternatively, *minis* are thought to underlie the release of a single quantum of neurotransmitter thus providing the building blocks of the AP-dependent responses (Bekkers *et al.*, 1990; Forti *et al.*, 1997). Although recently Llano and colleagues (2000) identified cerebellar basket cell-mediated, TTX-resistant large amplitude events (lamIPSCs) resulting from the release of more than one quanta from the same or adjacent release sites. Enhancement of the AP-independent release process can be achieved via a variety of neuromodulators which serve to raise the cytosolic $[Ca^{2+}]_i$ in close proximity to release sites without requiring VACC activation. The question still remains as to whether AP-dependent and AP-independent release of neurotransmitter utilise the same signal cascade(s) downstream of the increase in $[Ca^{2+}]_i$ and whether they release quanta from separate vesicle pools. Recent work illustrated that the spontaneous release of glutamate contributed to the maintenance of dendritic structures (McKinney *et al.*, 1999) and that spontaneous vesicular release itself is not 'a memoryless stochastic process' (Lowen *et al.*, 1997). The present study examined changes in cerebellar inhibitory synaptic efficacy by monitoring changes in the rate of release and postsynaptic currents induced by the AP-independent release of GABA. Conducting experiments in the presence of TTX provided a system where the neurones of interest were in complete electrical isolation thus eliminating the possibility of reciprocal innervation of presynaptic interneurones subsequent to postsynaptic depolarisation. The work carried out in this study attempted to address the question as to whether the basal spontaneous release of neurotransmitter can undergo short- and/or long-term changes in synaptic efficacy and whether the underlying signalling cascade(s) are similar to that of AP-dependent synaptic plasticity. The main similarities and differences will be discussed later.

8.2 Hippocampal vs cerebellar DSI

Changes in inhibitory synaptic efficacy, due to single or repetitive postsynaptic depolarisation, have been known and examined for over a decade (Llano *et al.*, 1991; Pitler & Alger, 1992). The depolarisation-induced release of a retrograde messenger and subsequent depression of presynaptic vesicle release, termed DSI, has been the focal point of experiments in both the hippocampus and the cerebellum, common in the belief that similar signal transduction cascade(s) underlie both processes. Although similarities do exist there are some quite fundamental differences between hippocampal and cerebellar DSI illustrated both in previous studies and in the present study. The similarities are: Ca^{2+} dependence of retrograde transmitter release (Lenz & Alger, 1999; Glitsch *et al.*, 2000); transient nature of DSI (Pitler & Alger, 1992; Llano *et al.*, 1991); released transmitter mediating effects similar to glutamate or a 'glutamate-like' substance (Morishita & Alger, 1999; Glitsch *et al.*, 1996); activation of presynaptic mGluRs (Morishita *et al.*, 1998; Glitsch *et al.*, 1996) resulting in a decrease in the frequency of neurotransmitter release during DSI (Pitler & Alger, 1992; Llano *et al.*, 1991). Although on the surface hippocampal and cerebellar DSI look equivalent two major differences exist. Firstly, hippocampal DSI is postulated to be mediated via group I mGluRs (most likely $mGluR_5$ due to high expression levels in the hippocampus (Testa *et al.*, 1994)) or possibly an unknown subtype displaying Group I pharmacology. Although the involvement of a G-protein coupled receptor in hippocampal DSI has been established (Pitler & Alger, 1994), the downstream signalling cascade(s) underlying the decrease in neurotransmitter release have not yet been established. On the assumption that hippocampal DSI is mediated via group I mGluRs then activation of these presynaptic receptors would have to activate an alternative transduction pathway to the known PLC pathway, presumably via the same G-protein, because PLC activation would facilitate the release of GABA during DSI as opposed to the observed inhibition. In contrast, cerebellar DSI has been shown to be mediated by a mGluR with a pharmacological profile similar to a Group II mGluR, although immunohistochemical studies fail, so far, to display any staining for group II mGluRs in the molecular layer of the cerebellum (Ohishi *et al.*, 1994; present study). Activation of presynaptic group II mGluRs, negatively coupled to the adenylate cyclase pathway, would serve to reduce

the presynaptic release of GABA similar to that of hippocampal DSI. Secondly, hippocampal DSI only affects the TTX-sensitive neurotransmitter release process and is relatively ineffective at reducing spontaneous miniature release (Pitler & Alger, 1994). However, in the cerebellum there are two types of DSI one being TTX-sensitive and the other being TTX-insensitive. Presynaptic mGluR activation during cerebellar DSI facilitates a reduction in the AP-dependent and AP-independent release of neurotransmitter (Llano *et al.*, 1991). Morishita and colleagues (1998) proposed that TTX-sensitive DSI in the hippocampus and cerebellum are mediated via common signal transduction cascade(s) while cerebellar TTX-insensitive DSI may be meditated via alternative signal transduction pathways. As shown in the present study, TTX-insensitive cerebellar DSI is mediated via retrograde transmitter activation of a presynaptic 'group II-like mGluR'. Therefore, the possibility remains that hippocampal DSI and cerebellar DSI may be mediated via a common retrograde messenger although the presynaptic receptor subtype and subsequent signal transduction cascade(s) activated may be distinct.

Recent evidence has identified the release of endogenous cannabinoids upon repetitive postsynaptic depolarisation of hippocampal slice and culture preparations and cerebellar slice preparations (Ohno-Shosaku *et al.*, 2001; Wilson & Nicoll, 2001; Kreitzer & Regehr). The study by Wilson & Nicoll (2001) illustrated a robust DSI which could be largely blocked by the application of cannabinoid receptor type 1 (CB_1) antagonists. Interestingly, postsynaptic depolarisation induced a reduction in the amplitude of evoked IPSCs and a reduction in the frequency of mIPSCs, each of which could be occluded by the application of CB_1 antagonists. These findings are in complete contrast to that of previous work (Pitler & Alger, 1994) who were unable to induce any effect on the TTX-insensitive release of GABA during hippocampal DSI. Another discrepancy in the study by Wilson & Nicoll (2001) is the inability of the broad spectrum mGluR antagonists LY 341495 to block the induction of DSI. Previous work in the same tissue induced a significant block of DSI using the non-specific mGluR antagonist (S)-MCPG (Morishita *et al.*, 1998). Complimentary work on the role played by endogenous cannabinoids during hippocampal DSI induction failed to induce DSI in ~50% of the cells tested, presumed to be due to the differential CB_1 distribution on interneurones of the hippocampus, thus only the neurones innervated by presynaptic

interneurone terminals containing CB_1 would a robust DSI be induced (Ohno-Shosaku *et al.*, 2001). Clearly there are major discrepancies between previous work which eluded to glutamate or a 'glutamate-like' substance as being the retrograde transmitter and recent studies identifying an endogenous cannabinoid ligand as the retrograde messenger. One possible mechanism for the CB_1-mediated depression of AP-dependent release is via a direct G-protein modulation of presynaptic calcium channels (Twitchell *et al.*, 1997) as Ca^{2+} entry, subsequent to axon terminal depolarisation, is required for the release of neurotransmitter. However, this does not account for the CB_1-mediated modulation of AP-independent, spontaneous release of neurotransmitter which is, at least in the short term, entirely independent of Ca^{2+} entry via VACCs. A secondary effect of CB_1 activation is a negative regulation of adenylate cyclase (Felder *et al.*, 1995) which would facilitate the decrease in mIPSC frequency observed during DSI. Although the magnitude, Ca^{2+} dependence of retrograde transmitter release and transient timescale of depression is entirely comparable between this study and previous studies there still remains much controversy as to the exact nature of the retrograde messenger and the presynaptic receptors activated upon release. The conclusion reached by Ohno-Shosaku and colleagues (2001) did not discount the possibility that presynaptic mGluRs may play a role in hippocampal DSI thus proposing a dual regulatory mechanism controlled by the retrograde release of both glutamate and endogenous cannabinoids. Although this mechanism is appealing considerable work still has to be achieved in order address the discrepancies between studies.

The role of endogenous cannabinoids as retrograde messengers is not restricted to the hippocampus nor only to inhibitory afferent inputs. Concurrent work by Kreitzer and Regehr (2001) illustrated a form of depolarisation-induced presynaptic suppression of PF- and CF-mediated EPSCs recorded in PNs in cerebellar slice preparations, termed depolarisation-induced suppression of excitation (DSE). In parallel with recent studies on hippocampal DSI the postsynaptic depolarisation of mature PNs induced the release of endogenous cannabinoids activating CB_1 on excitatory afferent inputs thus mediating a reduction in the amplitude of eEPSCs. This study identified, using Ca^{2+} fluorescence, the CB_1-mediated suppression of Ca^{2+} influx via VACCs upon depolarisation of the presynaptic terminal. Therefore, it is plausible that hippocampal DSI and cerebellar DSE, if mediated via presynaptic CB_1, activate similar if not identical signal

transduction mechanisms to inhibit the prerequisite Ca^{2+} influx necessary for neurotransmitter exocytosis. To date no study has focussed on the possible role for endogenous cannabinoid ligands as the mediator of cerebellar DSI although cannabinoid-induced suppression of both sIPSC and mIPSCs has been illustrated in the cerebellum (Takahashi & Linden, 2000).

As previously illustrated the work done in this study attempted to address the mechanism(s) underlying synaptic plasticity of the TTX-insensitive, spontaneous neurotransmitter release process. Although hippocampal DSI, mediated either by 'glutamate' or endogenous cannabinoids, is primarily concerned with the direct inhibition of presynaptic VACCs this mechanism is unable to account for cerebellar DSI in the presence of TTX. Suppression of the spontaneous release of transmitter requires the disruption of the vesicle recycling machinery, downstream of the Ca^{2+} influx via VACCs, assuming that a) the readily-releasable vesicle pools are identical and b) release is mediated by similar if not identical signal transduction cascade(s). The work carried out in this study identifies the release of a retrograde transmitter, possessing properties similar to that of glutamate, which activates presynaptic mGluRs resulting in the direct disruption of spontaneous GABA release (refer to Fig. 8.1). Therefore, the present study is in accord with that of Ohno-Shosaku and colleagues (2001) in supporting the idea that more than one retrograde transmitter may mediate the presynaptic effects observed during cerebellar and hippocampal DSI. The similarities and differences in retrograde transmitter release and the subsequent activation of signal transduction cascade(s) will be the focal point of future studies.

8.3. Rebound potentiation of neuronal $GABA_A$ receptors

Repetitive depolarisation of mature PNs, similar to that required to induce DSI, induces a long lasting potentiation of $GABA_A$R-mediated eIPSCs, sIPSCs, mIPSCs and whole-cell currents (Llano *et al.*, 1991; Kano *et al.*, 1992; Kawaguchi & Hirano, 2000). Induction of a robust RP requires the postsynaptic influx of Ca^{2+} via PN VACCs, activation of downstream protein kinases and subsequent phosphorylation of $GABA_A$R subunits (Kano *et al.*, 1992; Hashimoto *et al.*, 1996; Kano & Konnerth, 1992; Kano *et*

Fig. 8.1. Overview of the signalling mechanisms involved in DSI.

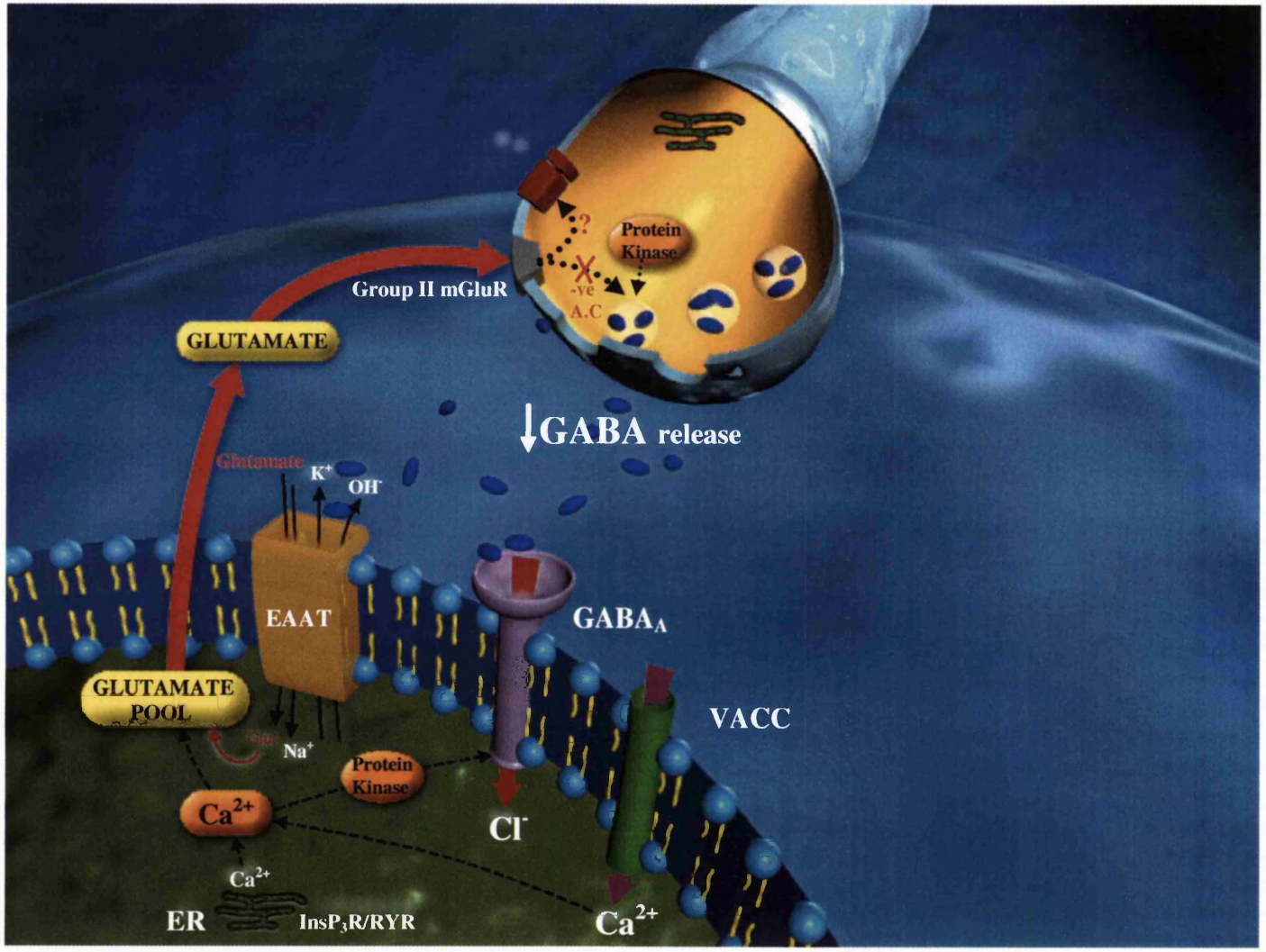

al., 1996; Kawaguchi & Hirano, 2000). Although $GABA_AR$ phosphorylation is a pivotal part of the RP induction phase the specific sites of phosphorylation and the role played by individual protein kinases still remains unclear. Over the past decade studies have attempted to separate the phenomena termed DSI and RP to examine either the exact nature of retrograde transmitter release or the phosphorylation process underlying the induction of RP. Studies concerned with the induction of DSI first apply a train of stimuli, the effects of which are ignored due to contamination with long-lasting postsynaptic $GABA_AR$ phosphorylation, then subsequently apply trains of stimuli at 4 min intervals to obtain a robust induction of cerebellar DSI (Glitsch *et al.*, 1996; Glitsch *et al.*, 2000). However, this induces a situation whereby changes in IPSC amplitude during DSI are normalised to an already potentiated amplitude plateau. Although this does separate DSI from the long-lasting effects of RP the question exists as to whether this relatively short-lasting, transient form of synaptic plasticity will significantly affect the excitability of PNs subsequent to the induction of RP. The present study attempted to examine the induction phase of both DSI and RP after a *single* train of depolarising stimuli thereby addressing the question as to the similarities between the signal transduction cascade(s) required to induce both 'phenomena'. Although previously considered separate, the findings of this study and after extensive review of the literature, it is evident that DSI and RP are entirely comparable and should be classified as a single 'phenomenon'. One plausible hypothesis as to the requirement for the release of a retrograde messenger during the induction of RP comes from the work conducted by Kawaguchi and Hirano (2000). This study concentrated on the synapse specificity of RP induction showing that the presynaptic release of GABA, coincident with repetitive postsynaptic depolarisation, will inhibit the induction of a robust RP via activation of PN $GABA_BRs$. The molecular mechanism of suppression has been postulated to be a $G_{i/o}$-mediated inhibition of adenylate cyclase thus reducing the level of $GABA_AR$ phosphorylation by PKA, previously identified to play a role in RP induction (Kano & Konnerth, 1992). The release of a retrograde messenger, facilitating the suppression of presynaptic neurotransmitter release, may serve to vastly reduce the possibility of coincident presynaptic GABA release during repetitive postsynaptic depolarisation. Therefore, the phenomenon known as DSI may exist as a subsidiary component of RP, present only to facilitate the induction of a robust, long-lasting RP of PN $GABA_ARs$.

One major finding of this study was a previously undocumented transient potentiation of mIPSC frequency observed subsequent to the cessation of DSI. The 'rebound' frequency increase was induced by the same depolarising stimuli required to induce a robust DSI. Therefore, it seems probable that the 'wave-like' increase in PN cytosolic Ca^{2+} levels facilitates the release of a retrograde messenger mediating not only a 'group II-like mGluR'-mediated decrease in GABA release during DSI but also a NMDAR-mediated enhancement of transmitter release at RP_{t3} (refer to Fig. 8.2). The initiation of mIPSC amplitude potentiation occurred immediately after stimulus cessation and continued for the duration of recording similar to that of previous work on RP (Llano *et al.*, 1991; Vincent *et al.*, 1992; Kano *et al.*, 1992; Kano & Konnerth, 1992; Hashimoto *et al.*, 1996; Kano *et al.*, 1996; Kawaguchi & Hirano, 2000). The findings of this study identify the separable components of postsynaptic receptor phosphorylation and the presynaptic retrograde transmitter-mediated modulation of neurotransmitter release. Presynaptic NMDARs underlie the 'rebound' frequency increase during RP due to the complete abolition of the frequency increase in the presence of D-APV and on removal of extracellular Na^+ while the exogenous application of NMDA mimicked the induction of the presynaptic plasticity observed (see chapter 6 discussion). Further, immunocytochemical evidence unequivocally identified the presence of presynaptic NMDARs at putative release sites on mature cerebellar interneurones. The present study is the first to show a role for presynaptic NMDARs in the induction of inhibitory synaptic plasticity in the cerebellum as previous work by Glitsch and Marty (1999) postulated the existence of presynaptic NMDARs on cerebellar interneurones through the exogenous application of NMDA, although this study did not address the possibility of presynaptic NMDAR-mediated synaptic plasticity. Interestingly, the former study observed only a modulation of mIPSC frequency upon application of NMDA with no discernible change in mEPSC frequency. These findings are intriguing in that a subsequent study by Casado and colleagues (2000) described an NMDAR-mediated reduction of PF-mediated EPSCs. Although the NMDAR-mediated effects were indirect, where presynaptic NMDAR activation induced the release of NO causing a depression of postsynaptic PN EPSCs, a precedent for the NMDAR-induced regulation of neurotransmitter release was set. The differences that exist between the two studies may concern the fact that the former study examined NMDAR-mediated changes in the

Fig. 8.2. Overview of the signalling mechanisms involved in RP.

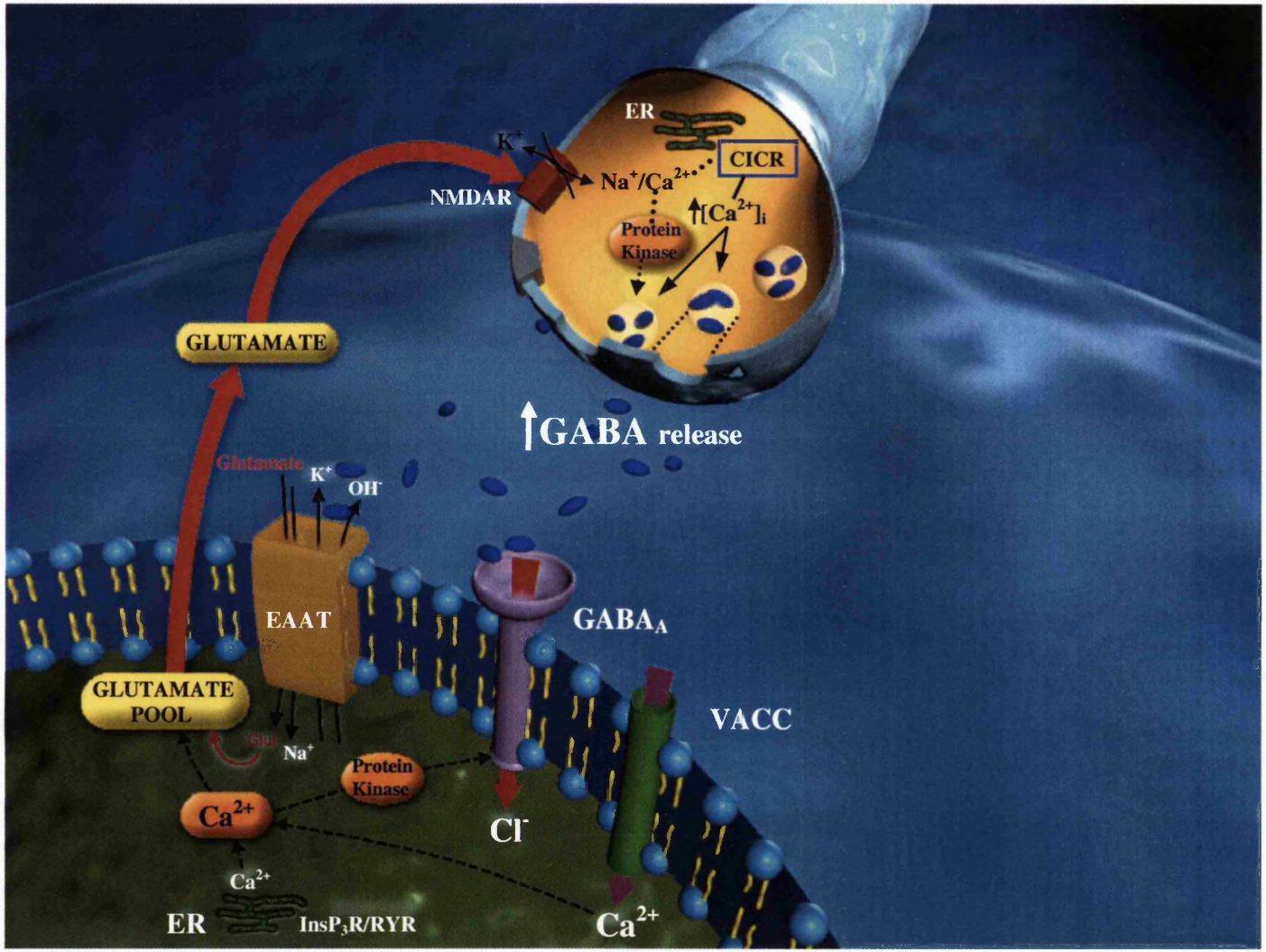

spontaneous miniature release of transmitter while the latter only examined evoked transmitter release. The question therefore exists as to whether AP-dependent release is governed by similar signal transduction cascade(s) as AP-independent release and whether they are differentially regulated by presynaptic receptor activation. This question may underlie the reasons why previous studies have failed to identify a change in the frequency of neurotransmitter release during RP. While this study was concerned with changes in the spontaneous AP-independent release of GABA, displaying a transient NMDAR-mediated increase subsequent to DSI, other studies have concentrated solely on the changes in spontaneous AP-dependent release where no changes in sIPSC frequency were observed (Kano *et al.*, 1992; Hashimoto *et al.*, 1996; Kano *et al.*, 1996).

Presynaptic NMDAR activation would result in a large influx of sodium (~90% of the NMDAR-mediated current) and Ca^{2+} (~10% of NMDAR-mediated current) into the presynaptic nerve terminal. In the present study NMDAR activation presumably facilitates the enhancement of neurotransmitter release at a point downstream of presynaptic VACC activation although it is possible that the large influx of Na^{+} may cause spatially distinct, focal depolarisations of the presynaptic nerve terminals thus facilitating the opening of presynaptic VACCs. The NMDAR-mediated activation of VACCs and subsequent Ca^{2+} spike has been illustrated in the basolateral amygdala and in the neocortex, the effect of which can be blocked by the application of cadmium (Markram & Sakmann, 1994; Calton *et al.*, 2000). This hypothesis, although inviting, would require the induction of Ca^{2+} spikes in the presynaptic nerve terminals as a result of the opening of the majority of VACCs present on the presynaptic nerve terminal. The result of a presynaptic Ca^{2+} spike at individual release sites would be to induce both multi-vesicular release and an increase in the probability of transmitter release. The large increase in $[Ca^{2+}]_i$ may also serve to induce the coordinated release from closely adjacent release sites even in the presence of TTX. The aforementioned effects would manifest as a large but transient increase in the amplitude and frequency of IPSCs. However, in all the control experiments conducted in this study at no time was there an indication of a 'switch' from spontaneous miniature release of transmitter to that of spontaneous AP-dependent 'like' release during the induction phase of RP. The aforementioned observations alone would negate any role for the presynaptic NMDAR-

mediated depolarisation of axon terminals in the onset of the 'rebound' mIPSC frequency increase observed during RP in this study. A previous study conducted by Cochilla and Alford (1999) identified the entry of Ca^{2+} via presynaptic NMDARs in the reticulospinal axons of the lamprey spinal cord, showing that activation of the NMDARs in the presence of TTX was insufficient to activate VACCs as the largest depolarisation induced by the application of 500μM NMDA was +9mV (mean +5.7 ± 1.4mV). In neurones of the lamprey spinal cord there are no low voltage-activated calcium channels such that a +9mV depolarisation, from a mean resting membrane potential of -76.3 ± 0.9mV, would be insufficient to recruit high voltage-activated calcium channels. Similarly, the interneurones used within this study contain N-, P/Q- and R-type high threshold voltage-activated calcium channels (Forti *et al.*, 2000) such that a presynaptic NMDAR-mediated depolarisation of approximately +9mV would not facilitate the opening of VACCs present on presynaptic axon terminals. Therefore, the likely mechanism underlying the NMDAR-mediated enhancement of GABA release may be either through direct activation of Ca^{2+}-sensitive substrates and/or subsequent liberation of intracellular Ca^{2+} stores (Bliss & Collingridge, 1993; Bliss & Lynch, 1988; Madison *et al.*, 1991; Korkotian & Segal, 1998; Savic & Sciancalepore, 1998; Caillard *et al.*, 2000; Llano *et al.*, 2000; Emptage *et al.*, 2001).

8.4. Modulation of AP-independent 'spontaneous' release during DSI/RP

In the past two years the question as to the mechanisms underlying the spontaneous AP-independent release of GABA (measured as mIPSCs) has began to be addressed. Convincing evidence now exists that the release mechanism involves the 'spontaneous' release of Ca^{2+} from ryanodine sensitive stores present in the axon terminals of both hippocampal and cerebellar interneurones (Emptage *et al.*, 2001; Caillard *et al.*, 2000; Llano *et al.*, 2000). Utilising both fluorescent imaging and electrophysiological techniques spontaneous AP-independent release has now been shown to be dependent upon $[Ca^{2+}]_o$ and can be seen as intermittent fluorescent 'sparks' at interneurone axon terminals. Blocking CICR reduces the frequency of these terminal 'sparks' while application of agonists for ryanodine-sensitive stores has the opposing

effect. Therefore, the work presented in this study presents two fundamental questions as to the regulation of AP-independent release of GABA during DSI and RP. Firstly, does the 'group II-like mGluR'-mediated reduction in mIPSC frequency observed during DSI involve the negative regulation of the adenylate cyclase pathway and does this occur downstream of adenylate cyclase itself at the level of cAMP/PKA? Secondly, does the NMDAR-mediated increase in mIPSC frequency observed during RP involve the enhancement of CICR from ryanodine-sensitive stores and does this enhancement directly facilitate the release of GABA? Although these questions were not addressed in the present study some tentative conclusions can be drawn from existing evidence. Group II mGluRs are known to be negatively coupled to adenylate cyclase system via $G_{i/o}$ (Prezeau *et al.*, 1992; Tanabe *et al.*, 1992) whereby activation facilitates a decrease in both AP-dependent and AP-independent release (Baskys & Malenka, 1991; Gereau & Conn, 1995; Hayashi *et al.*, 1995; Llano & Marty, 1995; Manzoni & Bockaert, 1995). The mGluR-mediated negative regulation of the adenylate cyclase pathway has been proposed to occur downstream of both VACCs and adenylate cyclase itself thus affecting the pathway at the level of cAMP/PKA (Chavis *et al.*, 1998). Therefore, the 'group II-like mGluR'-mediated reduction in mIPSCs, observed during cerebellar DSI in this study, could most likely underlie a negative regulation of presynaptic cAMP/PKA activity and subsequent transmitter release. In contrast, the transient enhancement in mIPSC frequency observed during RP presumably underlies an NMDAR-mediated increase in presynaptic Ca^{2+} having the effect of sensitising the ryanodine-sensitive stores such that when the threshold level of $[Ca^{2+}]_i$ has been reached an 'all-or-nothing' release of Ca^{2+} from intracellular stores occurs, termed CICR (Berridge, 1997; Usachev & Thayer, 1997). Therefore, the enhanced release from presynaptic Ca^{2+} stores may play a pivotal role in the induction of both short- and long-term synaptic plasticity throughout the mammalian CNS. In this study, presynaptic NMDAR activation facilitates the induction of a short-term synaptic plasticity subsequent to the termination of DSI.

One interesting feature of the present study is the evident time-lag between the onset of mIPSC frequency suppression during DSI and the onset of the 'rebound' frequency increase observed during RP. This could be explained by two separable pathways which may centre around similar and/or divergent presynaptic signal

cascade(s). Firstly, as previously mentioned, 'glutamate' release during PN depolarisation will activate presynaptic, G-protein coupled 'group II-like mGluR' resulting in the inhibition of the adenylate cyclase pathway at a site proposed to be downstream of both VACCs and adenylate cyclase itself (Chavis *et al.*, 1998). Presynaptic enhancement of the adenylate cyclase pathway has previously been shown to facilitate long-term changes in synaptic efficacy in the hippocampus (Frey *et al.*, 1993; Huang *et al.*, 1994; Weisskopf *et al.*, 1994; Brandon *et al.*, 1995; Capogna *et al.*, 1995; Sciancalepore & Cherubini, 1995; Sciancalepore *et al.*, 1995; Trudeau *et al.*, 1996; Bolshakov *et al.*, 1997) and in the cerebellum (Salin *et al.*, 1996; Chen & Regher, 1997) and therefore must play a pivotal role in the spontaneous AP-independent release of neurotransmitters throughout the mammalian CNS. The 'group II-like mGluR'-mediated inhibition of the adenylate cyclase pathway will inevitably lead to the depression in GABA release observed during DSI in this study. Secondly, the postsynaptic release of glutamate during depolarisation will induce the concurrent activation of presynaptic NMDARs, shown in this study to be present at putative presynaptic release sites on cerebellar interneurones. Recent evidence has identified that Ca^{2+} release from presynaptic ryanodine-sensitive stores during spontaneous CICR underlies the AP-independent release of neurotransmitter in both hippocampal neurones and cerebellar neurones (Savic & Sciancalepore, 1998; Emptage *et al.*, 2001; Llano *et al.*, 2000). The release of Ca^{2+} from intracellular stores can be enhanced either by the application of caffeine, due to the ability of this compound to lower the threshold $[Ca^{2+}]_i$ required to induce CICR (e.g. increasing the sensitivity of ryanodine receptors to Ca^{2+}), or by raising $[Ca^{2+}]_i$ to the threshold level required to induce CICR (Usachev & Thayer, 1997). Experimental data obtained from dorsal root ganglion (DRG) neurones displayed CICR which was entirely dependent upon raising $[Ca^{2+}]_i$ from a basal level of 50nM to 100nM (Usachev & Thayer, 1997) although the length of depolarisation required to achieve this was a rather non-physiological 39 seconds. More recently Korkotian and Segal (1998) used fast imaging of calcium responses in the spines and dendrites of cultured hippocampal neurones to display CICR as a result of caffeine application (5-10mM). The induction of CICR was shown to be almost immediate, subsequent to pressure ejection of caffeine near the recorded dendrite. The Ca^{2+} release phase reached a plateau on a time-scale of 50 to 100ms after initiation of the caffeine pulse thus

showing, at least in spine/dendrites, that the release of Ca^{2+} from ryanodine-sensitive stores is extremely rapid. However, an alternative study examining the effect of the pulse application of caffeine (10mM) on the AP-independent release of GABA in the hippocampus displayed an evident time-lag between the point of caffeine application and the resultant increase in mIPSC frequency observed (Savic & Sciancalepore, 1998). Pressure application of caffeine (10mM) resulted in a ~5-fold increase in the frequency of mIPSCs leading to bursting behaviour. Interestingly, this increase in frequency and bursting activity commenced 10-90s after cessation of the caffeine pulse and persisted for 20-50s. The release of Ca^{2+} during CICR has been proposed to activate the adenylate cyclase pathway (Savic & Sciancalepore, 1998) and thus may potentiate GABA release (Capogna *et al.*, 1995; Sciancalepore & Cherubini, 1995; Sciancalepore *et al.*, 1995). The discrepancy between the timing of the caffeine-induced change in spine/dendrite fluoresence and caffeine-induced increase in mIPSC frequency may underlie the downstream mechanisms required to enhance AP-independent neurotransmitter release subsequent to CICR as both experimental protocols were effectively identical (Korkotian & Segal, 1998; Savic & Sciancalepore, 1998). Therefore, the question arises as to why, if on glutamate release both presynaptic 'group II-like mGluRs' and presynaptic NMDARs are concurrently activated, the mIPSC frequency is first depressed then potentiated. One plausible hypothesis is that 'group II-like mGluR' activation inhibits the PKA-mediated release of GABA, occurring 'immediately' after the depolarisation-induced release of glutamate. Meanwhile, repetitive NMDAR activation results in a graded increase in the level of presynaptic $[Ca^{2+}]_i$. This increase in Ca^{2+} will act to 'sensitise' the axon terminal ryanodine-sensitive stores thus facilitating CICR, although an increase in mIPSC frequency may not be observed for ~10-90s (Savic & Sciancalepore, 1998). This time-lag before mIPSC frequency potentiation would be entirely consistent with the ~60s lag before the onset of the mIPSC frequency potentiation observed during RP in this study (refer to chapter 4). Further corroborating evidence arises from the experiments conducted in the presence of the $mGluR_{2/3}$ specific antagonist LY 341495 which completely blocked the mIPSC frequency decrease during DSI. In this situation the depolarisation-induced release of glutamate did not immediately enhance the mIPSC frequency and a time-lag of ~20s was observed (refer to chapter 5). Therefore, the evidence provided in this study is in accord with the

hypothesis of Savic and Sciancalepore (1998) in that the enhancement of presynaptic CICR does not immediately facilitate a rise in the frequency of GABA release. The possibility remains that in control conditions the presynaptic release of Ca^{2+}, during NMDAR-induced CICR, activates the adenylate cyclase pathway, previously inhibited by the activation of presynaptic 'group II-like mGluRs', therefore inducing the PKA-mediated enhancement of GABA release. The direct influx of Ca^{2+} upon presynaptic NMDAR activation may also facilitate the activation of various isoforms of PKC and CaMKII which have been implicated in the enhancement of spontaneous, miniature release (Bouron, 2001). The direct involvement of the aforementioned protein kinases during RP remains to be evaluated. In contrast, a recent study by Llano and colleagues (2000) concluded that presynaptic Ca^{2+} release from ryanodine-sensitive stores in the axon terminals of cerebellar basket cells resulted in the production of large amplitude mIPSCs (lamIPSCs), presumed to underlie multi-vesicular release. On removal of $[Ca^{2+}]_o$ there was a preferential decrease in the large amplitude, multi-vesicular events leaving small amplitude, presumably monovesicular events (mIPSCs) thus conferring a role for presynaptic CICR in the production of large amplitude events. Immediately after the removal of $[Ca^{2+}]_o$ there was a preferential reduction in the number of lamIPSCs suggesting a requirement for external Ca^{2+} for multi-vesicular release. However, during prolonged periods of 0mM external Ca^{2+} the mIPSC amplitude histograms displayed a reduction in the frequency of all mIPSC amplitudes thus intimating that CICR may underlie both multi- and mono-vesicular neurotransmitter release, although this was not eluded to. This hypothesis is further compounded upon switching back to a Ca^{2+}-containing medium after prolonged exposure to 0mM Ca^{2+} where there was an increase in the frequency of mIPSCs from 0.4Hz to 0.9Hz (in 2mM $[Ca^{2+}]_o$). This increase in frequency was not accompanied by a change in the mIPSC amplitude distribution, which would be expected if the increase in frequency concerned an increase in both small and large amplitude events, thus identifying that the removal of $[Ca^{2+}]_o$ does eventually lead to the reduction in the frequency of both mono- and multi-vesicular release, the latter being most susceptible to changes in $[Ca^{2+}]_o$. The findings mentioned above were not elaborated further in order to solely identify the mechanism(s) underlying the production of cerebellar basket cell-mediated lamIPSCs. Although the requirement for $[Ca^{2+}]_o$ in the spontaneous CICR-mediated release of

neurotransmitter seems quite plausible a previous study by Savic and Sciancalepore (1998) identified no change in the frequency or amplitude of mIPSCs in the hippocampus upon removal of $[Ca^{2+}]_o$, although they do display the presynaptic CICR-mediated Ca^{2+} dependence of AP-independent GABA release. Evidently there still remains many unanswered questions as to the role played by presynaptic Ca^{2+} stores in the AP-dependent and AP-independent release of neurotransmitter.

8.5 AMPA/KA receptor modulation of presynaptic release

The existence of presynaptic AMPARs on both cerebellar basket and stellate cell axon terminals has already been established (Bureau & Mulle, 1998; Satake *et al.*, 2000). Although in this study the non-NMDAR antagonist CNQX was used, in order to block direct AMPAR-mediated depolarisation of PNs, a putative role for AMPA and Kainate receptors in the induction and maintenance of DSI-RP has to be considered. Early studies identified that AMPAR activation on cerebellar stellate cells resulted in complex age- and transmitter release type-dependent effects. Application of the specific AMPAR agonist domoate to immature animals (PN 11-15) induced a large increase followed by a significant decrease (upon cessation of drug application) in the frequency of sIPSCs while displaying a large increase in the frequency of mIPSCs. Under the same application protocol mature animals (PN 21-25) displayed only a very modest increase in sIPSC frequency and negligible changes in mIPSC frequency (Bureau & Mulle, 1998). It thus appeared that presynaptic AMPAR-mediated modulation of GABA release occurred mainly as a developmental requirement. Interestingly, recent work identified that synaptic activation of AMPARs on cerebellar basket cells caused a reduction in the amplitude but not the frequency of sIPSCs in immature animals (PN 12-18) (Satake *et al.*, 2000). This work identified the role played by AMPA but not kainate receptors in the presynaptic reduction of GABA release due to 'spillover' of glutamate from stimulated CFs. These findings, as opposed to that of Bureau & Mulle (1998), intimate that repetitive climbing fibre stimulation and subsequent pre- and postsynaptic AMPAR activation causes both PN depolarisation and a reduction in GABA release from cerebellar basket cells. This effect of glutamate 'spillover' and

axon terminal AMPAR activation would result in a more profound depolarisation of the PN without any 'dampening' effects from cerebellar interneurones. The mechanism underlying the AMPAR-mediated decrease in neurotransmitter release, although unknown, may involve either a direct G-protein coupled effect on the downstream cAMP-associated pathways or possibly as a result of presynaptic autoreceptor activation of $GABA_BRs$ (Wang *et al.*, 1997; Rodriguez-Moreno & Lerma, 1998; Frerking *et al.*, 1999; Satake *et al.*, 2000). The possibility remains that presynaptic AMPARs may play differential roles on cerebellar basket and stellate cells during development although this seems unlikely. The study by Satake and colleagues (2000) intimated that they never observed RP upon PN depolarisation due to their relatively short timeframe of recording (e.g. 400ms immediately after CF stimulation) thus identifying that this AMPA-mediated reduction in GABA release may only be a very transient form of plasticity, possibly exacerbating the existing mGluR-mediated cerebellar DSI. Therefore, a plausible hypothesis could be that glutamate 'spillover' during repetitive CF stimulation and the release of glutamate subsequent to PN AMPAR-mediated depolarisation would serve to reduce GABA release, via presynaptic mGluRs and presynaptic AMPARs, for a short period of time during the induction phase of RP. Similar to the effects of presynaptic 'group II-like mGluR' activation in this study, presynaptic AMPAR activation may also serve to reduce the risk of PN $GABA_BR$-mediated suppression of RP induction (Kawaguchi & Hirano, 2000). It would seem plausible that presynaptic kainate receptors may also play a role in the induction and maintenance of cerebellar DSI and RP, however, this still remains to be evaluated.

8.6 Overview

The reductionist approach to this study was entirely intentional so as to illustrate the separable components of both DSI and RP. However, as indicated many similarities exist between the two phenomena including: identical induction protocol; Ca^{2+} dependence of retrograde transmitter release; presynaptic effects of the retrograde transmitter being similar to that of glutamate and mIPSC amplitude potentiation commencing during DSI and persisting for the duration of recording. All of the above

similarities point unequivocally to the fact that both 'phenomena' are actually a single depolarisation-induced 'phenomenon' (refer to Fig. 8.3). In this scenario the question exists as to whether DSI provides much of an impact to PN cell excitability subsequent to the induction of RP. During repetitive CF and PF stimulation *in vivo* the PN becomes repeatedly depolarised facilitating a rapid and large rise in $[Ca^{2+}]_i$ and subsequent activation of downstream signal cascade(s). Initially depolarisation promotes the phosphorylation of PN $GABA_A$ receptor subunits, manifest as an increase in the mean mIPSC amplitude, while simultaneously releasing 'glutamate' back into the synaptic cleft. The result of this 'glutamate' efflux is the activation of presynaptic 'group II-type mGluRs' and subsequent reduction in the frequency of GABA release. The presynaptic mGluR-mediated effects reach a peak at ~20s after stimulus cessation and persist for ~40s before returning to baseline. This short-term, transient form of synaptic plasticity termed DSI would serve to reduce the possibility of coincident GABA release during depolarisation of the PN as this has been shown to inhibit, via activation of PN $GABA_BRs$, the induction of a robust RP (Kawaguchi & Hirano, 2000). In view of the evidence in the present study and that of Kawaguchi & Hirano (2000) it seems probable that DSI exists as a subsidiary component of RP present only to facilitate the induction of a long-lasting robust increase in synaptic efficacy at the cerebellar interneurone-PN synapse. Interestingly, the increase in the mean mIPSC amplitude commences upon cessation of the depolarising stimuli and rises until reaching a plateau around ~1min, presumably at the point at which all postsynaptic PN $GABA_ARs$ may be fully phosphorylated. The fact remains that if the coincident release of GABA during PN depolarisation acts to suppress RP induction (Kawaguchi & Hirano, 2000) then when all PN $GABA_ARs$ have been phosphorylated (~1min after stimulus cessation) the risk of RP suppression, over the subsequent 20-40 min RP timecourse, is negligible due to the phenomenon of RP, unlike LTD, being irreversible (Hansel *et al.*, 2001). Therefore, the time-dependent changes in mIPSC frequency observed during the first 60s after stimulus cessation may act to reduce the risk of a $GABA_BR$-mediated suppression of RP. Once a robust RP has been induced a NMDAR-mediated increase in the mIPSC frequency is observed. At this stage the increase in the release rate of GABA and the increase in the sensitivity of PN $GABA_ARs$ to GABA results in a significant reduction in PN excitability. The question may be asked as to why the increase in the release of

Fig. 8.3. Cerebellar DSI and RP: One phenomenon or two?

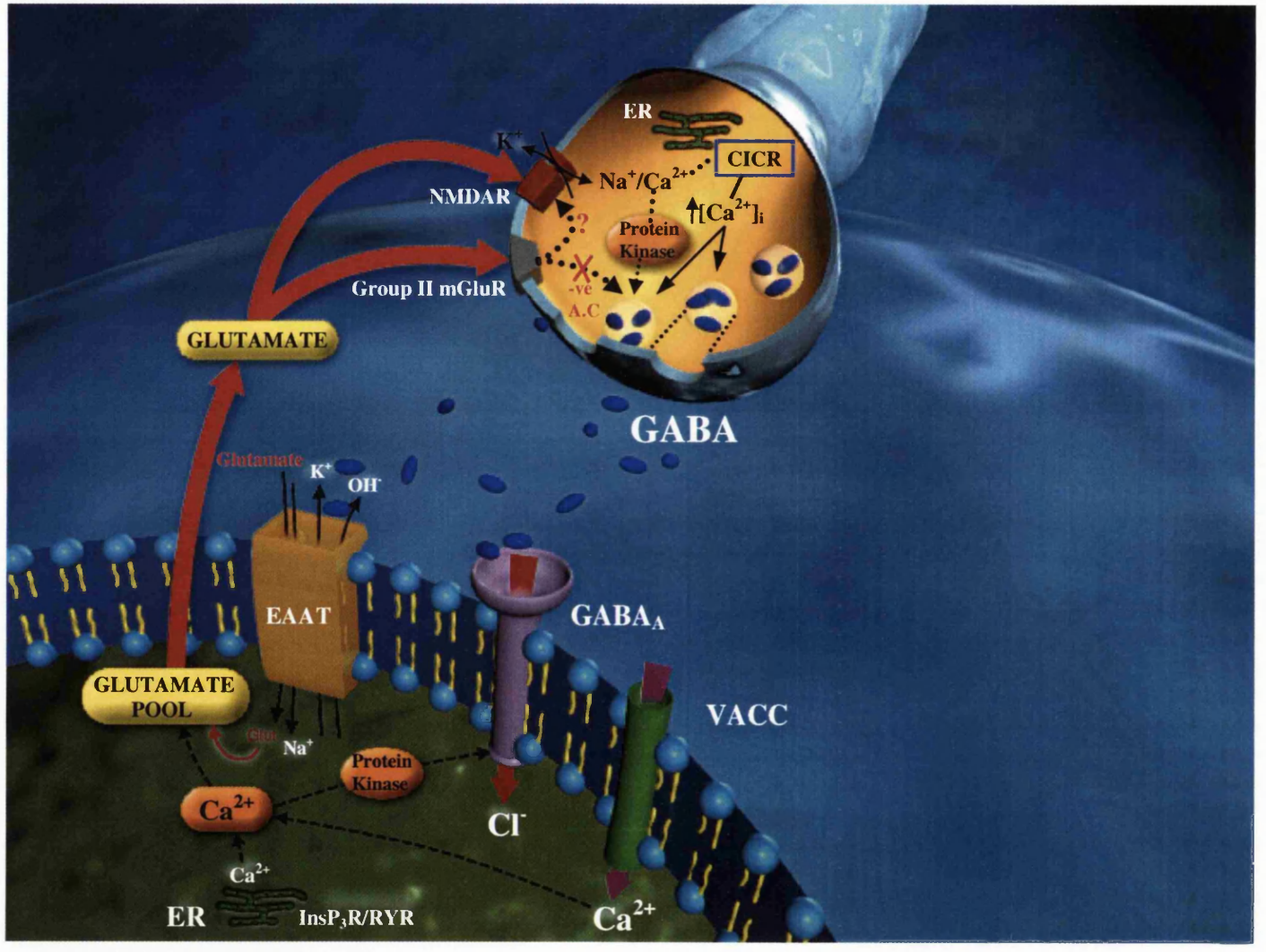

GABA at this time-point does not induce a $GABA_BR$-mediated suppression of RP. As previously mentioned the induction of RP occurs within the first 60s after stimulus cessation and cannot be reversed, over the subsequent 20-40 min RP timecourse, once RP has been established. The increase in the release of GABA does not occur until 60-90s after stimulus cessation thus having no further effect on RP induction but having a significant effect on PN excitability, effectively clamping the cell in a hyperpolarised state. The results in the present study reveal a small aspect of cerebellar synaptic plasticity which provides us with a glimpse of the true depth of the signal transduction cascade(s) and consequent timing involved in the induction of inhibitory synaptic plasticity within the cerebellum.

The prerequisite step in the induction of cerebellar LTD, DSI and RP is a rapid rise in $[Ca^{2+}]_i$ as a result of CF and PF stimulation thus displaying distinct similarities in their induction protocols. Although there are considerable differences between the specific signal transduction cascade(s) involved in the induction of LTD, DSI and RP there is ample evidence to suggest a substantial level of 'crosstalk'. If this is indeed the case then one tentative conclusion to be drawn from this and previous work is the possibility that cerebellar LTD and DSI-RP may occur concurrently. Separation of the two phenomena is simple as one deals with excitatory synaptic plasticity in the absence of any GABAergic input (recording in a Krebs containing bicuculline) while the other deals with inhibitory synaptic plasticity in the absence of any glutamatergic input (containing CNQX/NBQX). In order to observe both phenomena occurring simultaneously, using electrophysiological techniques, both excitatory and inhibitory inputs to the same PN would have to be monitored, which is technically impossible. The advent of new recording techniques coupled with advances in real-time confocal imaging may in the future allow us to examine the simultaneous induction of both excitatory and inhibitory synaptic plasticity within the mammalian CNS.

The cerebellum is unequivocally involved in the learning of a variety of relatively simple reflex behaviours as lesions within this structure will result in an inability to produce specific modifications in certain reflexes. Although lesions to other motor centres may result in complete paralysis or involuntary movements, lesions of the cerebellum produce distinct errors in the planning and execution of movements. The true depth of the plastic ability of the cerebellum lies in the fact that it can compare

internal feedback signals that reflect the *intended* movement with the external feedback signals that reflect the *actual* movement. Once an error has been detected during the information processing stage corrective adjustments are created in the form of feedback and feedforward controls which operate on the descending motor systems of the brain stem and cortex. The cerebellum also plays a predominant role in motor learning. Modulation of the climbing fibre spike patterns occurs during motor learning and this modulation may serve to reduce, by heterosynaptic inhibition, the strength of the mossy fibre input to Purkinje neurones. Early studies by Ito (1984) suggested that information coming into the cerebellum is processed in the deep cerebellar nuclei and that this processing is regulated by the changing levels of Purkinje cell inhibition. Therefore, the plasticity described within this study may in fact underlie one of the fundamental forms of motor learning which acts to decrease the excitability of the PN thus reducing the level of PN inhibition of the downstream deep cerebellar nuclei. The first work describing the effects of lesions to the cerebellum came from Gordon Holmes a physician during the first world war after studying patients who had received gunshot wounds to the cerebellum (Kandel *et al.*, 1991). This early work, although primitive, illustrated the ability of the cerebellum to show plasticity and learned motor activities. A quote from one of his patients, who had suffered a lesion of his right cerebellar hemisphere, underlies the requirement for us to examine and attempt to further understand the information processing pathways which exists in the cerebellum: " *The movements of my left arm are done subconsciously, but I have to think out each movement of the right (affected) arm. I come to a dead stop in turning and have to think before I start again*".

ACKNOWLEDGEMENTS

I would like to express my gratitude to my supervisor, Prof. Trevor G. Smart, for his invaluable guidance throughout the development of my studies in London and especially for his support outwith the School of Pharmacy.

I would like to thank my colleagues in the School of Pharmacy, particularly Dr. Philip Thomas, Dr Alastair Hosie, Dr Emma Dunne, Jonathan Mann & Megan Wilkins for their intellectual input and enjoyable company. I especially would like to thank Miss Helena da Silva for her unending assistance in attaining everything required for the development of my studies.

I am grateful to Dr. Fiona Marshall (Glaxo Wellcome) for her supervision and critical input and also to the BBSRC and Glaxo Wellcome for funding my project.

A large portion of the work achieved in this study would not have been possible without the generous gift of antibodies from Prof. Steve J. Moss (UCL) and the helpful advice of Darran Clements (UCL) and Chris Courtice (School of Pharmacy) in the fields of confocal microscopy and electronics, respectively.

I wish to thank Dr Malcolm Caulfield for introducing me to the world of neuroscience and electrophysiology and to Dr Roderick Scott (Aberdeen University) for his continuous advice throughout the development of my work.

The graphic design work included in this thesis was produced by my good friend Neil Foubister (Oxygenate, Aberdeen, Scotland)

Lastly I would like to thank my parents, Kenneth and Janet, for their devoted assistance throughout my university studies and to Miss Lyndsey McPherson for her support and patience through the long nights of writing.

REFERENCES

Abe, T., Sugihara, H., Nawa, H., Shigemoto, R., Mizuno, N., & Nakanishi, S. (1992). Molecular characterization of a novel metabotropic glutamate receptor mGluR5 coupled to inositol phosphate/Ca^{2+} signal transduction. *J Biol.Chem.* **267**, 13361-13368.

Akazawa, C., Shigemoto, R., Bessho, Y., Nakanishi, S., & Mizuno, N. (1994). Differential expression of five N-methyl-D-aspartate receptor subunit mRNAs in the cerebellum of developing and adult rats. *J Comp Neurol.* **347**, 150-160.

Alaluf, S., Mulvihill, E. R., & McIlhinney, R. A. (1995). Rapid agonist mediated phosphorylation of the metabotropic glutamate receptor 1 alpha by protein kinase C in permanently transfected BHK cells. *FEBS Lett.* **367**, 301-305.

Alford, S., Frenguelli, B. G., Schofield, J. G., & Collingridge, G. L. (1993). Characterization of Ca^{2+} signals induced in hippocampal CA1 neurones by the synaptic activation of NMDA receptors. *J Physiol* **469**, 693-716.

Alger, B. E. (1991). Gating of GABAergic inhibition in hippocampal pyramidal cells. *Ann.N.Y.Acad.Sci.* **627**, 249-263.

Alger, B. E., Pitler, T. A., Wagner, J. J., Martin, L. A., Morishita, W., Kirov, S. A., & Lenz, R. A. (1996). Retrograde signalling in depolarization-induced suppression of inhibition in rat hippocampal CA1 cells. *J Physiol* **496 (Pt 1)**, 197-209.

Altman, J. (1972). Postnatal development of the cerebellar cortex in the rat. II. Phases in the maturation of Purkinje cells and of the molecular layer. *J Comp Neurol.* **145**, 399-463.

Altman, J. & Bayer, S. A. (1978). Prenatal development of the cerebellar system in the rat. I. Cytogenesis and histogenesis of the deep nuclei and the cortex of the cerebellum. *J Comp Neurol.* **179**, 23-48.

Amato, A., Barbour, B., Szatkowski, M., & Attwell, D. (1994). Counter-transport of potassium by the glutamate uptake carrier in glial cells isolated from the tiger salamander retina. *J Physiol* **479 (Pt 3)**, 371-380.

Amin, J. & Weiss, D. S. (1993). $GABA_A$ receptor needs two homologous domains of the β-subunit for activation by GABA but not by pentobarbital [see comments]. *Nature* **366**, 565-569.

Anson, L. C., Chen, P. E., Wyllie, D. J., Colquhoun, D., & Schoepfer, R. (1998). Identification of amino acid residues of the NR2A subunit that control glutamate potency in recombinant NR1/NR2A NMDA receptors. *J.Neurosci.* **18**, 581-589.

Arriza, J. L., Fairman, W. A., Wadiche, J. I., Murdoch, G. H., Kavanaugh, M. P., & Amara, S. G. (1994). Functional comparisons of three glutamate transporter subtypes cloned from human motor cortex. *J Neurosci.* **14**, 5559-5569.

Arvola, M. & Keinanen, K. (1996). Characterization of the ligand-binding domains of glutamate receptor (GluR)-B and GluR-D subunits expressed in Escherichia coli as periplasmic proteins. *J Biol.Chem.* **271**, 15527-15532.

Asztely, F. & Gustafsson, B. (1996). Ionotropic glutamate receptors. Their possible role in the expression of hippocampal synaptic plasticity. *Mol.Neurobiol.* **12**, 1-11.

Attwell, D., Barbour, B., & Szatkowski, M. (1993). Nonvesicular release of neurotransmitter. *Neuron* **11**, 401-407.

Backus, K. H., Arigoni, M., Drescher, U., Scheurer, L., Malherbe, P., Mohler, H., & Benson, J. A. (1993). Stoichiometry of a recombinant $GABA_A$ receptor deduced from mutation-induced rectification. *Neuroreport* **5**, 285-288.

Baetge, E. E., Bulloch, K., & Stallcup, W. B. (1979). A comparison of glutamate transport in cloned cell lines from the central nervous system. *Brain Res.* **167**, 210-214.

Baimbridge, K. G., Miller, J. J., & Parkes, C. O. (1982). Calcium-binding protein distribution in the rat brain. *Brain Res.* **239**, 519-525.

Balazs, R., Jorgensen, O. S., & Hack, N. (1988). N-methyl-D-aspartate promotes the survival of cerebellar granule cells in culture. *Neuroscience* **27**, 437-451.

Balchen, T. & Diemer, N. H. (1992). The AMPA antagonist, NBQX, protects against ischemia-induced loss of cerebellar Purkinje cells. *Neuroreport* **3**, 785-788.

Baptista, C. A., Hatten, M. E., Blazeski, R., & Mason, C. A. (1994). Cell-cell interactions influence survival and differentiation of purified Purkinje cells in vitro. *Neuron* **12**, 243-260.

Barbour, B., Brew, H., & Attwell, D. (1988). Electrogenic glutamate uptake in glial cells is activated by intracellular potassium. *Nature* **335**, 433-435.

Barbour, B., Brew, H., & Attwell, D. (1991). Electrogenic uptake of glutamate and aspartate into glial cells isolated from the salamander (Ambystoma) retina. *J Physiol* **436**, 169-193.

Barbour, B., Keller, B. U., Llano, I., & Marty, A. (1994). Prolonged presence of glutamate during excitatory synaptic transmission to cerebellar Purkinje cells. *Neuron* **12**, 1331-1343.

Barks, J. D. & Silverstein, F. S. (1994). The glutamate uptake inhibitor L-trans-2,4-pyrrolidine dicarboxylate is neurotoxic in neonatal rat brain. *Mol.Chem.Neuropathol.* **23**, 201-215.

Barnard, E. A., Darlison, M. G., & Seeburg, P. (1987). Molecular biology of $GABA_A$ receptor: the receptor/channel superfamily. *TINS* **10**, 502-509.

Baskys, A. & Malenka, R. C. (1991). Agonists at metabotropic glutamate receptors presynaptically inhibit EPSCs in neonatal rat hippocampus. *J.Physiol* **444**, 687-701.

Baude, A., Nusser, Z., Roberts, J. D., Mulvihill, E., McIlhinney, R. A., & Somogyi, P. (1993). The metabotropic glutamate receptor (mGluR1 alpha) is concentrated at perisynaptic membrane of neuronal subpopulations as detected by immunogold reaction. *Neuron* **11**, 771-787.

Bean, B. P. (1989). Classes of calcium channels in vertebrate cells. *Annu.Rev.Physiol* **51**, 367-384.

Beattie, C. E., Kolva, B., & Siegel, R. E. (1995). $GABA_A$ receptor subunit mRNA expression in the weaver cerebellum: modulation by cell-cell interactions. *Brain Res.Dev.Brain Res.* **88**, 171-177.

Behe, P., Stern, P., Wyllie, D. J., Nassar, M., Schoepfer, R., & Colquhoun, D. (1995). Determination of NMDA NR1 subunit copy number in recombinant NMDA receptors. *Proc.R.Soc.Lond B Biol.Sci.* **262**, 205-213.

Bekkers, J. M. & Stevens, C. F. (1989). NMDA and non-NMDA receptors are co-localized at individual excitatory synapses in cultured rat hippocampus. *Nature* **341**, 230-233.

Bekkers, J. M., Richerson, G. B., & Stevens, C. F. (1990). Origin of variability in quantal size in cultured hippocampal neurons and hippocampal slices. *Proc.Natl.Acad.Sci.U.S.A* **87**, 5359-5362.

Benke, D., Mertens, S., Trzeciak, A., Gillessen, D., & Mohler, H. (1991). GABAA receptors display association of gamma 2-subunit with alpha 1- and beta 2/3-subunits. *J Biol.Chem.* **266**, 4478-4483.

Benveniste, H., Drejer, J., Schousboe, A., & Diemer, N. H. (1984). Elevation of the extracellular concentrations of glutamate and aspartate in rat hippocampus during transient cerebral ischemia monitored by intracerebral microdialysis. *J Neurochem* **43**, 1369-1374.

Berretta, N. & Jones, R. S. (1996). Tonic facilitation of glutamate release by presynaptic N-methyl-D- aspartate autoreceptors in the entorhinal cortex. *Neuroscience* **75**, 339-344.

Berridge, M. J. (1996). Inositol trisphosphate and Ca^{2+} in neural signalling. *Coincidence detection in the Nervous System* , 22-31. Strasbourg, HFSP.

Berridge, M. J. (1997). Elementary and global aspects of calcium signalling. *J Physiol* **499 (Pt 2)** , 291-306.

Berry, M. & Bradley, P. (1976). The growth of the dendritic trees of Purkinje cells in the cerebellum of the rat. *Brain Res.* **112**, 1-35.

Berthele, A., Platzer, S., Laurie, D. J., Weis, S., Sommer, B., Zieglgansberger, W., Conrad, B., & Tolle, T. R. (1999). Expression of metabotropic glutamate receptor subtype mRNA (mGluR1-8) in human cerebellum. *Neuroreport* **10**, 3861-3867.

Billups, B. & Attwell, D. (1996). Modulation of non-vesicular glutamate release by pH. *Nature* **379**, 171-174.

Bishop, G. A. (1993). An analysis of HRP-filled basket cell axons in the cat's cerebellum. I. Morphometry and configuration. *Anat.Embryol.(Berl)* **188**, 287-297.

Blahos, J. & Wenthold, R. J. (1996). Relationship between N-methyl-D-aspartate receptor NR1 splice variants and NR2 subunits. *J.Biol.Chem.* **271**, 15669-15674.

Bliss, T. V. & Collingridge, G. L. (1993). A synaptic model of memory: long-term potentiation in the hippocampus. *Nature* **361**, 31-39.

Bliss, T. V. P. & Lynch, M. A. (1988). Long-term potentiation of synaptic transmission in the hippocampus: properties and mechanisms. In: *Long-term potentiation: From biophysics to behaviour.* 3-72. New York, Liss.

Blond, O., Daniel, H., Otani, S., Jaillard, D., & Crepel, F. (1997). Presynaptic and postsynaptic effects of nitric oxide donors at synapses between parallel fibres and Purkinje cells: involvement in cerebellar long-term depression. *Neuroscience* **77**, 945-954.

Bockaert, J., Pin, J., & Fagni, L. (1993). Metabotropic glutamate receptors: an original family of G protein- coupled receptors. *Fundam.Clin.Pharmacol.* **7**, 473-485.

Bohme, G. A., Bon, C., Stutzmann, J. M., Doble, A., & Blanchard, J. C. (1991). Possible involvement of nitric oxide in long-term potentiation. *Eur.J.Pharmacol.* **199**, 379-381.

Bolshakov, V. Y., Golan, H., Kandel, E. R., & Siegelbaum, S. A. (1997). Recruitment of new sites of synaptic transmission during the cAMP- dependent late phase of LTP at CA3-CA1 synapses in the hippocampus. *Neuron* **19**, 635-651.

Bonnert, T. P., McKernan, R. M., Farrar, S., Le Bourdelles, B., Heavens, R. P., Smith, D. W., Hewson, L., Rigby, M. R., Sirinathsinghji, D. J., Brown, N., Wafford, K. A., &

Whiting, P. J. (1999). θ, a novel γ-aminobutyric acid type A receptor subunit. *Proc.Natl.Acad.Sci.U.S.A* **96**, 9891-9896.

Bormann, J., Hamill, O. P., & Sakmann, B. (1987). Mechanism of anion permeation through channels gated by glycine and gamma-aminobutyric acid in mouse cultured spinal neurones. *J Physiol* **385**, 243-286.

Bouron, A. & Reuter, H. (1999). The D1 dopamine receptor agonist SKF-38393 stimulates the release of glutamate in the hippocampus. *Neuroscience* **94**, 1063-1070.

Bouron, A. (2001). Modulation of spontaneous quantal release of neurotransmitters in the hippocampus. *Prog.Neurobiol.* **63**, 613-635.

Bouvier, M., Szatkowski, M., Amato, A., & Attwell, D. (1992). The glial cell glutamate uptake carrier countertransports pH-changing anions. *Nature* **360**, 471-474.

Boxall, A. R. & Marty, A. (1997). A critical time-window for the potentiation of synaptic GABA responses in rat cerebellar Purkinje cells. *Society for Neuroscience abstract* **23**, 2006.

Boxall, A. R. (2000). GABAergic mIPSCs in rat cerebellar Purkinje cells are modulated by TrkB and mGluR1-mediated stimulation of Src. *J Physiol* **524 Pt 3**, 677-684.

Bradley, S. R., Levey, A. I., Hersch, S. M., & Conn, P. J. (1996). Immunocytochemical localization of group III metabotropic glutamate receptors in the hippocampus with subtype-specific antibodies. *J.Neurosci.* **16**, 2044-2056.

Brakeman, P. R., Lanahan, A. A., O'Brien, R., Roche, K., Barnes, C. A., Huganir, R. L., & Worley, P. F. (1997). Homer: a protein that selectively binds metabotropic glutamate receptors. *Nature* **386**, 284-288.

Brandon, E. P., Zhuo, M., Huang, Y. Y., Qi, M., Gerhold, K. A., Burton, K. A., Kandel, E. R., McKnight, G. S., & Idzerda, R. L. (1995). Hippocampal long-term depression and depotentiation are defective in mice carrying a targeted disruption of the gene encoding the RI beta subunit of cAMP-dependent protein kinase. *Proc.Natl.Acad.Sci.U.S.A* **92**, 8851-8855.

Bredt, D. S., Hwang, P. M., & Snyder, S. H. (1990). Localization of nitric oxide synthase indicating a neural role for nitric oxide. *Nature* **347**, 768-770.

Brose, N., Gasic, G. P., Vetter, D. E., Sullivan, J. M., & Heinemann, S. F. (1993). Protein chemical characterization and immunocytochemical localization of the NMDA receptor subunit NMDA R1. *J.Biol.Chem.* **268**, 22663-22671.

Bueno, O. F., Robinson, L. C., Alvarez-Hernandez, X., & Leidenheimer, N. J. (1998). Functional characterization and visualization of a GABAA receptor-GFP chimera expressed in Xenopus oocytes. *Brain Res.Mol.Brain Res.* **59**, 165-177.

Burckhardt, G., Kinne, R., Stange, G., & Murer, H. (1980). The effects of potassium and membrane potential on sodium-dependent glutamic acid uptake. *Biochim.Biophys.Acta* **599**, 191-201.

Bureau, I. & Mulle, C. (1998). Potentiation of GABAergic synaptic transmission by AMPA receptors in mouse cerebellar stellate cells: changes during development. *J Physiol* **509 (Pt 3)**, 817-831.

Bureau, M. H. & Olsen, R. W. (1993). $GABA_A$ receptor subtypes: ligand binding heterogeneity demonstrated by photoaffinity labeling and autoradiography. *J Neurochem* **61**, 1479-1491.

Burger, P. M., Mehl, E., Cameron, P. L., Maycox, P. R., Baumert, M., Lottspeich, F., De Camilli, P., & Jahn, R. (1989). Synaptic vesicles immunoisolated from rat cerebral cortex contain high levels of glutamate. *Neuron* **3**, 715-720.

Burgoyne, R. D., Graham, M. E., & Cambray-Deakin, M. (1993). Neurotrophic effects of NMDA receptor activation on developing cerebellar granule cells. *J Neurocytol.* **22**, 689-695.

Burnashev, N., Monyer, H., Seeburg, P. H., & Sakmann, B. (1992). Divalent ion permeability of AMPA receptor channels is dominated by the edited form of a single subunit. *Neuron* **8** , 189-198.

Burnashev, N., Zhou, Z., Neher, E., & Sakmann, B. (1995). Fractional calcium currents through recombinant GluR channels of the NMDA, AMPA and kainate receptor subtypes. *J.Physiol* **485 (Pt 2)**, 403-418.

Burt, D. R. & Kamatchi, G. L. (1991). $GABA_A$ receptor subtypes: From pharmacology to molecular biology. *FASEB Journal* **5**, 2916-2923.

Bushell, T. J., Jane, D. E., Tse, H. W., Watkins, J. C., Garthwaite, J., & Collingridge, G. L. (1996). Pharmacological antagonism of the actions of group II and III mGluR agonists in the lateral perforant path of rat hippocampal slices. *Br.J.Pharmacol.* **117**, 1457-1462.

Caillard, O., Ben Ari, Y., & Gaiarsa, J. L. (1999). Long-term potentiation of GABAergic synaptic transmission in neonatal rat hippocampus. *J Physiol* **518 (Pt 1)**, 109-119.

Caillard, O., Ben Ari, Y., & Gaiarsa, J. L. (2000). Activation of Presynaptic and Postsynaptic Ryanodine-Sensitive Calcium Stores Is Required for the Induction of Long-

Term Depression at GABAergic Synapses in the Neonatal Rat Hippocampus Amphetamine. *J Neurosci.* **20**, RC94.

Calton, J. L., Kang, M. H., Wilson, W. A., & Moore, S. D. (2000). NMDA-Receptor-dependent synaptic activation of voltage-dependent calcium channels in basolateral amygdala. *J Neurophysiol.* **83**, 685-692.

Capogna, M., Gahwiler, B. H., & Thompson, S. M. (1995). Presynaptic enhancement of inhibitory synaptic transmission by protein kinases A and C in the rat hippocampus in vitro. *J Neurosci.* **15**, 1249-1260.

Carter, A. G. & Regehr, W. G. (2000). Prolonged synaptic currents and glutamate spillover at the parallel fiber to stellate cell synapse. *J Neurosci.* **20**, 4423-4434.

Cartmell, J. & Schoepp, D. D. (2000). Regulation of neurotransmitter release by metabotropic glutamate receptors. *J Neurochem.* **75**, 889-907.

Casado, M., Dieudonne, S., & Ascher, P. (2000). Presynaptic N-methyl-D-aspartate receptors at the parallel fiber- Purkinje cell synapse. *Proc.Natl.Acad.Sci.U.S.A* **97**, 11593-11597.

Catterall, W. A. (1998). Structure and function of neuronal Ca^{2+} channels and their role in neurotransmitter release. *Cell Calcium* **24**, 307-323.

Celio, M. R. (1990). Calbindin D-28k and parvalbumin in the rat nervous system. *Neuroscience* **35**, 375-475.

Chang, Y., Wang, R., Barot, S., & Weiss, D. S. (1996). Stoichiometry of a recombinant $GABA_A$ receptor. *Journal of Neuroscience* **16**, 5415-5424.

Chapell, R., Bueno, O. F., Alvarez-Hernandez, X., Robinson, L. C., & Leidenheimer, N. J. (1998). Activation of protein kinase C induces gamma-aminobutyric acid type A receptor internalization in Xenopus oocytes. *J Biol.Chem.* **273**, 32595-32601.

Chaudhry, F. A., Lehre, K. P., van Lookeren, C. M., Ottersen, O. P., Danbolt, N. C., & Storm-Mathisen, J. (1995). Glutamate transporters in glial plasma membranes: highly differentiated localizations revealed by quantitative ultrastructural immunocytochemistry. *Neuron* **15**, 711-720.

Chavis, P., Mollard, P., Bockaert, J., & Manzoni, O. (1998). Visualization of cyclic AMP-regulated presynaptic activity at cerebellar granule cells. *Neuron* **20**, 773-781.

Chazot, P. L. & Stephenson, F. A. (1997). Molecular dissection of native mammalian forebrain NMDA receptors containing the NR1 C2 exon: direct demonstration of NMDA

receptors comprising NR1, NR2A, and NR2B subunits within the same complex. *J.Neurochem.* **69**, 2138-2144.

Chen, C. & Regehr, W. G. (1997). The mechanism of cAMP-mediated enhancement at a cerebellar synapse. *J Neurosci.* **17**, 8687-8694.

Chen, L. & Huang, L. Y. (1992). Protein kinase C reduces Mg^{2+} block of NMDA-receptor channels as a mechanism of modulation. *Nature* **356**, 521-523.

Chen, W. R., Xiong, W., & Shepherd, G. M. (2000). Analysis of relations between NMDA receptors and GABA release at olfactory bulb reciprocal synapses. *Neuron* **25**, 625-633.

Cheung, W. T., Richards, D. E., & Rogers, J. H. (1993). Calcium binding by chick calretinin and rat calbindin D_{28k} synthesised in bacteria. *Eur.J.Biochem.* **215**, 401-410.

Choi, D. W., Maulucci-Gedde, M., & Kriegstein, A. R. (1987). Glutamate neurotoxicity in cortical cell culture. *J.Neurosci.* **7**, 357-368.

Ciruela, F., Soloviev, M. M., & McIlhinney, R. A. (1999). Co-expression of metabotropic glutamate receptor type 1alpha with homer- 1a/Vesl-1S increases the cell surface expression of the receptor. *Biochem.J.* **341 (Pt 3)**, 795-803.

Cochilla, A. J. & Alford, S. (1999). NMDA receptor-mediated control of presynaptic calcium and neurotransmitter release. *J Neurosci.* **19**, 193-205.

Coco, S., Verderio, C., Trotti, D., Rothstein, J. D., Volterra, A., & Matteoli, M. (1997). Non-synaptic localization of the glutamate transporter EAAC1 in cultured hippocampal neurons. *Eur.J.Neurosci.* **9**, 1902-1910.

Conn, P. J. & Pin, J. P. (1997). Pharmacology and functions of metabotropic glutamate receptors. *Annu.Rev.Pharmacol.Toxicol.* **37**, 205-237.

Connolly, C. N., Wooltorton, J. R., Smart, T. G., & Moss, S. J. (1996). Subcellular localization of gamma-aminobutyric acid type A receptors is determined by receptor beta subunits. *Proc.Natl.Acad.Sci.U.S.A* **93**, 9899-9904.

Connolly, C. N., Kittler, J. T., Thomas, P., Uren, J. M., Brandon, N. J., Smart, T. G., & Moss, S. J. (1999). Cell surface stability of γ-aminobutyric acid type A receptors. Dependence on protein kinase C activity and subunit composition. *J.Biol.Chem.* **274**, 36565-36572.

Crepel, F. (1974). Excitatory and inhibitory processes acting upon cerebellar Purkinje cells during maturation in the rat; influence of hypothyroidism. *Exp.Brain Res.* **20**, 403-420.

Crepel, F. & Krupa, M. (1988). Activation of protein kinase C induces a long-term depression of glutamate sensitivity of cerebellar Purkinje cells. An in vitro study. *Brain Res.* **458**, 397-401.

Crepel, F., Audinat, E., Daniel, H., Hemart, N., Jaillard, D., Rossier, J., & Lambolez, B. (1994). Cellular locus of the nitric oxide-synthase involved in cerebellar long- term depression induced by high external potassium concentration. *Neuropharmacology* **33** , 1399-1405.

Dan, Y. & Poo, M. M. (1994). Calcium-dependent postsynaptic exocytosis: a possible mechanism for activity-dependent synaptic modulation. *J.Neurobiol.* **25**, 336-341.

Danbolt, N. C., Storm-Mathisen, J., & Kanner, B. I. (1992). An [Na^+ + K^+]coupled L-glutamate transporter purified from rat brain is located in glial cell processes. *Neuroscience* **51**, 295-310.

Daniel, H., Levenes, C., & Crepel, F. (1998). Cellular mechanisms of cerebellar LTD. *Trends Neurosci.* **21**, 401-407.

Davies, P. A., Hanna, M. C., Hales, T. G., & Kirkness, E. F. (1997). Insensitivity to anaesthetic agents conferred by a class of $GABA_A$ receptor subunit. *Nature* **385**, 820-823.

De Schutter, E. & Bower, J. M. (1994). An active membrane model of the cerebellar Purkinje cell. I. Simulation of current clamps in slice. *J Neurophysiol.* **71**, 375-400.

De Talamoni, N., Smith, C. A., Wasserman, R. H., Beltramino, C., Fullmer, C. S., & Penniston, J. T. (1993). Immunocytochemical localization of the plasma membrane calcium pump, calbindin-D_{28k}, and parvalbumin in Purkinje cells of avian and mammalian cerebellum. *Proc.Natl.Acad.Sci.U.S.A* **90**, 11949-11953.

DeBiasi, S., Minelli, A., Melone, M., & Conti, F. (1996). Presynaptic NMDA receptors in the neocortex are both. *Neuroreport* **7**, 2773-2776.

Dehnes, Y., Chaudhry, F. A., Ullensvang, K., Lehre, K. P., Storm-Mathisen, J., & Danbolt, N. C. (1998). The glutamate transporter EAAT4 in rat cerebellar Purkinje cells: a glutamate-gated chloride channel concentrated near the synapse in parts of the dendritic membrane facing astroglia. *J Neurosci.* **18**, 3606-3619.

Dingledine, R., Borges, K., Bowie, D., & Traynelis, S. F. (1999). The glutamate receptor ion channels. *Pharmacol.Rev.* **51**, 7-61.

Doyle, D. A., Morais, C. J., Pfuetzner, R. A., Kuo, A., Gulbis, J. M., Cohen, S. L., Chait, B. T., & MacKinnon, R. (1998). The structure of the potassium channel: molecular basis of K^+ conduction and selectivity. *Science* **280**, 69-77.

Draguhn, A., Verdoorn, T. A., Ewert, M., Seeburg, P. H., & Sakmann, B. (1990). Functional and molecular distinction between recombinant rat $GABA_A$ receptor subtypes by Zn^{2+}. *Neuron* **5**, 781-788.

Dumuis, A., Sebben, M., Haynes, L., Pin, J. P., & Bockaert, J. (1988). NMDA receptors activate the arachidonic acid cascade system in striatal neurons. *Nature* **336**, 68-70.

Dunah, A. W., Luo, J., Wang, Y. H., Yasuda, R. P., & Wolfe, B. B. (1998). Subunit composition of N-methyl-D-aspartate receptors in the central nervous system that contain the NR2D subunit. *Mol.Pharmacol.* **53**, 429-437.

Duvoisin, R. M., Zhang, C., & Ramonell, K. (1995). A novel metabotropic glutamate receptor expressed in the retina and olfactory bulb. *J.Neurosci.* **15**, 3075-3083.

Dzubay, J. A. & Jahr, C. E. (1996). Kinetics of NMDA channel opening. *J.Neurosci.* **16**, 4129-4134.

Eilers, J., Augustine, G. J., & Konnerth, A. (1995). Subthreshold synaptic Ca^{2+} signalling in fine dendrites and spines of cerebellar Purkinje neurons. *Nature* **373**, 155-158.

Ekerot, C. F. & Oscarsson, O. (1981). Prolonged depolarization elicited in Purkinje cell dendrites by climbing fibre impulses in the cat. *J.Physiol* **318**, 207-221.

Ekerot, C. F. & Kano, M. (1985). Long-term depression of parallel fibre synapses following stimulation of climbing fibres. *Brain Res.* **342**, 357-360.

Ellisman, M. H., Deerinck, T. J., Ouyang, Y., Beck, C. F., Tanksley, S. J., Walton, P. D., Airey, J. A., & Sutko, J. L. (1990). Identification and localization of ryanodine binding proteins in the avian central nervous system. *Neuron* **5**, 135-146.

Emptage, N. J., Reid, C. A., & Fine, A. (2001). Calcium stores in hippocampal synaptic boutons mediate short-term plasticity, store-operated Ca^{2+} entry, and spontaneous transmitter release. *Neuron* **29**, 197-208.

England, M. A. & Wakely, J. (1991). A colour atlas of the brain & spinal cord. **1st Edition**. 168-168. England, Wolfe Publishing Ltd.

Erecinska, M., Wantorsky, D., & Wilson, D. F. (1983). Aspartate transport in synaptosomes from rat brain. *J Biol.Chem.* **258**, 9069-9077.

Farrant, M. & Cull-Candy, S. G. (1991). Excitatory amino acid receptor-channels in Purkinje cells in thin cerebellar slices. *Proc.R.Soc.Lond B Biol.Sci.* **244**, 179-184.

Faull, R. L., Villiger, J. W., & Holford, N. H. (1987). Benzodiazepine receptors in the human cerebellar cortex: a quantitative autoradiographic and pharmacological study demonstrating the predominance of type I receptors. *Brain Res.* **411**, 379-385.

Felder, C. C., Joyce, K. E., Briley, E. M., Mansouri, J., Mackie, K., Blond, O., Lai, Y., Ma, A. L., & Mitchell, R. L. (1995). Comparison of the pharmacology and signal transduction of the human cannabinoid CB1 and CB2 receptors. *Mol.Pharmacol.* **48**, 443-450.

Ferrer-Montiel, A. V. & Montal, M. (1996). Pentameric subunit stoichiometry of a neuronal glutamate receptor. *Proc.Natl.Acad.Sci.U.S.A* **93**, 2741-2744.

Fierro, L. & Llano, I. (1996). High endogenous calcium buffering in Purkinje cells from rat cerebellar slices. *J Physiol* **496 (Pt 3)**, 617-625.

Fierro, L., DiPolo, R., & Llano, I. (1998). Intracellular calcium clearance in Purkinje cell somata from rat cerebellar slices. *J.Physiol* **510 (Pt 2)**, 499-512.

Finch, E. A. & Augustine, G. J. (1998). Local calcium signalling by inositol-1,4,5-trisphosphate in Purkinje cell dendrites. *Nature* **396**, 753-756.

Fitzjohn, S. M., Bortolotto, Z. A., Palmer, M. J., Doherty, A. J., Ornstein, P. L., Schoepp, D. D., Kingston, A. E., Lodge, D., & Collingridge, G. L. (1998). The potent mGlu receptor antagonist LY341495 identifies roles for both cloned and novel mGlu receptors in hippocampal synaptic plasticity. *Neuropharmacology* **37**, 1445-1458.

Fitzsimonds, R. M. & Dichter, M. A. (1996). Heterologous modulation of inhibitory synaptic transmission by metabotropic glutamate receptors in cultured hippocampal neurons. *J Neurophysiol.* **75**, 885-893.

Forti, L., Bossi, M., Bergamaschi, A., Villa, A., & Malgaroli, A. (1997). Loose-patch recordings of single quanta at individual hippocampal synapses. *Nature* **388**, 874-878.

Forti, L., Pouzat, C., & Llano, I. (2000). Action potential-evoked Ca^{2+} signals and calcium channels in axons of developing rat cerebellar interneurones. *J Physiol* **527 Pt 1**, 33-48.

Fotuhi, M., Sharp, A. H., Glatt, C. E., Hwang, P. M., von Krosigk, M., Snyder, S. H., & Dawson, T. M. (1993). Differential localization of phosphoinositide-linked metabotropic glutamate receptor (mGluR1) and the inositol 1,4,5-trisphosphate receptor in rat brain. *J.Neurosci.* **13**, 2001-2012.

Frerking, M., Petersen, C. C., & Nicoll, R. A. (1999). Mechanisms underlying kainate receptor-mediated disinhibition in the hippocampus. *Proc.Natl.Acad.Sci.U.S.A* **96**, 12917-12922.

Frey, U., Huang, Y. Y., & Kandel, E. R. (1993). Effects of cAMP simulate a late stage of LTP in hippocampal CA1 neurons. *Science* **260**, 1661-1664.

Fritschy, J. M., Benke, D., Mertens, S., Oertel, W. H., Bachi, T., & Mohler, H. (1992). Five subtypes of type A gamma-aminobutyric acid receptors identified in neurons by double and triple immunofluorescence staining with subunit- specific antibodies. *Proc.Natl.Acad.Sci.U.S.A* **89**, 6726-6730.

Frostholm, A., Zdilar, D., Chang, A., & Rotter, A. (1991). Stability of $GABA_A$/benzodiazepine receptor alpha 1 subunit mRNA expression in *reeler* mouse cerebellar Purkinje cells during postnatal development. *Brain Res.Dev.Brain Res.* **64**, 121-128.

Furuta, A., Martin, L. J., Lin, C. L., Dykes-Hoberg, M., & Rothstein, J. D. (1997). Cellular and synaptic localization of the neuronal glutamate transporters excitatory amino acid transporter 3 and 4. *Neuroscience* **81**, 1031-1042.

Gabellini, N., Manev, R. M., Candeo, P., Favaron, M., & Manev, H. (1993). Carboxyl domain of glutamate receptor directs its coupling to metabolic pathways. *Neuroreport* **4**, 531-534.

Gao, W. Q., Zheng, J. L., & Karihaloo, M. (1995). Neurotrophin-4/5 (NT-4/5) and brain-derived neurotrophic factor (BDNF) act at later stages of cerebellar granule cell differentiation. *J Neurosci.* **15**, 2656-2667.

Gereau, R. W. & Conn, P. J. (1995). Multiple presynaptic metabotropic glutamate receptors modulate excitatory and inhibitory synaptic transmission in hippocampal area CA1. *J.Neurosci.* **15**, 6879-6889.

German, D. C., Ng, M. C., Liang, C. L., McMahon, A., & Iacopino, A. M. (1997). Calbindin-D_{28k} in nerve cell nuclei. *Neuroscience* **81**, 735-743.

Ginsborg, B. L. & Jenkinson, D. N. (1976). Transmission of impulses from nerve to muscle. *Handbook of experimental pharmacology* , 229-364. Berlin, Springer-Verly.

Glaum, S. R. & Miller, R. J. (1993). Activation of metabotropic glutamate receptors produces reciprocal regulation of ionotropic glutamate and GABA responses in the nucleus of the tractus solitarius of the rat. *J.Neurosci.* **13**, 1636-1641.

Glitsch, M., Llano, I., & Marty, A. (1996). Glutamate as a candidate retrograde messenger at interneurone-Purkinje cell synapses of rat cerebellum. *J Physiol* **497 (Pt 2)**, 531-537.

Glitsch, M. & Marty, A. (1999). Presynaptic effects of NMDA in cerebellar Purkinje cells and interneurons. *J.Neurosci.* **19**, 511-519.

Glitsch, M., Parra, P., & Llano, I. (2000). The retrograde inhibition of IPSCs in rat cerebellar purkinje cells is highly sensitive to intracellular Ca^{2+}. *Eur.J.Neurosci.* **12**, 987-993.

Gomeza, J., Joly, C., Kuhn, R., Knopfel, T., Bockaert, J., & Pin, J. P. (1996). The second intracellular loop of metabotropic glutamate receptor 1 cooperates with the other intracellular domains to control coupling to G-proteins. *J.Biol.Chem.* **271**, 2199-2205.

Gutierrez, A., Khan, Z. U., & De Blas, A. L. (1994). Immunocytochemical localization of gamma 2 short and gamma 2 long subunits of the $GABA_A$ receptor in the rat brain. *J Neurosci.* **14**, 7168-7179.

Haak, L. L. (1999). Metabotropic glutamate receptor modulation of glutamate responses in the suprachiasmatic nucleus. *J Neurophysiol.* **81**, 1308-1317.

Hafidi, A. & Hillman, D. E. (1997). Distribution of glutamate receptors GluR 2/3 and NR1 in the developing rat cerebellum. *Neuroscience* **81**, 427-436.

Haines, D. E. (1997). Fundamental Neuroscience. **1st Edition**. Edinburgh, Churchill Livingstone.

Hamilton, S. L., Serysheva, I., & Strasburg, G. M. (2000). Calmodulin and excitation-contraction coupling. *News in physiological sciences* **15**, 281-284.

Hampson, D. R., Theriault, E., Huang, X. P., Kristensen, P., Pickering, D. S., Franck, J. E., & Mulvihill, E. R. (1994). Characterization of two alternatively spliced forms of a metabotropic glutamate receptor in the central nervous system of the rat. *Neuroscience* **60**, 325-336.

Harrison, N. L. & Lambert, N. A. (1989). Modification of $GABA_A$ receptor function by an analog of cyclic AMP. *Neurosci.Lett.* **105**, 137-142.

Hartell, N. A. (2001). Receptors, second messengers and protein kinases required for heterosynaptic cerebellar long-term depression. *Neuropharmacology* **40**, 148-161.

Hashimoto, T., Ishii, T., & Ohmori, H. (1996). Release of Ca^{2+} is the crucial step for the potentiation of IPSCs in the cultured cerebellar Purkinje cells of the rat. *J Physiol* **497 (Pt 3)**, 611-627.

Hayashi, Y., Momiyama, A., Takahashi, T., Ohishi, H., Ogawa-Meguro, R., Shigemoto, R., Mizuno, N., & Nakanishi, S. (1993). Role of a metabotropic glutamate receptor in synaptic modulation in the accessory olfactory bulb. *Nature* **366**, 687-690.

Hedblom, E. & Kirkness, E. F. (1997). A novel class of $GABA_A$ receptor subunit in tissues of the reproductive system. *Journal of Biological Chemistry* **272**, 15346-15350.

Hendelman, W. J. & Aggerwal, A. S. (1980). The Purkinje neuron: I. A Golgi study of its development in the mouse and in culture. *J Comp Neurol.* **193**, 1063-1079.

Heuschneider, G. & Schwartz, R. D. (1989). cAMP and forskolin decrease gamma-aminobutyric acid-gated chloride flux in rat brain synaptoneurosomes. *Proc.Natl.Acad.Sci.U.S.A* **86**, 2938-2942.

Hidaka, H., Tanaka, T., Onoda, K., Hagiwara, M., Watanabe, M., Ohta, H., Ito, Y., Tsurudome, M., & Yoshida, T. (1988). Cell type-specific expression of protein kinase C isozymes in the rabbit cerebellum. *J Biol.Chem.* **263**, 4523-4526.

Hille, B. (1992). Ion channels of excitable membranes. **2nd edition**. Sunderland, MA, USA. Sinauer Associates, Inc.

Hirai, H., Kirsch, J., Laube, B., Betz, H., & Kuhse, J. (1996). The glycine binding site of the N-methyl-D-aspartate receptor subunit NR1: identification of novel determinants of co-agonist potentiation in the extracellular M3-M4 loop region. *Proc.Natl.Acad.Sci.U.S.A* **93**, 6031-6036.

Hirai, H. & Launey, T. (2000). The regulatory connection between the activity of granule cell NMDA receptors and dendritic differentiation of cerebellar Purkinje cells. *J Neurosci.* **20**, 5217-5224.

Hirai, H. (2001). Modification of AMPA receptor clustering regulates cerebellar synaptic plasticity. *Neurosci.Res.* **39**, 261-267

Hofmann, K., Duker, M., Fink, T., Lichter, P., & Stoffel, W. (1994). Human neutral amino acid transporter ASCT1: structure of the gene (SLC1A4) and localization to chromosome 2p13-p15. *Genomics* **24**, 20-26.

Huang, Y. Y., Li, X. C., & Kandel, E. R. (1994). cAMP contributes to mossy fiber LTP by initiating both a covalently mediated early phase and macromolecular synthesis-dependent late phase. *Cell* **79**, 69-79.

Huettner, J. E. & Bean, B. P. (1988). Block of N-methyl-D-aspartate-activated current by the anticonvulsant MK-801: selective binding to open channels. *Proc.Natl.Acad.Sci.U.S.A* **85**, 1307-1311.

Iino, M., Ozawa, S., & Tsuzuki, K. (1990). Permeation of calcium through excitatory amino acid receptor channels in cultured rat hippocampal neurones. *J Physiol* **424**, 151-165.

Isaacson, J. S. & Nicoll, R. A. (1993). The uptake inhibitor L-trans-PDC enhances responses to glutamate but fails to alter the kinetics of excitatory synaptic currents in the hippocampus. *J.Neurophysiol.* **70**, 2187-2191.

Ishida, M., Saitoh, T., Shimamoto, K., Ohfune, Y., & Shinozaki, H. (1993). A novel metabotropic glutamate receptor agonist: marked depression of monosynaptic excitation in the newborn rat isolated spinal cord. *Br.J.Pharmacol.* **109**, 1169-1177.

Ito, M. (1984). The cerebellum and neural control. New York, Raven Press.

Ito, M., Sakurai, M., & Tongroach, P. (1982). Climbing fibre induced depression of both mossy fibre responsiveness and glutamate sensitivity of cerebellar Purkinje cells. *J Physiol* **324**, 113-134.

Jahr, C. E. (1992). High probability opening of NMDA receptor channels by L-glutamate. *Science* **255** , 470-472.

Jahr, C. E. & Stevens, C. F. (1990). Voltage dependence of NMDA-activated macroscopic conductances predicted by single-channel kinetics. *J.Neurosci.* **10**, 3178-3182.

Jahr, C. E. & Stevens, C. F. (1990). A quantitative description of NMDA receptor-channel kinetic behavior. *J Neurosci.* **10**, 1830-1837.

Janaky, R., Varga, V., Saransaari, P., & Oja, S. S. (1994). Glutamate agonists and [^{3}H]GABA release from rat hippocampal slices: involvement of metabotropic glutamate receptors in the quisqualate- evoked release. *Neurochem Res.* **19**, 729-734.

Jarolimek, W. & Misgeld, U. (1997). $GABA_B$ receptor-mediated inhibition of tetrodotoxin-resistant GABA release in rodent hippocampal CA1 pyramidal cells. *J Neurosci.* **17**, 1025-1032.

Johnson, J. W. & Ascher, P. (1987). Glycine potentiates the NMDA response in cultured mouse brain neurons. *Nature* **325**, 529-531.

Johnson, M. P., Chamberlain, M., & Kelly, G. M. (1999). Phosphoinositide hydrolysis in vivo with group I metabotropic glutamate receptor agonists. *Brain Res.* **821**, 539-545.

Johnston, D. & Wu, S. M. S. (1995). Foundations of Cellular Neurophysiology. Cambridge, MA, USA, MIT.

Jouvenceau, A., Dutar, P., & Billard, J. M. (1995). Presynaptic depression of inhibitory postsynaptic potentials by metabotropic glutamate receptors in rat hippocampal CA1 pyramidal cells. *Eur.J Pharmacol.* **281**, 131-139.

Kanai, Y. & Hediger, M. A. (1992). Primary structure and functional characterization of a high-affinity glutamate transporter. *Nature* **360**, 467-471.

Kanai, Y., Nussberger, S., Romero, M. F., Boron, W. F., Hebert, S. C., & Hediger, M. A. (1995). Electrogenic properties of the epithelial and neuronal high affinity glutamate transporter. *J Biol.Chem.* **270**, 16561-16568.

Kandel, E. R., Schwartz, J. H., & Jessell, T. M. (1991). Principles of neural science. **3rd edition**, 98-100.

Kanner, B. I. (1993). Glutamate transporters from brain. A novel neurotransmitter transporter family. *FEBS Lett.* **325**, 95-99.

Kanner, B. I. & Sharon, I. (1978). Active transport of L-glutamate by membrane vesicles isolated from rat brain. *Biochemistry* **17**, 3949-3953.

Kanner, B. I. & Schuldiner, S. (1987). Mechanism of transport and storage of neurotransmitters. *CRC Crit Rev.Biochem.* **22**, 1-38.

Kano, M. & Konnerth, A. (1992). Potentiation of GABA-mediated currents by cAMP-dependent protein kinase. *Neuroreport* **3**, 563-566.

Kano, M., Rexhausen, U., Dreessen, J., & Konnerth, A. (1992). Synaptic excitation produces a long-lasting rebound potentiation of inhibitory synaptic signals in cerebellar Purkinje cells. *Nature* **356**, 601-604.

Kano, M., Garaschuk, O., Verkhratsky, A., & Konnerth, A. (1995). Ryanodine receptor-mediated intracellular calcium release in rat cerebellar Purkinje neurones. *J Physiol* **487 (Pt 1)**, 1-16.

Kano, M., Kano, M., Fukunaga, K., & Konnerth, A. (1996). Ca^{2+}-induced rebound potentiation of gamma-aminobutyric acid-mediated currents requires activation of Ca^{2+}/calmodulin-dependent kinase II. *Proc.Natl.Acad.Sci.U.S.A* **93**, 13351-13356.

Katsumori, H., Baldwin, R. A., & Wasterlain, C. G. (1999). Reverse transport of glutamate during depolarization in immature hippocampal slices. *Brain Res.* **819**, 160-164.

Katz, B. (1969). The release of Neural Transmitter substances. Liverpool, Liverpool University Press.

Kawaguchi, S. & Hirano, T. (2000). Suppression of inhibitory synaptic potentiation by presynaptic activity through postsynaptic GABA(B) receptors in a Purkinje neuron. *Neuron* **27**, 339-347.

Kellenberger, S., Malherbe, P., & Sigel, E. (1992). Function of the α1 β2 γ2S γ-aminobutyric acid type A receptor is modulated by protein kinase C via multiple phosphorylation sites. *J.Biol.Chem.* **267**, 25660-25663.

Kemp, J. A., Foster, A. C., Leeson, P. D., Priestley, T., Tridgett, R., Iversen, L. L., & Woodruff, G. N. (1988). 7-Chlorokynurenic acid is a selective antagonist at the glycine modulatory site of the N-methyl-D-aspartate receptor complex. *Proc.Natl.Acad.Sci.U.S.A* **85**, 6547-6550.

Khakh, B. S. & Henderson, G. (2000). Modulation of fast synaptic transmission by presynaptic ligand-gated cation channels. *J. Autonom. Nerv. Syst.* **81**, 110-121.

Khodakhah, K. & Armstrong, C. M. (1997). Induction of long-term depression and rebound potentiation by inositol trisphosphate in cerebellar Purkinje neurons. *Proc.Natl.Acad.Sci.U.S.A* **94**, 14009-14014.

Kilbride, J., Huang, L. Q., Rowan, M. J., & Anwyl, R. (1998). Presynaptic inhibitory action of the group II metabotropic glutamate receptor agonists, LY354740 and DCG-IV. *Eur.J.Pharmacol.* **356**, 149-157.

Kindler, S. & Kennedy, M. B. (1996). Visualization of autophosphorylation of Ca^{2+}/calmodulin-dependent protein kinase II in hippocampal slices. *J Neurosci.Methods* **68**, 61-70.

Kingston, A. E., Ornstein, P. L., Wright, R. A., Johnson, B. G., Mayne, N. G., Burnett, J. P., Belagaje, R., Wu, S., & Schoepp, D. D. (1998). LY341495 is a nanomolar potent and selective antagonist of group II metabotropic glutamate receptors. *Neuropharmacology* **37**, 1-12.

Kingston, A. E., Lowndes, J., Evans, N., Clark, B., Tomlinson, R., Burnett, J. P., Mayne, N. G., Cockerham, S. L., & Lodge, D. (1998). Sulphur-containing amino acids are agonists for group 1 metabotropic receptors expressed in clonal RGT cell lines. *Neuropharmacology* **37**, 277-287.

Kleckner, N. W. & Dingledine, R. (1988). Requirement for glycine in activation of NMDA-receptors expressed in Xenopus oocytes. *Science* **241**, 835-837.

Koerner, J. F. & Cotman, C. W. (1981). Micromolar L-2-amino-4-phosphonobutyric acid selectively inhibits perforant path synapses from lateral entorhinal cortex. *Brain Res.* **216**, 192-198.

Konnerth, A., Llano, I., & Armstrong, C. M. (1990). Synaptic currents in cerebellar Purkinje cells. *Proc.Natl.Acad.Sci.U.S.A* **87**, 2662-2665.

Konnerth, A., Dreessen, J., & Augustine, G. J. (1992). Brief dendritic calcium signals initiate long-lasting synaptic depression in cerebellar Purkinje cells. *Proc.Natl.Acad.Sci.U.S.A* **89**, 7051-7055.

Korbo, L., Andersen, B. B., Ladefoged, O., & Moller, A. (1993). Total numbers of various cell types in rat cerebellar cortex estimated using an unbiased stereological method. *Brain Res.* **609**, 262-268.

Korkotian, E. & Segal, M. (1998). Fast confocal imaging of calcium released from stores in dendritic spines. *Eur.J Neurosci.* **10**, 2076-2084.

Kornhuber, J. & Weller, M. (1997). Psychotogenicity and N-methyl-D-aspartate receptor antagonism: implications for neuroprotective pharmacotherapy. *Biol.Psychiatry* **41**, 135-144.

Kreitzer, A. C. & Regehr, W. G. (2001). Retrograde inhibition of presynaptic calcium influx by endogenous cannabinoids at excitatory synapses onto Purkinje cells. *Neuron* **29**, 717-727.

Krishek, B. J., Xie, X., Blackstone, C., Huganir, R. L., Moss, S. J., & Smart, T. G. (1994). Regulation of $GABA_A$ receptor function by protein kinase C phosphorylation. *Neuron* **12**, 1081-1095.

Kuner, T., Wollmuth, L. P., Karlin, A., Seeburg, P. H., & Sakmann, B. (1996). Structure of the NMDA receptor channel M2 segment inferred from the accessibility of substituted cysteines. *Neuron* **17**, 343-352.

Kuryatov, A., Laube, B., Betz, H., & Kuhse, J. (1994). Mutational analysis of the glycine-binding site of the NMDA receptor: structural similarity with bacterial amino acid-binding proteins. *Neuron* **12**, 1291-1300.

Kuusinen, A., Arvola, M., & Keinanen, K. (1995). Molecular dissection of the agonist binding site of an AMPA receptor. *EMBO J* **14**, 6327-6332.

Kuwajima, G., Futatsugi, A., Niinobe, M., Nakanishi, S., & Mikoshiba, K. (1992). Two types of ryanodine receptors in mouse brain: skeletal muscle type exclusively in Purkinje cells and cardiac muscle type in various neurons. *Neuron* **9**, 1133-1142.

Lambolez, B., Audinat, E., Bochet, P., Crepel, F., & Rossier, J. (1992). AMPA receptor subunits expressed by single Purkinje cells. *Neuron* **9**, 247-258.

Lasher, R. S. & Zagon, I. S. (1972). The effect of potassium on neuronal differentiation in cultures of dissociated newborn rat cerebellum. *Brain Res.* **41**, 482-488.

Laube, B., Hirai, H., Sturgess, M., Betz, H., & Kuhse, J. (1997). Molecular determinants of agonist discrimination by NMDA receptor subunits: analysis of the glutamate binding site on the NR2B subunit. *Neuron* **18**, 493-503.

Laurie, D. J., Seeburg, P. H., & Wisden, W. (1992). The distribution of 13 $GABA_A$ receptor subunit mRNAs in the rat brain. II. Olfactory bulb and cerebellum. *J Neurosci.* **12**, 1063-1076.

Laurie, D. J., Wisden, W., & Seeburg, P. H. (1992). The distribution of thirteen $GABA_A$ receptor subunit mRNAs in the rat brain. III. Embryonic and postnatal development. *J Neurosci.* **12**, 4151-4172.

Laxson, L. C. & King, J. S. (1983). The development of the Purkinje cell in the cerebellar cortex of the opossum. *J Comp Neurol.* **214**, 290-308.

Lehre, K. P., Levy, L. M., Ottersen, O. P., Storm-Mathisen, J., & Danbolt, N. C. (1995). Differential expression of two glial glutamate transporters in the rat brain: quantitative and immunocytochemical observations. *J Neurosci.* **15**, 1835-1853.

Leidenheimer, N. J., Browning, M. D., & Harris, R. A. (1991). $GABA_A$ receptor phosphorylation: multiple sites, actions and artifacts. *Trends Pharmacol.Sci.* **12**, 84-87.

Leidenheimer, N. J., McQuilkin, S. J., Hahner, L. D., Whiting, P., & Harris, R. A. (1992). Activation of protein kinase C selectively inhibits the γ- aminobutyric $acid_A$ receptor: role of desensitization. *Mol.Pharmacol.* **41**, 1116-1123.

Leidenheimer, N. J., Whiting, P. J., & Harris, R. A. (1993). Activation of calcium-phospholipid-dependent protein kinase enhances benzodiazepine and barbiturate potentiation of the $GABA_A$ receptor. *J.Neurochem.* **60**, 1972-1975.

Lenz, R. A. & Alger, B. E. (1999). Calcium dependence of depolarization-induced suppression of inhibition in rat hippocampal CA1 pyramidal neurons. *J.Physiol* **521 Pt 1**, 147-157.

Leonard, A. S. & Hell, J. W. (1997). Cyclic AMP-dependent protein kinase and protein kinase C phosphorylate N-methyl-D-aspartate receptors at different sites. *J.Biol.Chem.* **272**, 12107-12115.

Lester, R. A., Quarum, M. L., Parker, J. D., Weber, E., & Jahr, C. E. (1989). Interaction of 6-cyano-7-nitroquinoxaline-2,3-dione with the N-methyl-D- aspartate receptor-associated glycine binding site. *Mol.Pharmacol.* **35**, 565-570.

Levenes, C., Daniel, H., & Crepel, F. (1998). Long-term depression of synaptic transmission in the cerebellum: cellular and molecular mechanisms revisited. *Prog.Neurobiol.* **55**, 79-91.

Levi, G. & Raiteri, M. (1993). Carrier-mediated release of neurotransmitters. *Trends Neurosci.* **16**, 415-419.

Levy, L. M., Lehre, K. P., Rolstad, B., & Danbolt, N. C. (1993). A monoclonal antibody raised against an [Na^++K^+]coupled L-glutamate transporter purified from rat brain confirms glial cell localization. *FEBS Lett.* **317**, 79-84.

Lieberman, D. N. & Mody, I. (1994). Regulation of NMDA channel function by endogenous Ca^{2+}-dependent phosphatase. *Nature* **369**, 235-239.

Lin, Y. F., Browning, M. D., Dudek, E. M., & MacDonald, R. L. (1994). Protein kinase C enhances recombinant bovine $\alpha 1\beta 1\gamma 2L$ $GABA_A$ receptor whole-cell currents expressed in L929 fibroblasts. *Neuron* **13**, 1421-1431.

Linden, D. J. & Connor, J. A. (1991). Participation of postsynaptic PKC in cerebellar long-term depression in culture. *Science* **254**, 1656-1659.

Linden, D. J., Dickinson, M. H., Smeyne, M., & Connor, J. A. (1991). A long-term depression of AMPA currents in cultured cerebellar Purkinje neurons. *Neuron* **7**, 81-89.

Lissin, D. V., Carroll, R. C., Nicoll, R. A., Malenka, R. C., & von Zastrow, M. (1999). Rapid, activation-induced redistribution of ionotropic glutamate receptors in cultured hippocampal neurons. *J Neurosci.* **19**, 1263-1272.

Liu, D. T., Tibbs, G. R., & Siegelbaum, S. A. (1996). Subunit stoichiometry of cyclic nucleotide-gated channels and effects of subunit order on channel function. *Neuron* **16**, 983-990.

Liu, H., Wang, H., Sheng, M., Jan, L. Y., Jan, Y. N., & Basbaum, A. I. (1994). Evidence for presynaptic N-methyl-D-aspartate autoreceptors in the spinal cord dorsal horn. *Proc.Natl.Acad.Sci.U.S.A* **91**, 8383-8387.

Liu, J., Conklin, B. R., Blin, N., Yun, J., & Wess, J. (1995). Identification of a receptor/G-protein contact site critical for signaling specificity and G-protein activation. *Proc.Natl.Acad.Sci.U.S.A* **92**, 11642-11646.

Liu, Q. S., Patrylo, P. R., Gao, X. B., & van den Pol, A. N. (1999). Kainate acts at presynaptic receptors to increase GABA release from hypothalamic neurons. *J Neurophysiol.* **82**, 1059-1062.

Liu, Y. B., Disterhoft, J. F., & Slater, N. T. (1993). Activation of metabotropic glutamate receptors induces long-term depression of GABAergic inhibition in hippocampus. *J Neurophysiol.* **69**, 1000-1004.

Llano, I., Marty, A., Johnson, J. W., Ascher, P., & Gahwiler, B. H. (1988). Patch-clamp recording of amino acid-activated responses in "organotypic" slice cultures. *Proc.Natl.Acad.Sci.U.S.A* **85**, 3221-3225.

Llano, I., Leresche, N., & Marty, A. (1991). Calcium entry increases the sensitivity of cerebellar Purkinje cells to applied GABA and decreases inhibitory synaptic currents. *Neuron* **6**, 565-574.

Llano, I. & Gerschenfeld, H. M. (1993). Inhibitory synaptic currents in stellate cells of rat cerebellar slices. *J Physiol* **468**, 177-200.

Llano, I., DiPolo, R., & Marty, A. (1994). Calcium-induced calcium release in cerebellar Purkinje cells. *Neuron* **12**, 663-673.

Llano, I. & Marty, A. (1995). Presynaptic metabotropic glutamatergic regulation of inhibitory synapses in rat cerebellar slices. *J.Physiol* **486 (Pt 1)**, 163-176.

Llano, I., Gonzalez, J., Caputo, C., Lai, F. A., Blayney, L. M., Tan, Y. P., & Marty, A. (2000). Presynaptic calcium stores underlie large-amplitude miniature IPSCs and spontaneous calcium transients. *Nat.Neurosci.* **3**, 1256-1265.

Llinas, R. & Sugimori, M. (1980). Electrophysiological properties of in vitro Purkinje cell somata in mammalian cerebellar slices. *J Physiol* **305**, 171-195.

Llinas, R. & Walton, K. D. Cerebellum. (1990). The synaptic organization of the brain (Shepherd G. M., Ed). 214-245. Oxford, Oxford University Press.

Llinas, R., Sugimori, M., Hillman, D. E., & Cherksey, B. (1992). Distribution and functional significance of the P-type, voltage- dependent Ca^{2+} channels in the mammalian central nervous system. *Trends Neurosci.* **15**, 351-355.

Loopuijt, L. D. & Schmidt, W. J. (1998). The role of NMDA receptors in the slow neuronal degeneration of Parkinson's disease. *Amino.Acids* **14**, 17-23.

Lovinger, D. M. & McCool, B. A. (1995). Metabotropic glutamate receptor-mediated presynaptic depression at corticostriatal synapses involves mGLuR2 or 3. *J.Neurophysiol.* **73**, 1076-1083.

Lowen, S. B., Cash, S. S., Poo, M., & Teich, M. C. (1997). Quantal neurotransmitter secretion rate exhibits fractal behavior. *J Neurosci.* **17**, 5666-5677.

Lu, Y. M., Roder, J. C., Davidow, J., & Salter, M. W. (1998). Src activation in the induction of long-term potentiation in CA1 hippocampal neurons. *Science* **279**, 1363-1367.

Lucas, D. R. & Newhouse, J. P. (1957). The toxic effect of sodium L-glutamate on the inner layers of the retina. *Archives of opthamology* **58**, 193-201.

Luddens, H., Korpi, E. R., & Seeburg, P. H. (1995). Neurotransmitter Receptors III. $GABA_A$/Benzodiazepine receptor heterogeneity: Neurophysiological implications. *Neuropharmacology* **34**, 245-254.

Lujan, R., Nusser, Z., Roberts, J. D., Shigemoto, R., & Somogyi, P. (1996). Perisynaptic location of metabotropic glutamate receptors mGluR1 and mGluR5 on dendrites and dendritic spines in the rat hippocampus. *Eur.J.Neurosci.* **8**, 1488-1500.

Lujan, R., Roberts, J. D., Shigemoto, R., Ohishi, H., & Somogyi, P. (1997). Differential plasma membrane distribution of metabotropic glutamate receptors mGluR1 alpha, mGluR2 and mGluR5, relative to neurotransmitter release sites. *J.Chem.Neuroanat.* **13**, 219-241.

Luntz-Leybman, V., Frostholm, A., Fernando, L., De Blas, A., & Rotter, A. (1993). $GABA_A$/benzodiazepine receptor gamma 2 subunit gene expression in developing normal and mutant mouse cerebellum. *Brain Res.Mol.Brain Res.* **19**, 9-21.

Luo, J., Wang, Y., Yasuda, R. P., Dunah, A. W., & Wolfe, B. B. (1997). The majority of N-methyl-D-aspartate receptor complexes in adult rat cerebral cortex contain at least three different subunits (NR1/NR2A/NR2B). *Mol.Pharmacol.* **51**, 79-86.

MacDermott, A. B., Role, L. W., & Siegelbaum, S. A. (1999). Presynaptic ionotropic receptors and the control of transmitter release. *Annu.Rev.Neurosci.* **22**, 443-485.

MacDonald, J. F., Bartlett, M. C., Mody, I., Pahapill, P., Reynolds, J. N., Salter, M. W., Schneiderman, J. H., & Pennefather, P. S. (1991). Actions of ketamine, phencyclidine and MK-801 on NMDA receptor currents in cultured mouse hippocampal neurones. *J.Physiol* **432**, 483-508.

Madison, D. V., Malenka, R. C., & Nicoll, R. A. (1991). Mechanisms underlying long-term potentiation of synaptic transmission. *Annu.Rev.Neurosci.* **14**, 379-397.

Manzoni, O. & Bockaert, J. (1995). Metabotropic glutamate receptors inhibiting excitatory synapses in the CA1 area of rat hippocampus. *Eur.J.Neurosci.* **7**, 2518-2523.

Marini, A. M., Rabin, S. J., Lipsky, R. H., & Mocchetti, I. (1998). Activity-dependent release of brain-derived neurotrophic factor underlies the neuroprotective effect of N-methyl-D-aspartate. *J Biol.Chem.* **273**, 29394-29399.

Markram, H. & Sakmann, B. (1994). Calcium transients in dendrites of neocortical neurons evoked by single subthreshold excitatory postsynaptic potentials via low-voltage- activated calcium channels. *Proc.Natl.Acad.Sci.U.S.A* **91**, 5207-5211.

Martin, G., Nie, Z., & Siggins, G. R. (1997). Metabotropic glutamate receptors regulate N-methyl-D-aspartate-mediated synaptic transmission in nucleus accumbens. *J Neurophysiol.* **78**, 3028-3038.

Martin, L. J., Blackstone, C. D., Huganir, R. L., & Price, D. L. (1992). Cellular localization of a metabotropic glutamate receptor in rat brain. *Neuron* **9**, 259-270.

Mason, C. A., Christakos, S., & Catalano, S. M. (1990). Early climbing fiber interactions with Purkinje cells in the postnatal mouse cerebellum. *J Comp Neurol.* **297**, 77-90.

Masu, M., Tanabe, Y., Tsuchida, K., Shigemoto, R., & Nakanishi, S. (1991). Sequence and expression of a metabotropic glutamate receptor. *Nature* **349**, 760-765.

Mateos, J. M., Benitez, R., Elezgarai, I., Azkue, J. J., Lazaro, E., Osorio, A., Bilbao, A., Donate, F., Sarria, R., Conquet, F., Ferraguti, F., Kuhn, R., Knopfel, T., & Grandes, P. (2000). Immunolocalization of the mGluR1b splice variant of the metabotropic glutamate receptor 1 at parallel fiber-Purkinje cell synapses in the rat cerebellar cortex. *J Neurochem.* **74**, 1301-1309.

Mayer, M. L., Westbrook, G. L., & Guthrie, P. B. (1984). Voltage-dependent block by Mg^{2+} of NMDA responses in spinal cord neurones. *Nature* **309**, 261-263.

Mayer, M. L. (1985). A calcium-activated chloride current generates the after-depolarization of rat sensory neurones in culture. *J Physiol* **364**, 217-239.

Mayer, M. L. & Westbrook, G. L. (1987). Permeation and block of N-methyl-D-aspartic acid receptor channels by divalent cations in mouse cultured central neurones. *J.Physiol* **394**, 501-527.

McDonald, B. J., Amato, A., Connolly, C. N., Benke, D., Moss, S. J., & Smart, T. G. (1998). Adjacent phosphorylation sites on $GABA_A$ receptor β subunits determine regulation by cAMP-dependent protein kinase. *Nat.Neurosci.* **1**, 23-28.

McKinney, R. A., Capogna, M., Durr, R., Gahwiler, B. H., & Thompson, S. M. (1999). Miniature synaptic events maintain dendritic spines via AMPA receptor activation. *Nat.Neurosci.* **2**, 44-49.

McPherson, P. S. & Campbell, K. P. (1993). The ryanodine receptor/Ca^{2+} release channel. *J Biol.Chem.* **268**, 13765-13768.

Meguro, R., Ohishi, H., Hoshino, K., Hicks, T. P., & Norita, M. (1999). Metabotropic glutamate receptor 2/3 immunoreactivity in the developing rat cerebellar cortex. *J Comp Neurol.* **410**, 243-255.

Mennerick, S. & Zorumski, C. F. (1994). Glial contributions to excitatory neurotransmission in cultured hippocampal cells. *Nature* **368**, 59-62.

Mertz, K., Koscheck, T., & Schilling, K. (2000). Brain-derived neurotrophic factor modulates dendritic morphology of cerebellar basket and stellate cells: an in vitro study. *Neuroscience* **97**, 303-310.

Midtgaard, J. (1992). Membrane properties and synaptic responses of Golgi cells and stellate cells in the turtle cerebellum in vitro. *J Physiol* **457**, 329-354.

Mikoshiba, K. (1996). Role of Ca^{2+} and inositol polyphosphates in coincidence detection. *Coincidence detection in the Nervous System* , 31-38. Strasbourg, HFSP.

Miller, R. J. (1987). Multiple calcium channels and neuronal function. *Science* **235**, 46-52.

Min, M. Y., Melyan, Z., & Kullmann, D. M. (1999). Synaptically released glutamate reduces gamma-aminobutyric acid (GABA)ergic inhibition in the hippocampus via kainate receptors. *Proc.Natl.Acad.Sci.U.S.A* **96**, 9932-9937.

Mintz, I. M., Venema, V. J., Swiderek, K. M., Lee, T. D., Bean, B. P., & Adams, M. E. (1992). P-type calcium channels blocked by the spider toxin omega-Aga-IVA. *Nature* **355**, 827-829.

Mintz, I. M., Adams, M. E., & Bean, B. P. (1992). P-type calcium channels in rat central and peripheral neurons. *Neuron* **9**, 85-95.

Miralles, C. P., Gutierrez, A., Khan, Z. U., Vitorica, J., & De Blas, A. L. (1994). Differential expression of the short and long forms of the gamma 2 subunit of the $GABA_A$/benzodiazepine receptors. *Brain Res.Mol.Brain Res.* **24**, 129-139.

Momiyama, A., Feldmeyer, D., & Cull-Candy, S. G. (1996). Identification of a native low-conductance NMDA channel with reduced sensitivity to Mg^{2+} in rat central neurones. *J Physiol* **494 (Pt 2)**, 479-492.

Monyer, H., Burnashev, N., Laurie, D. J., Sakmann, B., & Seeburg, P. H. (1994). Developmental and regional expression in the rat brain and functional properties of four NMDA receptors. *Neuron* **12**, 529-540.

Moran, J. & Patel, A. J. (1989). Stimulation of the N-methyl-D-aspartate receptor promotes the biochemical differentiation of cerebellar granule neurons and not astrocytes. *Brain Res.* **486**, 15-25.

Morishita, W. & Alger, B. E. (1997). Sr^{2+} supports depolarization-induced suppression of inhibition and provides new evidence for a presynaptic expression mechanism in rat hippocampal slices. *J.Physiol* **505 (Pt 2)**, 307-317.

Morishita, W., Kirov, S. A., Pitler, T. A., Martin, L. A., Lenz, R. A., & Alger, B. E. (1997). N-ethylmaleimide blocks depolarization-induced suppression of inhibition and enhances GABA release in the rat hippocampal slice in vitro. *J.Neurosci.* **17**, 941-950.

Morishita, W., Kirov, S. A., & Alger, B. E. (1998). Evidence for metabotropic glutamate receptor activation in the induction of depolarization-induced suppression of inhibition in hippocampal CA1. *J.Neurosci.* **18**, 4870-4882.

Morishita, W. & Alger, B. E. (1999). Evidence for endogenous excitatory amino acids as mediators in DSI of GABA(A)ergic transmission in hippocampal CA1. *J.Neurophysiol.* **82**, 2556-2564.

Moriyoshi, K., Masu, M., Ishii, T., Shigemoto, R., Mizuno, N., & Nakanishi, S. (1991). Molecular cloning and characterization of the rat NMDA receptor. *Nature* **354**, 31-37.

Morrison, M. E. & Mason, C. A. (1998). Granule neuron regulation of Purkinje cell development: striking a balance between neurotrophin and glutamate signaling. *J.Neurosci.* **18**, 3563-3573.

Moss, S. J., Smart, T. G., Blackstone, C. D., & Huganir, R. L. (1992). Functional modulation of $GABA_A$ receptors by cAMP-dependent protein phosphorylation. *Science* **257**, 661-665.

Moss, S. J., Gorrie, G. H., Amato, A., & Smart, T. G. (1995). Modulation of $GABA_A$ receptors by tyrosine phosphorylation. *Nature* **377**, 344-348.

Moss, S. J. & Smart, T. G. (1996). Modulation of amino acid-gated ion channels by protein phosphorylation. *Int.Rev.Neurobiol.* **39**, 1-52.

Nakajima, Y., Iwakabe, H., Akazawa, C., Nawa, H., Shigemoto, R., Mizuno, N., & Nakanishi, S. (1993). Molecular characterization of a novel retinal metabotropic glutamate receptor mGluR6 with a high agonist selectivity for L-2-amino-4- phosphonobutyrate. *J.Biol.Chem.* **268**, 11868-11873.

Nakanishi, S., Kuwajima, G., & Mikoshiba, K. (1992). Immunohistochemical localization of ryanodine receptors in mouse central nervous system. *Neurosci.Res.* **15**, 130-142.

Nakanishi, S. (1992). Molecular diversity of glutamate receptors and implications for brain function. *Science* **258**, 597-603.

Neki, A., Ohishi, H., Kaneko, T., Shigemoto, R., Nakanishi, S., & Mizuno, N. (1996). Metabotropic glutamate receptors mGluR2 and mGluR5 are expressed in two non-overlapping populations of Golgi cells in the rat cerebellum. *Neuroscience* **75**, 815-826.

Nelson, P. J., Dean, G. E., Aronson, P. S., & Rudnick, G. (1983). Hydrogen ion cotransport by the renal brush border glutamate transporter. *Biochemistry* **22**, 5459-5463.

Netzeband, J. G., Parsons, K. L., Sweeney, D. D., & Gruol, D. L. (1997). Metabotropic glutamate receptor agonists alter neuronal excitability and Ca^{2+} levels via the phospholipase C transduction pathway in cultured Purkinje neurons. *J Neurophysiol.* **78**, 63-75.

Niddam, R., Dubois, A., Scatton, B., Arbilla, S., & Langer, S. Z. (1987). Autoradiographic localization of [^{3}H]zolpidem binding sites in the rat CNS: comparison with the distribution of [^{3}H]flunitrazepam binding sites. *J Neurochem* **49**, 890-899.

Nishizuka, Y. (1986). Studies and perspectives of protein kinase C. *Science* **233**, 305-312.

Nowak, L., Bregestovski, P., Ascher, P., Herbet, A., & Prochiantz, A. (1984). Magnesium gates glutamate-activated channels in mouse central neurones. *Nature* **307**, 462-465.

Nusser, Z., Mulvihill, E., Streit, P., & Somogyi, P. (1994). Subsynaptic segregation of metabotropic and ionotropic glutamate receptors as revealed by immunogold localization. *Neuroscience* **61**, 421-427.

O'Dell, T. J., Kandel, E. R., & Grant, S. G. (1991). Long-term potentiation in the hippocampus is blocked by tyrosine kinase inhibitors. *Nature* **353**, 558-560.

O'Hara, P. J., Sheppard, P. O., Thogersen, H., Venezia, D., Haldeman, B. A., McGrane, V., Houamed, K. M., Thomsen, C., Gilbert, T. L., & Mulvihill, E. R. (1993). The ligand-binding domain in metabotropic glutamate receptors is related to bacterial periplasmic binding proteins. *Neuron* **11**, 41-52.

O'Shea, R. D., Manallack, D. T., Conway, E. L., Mercer, L. D., & Beart, P. M. (1991). Evidence for heterogenous glycine domains but conserved multiple states of the excitatory amino acid recognition site of the NMDA receptor: regional binding studies with [^{3}H]glycine and [3H]L-glutamate. *Exp.Brain Res.* **86**, 652-662.

Ohishi, H., Shigemoto, R., Nakanishi, S., & Mizuno, N. (1993). Distribution of the messenger RNA for a metabotropic glutamate receptor, mGluR2, in the central nervous system of the rat. *Neuroscience* **53**, 1009-1018.

Ohishi, H., Ogawa-Meguro, R., Shigemoto, R., Kaneko, T., Nakanishi, S., & Mizuno, N. (1994). Immunohistochemical localization of metabotropic glutamate receptors, mGluR2 and mGluR3, in rat cerebellar cortex. *Neuron* **13**, 55-66.

Ohno-Shosaku, T., Maejima, T., & Kano, M. (2001). Endogenous cannabinoids mediate retrograde signals from depolarized postsynaptic neurons to presynaptic terminals. *Neuron* **29**, 729-738.

Olney, J. W. & Sharpe, L. G. (1969). Brain lesions in an infant rhesus monkey treated with monosodium glutamate. *Science* **166**, 386-388.

Olney, J. W., Adamo, N. J., & Ratner, A. (1971). Monosodium glutamate effects. *Science* **172**, 294.

Olsen, R. W., McCabe, R. T., & Wamsley, J. K. (1990). $GABA_A$ receptor subtypes: autoradiographic comparison of GABA, benzodiazepine, and convulsant binding sites in the rat central nervous system. *J Chem.Neuroanat.* **3**, 59-76.

Omkumar, R. V., Kiely, M. J., Rosenstein, A. J., Min, K. T., & Kennedy, M. B. (1996). Identification of a phosphorylation site for calcium/calmodulindependent protein kinase II in the NR2B subunit of the N-methyl-D-aspartate receptor. *J.Biol.Chem.* **271**, 31670-31678.

Ornstein, P. L., Bleisch, T. J., Arnold, M. B., Kennedy, J. H., Wright, R. A., Johnson, B. G., Tizzano, J. P., Helton, D. R., Kallman, M. J., Schoepp, D. D., & Herin, M. (1998). 2-substituted (2SR)-2-amino-2-((1SR,2SR)-2-carboxycycloprop-1- yl)glycines as potent and selective antagonists of group II metabotropic glutamate receptors. 2. Effects of aromatic substitution, pharmacological characterization, and bioavailability. *J Med.Chem.* **41**, 358-378.

Ostrowski, J., Kjelsberg, M. A., Caron, M. G., & Lefkowitz, R. J. (1992). Mutagenesis of the beta 2-adrenergic receptor: how structure elucidates function. *Annu.Rev.Pharmacol.Toxicol.* **32**, 167-183.

Owen, D. G., Segal, M., & Barker, J. L. (1986). Voltage-clamp analysis of a Ca^{2+}- and voltage-dependent chloride conductance in cultured mouse spinal neurons. *J Neurophysiol.* **55**, 1115-1135.

Ozawa, S. (1998). [Ca^{2+} permeation through the ionotropic glutamate receptor]. *Tanpakushitsu Kakusan Koso* **43**, 1589-1595.

Palacin, M., Estevez, R., Bertran, J., & Zorzano, A. (1998). Molecular biology of mammalian plasma membrane amino acid transporters. *Physiol Rev.* **78**, 969-1054.

Paquet, M. & Smith, Y. (2000). Presynaptic NMDA receptor subunit immunoreactivity in GABAergic terminals in rat brain. *J.Comp Neurol.* **423**, 330-347.

Parfitt, K. D., Hoffer, B. J., & Bickford-Wimer, P. C. (1990). Potentiation of γ-aminobutyric acid-mediated inhibition by isoproterenol in the cerebellar cortex: receptor specificity. *Neuropharmacology* **29**, 909-916.

Parnas, I., Rashkovan, G., Ravin, R., & Fischer, Y. (2000). Novel mechanism for presynaptic inhibition: $GABA_A$ receptors affect the release machinery. *J Neurophysiol.* **84**, 1240-1246.

Parpura, V., Basarsky, T. A., Liu, F., Jeftinija, K., Jeftinija, S., & Haydon, P. G. (1994). Glutamate-mediated astrocyte-neuron signalling. *Nature* **369**, 744-747.

Patneau, D. K. & Mayer, M. L. (1990). Structure-activity relationships for amino acid transmitter candidates acting at N-methyl-D-aspartate and quisqualate receptors. *J.Neurosci.* **10**, 2385-2399.

Peghini, P., Janzen, J., & Stoffel, W. (1997). Glutamate transporter EAAC-1-deficient mice develop dicarboxylic aminoaciduria and behavioral abnormalities but no neurodegeneration. *EMBO J.* **16**, 3822-3832.

Persohn, E., Malherbe, P., & Richards, J. G. (1992). Comparative molecular neuroanatomy of cloned $GABA_A$ receptor subunits in the rat CNS. *J Comp Neurol.* **326**, 193-216.

Petralia, R. S., Wang, Y. X., & Wenthold, R. J. (1994). The NMDA receptor subunits NR2A and NR2B show histological and ultrastructural localization patterns similar to those of NR1. *J.Neurosci.* **14**, 6102-6120.

Petralia, R. S., Wang, Y. X., Niedzielski, A. S., & Wenthold, R. J. (1996). The metabotropic glutamate receptors, $mGluR_2$ and $mGluR_3$, show unique postsynaptic, presynaptic and glial localizations. *Neuroscience* **71**, 949-976.

Phillips, T., Makoff, A., Murrison, E., Mimmack, M., Waldvogel, H., Faull, R., Rees, S., & Emson, P. (1998). Immunohistochemical localisation of mGluR7 protein in the rodent and human cerebellar cortex using subtype specific antibodies. *Brain Res.Mol.Brain Res.* **57**, 132-141.

Pickering, D. S., Thomsen, C., Suzdak, P. D., Fletcher, E. J., Robitaille, R., Salter, M. W., MacDonald, J. F., Huang, X. P., & Hampson, D. R. (1993). A comparison of two alternatively spliced forms of a metabotropic glutamate receptor coupled to phosphoinositide turnover. *J.Neurochem.* **61**, 85-92.

Pin, J. P., Waeber, C., Prezeau, L., Bockaert, J., & Heinemann, S. F. (1992). Alternative splicing generates metabotropic glutamate receptors inducing different patterns of calcium release in Xenopus oocytes. *Proc.Natl.Acad.Sci.U.S.A* **89**, 10331-10335.

Pin, J. P., Joly, C., Heinemann, S. F., & Bockaert, J. (1994). Domains involved in the specificity of G protein activation in phospholipase C-coupled metabotropic glutamate receptors. *EMBO J.* **13**, 342-348.

Pin, J. P. & Bockaert, J. (1995). Get receptive to metabotropic glutamate receptors. *Curr.Opin.Neurobiol.* **5**, 342-349.

Pin, J. P. & Duvoisin, R. (1995). The metabotropic glutamate receptors: structure and functions. *Neuropharmacology* **34**, 1-26.

Pines, G., Danbolt, N. C., Bjoras, M., Zhang, Y., Bendahan, A., Eide, L., Koepsell, H., Storm-Mathisen, J., Seeberg, E., & Kanner, B. I. (1992). Cloning and expression of a rat brain L-glutamate transporter. *Nature* **360**, 464-467.

Pisani, A., Calabresi, P., Centonze, D., & Bernardi, G. (1997). Activation of group III metabotropic glutamate receptors depresses glutamatergic transmission at corticostriatal synapse. *Neuropharmacology* **36**, 845-851.

Pitler, T. A. & Alger, B. E. (1992). Postsynaptic spike firing reduces synaptic $GABA_A$ responses in hippocampal pyramidal cells. *J.Neurosci.* **12**, 4122-4132.

Pitler, T. A. & Alger, B. E. (1994). Depolarization-induced suppression of GABAergic inhibition in rat hippocampal pyramidal cells: G protein involvement in a presynaptic mechanism. *Neuron* **13**, 1447-1455.

Porter, N. M., Twyman, R. E., Uhler, M. D., & MacDonald, R. L. (1990). Cyclic AMP-dependent protein kinase decreases $GABA_A$ receptor current in mouse spinal neurons. *Neuron* **5**, 789-796.

Pouzat, C. & Kondo, S. (1996). An analysis of neurobiotin-filled stellate axons in the rat cerebellum. *Society for Neuroscience abstract* **22**, 1632.

Pouzat, C. & Hestrin, S. (1997). Developmental regulation of basket/stellate cell-->Purkinje cell synapses in the cerebellum. *J Neurosci.* **17**, 9104-9112.

Pouzat, C. & Marty, A. (1998). Autaptic inhibitory currents recorded from interneurones in rat cerebellar slices. *J Physiol* **509 (Pt 3)**, 777-783.

Pouzat, C. & Marty, A. (1999). Somatic recording of GABAergic autoreceptor current in cerebellar stellate and basket cells. *J Neurosci.* **19**, 1675-1690.

Poyatos, I., Ponce, J., Aragon, C., Gimenez, C., & Zafra, F. (1997). The glycine transporter GLYT2 is a reliable marker for glycine-immunoreactive neurons. *Brain Res.Mol.Brain Res.* **49**, 63-70.

Premkumar, L. S. & Auerbach, A. (1997). Stoichiometry of recombinant N-methyl-D-aspartate receptor channels inferred from single-channel current patterns. *J Gen Physiol* **110**, 485-502.

Prezeau, L., Manzoni, O., Homburger, V., Sladeczek, F., Curry, K., & Bockaert, J. (1992). Characterization of a metabotropic glutamate receptor: direct negative coupling to adenylyl cyclase and involvement of a pertussis toxin- sensitive G protein. *Proc.Natl.Acad.Sci.U.S.A* **89**, 8040-8044.

Prezeau, L., Gomeza, J., Ahern, S., Mary, S., Galvez, T., Bockaert, J., & Pin, J. P. (1996). Changes in the carboxyl-terminal domain of metabotropic glutamate receptor 1 by alternative splicing generate receptors with differing agonist-independent activity. *Mol.Pharmacol.* **49**, 422-429.

Pullan, L. M., Olney, J. W., Price, M. T., Compton, R. P., Hood, W. F., Michel, J., & Monahan, J. B. (1987). Excitatory amino acid receptor potency and subclass specificity of sulfur-containing amino acids. *J Neurochem* **49**, 1301-1307.

Raman, I. M., Tong, G., & Jahr, C. E. (1996). Beta-adrenergic regulation of synaptic NMDA receptors by cAMP-dependent protein kinase. *Neuron* **16**, 415-421.

Ramon Y Cajal, S. (1960). Studies on vertebrate neurogenesis. Springfield, Illinois: Charles C Thomas .

Rapp, M., Segev, I., & Yarom, Y. (1994). Physiology, morphology and detailed passive models of guinea-pig cerebellar Purkinje cells. *J Physiol* **474**, 101-118.

Reyes, A., Lujan, R., Rozov, A., Burnashev, N., Somogyi, P., & Sakmann, B. (1998). Target-cell-specific facilitation and depression in neocortical circuits. *Nat.Neurosci.* **1**, 279-285.

Richards, J. G., Schoch, P., Haring, P., Takacs, B., & Mohler, H. (1987). Resolving $GABA_A$/benzodiazepine receptors: cellular and subcellular localization in the CNS with monoclonal antibodies. *J Neurosci.* **7**, 1866-1886.

Robello, M., Amico, C., & Cupello, A. (1993). Regulation of $GABA_A$ receptor in cerebellar granule cells in culture: differential involvement of kinase activities. *Neuroscience* **53**, 131-138.

Roberts, W. M. (1993). Spatial calcium buffering in saccular hair cells. *Nature* **363**, 74-76.

Robinson, M. B., Djali, S., & Buchhalter, J. R. (1993). Inhibition of glutamate uptake with L-trans-pyrrolidine-2,4- dicarboxylate potentiates glutamate toxicity in primary hippocampal cultures. *J.Neurochem.* **61**, 2099-2103.

Rocamora, N., Garcia-Ladona, F. J., Palacios, J. M., & Mengod, G. (1993). Differential expression of brain-derived neurotrophic factor, neurotrophin-3, and low-affinity nerve growth factor receptor during the postnatal development of the rat cerebellar system. *Brain Res.Mol.Brain Res.* **17**, 1-8.

Rodriguez-Moreno, A., Herreras, O., & Lerma, J. (1997). Kainate receptors presynaptically downregulate GABAergic inhibition in the rat hippocampus. *Neuron* **19**, 893-901.

Rodriguez-Moreno, A. & Lerma, J. (1998). Kainate receptor modulation of GABA release involves a metabotropic function. *Neuron* **20**, 1211-1218.

Roettger, V. & Lipton, P. (1996). Mechanism of glutamate release from rat hippocampal slices during in vitro ischemia. *Neuroscience* **75**, 677-685.

Rosenmund, C., Legendre, P., & Westbrook, G. L. (1992). Expression of NMDA channels on cerebellar Purkinje cells acutely dissociated from newborn rats. *J Neurophysiol.* **68**, 1901-1905.

Rosenmund, C., Stern-Bach, Y., & Stevens, C. F. (1998). The tetrameric structure of a glutamate receptor channel. *Science* **280**, 1596-1599.

Ross, C. A., Danoff, S. K., Schell, M. J., Snyder, S. H., & Ullrich, A. (1992). Three additional inositol 1,4,5-trisphosphate receptors: molecular cloning and differential localization in brain and peripheral tissues. *Proc.Natl.Acad.Sci.U.S.A* **89**, 4265-4269.

Rossi, D. J., Oshima, T., & Attwell, D. (2000). Glutamate release in severe brain ischaemia is mainly by reversed uptake. *Nature* **403**, 316-321.

Rothstein, J. D., Jin, L., Dykes-Hoberg, M., & Kuncl, R. W. (1993). Chronic inhibition of glutamate uptake produces a model of slow neurotoxicity. *Proc.Natl.Acad.Sci.U.S.A* **90**, 6591-6595.

Rothstein, J. D., Martin, L., Levey, A. I., Dykes-Hoberg, M., Jin, L., Wu, D., Nash, N., & Kuncl, R. W. (1994). Localization of neuronal and glial glutamate transporters. *Neuron* **13**, 713-725.

Rothstein, J. D., Dykes-Hoberg, M., Pardo, C. A., Bristol, L. A., Jin, L., Kuncl, R. W., Kanai, Y., Hediger, M. A., Wang, Y., Schielke, J. P., & Welty, D. F. (1996). Knockout of glutamate transporters reveals a major role for astroglial transport in excitotoxicity and clearance of glutamate. *Neuron* **16**, 675-686.

Rudy, B. (1988). Diversity and ubiquity of K channels. *Neuroscience* **25**, 729-749.

Saitoh, T. & Schwartz, J. H. (1985). Phosphorylation-dependent subcellular translocation of a Ca^{2+}/calmodulin-dependent protein kinase produces an autonomous enzyme in Aplysia neurons. *J.Cell Biol.* **100**, 835-842.

Sakurai, M. (1987). Synaptic modification of parallel fibre-Purkinje cell transmission in in vitro guinea-pig cerebellar slices. *J Physiol* **394**, 463-480.

Sakurai, M. (1990). Calcium is an intracellular mediator of the climbing fiber in induction of cerebellar long-term depression. *Proc.Natl.Acad.Sci.U.S.A* **87**, 3383-3385.

Salin, P. A., Malenka, R. C., & Nicoll, R. A. (1996). Cyclic AMP mediates a presynaptic form of LTP at cerebellar parallel fiber synapses. *Neuron* **16**, 797-803.

Sarantis, M., Ballerini, L., Miller, B., Silver, R. A., Edwards, M., & Attwell, D. (1993). Glutamate uptake from the synaptic cleft does not shape the decay of the non-NMDA component of the synaptic current. *Neuron* **11**, 541-549.

Satake, S., Saitow, F., Yamada, J., & Konishi, S. (2000). Synaptic activation of AMPA receptors inhibits GABA release from cerebellar interneurons. *Nat.Neurosci.* **3**, 551-558.

Satoh, T., Ross, C. A., Villa, A., Supattapone, S., Pozzan, T., Snyder, S. H., & Meldolesi, J. (1990). The inositol 1,4,5,-trisphosphate receptor in cerebellar Purkinje cells: quantitative immunogold labeling reveals concentration in an ER subcompartment. *J.Cell Biol.* **111**, 615-624.

Savarese, T. M. & Fraser, C. M. (1992). In vitro mutagenesis and the search for structure-function relationships among G protein-coupled receptors. *Biochem.J* **283 (Pt 1)**, 1-19.

Savic, N. & Sciancalepore, M. (1998). Intracellular calcium stores modulate miniature GABA-mediated synaptic currents in neonatal rat hippocampal neurons. *Eur.J Neurosci.* **10**, 3379-3386.

Scanziani, M., Salin, P. A., Vogt, K. E., Malenka, R. C., & Nicoll, R. A. (1997). Use-dependent increases in glutamate concentration activate presynaptic metabotropic glutamate receptors. *Nature* **385**, 630-634.

Schilling, K., Dickinson, M. H., Connor, J. A., & Morgan, J. I. (1991). Electrical activity in cerebellar cultures determines Purkinje cell dendritic growth patterns. *Neuron* **7**, 891-902.

Schneggenburger, R., Zhou, Z., Konnerth, A., & Neher, E. (1993). Fractional contribution of calcium to the cation current through glutamate receptor channels. *Neuron* **11**, 133-143.

Schoepp, D., Bockaert, J., & Sladeczek, F. (1990). Pharmacological and functional characteristics of metabotropic excitatory amino acid receptors. *Trends Pharmacol.Sci.* **11**, 508-515.

Schoepp, D. D. & Conn, P. J. (1993). Metabotropic glutamate receptors in brain function and pathology. *Trends Pharmacol.Sci.* **14**, 13-20.

Schoepp, D. D., Jane, D. E., & Monn, J. A. (1999). Pharmacological agents acting at subtypes of metabotropic glutamate receptors. *Neuropharmacology* **38**, 1431-1476.

Schofield, P. R., Darlison, M. G., Fujita, N., Burt, D. R., Stephenson, F. A., Rodriguez, H., Rhee, L. M., Ramachandran, J., Reale, V., Glencorse, T. A., Seeburg, P. H., & Barnard, E. A. (1987). Sequence and functional expression of the $GABA_A$ receptor shows a ligand-gated receptor super-family. *Nature* **328**, 221-227.

Schulte, S. & Stoffel, W. (1995). UDP galactose:ceramide galactosyltransferase and glutamate/aspartate transporter. Copurification, separation and characterization of the two glycoproteins. *Eur.J Biochem.* **233**, 947-953.

Schwartz, P. M., Borghesani, P. R., Levy, R. L., Pomeroy, S. L., & Segal, R. A. (1997). Abnormal cerebellar development and foliation in BDNF-/- mice reveals a role for neurotrophins in CNS patterning. *Neuron* **19**, 269-281.

Schwartz, R. D., Heuschneider, G., Edgar, P. P., & Cohn, J. A. (1991). cAMP analogs inhibit γ-aminobutyric acid-gated chloride flux and activate protein kinase A in brain synaptoneurosomes. *Mol.Pharmacol.* **39**, 370-375.

Sciancalepore, M. & Cherubini, E. (1995). Protein kinase A-dependent increase in frequency of miniature GABAergic currents in rat CA3 hippocampal neurons. *Neurosci.Lett.* **187**, 91-94.

Sciancalepore, M., Stratta, F., Fisher, N. D., & Cherubini, E. (1995). Activation of metabotropic glutamate receptors increase the frequency of spontaneous GABAergic currents through protein kinase A in neonatal rat hippocampal neurons. *J Neurophysiol.* **74**, 1118-1122.

Scott, R. H., McGuirk, S. M., & Dolphin, A. C. (1988). Modulation of divalent cation-activated chloride ion currents. *Br.J Pharmacol.* **94**, 653-662.

Seagar, M., Leveque, C., Charvin, N., Marqueze, B., Martin-Moutot, N., Boudier, J. A., Boudier, J. L., Shoji-Kasai, Y., Sato, K., & Takahashi, M. (1999). Interactions between proteins implicated in exocytosis and voltage- gated calcium channels. *Philos.Trans.R.Soc.Lond B Biol.Sci.* **354**, 289-297.

Segal, M. & Manor, D. (1992). Confocal microscopic imaging of $[Ca^{2+}]_i$ in cultured rat hippocampal neurons following exposure to N-methyl-D-aspartate. *J Physiol* **448**, 655-676.

Segal, R. A., Takahashi, H., & McKay, R. D. (1992). Changes in neurotrophin responsiveness during the development of cerebellar granule neurons. *Neuron* **9**, 1041-1052.

Segal, R. A., Pomeroy, S. L., & Stiles, C. D. (1995). Axonal growth and fasciculation linked to differential expression of BDNF and NT3 receptors in developing cerebellar granule cells. *J Neurosci.* **15**, 4970-4981.

Sheng, M., Cummings, J., Roldan, L. A., Jan, Y. N., & Jan, L. Y. (1994). Changing subunit composition of heteromeric NMDA receptors during development of rat cortex. *Nature* **368**, 144-147.

Shigemoto, R., Nakanishi, S., & Mizuno, N. (1992). Distribution of the mRNA for a metabotropic glutamate receptor ($mGluR_1$) in the central nervous system: an in situ hybridization study in adult and developing rat. *J Comp Neurol.* **322**, 121-135.

Shigemoto, R., Abe, T., Nomura, S., Nakanishi, S., & Hirano, T. (1994). Antibodies inactivating $mGluR_1$ metabotropic glutamate receptor block long-term depression in cultured Purkinje cells. *Neuron* **12**, 1245-1255.

Shigemoto, R., Kinoshita, A., Wada, E., Nomura, S., Ohishi, H., Takada, M., Flor, P. J., Neki, A., Abe, T., Nakanishi, S., & Mizuno, N. (1997). Differential presynaptic localization of metabotropic glutamate receptor subtypes in the rat hippocampus. *J.Neurosci.* **17**, 7503-7522.

Sigel, E., Baur, R., Trube, G., Mohler, H., & Malherbe, P. (1990). The effect of subunit composition of rat brain $GABA_A$ receptors on channel function. *Neuron* **5**, 703-711.

Sigel, E., Baur, R., & Malherbe, P. (1991). Activation of protein kinase C results in down-modulation of different recombinant $GABA_A$-channels. *FEBS Lett.* **291**, 150-152.

Sigel, E., Baur, R., Kellenberger, S., & Malherbe, P. (1992). Point mutations affecting antagonist affinity and agonist dependent gating of $GABA_A$ receptor channels. *EMBO J.* **11**, 2017-2023.

Smart, T. G., Moss, S. J., Xie, X., & Huganir, R. L. (1991). $GABA_A$ receptors are differentially sensitive to zinc: dependence on subunit composition. *British Journal of Pharmacology* **103**, 1837-1839.

Smart, T. G. (1992). A novel modulatory binding site for zinc on the $GABA_A$ receptor complex in cultured rat neurones. *J.Physiol (Lond)* **447**, 587-625.

Somogyi, P., Takagi, H., Richards, J. G., & Mohler, H. (1989). Subcellular localization of benzodiazepine/$GABA_A$ receptors in the cerebellum of rat, cat, and monkey using monoclonal antibodies. *J Neurosci.* **9**, 2197-2209.

Sonsalla, P. K., Albers, D. S., & Zeevalk, G. D. (1998). Role of glutamate in neurodegeneration of dopamine neurons in several animal models of parkinsonism. *Amino.Acids* **14**, 69-74.

Sorrentino, V. & Volpe, P. (1993). Ryanodine receptors: how many, where and why? *Trends Pharmacol.Sci.* **14**, 98-103.

Southam, E., Morris, R., & Garthwaite, J. (1992). Sources and targets of nitric oxide in rat cerebellum. *Neurosci.Lett.* **137**, 241-244.

Stallcup, W. B., Bulloch, K., & Baetge, E. E. (1979). Coupled transport of glutamate and sodium in a cerebellar nerve cell line. *J Neurochem* **32**, 57-65.

Stelzer, A. (1992). $GABA_A$ receptors control the excitability of neuronal populations. *Int.Rev.Neurobiol.* **33**, 195-287.

Stelzer, A. (1992). Intracellular regulation of $GABA_A$-receptor function. *Ion Channels* **3**, 83-136.

Stern-Bach, Y., Bettler, B., Hartley, M., Sheppard, P. O., O'Hara, P. J., & Heinemann, S. F. (1994). Agonist selectivity of glutamate receptors is specified by two domains structurally related to bacterial amino acid-binding proteins. *Neuron* **13**, 1345-1357.

Storck, T., Schulte, S., Hofmann, K., & Stoffel, W. (1992). Structure, expression, and functional analysis of a Na^+-dependent glutamate/aspartate transporter from rat brain. *Proc.Natl.Acad.Sci.U.S.A* **89**, 10955-10959.

Strichartz GR. (1973). The inhibition of sodium currents in myelinated nerve by quaternary derivatives of lidocaine. *J Gen Physiol* **62[1]**, 37-57.

Sun, L., Margolis, F. L., Shipley, M. T., & Lidow, M. S. (1998). Identification of a long variant of mRNA encoding the NR3 subunit of the NMDA receptor: its regional distribution and developmental expression in the rat brain. *FEBS Lett.* **441**, 392-396.

Swandulla, D., Carbone, E., & Lux, H. D. (1991). Do calcium channel classifications account for neuronal calcium channel diversity? *Trends Neurosci.* **14**, 46-51.

Szatkowski, M., Barbour, B., & Attwell, D. (1990). Non-vesicular release of glutamate from glial cells by reversed electrogenic glutamate uptake. *Nature* **348**, 443-446.

Szatkowski, M. & Attwell, D. (1994). Triggering and execution of neuronal death in brain ischaemia: two phases of glutamate release by different mechanisms. *Trends Neurosci.* **17**, 359-365.

Takahashi, K. A. & Linden, D. J. (2000). Cannabinoid receptor modulation of synapses received by cerebellar Purkinje cells. *J Neurophysiol.* **83**, 1167-1180.

Takahashi, M., Sarantis, M., & Attwell, D. (1996). Postsynaptic glutamate uptake in rat cerebellar Purkinje cells. *J Physiol* **497 (Pt 2)**, 523-530.

Takahashi, M., Billups, B., Rossi, D., Sarantis, M., Hamann, M., & Attwell, D. (1997). The role of glutamate transporters in glutamate homeostasis in the brain. *J Exp.Biol.* **200 (Pt 2)**, 401-409.

Takechi, H., Eilers, J., & Konnerth, A. (1998). A new class of synaptic response involving calcium release in dendritic spines. *Nature* **396**, 757-760.

Takei, K., Stukenbrok, H., Metcalf, A., Mignery, G. A., Sudhof, T. C., Volpe, P., & De Camilli, P. (1992). Ca^{2+} stores in Purkinje neurons: endoplasmic reticulum subcompartments demonstrated by the heterogeneous distribution of the $InsP_3$ receptor, Ca^{2+}-ATPase, and calsequestrin. *J.Neurosci.* **12**, 489-505.

Tanabe, Y., Masu, M., Ishii, T., Shigemoto, R., & Nakanishi, S. (1992). A family of metabotropic glutamate receptors. *Neuron* **8**, 169-179.

Tanabe, Y., Nomura, A., Masu, M., Shigemoto, R., Mizuno, N., & Nakanishi, S. (1993). Signal transduction, pharmacological properties, and expression patterns of two rat metabotropic glutamate receptors, $mGluR_3$ and $mGluR_4$. *J.Neurosci.* **13**, 1372-1378.

Tanaka, J., Ichikawa, R., Watanabe, M., Tanaka, K., & Inoue, Y. (1997). Extra-junctional localization of glutamate transporter EAAT4 at excitatory Purkinje cell synapses. *Neuroreport* **8**, 2461-2464.

Tanaka, K., Watase, K., Manabe, T., Yamada, K., Watanabe, M., Takahashi, K., Iwama, H., Nishikawa, T., Ichihara, N., Kikuchi, T., Okuyama, S., Kawashima, N., Hori, S., Takimoto, M., & Wada, K. (1997). Epilepsy and exacerbation of brain injury in mice lacking the glutamate transporter GLT-1. *Science* **276**, 1699-1702.

Tehrani, M. H., Hablitz, J. J., & Barnes, E. M., Jr. (1989). cAMP increases the rate of $GABA_A$ receptor desensitization in chick cortical neurons. *Synapse* **4**, 126-131.

Tempia, F., Kano, M., Schneggenburger, R., Schirra, C., Garaschuk, O., Plant, T., & Konnerth, A. (1996). Fractional calcium current through neuronal AMPA-receptor channels with a low calcium permeability. *J.Neurosci.* **16**, 456-466.

Testa, C. M., Catania, M. V., & Young, A. B. (1994). Anatomical distribution of metabotropic glutamate receptors in mammalian brain. In: *The metabotropic glutamate receptors* (Conn PJ, Patel J, eds). 99-123. Totowa, NJ, Humana.

Thompson, C. L., Drewery, D. L., Atkins, H. D., Stephenson, F. A., & Chazot, P. L. (2000). Immunohistochemical localization of N-methyl-D-aspartate receptor NR1, NR2A, NR2B and NR2C/D subunits in the adult mammalian cerebellum. *Neurosci.Lett.* **283**, 85-88.

Thomsen, C., Hansen, L., & Suzdak, P. D. (1994). L-glutamate uptake inhibitors may stimulate phosphoinositide hydrolysis in baby hamster kidney cells expressing $mGluR_{1a}$ via heteroexchange with L-glutamate without direct activation of $mGluR_{1a}$. *J Neurochem* **63**, 2038-2047.

Tingley, W. G., Ehlers, M. D., Kameyama, K., Doherty, C., Ptak, J. B., Riley, C. T., & Huganir, R. L. (1997). Characterization of protein kinase A and protein kinase C phosphorylation of the N-methyl-D-aspartate receptor NR1 subunit using phosphorylation site-specific antibodies. *J Biol.Chem.* **272**, 5157-5166.

Tretter, V., Ehya, N., Fuchs, K., & Sieghart, W. (1997). Stoichiometry and assembly of a recombinant $GABA_A$ receptor subtype. *Journal of Neuroscience* **17**, 2728-2737.

Trombley, P. Q. & Westbrook, G. L. (1992). L-AP4 inhibits calcium currents and synaptic transmission via a G- protein-coupled glutamate receptor. *J.Neurosci.* **12**, 2043-2050.

Trudeau, L. E., Emery, D. G., & Haydon, P. G. (1996). Direct modulation of the secretory machinery underlies PKA-dependent synaptic facilitation in hippocampal neurons. *Neuron* **17** , 789-797.

Trudeau, L. E., Fang, Y., & Haydon, P. G. (1998). Modulation of an early step in the secretory machinery in hippocampal nerve terminals. *Proc.Natl.Acad.Sci.U.S.A* **95**, 7163-7168.

Tsien, R. W., Lipscombe, D., Madison, D. V., Bley, K. R., & Fox, A. P. (1988). Multiple types of neuronal calcium channels and their selective modulation. *Trends Neurosci.* **11**, 431-438.

Twitchell, W., Brown, S., & Mackie, K. (1997). Cannabinoids inhibit N- and P/Q-type calcium channels in cultured rat hippocampal neurons. *J Neurophysiol.* **78**, 43-50.

Unwin, N. (1993). Neurotransmitter action: opening of ligand-gated ion channels. *Cell* **72 Suppl**, 31-41.

Usachev, Y. M. & Thayer, S. A. (1997). All-or-none Ca^{2+} release from intracellular stores triggered by Ca^{2+} influx through voltage-gated Ca^{2+} channels in rat sensory neurons. *J Neurosci.* **17**, 7404-7414.

Valenzuela, C. F., Machu, T. K., McKernan, R. M., Whiting, P., VanRenterghem, B. B., McManaman, J. L., Brozowski, S. J., Smith, G. B., Olsen, R. W., & Harris, R. A. (1995). Tyrosine kinase phosphorylation of $GABA_A$ receptors. *Brain Res.Mol.Brain Res.* **31**, 165-172.

Vandenberg, R. J., Arriza, J. L., Amara, S. G., & Kavanaugh, M. P. (1995). Constitutive ion fluxes and substrate binding domains of human glutamate transporters. *J Biol.Chem.* **270** , 17668-17671.

Vandenberg, R. J., Mitrovic, A. D., & Johnston, G. A. (1998). Serine-O-sulphate transport by the human glutamate transporter, EAAT2. *Br.J Pharmacol.* **123**, 1593-1600.

Verdoorn, T. A., Draguhn, A., Ymer, S., Seeburg, P. H., & Sakmann, B. (1990). Functional properties of recombinant rat $GABA_A$ receptors depend upon subunit composition. *Neuron* **4**, 919-928.

Verdoorn, T. A., Burnashev, N., Monyer, H., Seeburg, P. H., & Sakmann, B. (1991). Structural determinants of ion flow through recombinant glutamate receptor channels. *Science* **252** , 1715-1718.

Veruki, M. L. & Yeh, H. H. (1992). Vasoactive intestinal polypeptide modulates $GABA_A$ receptor function in bipolar cells and ganglion cells of the rat retina. *J.Neurophysiol.* **67**, 791-797.

Veruki, M. L. & Yeh, H. H. (1994). Vasoactive intestinal polypeptide modulates $GABA_A$ receptor function through activation of cyclic AMP. *Vis.Neurosci.* **11**, 899-908.

Vincent, P., Armstrong, C. M., & Marty, A. (1992). Inhibitory synaptic currents in rat cerebellar Purkinje cells: modulation by postsynaptic depolarization. *J Physiol* **456**, 453-471.

Vincent, P. & Marty, A. (1993). Neighboring cerebellar Purkinje cells communicate via retrograde inhibition of common presynaptic interneurons. *Neuron* **11**, 885-893.

Walton, P. D., Airey, J. A., Sutko, J. L., Beck, C. F., Mignery, G. A., Sudhof, T. C., Deerinck, T. J., & Ellisman, M. H. (1991). Ryanodine and inositol trisphosphate receptors coexist in avian cerebellar Purkinje neurons. *J Cell Biol.* **113**, 1145-1157.

Wan, Q., Man, H. Y., Braunton, J., Wang, W., Salter, M. W., Becker, L., & Wang, Y. T. (1997). Modulation of $GABA_A$ receptor function by tyrosine phosphorylation of β subunits. *J.Neurosci.* **17**, 5062-5069.

Wang, J. & Johnson, K. M. (1995). Regulation of striatal cyclic-3',5'-adenosine monophosphate accumulation and GABA release by glutamate metabotropic and dopamine D1 receptors. *J Pharmacol.Exp.Ther.* **275**, 877-884.

Wang, L. Y., Orser, B. A., Brautigan, D. L., & MacDonald, J. F. (1994). Regulation of NMDA receptors in cultured hippocampal neurons by protein phosphatases 1 and 2A. *Nature* **369**, 230-232.

Wang, R. A., Cheng, G., Kolaj, M., & Randic, M. (1995). Alpha-subunit of calcium/calmodulin-dependent protein kinase II enhances gamma-aminobutyric acid and inhibitory synaptic responses of rat neurons in vitro. *J Neurophysiol.* **73**, 2099-2106.

Wang, Y., Small, D. L., Stanimirovic, D. B., Morley, P., & Durkin, J. P. (1997). AMPA receptor-mediated regulation of a G_i-protein in cortical neurons. *Nature* **389**, 502-504.

Wang, Y. T. & Linden, D. J. (2000). Expression of cerebellar long-term depression requires postsynaptic clathrin-mediated endocytosis. *Neuron* **25**, 635-647.

Watkins, J. C. (1984). Excitatory amino acids and central synaptic transmission. *Trends Pharmacol.Sci.* **5**, 373-376.

Watson, E. L. (1999). GTP-binding proteins and regulated exocytosis. *Crit Rev.Oral Biol.Med.* **10**, 284-306.

Weiner, J. L., Zhang, L., & Carlen, P. L. (1994). Potentiation of $GABA_A$-mediated synaptic current by ethanol in hippocampal CA1 neurons: possible role of protein kinase C. *J.Pharmacol.Exp.Ther.* **268**, 1388-1395.

Weisskopf, M. G., Castillo, P. E., Zalutsky, R. A., & Nicoll, R. A. (1994). Mediation of hippocampal mossy fiber long-term potentiation by cyclic AMP. *Science* **265**, 1878-1882.

Westbrook, G. L. & Mayer, M. L. (1987). Micromolar concentrations of Zn^{2+} antagonize NMDA and GABA responses of hippocampal neurons. *Nature* **328**, 640-643.

Wheeler, D. B., Randall, A., Sather, W. A., & Tsien, R. W. (1995). Neuronal calcium channels encoded by the alpha 1A subunit and their contribution to excitatory synaptic transmission in the CNS. *Prog.Brain Res.* **105**, 65-78.

White, G., Li, C., & Ishac, E. (1992). 1,9-Dideoxyforskolin does not mimick all cAMP and protein kinase A independent effects of forskolin on GABA activated ion currents in adult rat sensory neurons. *Brain Res.* **586**, 157-161.

Whiting, P. J., McKernan, R. M., & Wafford, K. A. (1995). Structure and pharmacology of vertebrate $GABA_A$ receptor subtypes. *International Review of Neurobiology* **38**, 95-138.

Whiting, P. J., McAllister, G., Vasilatis, D., Bonnert, T. P., Heavens, R. P., Smith, D. W., Hewson, L., O'Donnell, R., Rigby, M. R., Sirinathsinghji, D. J. S., Marshall, G., Thompson, S. A., & Wafford, K. A. (1997). Neuronally restricted RNA splicing regulates the expression of a novel $GABA_A$ receptor subunit conferring atypical functional properties. *Journal of Neuroscience* **17**, 5027-6037.

Wilson, R. I. & Nicoll, R. A. (2001). Endogenous cannabinoids mediate retrograde signalling at hippocampal synapses. *Nature* **410**, 588-592.

Winkler, A., Mahal, B., Zieglgansberger, W., & Spanagel, R. (1999). Accurate quantification of the mRNA of NMDAR1 splice variants measured by competitive RT-PCR. *Brain Res.Brain Res.Protoc.* **4**, 69-81.

Wisden, W., Korpi, E. R., & Bahn, S. (1996). The cerebellum: a model system for studying $GABA_A$ receptor diversity. *Neuropharmacology* **35**, 1139-1160.

Wollmuth, L. P. & Sakmann, B. (1998). Different mechanisms of Ca^{2+} transport in NMDA and Ca^{2+}-permeable AMPA glutamate receptor channels. *J Gen Physiol* **112**, 623-636.

Wong, E. H. & Kemp, J. A. (1991). Sites for antagonism on the N-methyl-D-aspartate receptor channel complex. *Annu.Rev.Pharmacol.Toxicol.* **31**, 401-425.

Woodward, D. J., Hoffer, B. J., Siggins, G. R., & Bloom, F. E. (1971). The ontogenic development of synaptic functions, synaptic activation and responsiveness to neurotransmitter substances in rat cerebellar Purkinje neurones. *Brain Research* **34**, 7-97.

Woodward, D. J., Hoffer, B. J., Siggins, G. R., & Oliver, A. P. (1971). Inhibition of Purkinje cells in the frog cerebellum. II. Evidence for GABA as the inhibitory transmitter. *Brain Res.* **33**, 91-100.

Worley, P. F. (1999). Homer signaling complex links group I metabotropic and IP_3 receptors. *J Neurochem* **73**, S103.

Xia, J., Chung, H. J., Wihler, C., Huganir, R. L., & Linden, D. J. (2000). Cerebellar long-term depression requires PKC-regulated interactions between GluR2/3 and PDZ domain-containing proteins. *Neuron* **28**, 499-510.

Yakushiji, T., Shirasaki, T., Munakata, M., Hirata, A., & Akaike, N. (1993). Differential properties of type I and type II benzodiazepine receptors in mammalian CNS neurones. *Br.J Pharmacol.* **109**, 819-825.

Yamakuni, T., Kuwano, R., Odani, S., Miki, N., Yamaguchi, K., & Takahashi, Y. (1987). Molecular cloning of cDNA to mRNA for a cerebellar spot 35 protein. *J Neurochem* **48**, 1590-1596.

Yokoi, M., Kobayashi, K., Manabe, T., Takahashi, T., Sakaguchi, I., Katsuura, G., Shigemoto, R., Ohishi, H., Nomura, S., Nakamura, K., Nakao, K., Katsuki, M., & Nakanishi, S. (1996). Impairment of hippocampal mossy fiber LTD in mice lacking $mGluR_2$. *Science* **273**, 645-647.

Yu, X. M., Askalan, R., Keil, G. J., & Salter, M. W. (1997). NMDA channel regulation by channel-associated protein tyrosine kinase Src. *Science* **275**, 674-678.

Zafra, F., Gomeza, J., Olivares, L., Aragon, C., & Gimenez, C. (1995). Regional distribution and developmental variation of the glycine transporters GLYT1 and GLYT2 in the rat CNS. *Eur.J Neurosci.* **7**, 1342-1352.

Zdilar, D., Rotter, A., & Frostholm, A. (1991). Expression of $GABA_A$/benzodiazepine receptor alpha 1-subunit mRNA and [^{3}H]flunitrazepam binding sites during postnatal development of the mouse cerebellum. *Brain Res.Dev.Brain Res.* **61**, 63-71.

Zdilar, D., Luntz-Leybman, V., Frostholm, A., & Rotter, A. (1992). Differential expression of $GABA_A$/benzodiazepine receptor beta 1, beta 2, and beta 3 subunit mRNAs in the developing mouse cerebellum. *J Comp Neurol.* **326**, 580-594.

Zempel, J. M. & Steinbach, J. H. (1995). Neonatal rat cerebellar granule and Purkinje neurons in culture express different $GABA_A$ receptors. *Eur.J Neurosci.* **7**, 1895-1905.

Zerangue, N. & Kavanaugh, M. P. (1996). Flux coupling in a neuronal glutamate transporter. *Nature* **383**, 634-637.

Zhang, L. & Goldman, J. E. (1996). Generation of cerebellar interneurons from dividing progenitors in white matter. *Neuron* **16**, 47-54.

Zheng, F., Gingrich, M. B., Traynelis, S. F., & Conn, P. J. (1998). Tyrosine kinase potentiates NMDA receptor currents by reducing tonic zinc inhibition. *Nat.Neurosci.* **1**, 185-191.

Zheng, J. & Sigworth, F. J. (1997). Selectivity changes during activation of mutant Shaker potassium channels. *J Gen Physiol* **110**, 101-117.

Zilberter, Y., Kaiser, K. M., & Sakmann, B. (1999). Dendritic GABA release depresses excitatory transmission between layer 2/3 pyramidal and bitufted neurons in rat neocortex. *Neuron* **24**, 979-988.